Investigating the effect of low dietary iodine on cardiovascular disease parameters, gene expression and thyroid function in stroke-prone spontaneously hypertensive rats

Phillip Moseki
HND, BSc, MSc

This thesis is being submitted for the
degree of Doctor of Philosophy
(Ph.D.)
in the College of Medical, Veterinary and Life Sciences at
the University of Glasgow

December 2023

Abstract

Despite progress in strategies for preventing and controlling iodine deficiency, iodine deficiency disorders (IDD) continue to be a major public health problem throughout the world. At the same time, cardiovascular disease (CVD) remains a global health problem. Hypertension is the leading risk factor for CVD. The number of people with hypertension is expected to rise to 1.56 billion in 2025 while it is also estimated that >2000 million people worldwide are still at risk of insufficient iodine intake. Iodine is an essential microelement in human physiology. Its role in thyroid function is well known and documented in the literature. However, recent evidence links iodine with direct cardiovascular functional changes independent of thyroid hormones (TH). The stroke-prone spontaneously hypertensive (SHRSP) rat is a well-established model of primary hypertension and endothelial dysfunction which can be used for investigating CVD mechanisms and novel interventions. It has been established that Wistar Kyoto (WKY) and SHRSP rats have similar thyroid function under baseline conditions.

In this thesis, I aimed to understand the direct effect of iodine on cardiovascular function and disease development in young Wistar Kyoto (WKY) and stroke-prone spontaneously hypertensive (SHRSP) male and female rats. I also employed RNA sequencing (RNA-Seq) to determine the effect of low iodine diet (LID) on protein coding genes in thoracic aorta from WKY and SHRSP male rats. Moreover, I determined the effect of iodide on contractile signalling in mesenteric artery vascular smooth muscle cells (VSMCs) isolated from WKY and SHRSP males.

In chapter 3, 5-week-old WKY and SHRSP males and females (n =7-8 per group) were assigned a normal (NID) or LID for 4 weeks. Tail cuff blood pressure (BP) and body weight (BW) were measured weekly while water consumption, urine production and echocardiography measurements were determined fortnightly. Plasma was collected for assessment of thyroid-stimulating hormone (TSH), free triiodothyronine (fT3), free thyroxine (fT4) and thyroglobulin (Tg). At sacrifice, thyroid gland and heart tissues were snap-frozen for assessing sodium iodide symporter (SLC5a5) and pendrin (SLC26a4) gene expression. Mesenteric arteries were assessed for vascular function using wire myography. At baseline there were no significant differences in urinary iodine concentration (UIC) and TH

profiles between WKY and SHRSP males and females, however following the 4-week dietary period, UIC significantly reduced in LID fed rats irrespective of strain and sex. Contrary to the stable levels of fT3 and fT4, levels of TSH significantly increased in SHRSP but remained unchanged in WKY males and females. Strain differences in homeostatic mechanisms in response to LID were further revealed when SLC5a5 gene expression was significantly increased in the thyroid gland from WKY males but not SHRSP males fed LID. There were no significant effects of LID on BW, BP and cardiac function parameters. Contractile responses to U46619 in mesenteric arteries from SHRSP and WKY males fed LID increased in a dose dependent manner concomitant with significantly reduced UIC which were independent of fT3 and fT4.

In chapter 4, thoracic aorta was snap frozen for transcriptomic profiling using RNA sequencing (RNA-Seq). Moreover, ingenuity pathway analysis (IPA) software was used to understand the biology linking to the differential gene expressions (DEGs). In support of the vascular function data (chapter 3), RNA-Seq analysis demonstrated DEGs in SHRSP fed LID. 438 DEGs were significantly increased in thoracic aorta from SHRSP fed LID when compared to those fed NID. The DEGs in IPA identified dilated cardiomyopathy as the most significant canonical pathway and within this pathway contractile protein coding genes such as Mhy7, Myh6, Actc1, Tnnc1, Tnni3, Tnnt2 and Ttn were significantly increased. Moreover, expression of these genes was also significantly increased in Ca2+, integrin-linked kinase (ILK) and actin cytoskeleton signalling pathways. The DEGs in ingenuity pathway analysis (IPA) software identified growth failure or short stature as one of the diseases and functions associated with LID. This suggest that SHRSP fed LID are likely to experience growth restriction independent of thyroid dysfunction.

In chapter 5, mesenteric artery VSMCs were isolated from WKY and SHRSP males and used for assessing the effect of iodide on contractile signalling. This allowed investigation of the molecular mechanisms underlying enhanced vascular contractility secondary to iodine modification. I demonstrated that phospho-myosin light chain (phospho-MLC) was significantly reduced in SHRSP VSMCs incubated in cell culture media supplemented with iodide while there was no significant difference in VSMCs isolated from WKY male rats. In general, I

demonstrated an anticontractile effect of iodide on VSMC isolated from SHRSP male rats. Furthermore, I demonstrated the presence of SLC5a5 protein in VSMCs from WKY and SHRSP male rats.

To conclude, the results in this thesis demonstrate that short-term LID increases vascular reactivity in SHRSP and WKY male rats through increased expression of genes encoding contractile proteins in SHRSP but not WKY rats. Moreover, enhanced contractile response occurred independent of changes in TH profiles suggesting a direct effect of iodine on vascular function. This PhD thesis work therefore suggests that short-term LID is likely to have a greater detrimental effect on the hypertensive than the normotensive rat model and could potentially effect individuals with hypertension. Our work supports the hypothesis that dietary iodine has a direct effect on cardiovascular function and disease outcomes independent of TH levels and might be a new modifiable risk factor for CVD.

Table of Contents

List of Tables

List of Figures

List of Publications, Conferences and Awards

Oral Presentation at British and Irish Hypertension Society (BIHS) annual scientific meeting 2022, the Barbican, York, UK.

Short-term low iodine diet alters vascular reactivity independent of thyroid hormone levels in stroke-prone spontaneously hypertensive rats. Phillip Moseki*[1], Delyth Graham[1], Ian Salt[1], Emilie Combet[1]. Abstracts from the 2022 Annual Scientific Meeting of the British and Irish Hypertension Society (BIHS). *J Hum Hypertens* **36**(Suppl 1), 1–22 (2022). https://doi.org/10.1038/s41371-022-00734-5.

Poster presentation at the 29th Scientific meeting of the International Society of Hypertension (ISH) 2022, Kyoto, Japan.

Short-term low iodine diet exacerbates vascular reactivity without altering thyroid hormone profiles in stroke-prone spontaneously hypertensive rats. Phillip Moseki*[1]Delyth Graham[1], Ian Salt[1], Emilie Combet[1]. Journal of Hypertension 41 (Suppl 1): p e360, January 2023. DOI: 10.1097/01.hjh.0000916444.04285.9d.

Grants and Awards

Lead Applicant: Wellcome Trust Institutional Strategic Support Fund (ISSF) [204820/Z/16/Z] (£4,302).

Bioinformatics and R Wet Lab for Biologists Course Funding (£250).

MVLS Conference Funding to attend International Society of Hypertension in Kyoto, Japan (£750).

Acknowledgements

First and foremost, I would like to extend my sincere gratitude to Eleanor Emery PhD scholarship programme for funding my PhD training. Additionally, this PhD would not have been possible without the generous support from my employer, the University of Botswana who gave me a 4-year study leave.

I would like to thank my primary supervisor Dr Delyth Graham for her invaluable support and guidance throughout my PhD training. She has played a major role in my professional and personal development, and I will forever be grateful. I also like to thank my secondary supervisor Dr Ian Salt for his technical insights in cell culture and western blotting. Moreover, I want to thank Dr Emilie Combet for her technical support and training in assessment of urinary iodine concentrations. Finally, I want to also thank Dr Martin W McBride for offering support and training in molecular techniques including, RNA extraction, qPCR, and analysis of my RNA-sequencing data.

A huge thank you to all British heart foundation (BHF) animal house staff for their support and interaction during the 3 years of animal work. Another big thank you to John McClure for your guidance and training in wire myography, a skill I cherish so much. Thank you to Wendy Beattie for your kindness, patience, and guidance in primary cell culture techniques. A big thanks to Wellcome Institutional Strategic Support Fund (ISSF) for funding my RNA sequencing experiment and thanks to Glasgow Polyomics for analysing my samples. I would also like to appreciate, all staff members and students from Thursday meetings for their interaction and advice which contributed positively to my PhD. Thanks to Simon, Amrita and Kayley for welcoming me into the lab and taking time to train me in molecular techniques and animal handling.

I would like to thank my family for their emotional support and prayers. Thank you, mum, for believing in me. To my partner Boi and my daughters Rene and Bone, thank you so much for your support and patience. Your presence was enough motivation to keep me going.

Finally, I give thanks to the Lord who gave breath of life. My faith in you has kept me strong for I know nothing is impossible in your presence.

Author's Declaration

I Phillip Moseki declare that this thesis has been written by myself and is a record of research conducted by myself except for the following: RNA-Sequencing, generation of heatmaps, PCA plots and volcano plots which were conducted by Glasgow Polyomics. Contribution from others has been referenced and reproduced with permission. This PhD work was supervised by Dr Delyth Graham, Dr Ian Salt, and Dr Emilie Combet, and has not been submitted for any other degree at the University of Glasgow or any other institution.

Definitions/Abbreviations

Abbreviations	Full name
ΔCT	Delta cycle threshold
µg	Micrograms
µL	Microliter
µM	Micromolar
ACE	Angiotensin-converting enzyme
Ach	Acetylcholine
ACTA2	Smooth muscle cell actin
ACTB	Beta-Actin
Actc1	Actin alpha cardiac muscle 1
ADH	Antidiuretic hormone
ADP	Adenosine diphosphate
AF	Atrial fibrillation
AMI	Acute myocardial infarction
AMP	Adenosine monophosphate
ANS	Autonomic nervous system
ARRIVE	Animal Research: Reporting of In Vivo Experiments
ATP2C1	ATPase secretory pathway Ca^{2+}
BCA	Bicinchoninic acid
BP	Blood pressure
BSA	Bovine serum albumin
Ca	Calcium
Ca^{2+}	Calcium ion
CAD	Coronary Artery Disease
CaM	Calmodulin
cAMP	Cyclic Adenosine Monophosphate
cDNA	Complementary deoxyribonucleic acid
CNN2	Calponin 2
CNS	Central nervous system
CO	Cardiac output
COX	Cyclooxygenase
CSN	Carotid sinus nerve
csv	Comma-separated-values
CT	Cycle threshold
CVD	Cardiovascular Disease
CVS	Cardiovascular System
D1	Type 1 iodothyronine deiodinases
D2	Type 2 iodothyronine deiodinases
D3	Type 3 iodothyronine deiodinases
DAG	Diacylglycerol
DASH	Dietary Approaches to Stop Hypertension
DE	Differentially expressed.
DEGs	Differentially expressed genes.
dH2O	Distilled water.
DMEM	Dulbecco's Modified Eagle's medium
DMSO	Dimethyl sulfoxide
DMT	Danish Myo Technologies
DNA	Deoxyribonucleic acid

DPBS	Dulbecco's phosphate buffered saline
DTT	DL-Dithiothreitol; Clelands reagent
EDCF	Endothelium-dependent contracting factor
EDHF	Endothelium-derived hyperpolarizing factors
EDRF	Endothelium-dependent relaxing factor
EDTA	Ethylenediaminetetraacetic acid
EDV	End diastolic volume
eNOS	Endothelial nitric oxide synthase
FAM	Fluorescein amidites
FBS	Foetal bovine serum
FDR	Falso discovery rate
fT3	Free triiodothyronine
fT4	Free thyroxine
GAPDH	Gyceraldehyde-3-Phosphate Dehydrogenase
GDI	Guanine nucleotide dissociation inhibitor
GPCRs	G protein-coupled receptors
GSH	Reduced glutathione
GWAS	Genome wide association study
H_2O_2	Hydrogen peroxide
HO	Hydroxyl radical
HOCl	Hypochlorous acid
HPT	Hypothalamic-pituitary-thyroid
HR	Heart rate
hr	Hour
ICAM-1	Intercellular adhesion molecule-1
ICCIDD	International Council for the Control of Iodine Deficiency Disorders
IDD	Iodine deficiency disorders
ILK	Integrin-linked kinase
IncRNA	Long non-coding RNA
iNOS	Inducible nitric oxide
IPA	Ingenuity® Pathway Analysis
ISSF	Institutional Strategic Support Fund
KI	Potassium iodide
L	Liter
LA	Left atrium
LDL	Low density lipoprotein
LID	Low iodine diet
LV	Left ventricle
LVMI	Left ventricular mass index
MA plot	Mean Average plot.
Mg	Magnesium
MHC	Myosin heavy chain
min	Minute
miRNA	MicroRNA
mIU/L	Milli-international units per litre
mL	Millilitre
MLC	Myosin light chain
MLCK	Myosin light chain kinase
MLC-P	Myosin light chain phosphorylation
MYH11	Myosin heavy chain 11
Myh6	Myosin heavy chain 6
Myh7	Myosin heavy chain 7

Myl4	Myosin light chain 4
Myo10	Myosin X
MYOCD	Myocardin
NaCl	Sodium chloride
NaI	Sodium iodide
NE	Norepinephrine
ng	Nanogram
NGS	Next-generation sequencing
NID	Normal iodine diet
NIS	Sodium iodide symporter (SLC5a5)
NO	Nitric oxide
NO	Nitrogen oxide
NUE	NIS upstream enhancer
^{o}C	Degrees Celsius
$ONOO^{-}$	Peroxynitrite
padj	Adjusted p-value for false discovery rate
PAGE	Polyacrylamide gel electrophoresis
PBS	Phosphate-buffered saline
PCA	Principal component analysis
PCR	Polymerase chain reaction
Pg	Picogram
PIL	Personal license
PKC	Phosphokinase C
PLC	Phospholipase C
PLN	Phospholamban
pmol	Picomole
PSS	Physiological saline solution
RA	Right atrium
RAAS	Renin-angiotensin aldosterone system
RDD	RNase-Free DNase Set buffer
RIPA	Radioimmunoprecipitation assay buffer
RNA	Ribonucleic acid
RNA-Seq	RNA Sequencing
ROCK	RhoA-Rho kinase
ROS	Reactive oxygen species
RPKM	Reads per kilobase million
RPM	Reads per million
rT3	Reverse Triiodothyronine
RT-PCR	Reverse transcription PCR
RV	Right ventricle
RWT	Relative wall thickness
SAGE	Serial analysis of gene expression
SBP	Systolic blood pressure
SERCA	Sarcoendoplasmic reticulum Ca2+ ATPase
SHR	Spontaneously hypertensive rats
SHRSP	Stroke-prone spontaneously hypertensive rat
SLC26a4	Pendrin
SLC5a5	Sodium iodide symporter
SM22a/taglin	Smooth muscle 22a/taglin
SMC	Smooth muscle cell
SNA	Sympathetic nerve activity
SNPs	Single nucleotide polymorphisms

snRNA	Small nuclear RNA
SOD	Superoxide dismutase
SR	Sarcoplasmic reticulum
SRF	Serum response factor
SV	Stroke volume
SVR	Systemic vascular resistance
T3	Triiodothyronine
T4	Thyroxine
TBS	Tri-Buffered Saline
TBST	Tris-Buffered Saline tween
TC	Total cholesterol
TFs	Transcription factors
Tg	Thyroglobulin
TG	Triglyceride
TH	Thyroid hormone
TnC	Troponin C
TnI	Troponin I
Tnn	Titin
Tnnc1	Troponin C1, slow skeletal and cardiac type
Tnni3	Troponin I3, cardiac type
Tnnt2	Troponin T2, cardiac type
TnT	Troponin T
TPM	Transcripts per million
TPM	Transcripts per million
Tpm1	Tropomyosin 1, alpha
TPO	Thyroid peroxidase
TPR	Total peripheral resistance
TRH	Thyroid releasing hormone
TRs	Thyroid hormone receptors
TRα1	Thyroid receptor alpha
TRß	Thyroid receptor beta
TSH	Thyroid stimulating hormone.
TSH-R	TSH-receptor
UIC	Urinary iodine concentration
UIE	Urinary iodine excretion
UNICEF	United Nations Children’s Fund
URA	Upstream regulator analysis
VCAM-1	Vascular cell adhesion molecule-1
VCP	Valosin containing protein
VEGF	Vascular endothelial growth factor
VSMC	Vascular smooth muscle cell
WHO	World health organization
Wks	Weeks
WKY	Wistar Kyoto rat
ZIPK	Zipper-interacting protein kinase

Chapter 1 General Introduction

1.1 Cardiovascular system

The cardiovascular system (CVS) starts to develop and reaches a functional state before any other major organ system(Levick, 2009). It is active by the beginning of the fourth week during which the placenta is unable to meet the requirements of the growing embryo (Larsen, 1993). Its main function is to supply blood and nutrients throughout the body. The CVS consists of two main circuits: systemic circulation and pulmonary circulation. Pulmonary circulation allows for the oxygenation of blood while systemic circulation provides for oxygenated blood and nutrients to reach the rest of the body (Graham, 2019). The main components include the heart, arteries, vein, and capillaries. The heart is the muscular pump consisting of the right ventricle (RV) and the left ventricle (LV) which are filled from the right atrium (RA) and left atrium (LA) respectively. The RV pumps blood through the lungs (the pulmonary circulation) and the LV simultaneously pumps blood through the rest of the body and back to the heart (the systemic circulation) (Figure 1-1). The CVS responds to various stimuli such as changing blood volume, hormones, electrolytes, and medication which control the velocity and the amount of blood carried through the blood vessels. The control of blood flow is achieved by changes in cardiac output (CO), vascular resistance, and control of arterial blood pressure (BP) which are mediated by the autonomic nervous system (ANS) (Graham, 2019).The ANS has two interacting systems: the sympathetic nervous system releases norepinephrine (NE) which increases heart rate and vasoconstriction while parasympathetic releases acetylcholine (Ach) which decreases heart rate (HR). Blood vessels lack parasympathetic innervations and their diameter is regulated by the sympathetic nervous system i.e. a decrease in sympathetic tone allows vasodilatation (Gordan et al., 2015).

1.1.1 Systemic circulation

The LV contracts virtually simultaneously with the RV and ejects the same volume of blood but at a much higher pressure. The blood flows through the aorta and branching arterial system. Arteries carry blood away from the heart and divide into large and small arteries. Large arteries receive the highest

pressure of blood flow and are thicker and more elastic to accommodate the high pressure while small arteries such as arterioles have more smooth muscle cell (SMC) which contracts and relaxes to regulate blood flow to specific regions of the body (Gopolan & Kirk, 2022).

1.1.2 Cardiac output

The LV and the RV work together to maintain an adequate CO. The RV must supply an adequate preload to the left side of the heart(Della Rocca et al., 2009). The amount of blood in the ventricle before ventricular contraction is called end diastolic volume (EDV). According to the Frank-Starling principle, the strength of cardiac contraction is related to the muscle fibre length at the end of diastole. An increase of EDV means an increase of preload of the heart, and finally, it increases stroke volume (SV) (Della Rocca et al., 2009). CO is defined as SV (the volume of blood ejected by one ventricle per contraction) multiplied by HR (the number of contractions per minute). In a resting 70 kg adult, the SV is 70-80 mL, and the HR is 65-75 beats/min, so the resting CO is approximately 75 mL × 70 beats per min. The CO is not fixed, it adapts rapidly to changing internal or external circumstances such as exercise (Levick, 2009).

1.1.3 Blood pressure

Blood pressure (BP) is the force of blood against the arterial walls. Blood pressure is a generic term with several interpretations such as intraventricular blood pressure, systemic arterial blood pressure, capillary hydrostatic pressure or systemic venous return. In the context of this thesis blood pressure will refer to systemic blood pressure. A pressure gradient along the vessel is required to drive blood through the CVS. Ventricular contraction raises aortic BP to approximately 120 mmHg above the atmospheric pressure while the pressure in the great veins is close to atmospheric pressure, and the pressure difference drives blood from artery to vein (Levick, 2009). Arterial pressure is pulsatile rather than steady because the heart ejects blood intermittently. The systemic arterial pressure ranges from 120 mmHg during systole to approximately 80 mmHg during diastole, while the pulmonary pressure is between 25 mmHg and 10 mmHg in systole and diastole respectively. Normal arterial BP is therefore reported as 120/80 mmHg (Pickering & Stevens, 2013).

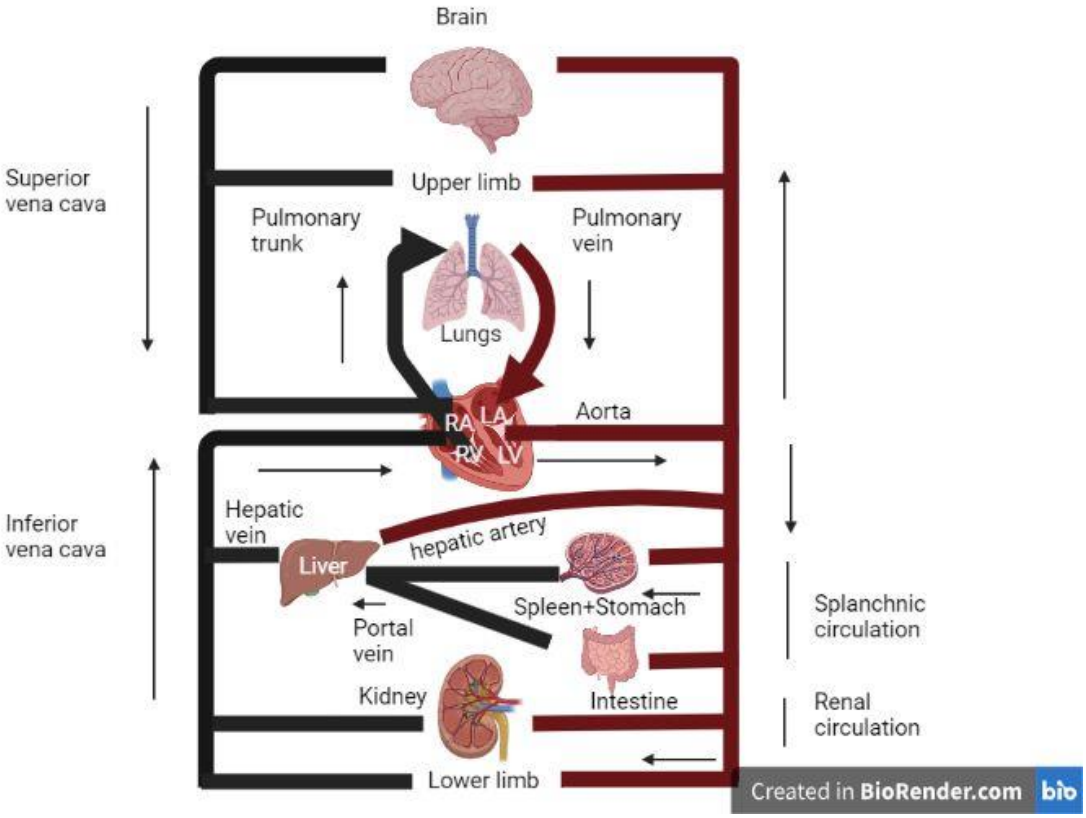

Figure 1-1: Schematic diagram of the circulatory system.

The systemic and pulmonary systems are arranged in series. The systemic circulation provides the blood supply to all body tissues. It carries oxygen and nutrients to the cells and picks up carbon dioxide and waste products. Systemic circulation carries oxygenated blood from the left ventricle (LV), through arteries, to the capillaries in the tissues of the body. From the tissue capillaries, the deoxygenated blood returns through the vein to the right atrium (RA) before it enters the right ventricle (RV). From the RV blood is circulated to the lungs for oxygenation and then enters the left atrium (LA) then the LV.

1.1.4 Blood pressure regulation

The control of BP is an integrated response that includes regulation by neural receptors, hormones, and renal fluid balance (Guyton, 1991). During acute BP changes the body responds through baroreceptors located within blood vessels and atria in the heart. The sensory information is conveyed to the central nervous system (CNS) and influences peripheral vascular resistance and CO (Graham, 2019). There are two major forms of baroreceptors which are low- and high-pressure baroreceptors. The carotid baroreceptor responds to both increases and decreases in BP and sends afferent signals via the glossopharyngeal nerve. On the other hand, the aortic arch baroreceptor responds only to increases in BP, sending its signals through the vagus nerve. These two high pressure baroreceptors send signals in response to the physical vessel distortion. The stretch increases action potential relayed from sensory endings in the adventitia of the artery to the solitary nucleus that signals to autonomic neurons to release hormones such as renin and aldosterone to affect the CVS (Figure 1-2) (Gordan et al., 2015; Graham, 2019). Low-pressure baroreceptors are present within the vena cava, pulmonary arteries, and atria. The venous system has compliance approximately 30 times greater than that of the arterial system (Gelman, 2008). Baroreceptors in the venous system are largely sensitive to changes in volume. BP can also be regulated through chemoreceptors. The carotid bodies which are located on carotid arteries are responsible for detecting changes in arterial blood O_2 levels and chemoreflex regulation of cardio-respiratory functions. The carotid body receives sensory innervation from a branch of the glossopharyngeal nerve called the carotid sinus nerve (CSN). Hypoxia increases the CNS activity, which in turn stimulates breathing, sympathetic nerve activity and increases BP (Prabhakar et al., 2015).

Intermediate and long-term control of BP is affected through hormones and renal fluid balance. Antidiuretic hormone (ADH) is synthesized and released in response to multiple triggers which include high serum osmolarity, decrease in BP and low blood volume. It mainly functions to increase water reabsorption in the collecting duct of the nephrons, thereby causing an increase in plasma volume and arterial pressure (Guyton, 1991).

The renin-angiotensin aldosterone system (RAAS) responds to decreased arterial pressure and/or decrease of Na^+ concentration which causes a decrease in kidney perfusion. In response to these triggers, renin is released from the juxtaglomerular cells in the afferent arterioles of the kidney and enters the blood where it encounters angiotensinogen which is produced continuously by the liver. Renin coverts angiotensinogen into angiotensin I. The angiotensin I then make its way to the pulmonary vessels, where the endothelium produces the angiotensin-converting enzyme (ACE). Angiotensin I is then converted to angiotensin II by ACE. Angiotensin II has many functions to increase arterial pressure, including: (1) vasoconstriction of arterioles throughout the body, (2) vasoconstriction of the efferent arterioles within the glomerulus of the kidney, resulting in the maintenance of glomerular filtration rate, (3) Increased sodium (Na^+) reabsorption within the kidney tubules which results in passive water reabsorption. The release of aldosterone from the zona glomerulosa of the adrenal cortex will increase arterial pressure through increased reabsorption of Na^+ and increased secretion of potassium (K^+) in the distal convoluted tubule and collecting duct with the nephron (Graham, 2019). Figure 1-2 gives a summary of intermediate and long-term control of BP by hormones.

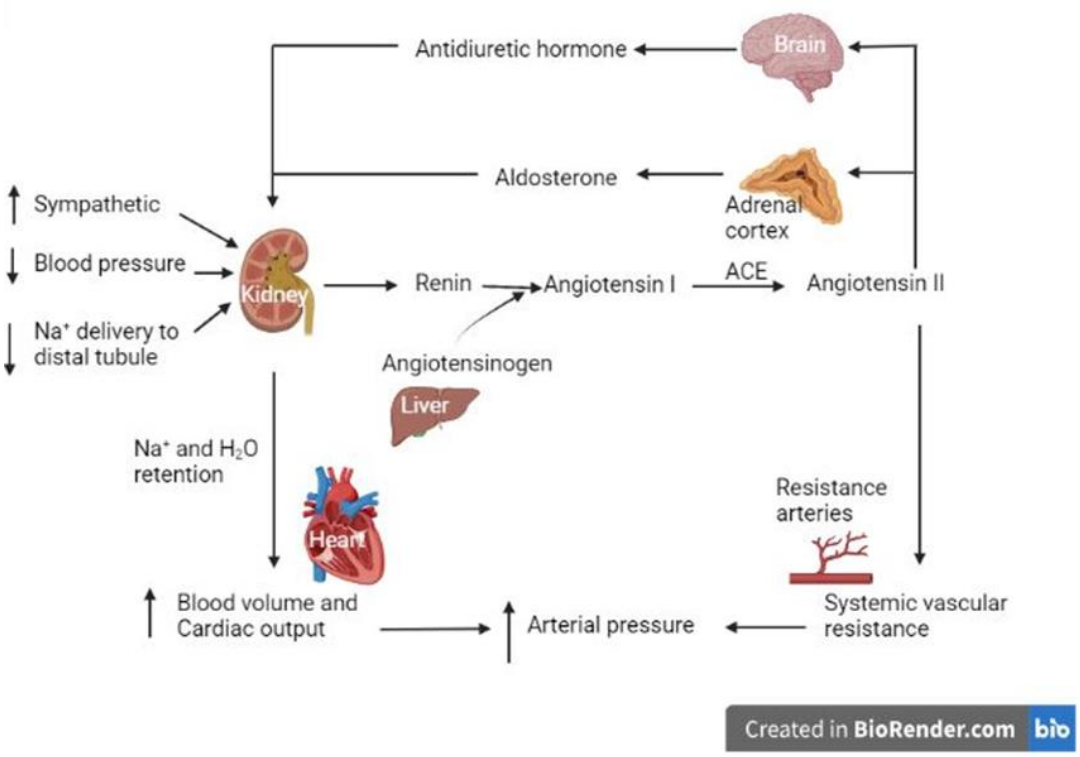

Figure 1-2: Intermediate and long-term regulation of blood pressure.

The renin-angiotensin-aldosterone system (RAAS) plays an important role in regulating blood volume and systemic vascular resistance (SVR). The system is dependent on hormonal changes which induce transcription of genes to produce vasoactive proteins, making it a longer term means of controlling BP.

1.1.5 Maintenance of vascular tone

The arterial system is made up of large conduit vessels, medium seized arteries, small arterioles, and capillaries (Touyz et al., 2018). Small resistance arteries with lumen diameters measuring < 300 µm when relaxed constitute the major site of generation of vascular resistance (Schiffrin, 1992). Vascular tone is maintained by the release of numerous vasodilator and vasoconstrictor substances. Three different layers form the blood vessel wall: intima, media, and adventitia. The intima, which is a monolayer made of endothelial cells separates circulating blood from the medial layer, which comprises of concentric layers of SMC and elastic lamella. The outer most layer is the tunica adventitia which is formed of collagen bundles, elastic fibres, fibroblasts, and vasa vasorum. Moreover, it also houses perivascular nerve endings (Fernández-Alfonso, 2004). VSMCs are specialised cells responsible for maintaining vascular homeostasis through active contraction and relaxation in healthy, blood vessels.

1.1.5.1 Vasoconstriction

In the presence of vasoconstrictor stimuli, intracellular stores and/or the extracellular space mobilize calcium(Ca^{2+}) to increase cytosolic Ca^{2+} in VSMC. The increased cytosolic Ca^{2+} will bind to calmodulin (CaM) and form a complex which activate myosin light chain (MLC) kinase and allow the interaction of actin and myosin to generate tonic contraction (Figure 1-3) (Carrillo-Sepúlveda & Barreto-Chaves, 2010).

In addition to the dependency on amount of Ca^{2+} in the cytoplasm, Ca^{2+}-independent processes regulate vascular smooth muscle contraction, by influencing the sensitivity of MLC to Ca^{2+}. Following the initial Ca2+ sensitization process, force generation is maintained. The two main signalling pathways implicated in Ca^{2+} sensitization, include the diacylglycerol (DAG)-phospholipase C (PLC)-phosphokinase C (PKC) pathway and the RhoA-Rho kinase (ROCK) pathway (Guzik et al., 2017; Loirand & Pacaud, 2010). Moreover, other kinases such as the integrin-linked kinase (ILK), p21-activated protein kinase and zipper-interacting protein kinase (ZIPK) are also implicated (Endo et al., 2004). The Ca^{2+} sensitization mechanism regulates the phosphorylation state of MLC20

independently of Ca^{2+}–calmodulin–MLCK signalling (Touyz et al., 2018). The Ca^{2+} independent regulation of VSMC involving rock is illustrated in Figure 1-4.

1.1.5.2 Vasodilatation

In healthy blood vessels, the epithelial cell lining of blood vessels (the endothelium) controls vascular reactivity by releasing paracrine signalling molecules, such as nitric oxide (NO) and prostacyclin (Wilson et al., 2019). Vasodilatation occurs when the VSMC relax. Relaxation can either be due to removal of a contractile stimulus or inhibition of contractility. Numerous vasoactive molecules such as acetylcholine, ATP, adenosine, bradykinin, and, histamine can activate endothelial nitric oxide synthase (eNOS) and cyclooxygenase (COX) pathways to form NO and prostacyclin respectively (Vanhoutte et al., 2017). NO uses cyclic guanosine monophosphate (cGMP) while prostacyclin utilises cyclic adenosine monophosphate (cAMP) intracellular secondary messengers for cellular effects (Hellsten et al., 2012). These secondary messengers have downstream effects of causing a decrease in intracellular Ca^{2+} and increase in myosin light chain (MLC) phosphatase activity which dephosphorylates the contracted actin MLC complex, causing relaxation (Hai & Murphy, 1989; Kuo & Ehrlich, 2015). Moreover, Ca^{2+} is removed by sarcoendoplasmic reticulum Ca^{2+} ATPase (SERCA) that sequester Ca^{2+} back into the sarcoplasmic reticulum. The Na^{+}/Ca^{2+} antiporters located in the plasma membrane can decrease intracellular $Ca^{2+}$by allowing Na^{+} to flow down its gradient in exchange of Ca^{2+} (Webb, 2003).

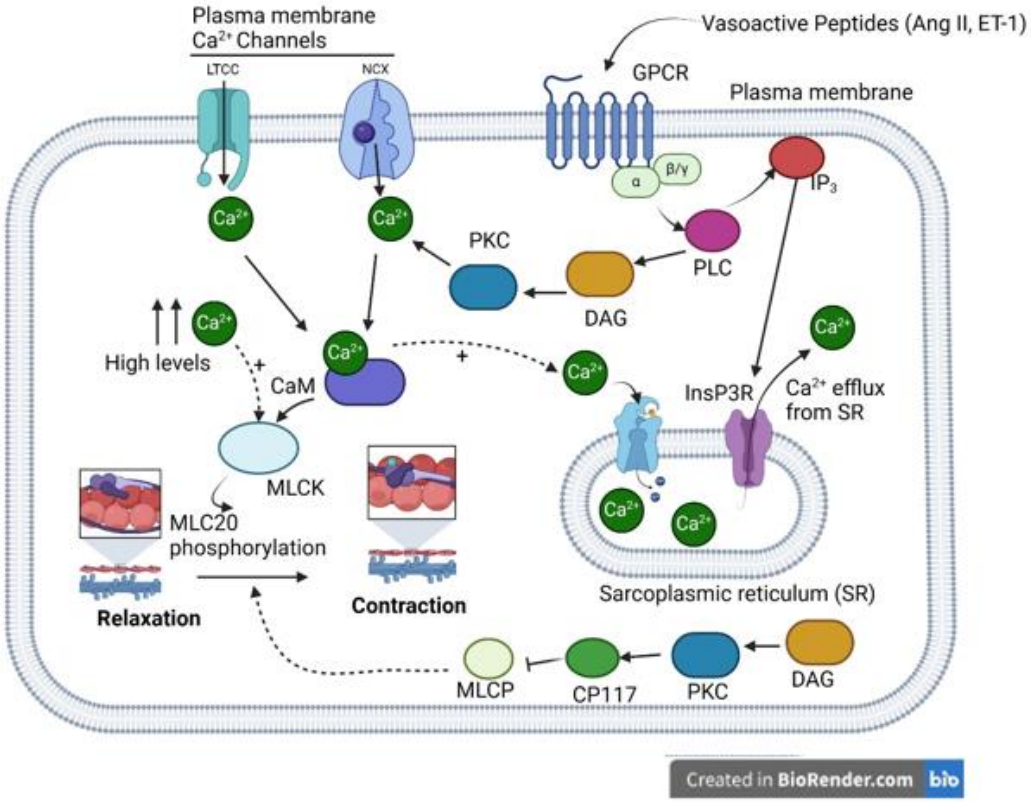

Figure 1-3: Diagrammatic representation of Ca^{2+} dependent regulation of vascular smooth muscle cell contraction.

Vasoconstrictors induce VSMC contraction by increasing the intracellular levels of Ca^{2+}. Vasoactive peptides, such as Ang II, bind to G protein-coupled receptors (GPCRs) activating PLC leading to (i) production of IP_3 and (ii) formation of DAG. IP_3 binds to the IP receptor Ca^{2+}channel (InsP3R) and induces Ca^{2+} release from the sarcoplasmic reticulum (SR). DAG causes activation of PKC, which influences Ca^{2+} channels such as L-type calcium channel (LTCC) and the Na^{+}-Ca^{2+} (NCX) to open. MLCP activity is reduced by CPI-17 phosphorylation. Ca^{2+} binds to calmodulin and activates the MLCK, leading to MLC20 phosphorylation at Ser19, actin polymerization, and vascular contraction.

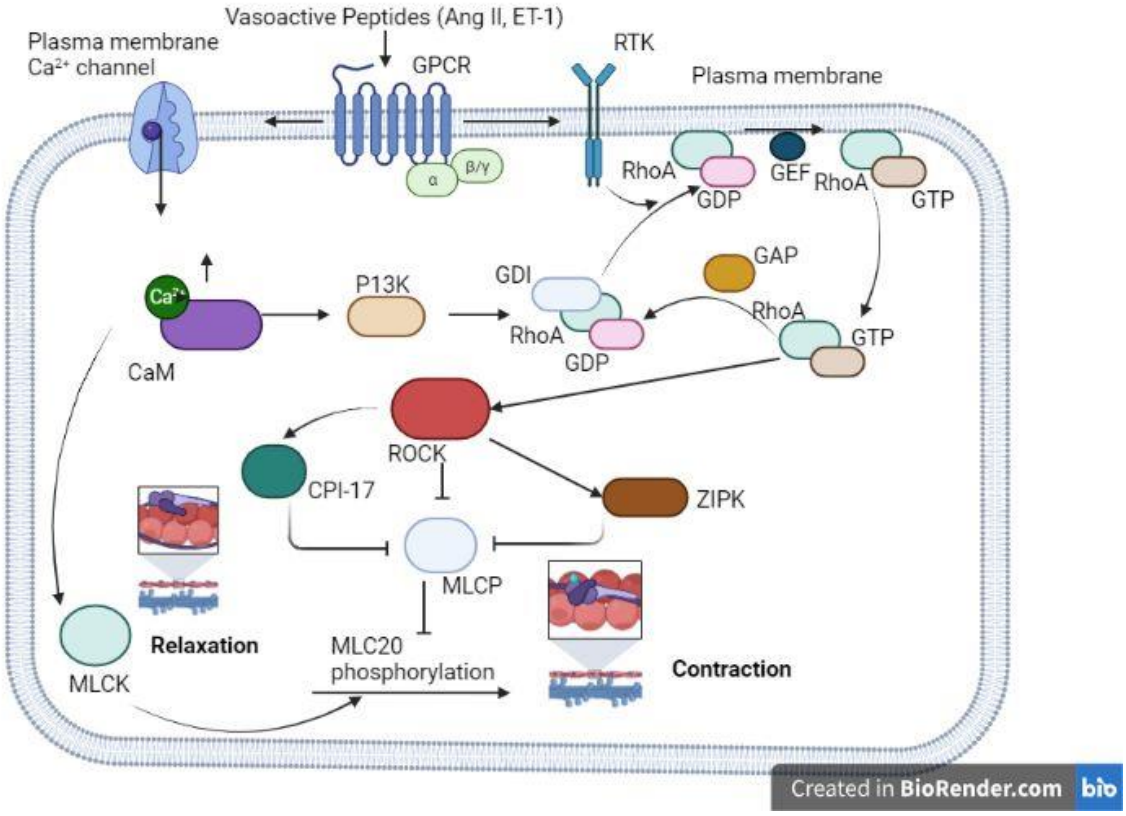

Figure 1-4: Diagrammatic representation of Ca^{2+} independent regulation of VSMC contraction.

Vasoactive agents bind to their respective GPCRs leading to release of RhoA from a guanine nucleotide dissociation inhibitor (GDI). RhoA translocate to the membrane. Mechanisms involving RhoA activation also involve transactivation of receptor tyrosine kinases (RTKs). GEFs promote exchange of Guanosine diphosphate (GDP) to Guanosine triphosphate (GTP), activating the RhoA-ROCK pathway. Activated ROCK renders MLCP inactive by phosphorylation of CPI-17 and/or zipper-interacting protein (ZIPK), facilitating MLC20 phosphorylation and vascular contraction. Increased Ca^{2+} may directly activate ROCK through phosphatidylinositol-4, 5-bisphosphate 3-kinase (PI3K)-dependent pathways.

1.2 Cardiovascular diseases

Cardiovascular disease (CVD) is a broad, umbrella term used to describe all conditions affecting the heart and circulatory system. They are often named after the region of the body they affect, and the major CVDs include coronary heart disease, stroke, heart attack and aortic disease (British et al., 2021). CVD are the leading cause of death worldwide with many lives lost each year from CVDs than from any other cause. In 2008 it was estimated that 17 million out of 57 million annual deaths were a result of CVD with an alarming 80% of deaths occurring in low- and middle-income countries (WHO, 2014). Among these deaths, 85% are because of heart attack and stroke (WHO, 2017, May 17). The cause of heart attacks and strokes are usually the presence of a combination of risk factors, such as tobacco use, unhealthy diet and obesity, physical inactivity and harmful use of alcohol, hypertension, diabetes and hyperlipidaemia (WHO, 2017, May 17).

While the underlying causes of CVD are still unclear, it is considered a non-communicable disease that is associated with both modifiable and non-modifiable risk factors. Non-modifiable risk factors for CVD include age, sex, genetics, family history, race, and ethnicity. However considerable population risk of CVD is the result of nine modifiable traditional risk factors, including smoking, history of hypertension or diabetes, obesity, unhealthy diet, lack of physical activity, excessive dependence on alcohol, raised blood lipids and psychological factors (Gersh et al., 2010). The effects of behavioural risk factors may show up in individuals as raised BP, raised blood glucose, raised blood lipids, overweight and obesity. These “transitional risks factors” can be assessed in primary health care facilities and indicate an increased risk of developing a heart attack, stroke, heart failure and other complications (Gersh et al., 2010).

Termination of tobacco use, reduction of salt in the diet, consuming fruits and vegetables, regular physical activity and avoiding harmful use of alcohol have been shown to reduce the risk of cardiovascular disease. Additionally, drug management of diabetes, hypertension and high blood lipids may be necessary to reduce cardiovascular risk and prevent heart attacks and strokes (Buttar et al., 2005). Health policies that create encouraging atmospheres for making healthy

choices reasonable and accessible are essential for inspiring individuals to adopt and sustain healthy behaviour.

1.2.1 Hypertension as a risk factor for cardiovascular disease

Hypertension is the number one associated risk factor for CVD, stroke and end-stage renal damage (Brozovich et al., 2016; Lim et al., 2012; Lozano et al., 2012). High blood pressure accounts for 9.4 million deaths, more than elevated body mass index (Rust & Ekmekcioglu, 2017), fasting plasma glucose, and total cholesterol (TC) combined (Lim et al., 2012). The prevalence of hypertension is approximately 40 % among adults over the age of 25 years and contributes to 45-50 % of deaths due to heart disease and stroke (Singh et al., 2017). By the year 2008, almost 1 billion people had uncontrolled hypertension globally (World health organization, 2013). The number of adults with hypertension in 2025 is projected to increase by about 60% to a total of 1.56 billion (Kearney et al., 2005). The prevention and control of hypertension represent a crucial global public health strategy in the effort to prevent premature death from CVD (Sudharsanan et al., 2021).

Hypertension is defined as systolic and diastolic blood pressures (SBP/DBP) >140 and 90 mmHg, respectively. Precisely hypertension has two stages, with stage I hypertension accepted as readings of ≥ 160mmHg and ≥ 100 mmHg in systolic and diastolic and stage II for any higher BP levels (Buelt et al., 2021). Moreover, hypertension can also be diagnosed from a single reading if the measurement is 180/110 mm Hg. Although the prevalence of hypertension is high in the general population, only in around 10 % of cases an underlying specific cause can be identified, whereas the remaining 90% have no identifiable cause (Lin et al., 2016). According to the causality, hypertension is classified as primary and secondary both which present with great clinical heterogeneity.

1.2.2 Primary hypertension

Hypertension with unknown cause but with multiple risk factors is known as primary hypertension. Precisely it a multifactorial disease caused by interacting environmental and polygenic factors (Deng, 2007). Primary hypertension is a heterogeneous disorder, with different patients having different causal factors

that lead to high BP. It is driven by several risk factors classified as modifiable and non-modifiable. Modifiable risk factors include obesity, high alcohol and/or salt intake, insulin resistance, low potassium and/or low Ca^{2+} intake while non-modifiable risk factors include sex, age and genetics (Carretero & Oparil, 2000). From a genetic perspective, many single nucleotide polymorphisms (SNPs), gene and epigenetic factors are associated with primary hypertension (Natekar et al., 2014).

1.2.3 Secondary hypertension

Secondary hypertension is elevated BP with an identifiable cause(Rimoldi et al., 2014). It accounts for 10% of hypertension cases due to renovascular hypertension, renal disease, endocrine disorders, and other medical conditions (Lin et al., 2016; Young, 2010). Many cases of endocrine hypertension result from primary aldosteronism through RAAS and is found in as high as 5% of patients with hypertension. Additional conditions that can cause endocrine hypertension are; congenital adrenal hyperplasia, Liddle syndrome, pheochromocytomas, Cushing's syndrome, acromegaly, thyroid diseases, primary hyperparathyroidism and iatrogenic hormone manipulation (Pappachan & Buch, 2017). A diagnosis of endocrine hypertension may be obvious when patients present with typical clinical features of the underlying condition like acromegaly, Cushing syndrome, hyperthyroidism, hypothyroidism and features of virilisation in congenital adrenal hyperplasia (Young, 2010). The role of thyroid hormones (TH), in supporting a healthy CVS has been acknowledged (Razvi et al., 2018) and thyroid disorders contributes 1% of hypertension cases (Rivas et al., 2021).

1.2.4 Genetics of hypertension

Epidemiological studies have improved our understanding of environmental factors in relation to BP regulation, especially with regards to diet and exercise, however the role of genetics has been a challenge to determine (Patel et al., 2017). Systematically acquired data on BP across three generations of the Framingham heart study revealed that higher BP in both grandparents and parents is associated with the risk of the same condition appearing in the third generation. Specifically, a family history of hypertension developed before 55

years of age represents the strongest risk factor for high BP in the offspring, independently of several measured environmental factors. Moreover, twin-and family- based studies have indicated that 30-50% of the variance in BP readings may be heritable, while a list of rare disorders have led to the identification of clear and causal Mendelian mutations (Ehret & Caulfield, 2013). Heritability studies and genome-wide association studies (GWAS) have been used to determine common genetic variants and explore complex diseases such as hypertension (Hoffmann et al., 2017; Warren et al., 2017). More recent studies conducted, bring the total number of variants associated with the risk of hypertension to 280 (Patel et al., 2017). Despite small contribution of each single nucleotide polymorphism (SNP) to systolic and diastolic BP values, their combined cumulative impact is more revealing (Ehret et al., 2011). A study conducted by Warren et al demonstrated that a combination of multiple SNPs in a risk score accounted for a difference in systolic BP values up to 10 mmHg between individuals (Warren et al., 2017). Though GWAS primarily focused on identifying genetic factors through modelling main effects of common SNPs, a focus on modelling gene-environment (GxE) and gene-gene (GxG) interaction may identify additional causal factors in human disease (Manolio et al., 2009). Table 1-1 shows a list of some of genes identified with their physiological function related to primary hypertension.

Data presented in the GWAS and heritability studies emphasize that primary hypertension is a syndrome, not a disease. Thus hypertensive subgroups have been categorised into a traditional four-tiered genetic approach: (i) distant phenotype (hypertension) (ii) intermediate phenotype (salt-sensitive and salt-resistant hypertension) (iii) sub intermediate phenotypes under salt-sensitive hypertension (normal renin and low renin) and (iv) proximate phenotypes (specific genotype-driven hypertensive subgroup) (Agarwal et al., 2005). Of importance is that each genetic subtype of primary hypertension has a substantial endocrine component (secondary hypertension) (Manosroi & Williams, 2019). Many of the mutated genes identified correspond to rare variants which are associated with Na^+ re-absorption (Munroe et al., 2013). Various mechanisms have been proposed to underlie salt-sensitive hypertension. Renal dysfunction and/or dysfunction of an endocrine system, involving the RAAS system is the

most common cause of hypertension (Chamarthi et al., 2010; Fisher et al., 1999).

Table 1-1: Genes identified with their associated physiological functions related to essential hypertension.

Genes	Pathway related to primary hypertension
NOS3	RAAS pathway
SH2B3	Endothelial cell function
AGT	Renal electrolyte balance
NPPA	Control of extracellular fluid volume and electrolyte homeostasis
NPPB	Involved in vasorelaxation and inhibition of renin and aldosterone.
NPR3	Involved with regulating blood pressure, pulmonary hypertension, and cardiac function.
UMOD	Constitutive inhibitor of Ca^{2+} crystallization in renal fluids
CYP17A1	Involved with steroid/aldosterone synthesis. Enzyme dysfunction leads to increased levels of mineralocorticoid activating hormones.
ATP2B1	Codes for enzymes that have a critical role in intracellular Ca^{2+} homeostasis.
CACNB2	Encodes for a subunit of a voltage-dependent Ca^{2+} channel protein that is a member of the voltage-gated Ca^{2+} channel superfamily.
SLC24A4	Encodes for a member of the potassium-dependent sodium/Ca^{2+} exchanger protein family.
EDN3	Endothelin-3 involved in vasoconstriction
CYP11B2	Enzymatic defects result in decreased aldosterone and increased salt-washing
TNNT3	Involved in Ca^{2+}-induced muscle contraction

Adapted from (Natekar et al., 2014)

1.2.5 Transcriptomics

Over the last 30 years, CVDs have remained a leading cause of death worldwide, however, there has been a notable decrease in both age-standardized death rates and age-standardized, disability-adjusted life years per 100,000 population (Zhang et al., 2023). The above-mentioned improvements were a largely due to understanding molecular and cellular processes underlying CVD. The polygenic nature of primary hypertension in humans presents a challenge to the identification of genes involved in the genesis of the disease (Ikawa et al., 2019). The advent of high-throughput techniques (e.g., next-generation sequencing, proteomic arrays, and high-resolution mass spectrometry) has revolutionized biomedical research and widened the scope for clinical research. It is now possible to uncover the multiple signalling pathways responsible for both physiological and pathological processes, and to pinpoint the molecular culprits of human disease (Kutikhin et al., 2018). RNA sequencing (RNA-Seq) has been in existence for more than a decade and it has become a useful tool in molecular biology that is shaping our understanding of the genomic function in humans and animal models (Dwinell et al., 2009; Emrich et al., 2007; Gonzaga-Jauregui et al., 2012; Lister et al., 2008). It has the ability to highlight all RNA populations in a cell including long non-coding RNAs (lncRNA), which are implicated in many cellular functions and diseases including regulation of gene expression (Wang & Chang, 2011). Table 1-2 shows the transcript biotype detected in humans and rats.

The transcriptome refers to all of the RNA transcripts in a cell or tissue (Lowe et al., 2017) while transcriptomics is the study of transcriptome and is involved in the function of cells, tissues, or organisms, across a wide range of biological conditions. The relationship between the transcriptome and the genome suggests that the information of an organism is stored in the DNA (the genome) and expressed by RNA (the transcriptome) (Khodadadian et al., 2020). The focus of the transcriptomics is to discover how transcripts of a cell, tissue, or living organism are influenced by disease or environmental factors (such as drugs, hormones, and nutritional elements such as iodine). Advancement in cardiovascular research has improved our understanding of BP and highlighted its complexity and pathophysiology, where genetic and environmental factors combine and ultimately form a phenotype (Patel et al., 2017). While

epidemiological studies have improved our understanding of environmental factors in relation to BP, especially with regards to diet and exercise, it does not address the changes that can occur in transcriptomics in relation to nutritional dietary elements. Comparison of the transcriptomics profiles with stratification based on the presence or absence of CVD would be a hypothesis-free approach that could reveal new pathways underlying disease processes.

1.2.6 Small resistance arteries in hypertension

Small resistance arteries play an important role in pathophysiology of many diseases including hypertension and its outcomes (Bohlen, 1986; Christensen & Mulvany, 2001; Rietzschel et al., 2008; Schiffrin, 1997). The underlying cause of increased peripheral resistance is a decrease in lumen diameter. According to Poiseuille's law, resistance varies inversely with the fourth power of the blood vessel radius, so that a small decrease in the lumen markedly increases resistance (Intengan & Schiffrin, 2000). The adverse effects of hypertension are mediated by changes in the structure and function of the arterial wall(Thom, 1997). Functional changes, in the form of altered vascular reactivity occur at the earliest stages of hypertension and contribute to the development and reinforcement of the condition (Wilson et al., 2019). Enhanced vasoconstriction is often cited as a mechanism for increased vascular tone in hypertension in both human vessels and in experimental hypertension (Lüscher & Vanhoutte, 1986; Mulvany et al., 1978). Nonetheless the precise mechanism contributing to altered vascular reactivity are not well understood. Endothelial dysfunction is, suggested to be responsible for dysfunctional vascular responses (increased contractile and decreased dilator responses), which accompany and aggravate chronic elevations in BP (Tang et al., 2007; Wang et al., 1995). Endothelial dysfunction is characterized by an imbalance between the release of endothelium-dependent relaxing (EDRF) and contracting (EDCF) factors. The production of EDCF is prominent in arteries of mature spontaneously hypertensive rats (SHR), but not in their age-matched normotensive control strain, Wistar–Kyoto rats (WKY) (Lüscher & Vanhoutte, 1986). Endothelial dysfunction is accelerated by ageing, diet, obesity, diabetes and hypertension, and the occurrence of EDCF-mediated contractions can be observed in arteries from aging normotensive and diabetic rats, and in humans with essential hypertension (De Vriese et al., 2000).

Table 1-2: Common transcript biotypes detected in RNA-Seq studies, and the number annotated in human and rat.

Transcript biotype	Human (GRCh38.p14 (Genome Reference Consortium Human Build 38), INSDC Assembly GCA_000001405.29, Dec 2013)	Rat (mRatBN7.2 (Genome Reference Consortium Rat Build 7.2), INSDC Assembly GCA_015227675.2, Nov 2020)
Protein coding	19,831	23,141
Non-coding	25,959	6,503
Small non-coding	4,864	3,952
Long noncoding	18,874	2,524
Misc. non-coding	2,221	27
Pseudogenes	15,239	918
All transcripts	252,894	54,993

Human and rats have approximately the same number of protein coding transcripts however there is under representation of none coding transcripts in rats mainly because they are not documented yet.

1.2.7 Reactive oxygen species and blood pressure

Reactive oxygen species (ROS) are a class of unstable molecules that contain O_2 or nitrogen and can easily react with other molecules in the cell and cause damage to the basic building blocks of the cell including DNA, protein and lipids. ROS or reactive nitrogen species (RNS) such as superoxide (O_2^-), hydroxyl radical (HO), hydrogen peroxide (H_2O_2), peroxynitrite ($ONOO^-$), nitrogen oxide (NO), and hypochlorous acid (HOCl) are products of normal metabolic pathways and are scavenged by antioxidant, however, in excess amounts, they can exert harmful reactions (Baradaran et al., 2014). In all biological systems there should be a balance between ROS and RNS formation and antioxidant activity (Rafieian-Kopaei et al., 2013). The human body has integrated antioxidant systems, which include enzymatic and nonenzymatic antioxidants that are usually effective in blocking harmful effects of ROS. Enzymatic antioxidants include superoxide dismutase (SOD) catalase, reduced glutathione (GSH), oxygenase-1 and redox proteins such as thioredoxins while nonenzymatic antioxidants include low molecular weight compounds such as vitamin C and E, ß carotene, uric acid and GSH (Birben et al., 2012). Several animal studies have supported the hypothesis that increased BP is associated with increase oxidative stress (Dobrian et al., 2004; Fukui et al., 1997; Wu et al., 2001). Oxidative stress promotes VSMC proliferation, hypertrophy, and collagen deposition, leading to thickening of the vascular media and narrowing of the vascular lumen. In addition, increased oxidative stress may damage the endothelium and impair endothelium-dependent vascular relaxation and increases vascular contractile activity (McIntyre et al., 1999). Observation from epidemiological studies have suggested that a higher circulating concentration of antioxidants may reduce BP and cardiovascular complications (Buijsse et al., 2015; Jayedi et al., 2019; Pfister et al., 2011). Despite the suggested association between antioxidants and CVD, several large randomised controlled trials have failed to corroborate the benefits of antioxidants in the prevention of CVD (Martín-Calvo & Martínez-González, 2017; Mirmiran et al., 2022; Myung et al., 2013; Vardi et al., 2013). However, the potential pro-oxidant activity of antioxidants is a phenomenon which should not be ignored (Ardalan & Rafieian-Kopaei, 2014).

1.2.8 Vascular smooth muscle cells and enhanced contractility in hypertension

VSMCs are specialised cells responsible for maintaining vascular homeostasis through active contraction and relaxation in healthy, blood vessels. They display considerable plasticity in the phenotype of blood vessels. Under normal circumstances, they express genes and proteins important for contraction/dilation, which allows them to control systemic and local pressure through the regulation of vascular tone (Coll-Bonfill et al., 2016). However, during the life span of an individual or in the early stage of hypertension, VSMC in conduit and resistance arteries may undergo a transition from a contractile phenotype to a more synthetic phenotype, including the production of both contractile and secreted proteins (Brozovich et al., 2016; Delbosc et al., 2008). As mentioned previously the primary mechanisms regulating the contractile state of VSMC are changes in cytosolic Ca^{2+} concentration. However, the VSMC intracellular Ca^{2+}concentration not only determines the contractile state, but also affects the activity of several Ca^{2+}dependent transcription factors and thereby determines VSMC phenotype (Brozovich et al., 2016).

In disease states such as hypertension, many of the mechanisms regulating intracellular Ca^{2+} homeostasis are perturbed, with experimental models and hypertensive patients demonstrating abnormal vascular Ca^{2+} handling and high intracellular Ca^{2+} (Touyz et al., 2018).

1.2.9 Clinical management of hypertension

Early treatment of hypertension is critical since it can lead to cerebral, cardiac, and renal complications. Available treatment regimens include antihypertensive drug treatment in addition to lifestyle modifications to adults of any age with persistent hypertension. The first line of drugs to treat essential hypertension include Ca^{2+} channel blockers, ACE inhibitors, angiotensin receptor blockers (ARBs), and thiazide diuretics. Other antihypertensive drugs include α blockers and ß blockers. Ca^{2+}-channel blockers (e.g., nifedipine) bind to L-type Ca^{2+} channels on VSMC, cardiac myocytes and cardiac nodal tissue thereby blocking Ca^{2+} entry into cells. These cause VSMC relaxation, decreased myocardial force generation, decreased heart rate and decreased conduction velocity (Lowenthal

et al., 1984). ACE inhibitors (e.g., benazepril) act by inhibiting the conversion of angiotensin I to angiotensin II thereby decreasing the vasoconstrictor effect of angiotensin II and the aldosterone production secondary to angiotensin II stimulation (Hurst et al., 2023). ARBs (e.g., losartan) have very similar effects to ACE inhibitors; however, their mechanism of action differs from ACE inhibitors. ARBs are receptor antagonists that block type 1 angiotensin II receptors on blood vessels and other tissues, such as the heart (Tamargo & Tamargo, 2017). Diuretics (e.g., hydrochlorothiazide) act as indirect vasodilators by depleting salt and water not only with the intravascular compartment but within the intramural portion of the arteriole, thereby diminishing its responsiveness to catecholamine and angiotensin II stimulation. ß-adrenergic blocking drugs act through a variety of mechanisms by either decreasing CO, decreasing renin release, inhibiting prejunctional release of norepinephrine or through central mechanisms (Lowenthal et al., 1984).

1.2.10 Dietary approaches to controlling hypertension.

Dietary approaches and recommendations have focused on scientific evidence examining foods consumed in combinations, or the overall dietary pattern, and its relationship with BP. A strong emphasis on dietary patterns has been endorsed by the Dietary Guidelines for Americans (Ozemek et al., 2018). Among the dietary patterns studied, the Dietary Approaches to Stop Hypertension (DASH) diet has been consistently endorsed by health organisations as an effective diet for controlling BP. Its development was influenced by observational studies highlighting the relation between low prevalence rates of hypertension and CVD in those who avoid eating animal products, where diets are low in saturated fat, high in polyunsaturated fat, and low in cholesterol (Sacks et al., 1974). Moreover, the adoption of a vegetable rich diet and devoid or limited consumption of red meat by normotensive or hypertensive individuals previously incorporating red meat frequently into their diet, has been shown to lower BP (Rouse et al., 1983). Dietary practices in countries along or near the Mediterranean are frequently recognised as being heart-healthy, and prolonging life free from CVD. Foods generally consumed in these areas include fruits, vegetables, breads, potatoes, beans, nuts, cheese, yoghurt, fish, and lean poultry. The mechanism by which these food products lower BP is not known. Nevertheless, it is important to note that the majority of the listed food items

are primary sources of iodine, so their benefits might be directly linked with this microelement.

1.3 Biological significance of iodine

1.3.1 Sources of iodine and recommended daily intakes.

Iodine is an essential microelement naturally obtained from food sources, particularly fish and crustaceans of marine origin, seaweeds, and sea vegetables such as kelp (Smyth, 2021). However, in many parts of the world, dairy products, including milk, cheese, yogurt, and eggs are the main source, especially where seafood is expensive or unavailable (Organisation, 2007). Some food sources are directly fortified with iodine (e.g., salt, infant formulas, and some meal replacements) (Santos et al., 2019). Iodine-supplemented animal feeds are an important contributor to the iodine content of milk (Castro et al., 2012) and eggs (Rottger et al., 2012). Furthermore, seaweed and seaweed-based food additives can contribute iodine to some foods (Bouga & Combet, 2015; Teas et al., 2004). Table 1-3 summaries iodine concentration (mg/kg) in 3 main classes of edible seaweeds, fish whole egg and milk. Iodization of table salt with potassium salts (iodides and iodates) at a level of 20-40 mg/kg provides a useful method of achieving population iodine sufficiency (Zimmermann & Andersson, 2012). However, the use of iodized table salt is only mandatory in some countries and almost absent in others such as the United Kingdom (UK) and Ireland (Bath et al., 2016; Lazarus & Smyth, 2008). While there are some discrepancies regarding optimal daily iodine intake between different regulatory bodies, there is an agreement that the level required by the body is relatively small. The daily recommended iodine intake for school children is 120 µg, and for adults is 150 µg (Organization, 2007). The World health organization (WHO) recommends 250 µg for pregnant women to account for additional needs due to increased maternal TH production and iodine uptake by the fetus, placenta, and amniotic fluid (Andersson et al., 2007; Scientific Opinion on Dietary Reference Values for iodine, 2014), however, the increase is not implemented by all countries in their recommendations. Table 1-4 summarises the recommended dietary allowances, recommended nutrient intake, and adequate iodine intake for men and women per age group as well as in pregnant women. The US Institute of Medicine, WHO, the United Nations Children's Fund (UNICEF), and

International Council for the Control of Iodine Deficiency Disorders (ICCIDD) state a tolerable upper level of 1,100 µg per day in adults (Cai et al., 2015) while the European Commission/Scientific Committee (EC/SCF) recommends an upper level of 600 µg per day in adults (Organization, 2007).

1.3.2 Measurement of iodine intakes and world iodine status

In healthy, iodine replete adults >90% of dietary iodine is absorbed from the stomach and upper small intestine by the sodium iodide symporter (NIS), a plasma membrane glycoprotein (Zimmermann et al., 2008) , and >90% is excreted within 24-48 hours(Rohner et al., 2014; Zimmermann & Andersson, 2012). Excretion of iodine in urine reflects recent iodine intake. Circulating iodide is cleared primarily by the thyroid and kidney, where it is used for TH synthesis or excreted, respectively. Healthy adults store 15-20 mg of iodine, with about 70%-80% located in the thyroid (Ahad & Ganie, 2010). In normal physiology, plasma iodine has a half-life of approximately 10 hours, yet this is reduced if the thyroid is overactive, as in iodine deficiency or hyperthyroidism (Chung, 2014).

Measurement of the urinary iodine concentration (UIC) is the WHO gold standard for the assessment of a population's iodine status (Organization, 2007). The UIC is conventionally expressed as a population median in µg/L (Organisation, 2007). Although spot urine UIC is useful for estimating the iodine status of a population, the low and high ends of the distribution must be interpreted with caution to avoid overestimating the respective prevalence of iodine deficiency and iodine excess (Pehrsson et al., 2016). Assessment of individual iodine status using spot urine samples is not recommended due to intradiurnal variations in intake (Vejbjerg et al., 2009). Urinary iodine excretion (UIE) in 24-hr collections is regarded as a better method, because, unlike spot urines, urinary iodine is determined from pooled 24-hr urine samples which might reflect an individual's true daily excretion (König et al., 2011). However, day-to-day, and seasonal variations in iodine uptake and kidney clearance are likely. Several methods such as colorimetric spectrophotometric procedure, the iodine specific electrode, neutron activation analysis and mass-spectrometry are used to determine iodine content in urine (Benotti et al., 1965; World Health Organization. & International Atomic Energy Agency., 1989; Yabu et al., 1986). The colorimetry

(spectrometry) procedure which is based on the Sandell-Kolthoff reaction, in which iodide acts as a catalyst in the reduction of ceric ammonium sulfate (yellow colour) to the cerous form (colourless) in the presence of arsenious acid is the most commonly used method (Benotti et al., 1965).

Table 1-5 shows cut-off values of iodine status for different populations. A UIC of 100 µg/L corresponds to about 150 µg iodine intake per day in adults. UIC below 100 µg/L in a population are associated with increases in median thyroid size and elevated serum thyroid stimulating hormone (TSH) and thyroglobulin (Tg) levels (Dunn et al., 1998). In euthyroid populations with a sufficient iodine intake, median serum Tg is normally <13 µg/L, though reference ranges are assay specific (Ma & Skeaff, 2014). TSH is routinely measured in many countries as part of neonatal congenital hypothyroidism screening programs, where data maybe be used to assess the iodine status of a population: a prevalence of >3% of TSH values >5 mIU/L in new-borns indicates iodine deficiency in a population (Organisation, 2007). TSH screening is also used routinely as a sensitive marker for hypo and hyperthyroidism and can be used as a diagnostic tool (alone or in conjunction with other tests) for thyrotoxicosis (Franklyn & Boelaert, 2012).

Table 1-3: Iodine concentration (mg/kg) in 3 main classes of edible seaweeds, fish whole egg and milk.

Food items	Average iodine content (mg/kg)
Seaweeds	
Alaria esculenta (Kelp)	220
Palmaria palmata (red algae)	260
Laminaria digitata (Kombu)	3100
Fish	
Melanogrammus aeglefinus (Haddock)	427.4
Mugil cephalus (Grey mullet)	52.2
Scomber scombrus (Atlantic mackerel)	34.5
Whole egg	0.21
Milk	0.20

Seaweeds contains the highest amount of iodine (mg/kg) followed by fish while whole egg and milk contain the lowest amount of iodine.(Maehre et al., 2014; Réhault-Godbert et al., 2019; Sprague et al., 2021; Trøan et al., 2015).

Table 1-4: Recommendations for iodine intake (µg/day) by age or population group

Age or population group[a]	U.S. Institute of Medicine	Age or population group[c]	World Health Organization
Infants 0–12 months [b]	110-130	Children 0-5 years	90
Children 1-8 years	90	Children 6-12 years	120
Children 9-13 years	120		
Adults n 9-13 years	150	Adults >12 years	150
Pregnancy	220	Pregnancy	250
Lactation	290	Lactation	250

[a] Recommended Daily Allowance and [b] Adequate iodine intake by the U.S Institute of medicine and [c] Recommended Nutrient Intake by the WHO in men and women per age group as well as in pregnant and lactating women.

.

Table 1-5: Cut-off for epidemiological classification of population iodine nutrition status based on median urinary iodine concentration.

Population group	Median UIC (µg/L)	Iodine intake	Iodine status
Children less than 2 years old	< 100	Insufficient	
	≥100	Adequate	
Pregnant women	< 150	Insufficient	
	150-249	Adequate	
	250-499	More than adequate	
	≥ 500	Excessive	
Lactating women	< 100	Insufficient	
	≥ 100	Adequate	
	< 20	Insufficient	Severe iodine deficiency
	20-49	Insufficient	Moderate iodine deficiency
	50-99	Insufficient	Mild iodine deficiency
	100-199	Adequate	Optimal iodine nutrition
School-aged children (6-12 years) and other adults	200-299	More than Adequate	Risk of iodide-induced hyperthyroidism within 5-10 years following introduction of iodised salt in susceptible groups
	≥ 300	Excessive	Risk of adverse health consequences (iodine induced hyperthyroidism, auto-immune thyroid diseases)

Adapted from (Andersson et al., 2007)

1.3.3 Iodine deficiency is a global health problem.

Millions of people have been adversely affected by iodine deficiency which leads to wide range of devastating health consequences collectively known as iodine deficiency disorders (IDD). At a global scale, approximately 2 billion people suffer from iodine deficiency of which 50 million present with clinical manifestations (Lazarus, 2015). In 1995, WHO and UNICEF launched a universal salt iodization as a direct action designed to prevent IDD (Al-Dakheel et al., 2018). Nevertheless, a quarter of a century later IDD remains a serious worldwide public health concern (Biban & Lichiardopol, 2017). The Iodine Global Network (IGN) compiles data from UIC studies conducted in 194 WHO member states and continually monitors global iodine status (Network, 2020). The number of countries with adequate iodine intake nearly doubled from 67 in 2003 to 118 in 2020. However, 19% of countries remain deficient, while 10% have excessive intakes, either due to excess groundwater iodine or over-iodized salt (Zimmermann & Andersson, 2021). Figure 1-5 shows the global iodine intake distribution based on UIC of school aged children. Some of the dietary iodine deficiency findings may, at first sight, seem unexpected. The data shows the populations of the pacific islands, Haiti, and Vanuatu for example, as having insufficient iodine dietary intake (mUIC<100µg/L). As island populations with a traditional fish diet, it would have been expected that their iodine intake would be optimal. However, in 2010 WHO reported that the Pacific Islands are facing serious health problems including IDD, with the islanders experiencing the consequences of replacing their traditional fish-based diet with imported, processed foods ("Pacific islanders pay heavy price for abandoning traditional diet," 2010). The data also shows countries such as Norway, Finland and Germany as having insufficient dietary iodine. The causes for this are less obvious. Inadequate iodine intake in some countries may be linked to low iodine content of the soil and consequently of the consumed food or low consumption of sea food in addition to failure of reinforcement of salt iodization.

Furthermore, restrictive diets may also play a role. For example, a study conducted by Krajcovicova-Kudlackova et al, indicated that around 25% of vegetarians and 80% of vegans may be iodine deficient compared to 9% in persons on a mixed diet (Krajcovicová-Kudlácková et al., 2003). This may be partly because of the disproportionate consumption of foods known as goitrogens

such as cruciferous vegetables and soya products which may affect iodine uptake and utilisation. Moreover, Bath et al have pointed to a change in milk/dairy consumption, with some groups drinking less milk, as a possible cause of lower iodine intakes and iodine deficiency (Bath et al., 2017). Bath et al., reports that organic milk has grown in popularity but has less iodine than conventional milk (study results indicate over 40% less) and he notes that milk alternatives such as soya, almond, coconut, oat drinks are not necessarily iodine fortified. Individuals who consume them in place of conventional milk may therefore be at risk of iodine deficiency (Bath et al., 2012). On the other hand, low iodine consumption may be due to the recent focus on countries trying to reduce dietary salt intake to tackle hypertension.

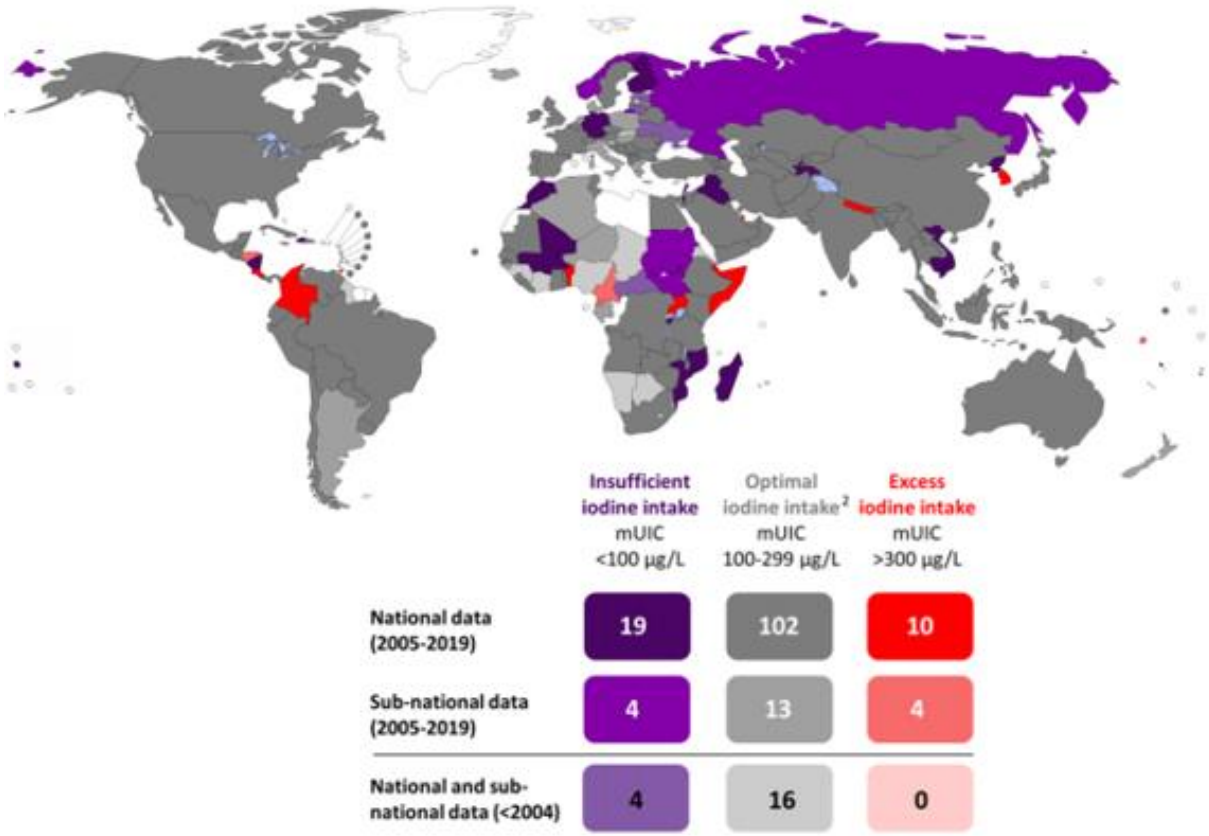

Figure 1-5: Global iodine intake distribution 2020 based on school aged children.

Purple shading indicates iodine deficient countries (mUIC < 100µg/L), grey shading indicates optimal iodine intake (mUIC 100-299µg/L) and red shading indicates excess iodine intake (mUIC > 300µg/L). Adapted from (Network, 2020)

1.3.4 Iodine and thyroid hormone synthesis

As already mentioned, total iodine content of the body is estimated at 15-20 mg with 70-80% found in the thyroid gland (Chung, 2014). Iodine is a precursor for TH. Production of TH begins with active iodide accumulation in the thyroid follicular cells mediated by NIS across a concentration gradient 20-50 time that of plasma by active transport (Dai et al., 1996; Zimmermann, 2009). NIS is a member of solute carrier family 5A and has been designated as SLC5a5 by the Gene Nomenclature Committee, according to the Human Genome Organization (Riesco-Eizaguirre et al., 2021). Accumulation of iodide in the thyroid is regulated by TSH, which is secreted from the pituitary gland in response to changes in circulating TH, through a negative feedback mechanism involving the hypothalamic-pituitary-thyroid (HPT) axis (Farebrother et al., 2019). TSH stimulation of TSH receptor (TSH-R) activates adenylate cyclase which generates cyclic AMP (cAMP) (Figure 1-6). Protein kinase A phosphorylation causes an increase in the activity of SLC5a5-mediated co-transport of two Na^+ and one iodide ion, driven by the transmembrane Na^+ gradient generated by the Na^+/K^+ ATPase pump (Spitzweg et al., 2001). Once taken up into the thyroid follicular cells, iodide is shuttled through pendrin (SLC26a4) into the thyroid colloid/lumen (Royaux et al., 2000). After entering the thyroid colloid/lumen, iodide is oxidized to iodine and bound to the tyrosine residues of Tg by the haem-dependent thyroid peroxidase (TPO) in the presence of an hydrogen peroxide (H_2O_2) generating system (Combet, 2017). H_2O_2 is formed from the oxidation of nicotinamide adenine dinucleotide phosphate by a thyroidal nicotinamide adenine dinucleotide phosphate oxidase (Li & Carayanniotis, 2007). The major iodinated Tg-derived product of thyroid peroxidase is thyroxine (T4), whereby Tg is iodinated at four sites. A minor but significant component is triiodothyronine (T3), in which Tg is iodinated at three sites (Carvalho & Dupuy, 2017; Dunn & Dunn, 1999), such that the human thyroid gland secretes T4:T3 in a ratio of 4-5:1.

T4 is more stable than T3 in the circulation, where the half-life of T4 is 7.5 and 6.2 days in hypothyroid and euthyroid individuals respectively. In contrast, T3 has a half-life of approximately 1.4 and 1.0 days in hypothyroid and euthyroid people respectively (Nicoloff et al., 1972). T3 is the most potent TH and T4 is converted into T3 by a process called (mono-) deiodination, which occurs

predominately in extrathyroidal tissues(Bianco & Kim, 2006). Deiodination is performed by type 1, type 2, and type 3 iodothyronine deiodinases (D1, D2, D3) (Darras & Van Herck, 2012). D1 is predominantly dominant in liver, kidney, and thyroid while D2 is dominant is heart brain and thyroid (Figure 1-7). While D1 and D2 converts T4 to T3, D3 coverts T4 to reverse T3 (rT3) in the placenta, skin, and liver. Deiodinases are selenocysteine-containing proteins and therefore deficiencies of selenium and iron can act together with iodine deficiency to impair thyroid metabolism and moderate the response to prophylactic iodine (Carvalho & Dupuy, 2017; Dunn & Dunn, 1999; Pearce et al., 2004).

1.3.4.1 Regulation of iodine uptake

Complex mechanisms control SLC5a5 expression in the thyroid and extra-thyroidal tissues (Kogai & Brent, 2012). TSH is the primary regulator of SLC5a5 activity in the thyroid at both the transcriptional and post-transcriptional level (Kogai et al., 1997; Levy et al., 1997; Weiss et al., 1984), increasing iodide uptake. TSH upregulates SLC5a5 mRNA and protein expression in vivo and in vitro (Bizhanova & Kopp, 2009). The elevation of endogenous cAMP by TSH stimulation induces SLC5a5 transcription by stimulating several signal pathways of cis-regulatory elements in SLC5a5 locus (Kogai et al., 2006), including the NIS upstream enhancer (NUE), the most potent TSH-responsive enhancer contained in the SLC5a5 promoter (Ohno et al., 1999; Taki et al., 2002). Another regulator of the SLC5a5 function is iodide itself. Its main effects are to decrease the response to TSH, to acutely inhibit its oxidation(Burns et al., 2013). Wolff & Chaikoff showed that when iodide reaches a critical high concentration in the plasma, TH biosynthesis decreases (the Wolff-Chaikoff effect) (Wolff & Chaikoff, 1948). Excess iodide may also have a deleterious effect on the thyroid by modifying the stability of SLC5a5 mRNA and increasing the production of ROS (Serrano-Nascimento et al., 2010). Nevertheless, there is protection from this acute Wolff-Chaikoff effect that restores normal TH biosynthesis even in the continued presence of high plasma iodide concentrations (Braverman & Ingbar, 1963). This protection is termed the escape phenomenon and occurs due to the downregulation of SLC5a5 (Uyttersprot et al., 1997).

Another regulator of SLC5a5 is valosin containing protein (VCP) which is involved in the extraction of unfolded or misfolded proteins from the endoplasmic

reticulum and can unfold polyubiquitinated proteins to facilitate their degradation by proteasomes (Bastola et al., 2016; Fletcher et al., 2020).

1.3.4.2 Regulation of thyroid hormone synthesis

It is important that T3 and T4 levels are maintained at optimum levels. The HPT axis regulates the release of TSH and hence T3 and T4 levels. The secretion of thyroid releasing hormone (TRH) by the hypothalamus stimulates thyrotrophs in the anterior pituitary to secrete TSH (Razvi et al., 2019). The secretion of TSH stimulates the thyroid follicular cells to release about 80% T4 and 20% T3. As discussed earlier T4 can be converted to T3 through the process of deiodination (Eghtedari & Correa, 2020). T4 and T3 can then exert negative feedback on TSH levels, with high levels of T3/T4 decreasing TSH and low levels of T3/T4 increasing TSH secretion from the anterior pituitary. T3 is the predominant inhibitor of TSH secretion. Because TSH secretion is so sensitive to minor changes in serum-free T4 through this negative feedback loop, abnormal TSH levels are detected earlier than those of free T4 in hypothyroidism and hyperthyroidism. There is a log-linear relationship between T3/T4 and TSH with minor changes in TH resulting in major changes in TSH (Eghtedari & Correa, 2020). Figure 1-8 gives a diagrammatic summary on regulation of TH biosynthesis.

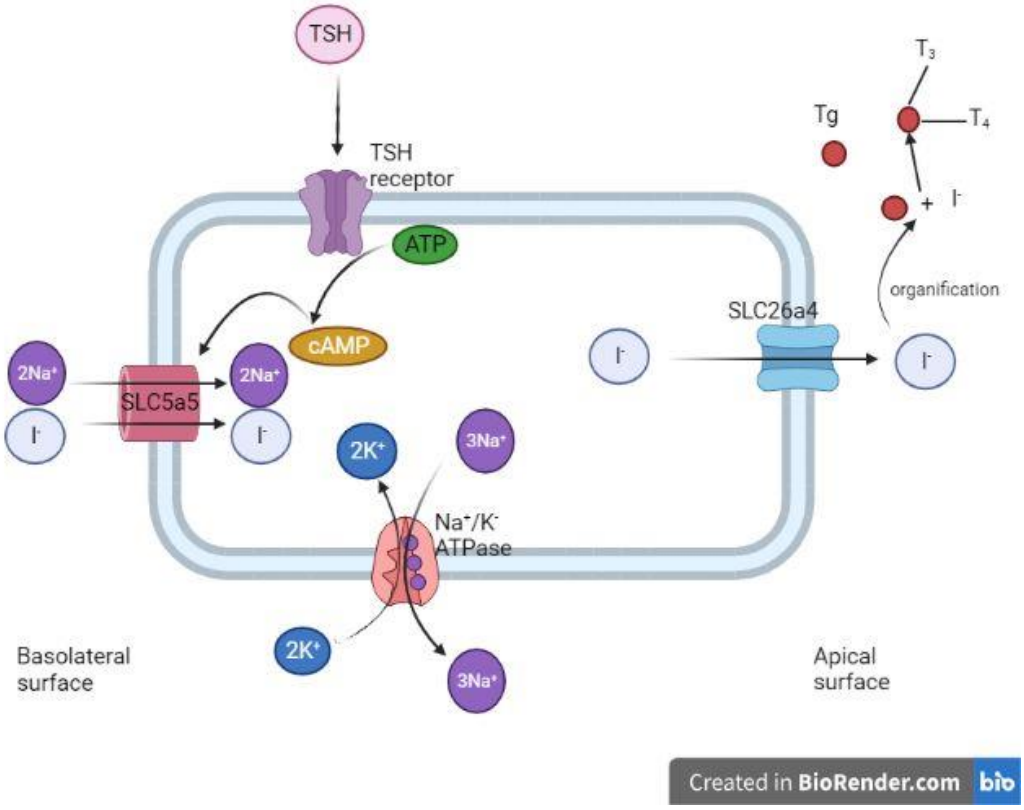

Figure 1-6: Regulation and transport of iodide in the thyroid gland.

The sodium iodide symporter SLC5a5 functions at the basolateral surface, to transfer iodide into the cell. Although several different hormones and molecules help regulate the SLC5a5 expression, thyroid-stimulating hormone (TSH) is the main regulator of the symporter. TSH binding to its receptor leads to increased intracellular cAMP concentrations that in turn stimulate the SLC5a5. SLC5a5 utilizes the Na^+ gradient to symport I^-, driven by the Na^+/K^+ ATPase. The efflux of iodide from the apical membrane to the follicular lumen is driven by SLC26a4. Iodide organification within the thyroid follicular lumen generates iodinated tyrosine residues with the thyroglobulin (Tg) backbone. These are then released as active TH, T3 and T4.

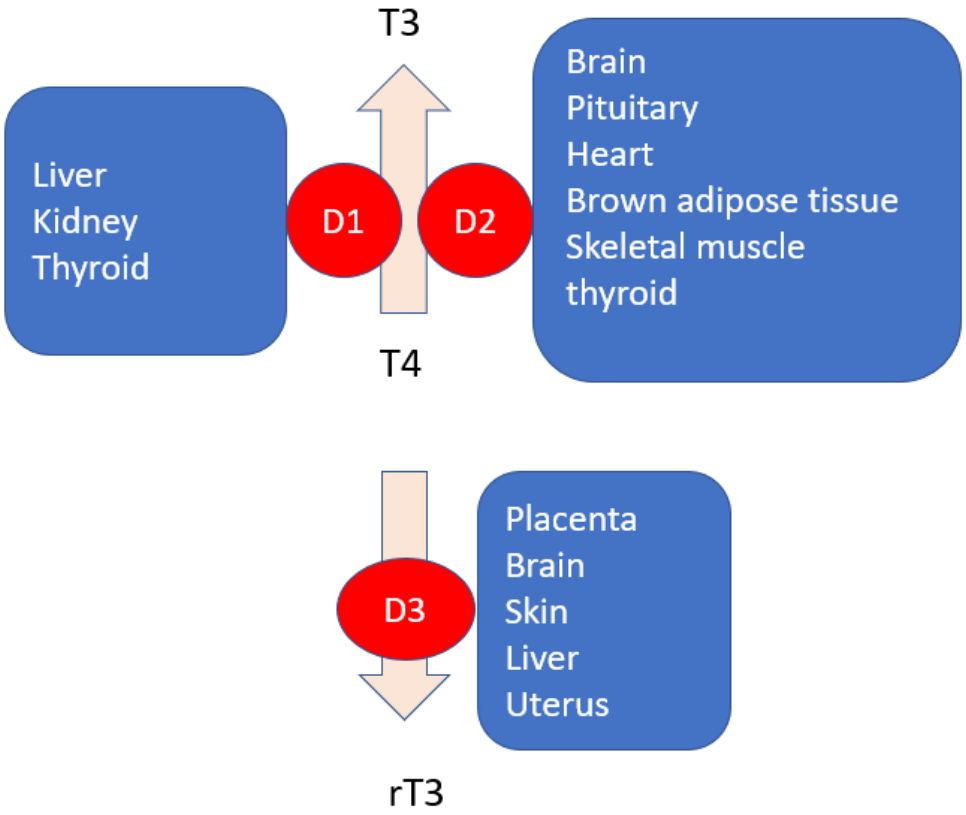

Figure 1-7: Pathways of iodothyronine deiodination and tissue distribution.

T4 can be converted to the active form of thyroid hormone, T3, by removal of an outer ring iodine. This reaction is catalyzed by the deiodinase isozymes, D1, type I 5′ iodothyronine deiodinase, and D2, type II 5′ iodothyronine deiodinase. The tissue distribution of D1 and D2 enzymes is shown. D3 deactivates T4 to reverse T3 (rT3)(Milanesi. & Brent., 2016)**.**

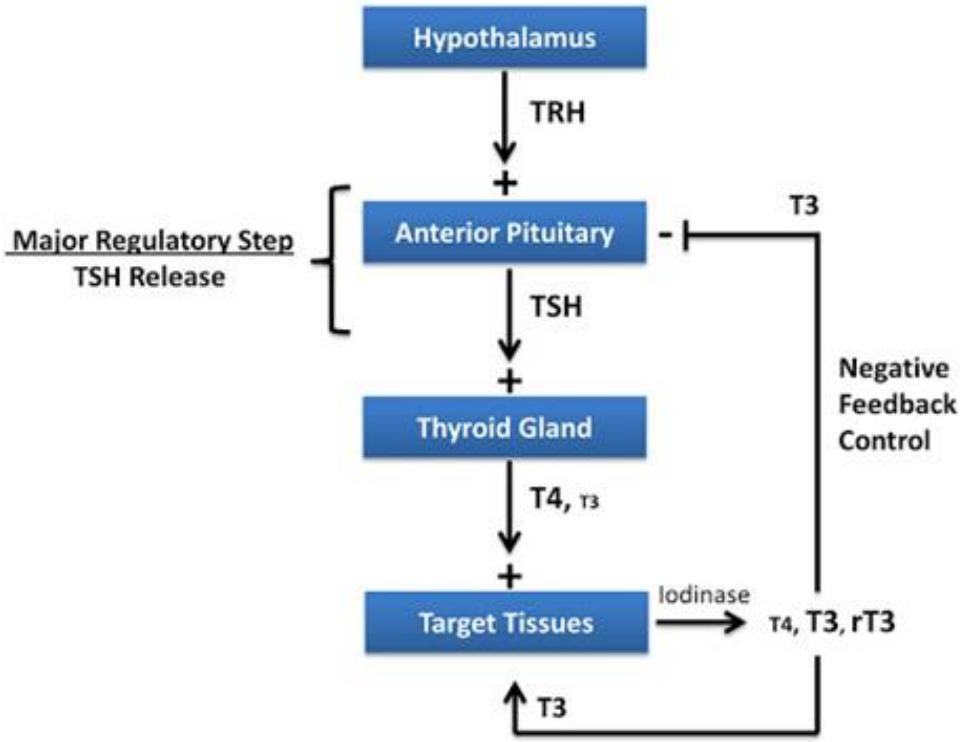

Figure 1-8: Regulation of thyroid hormone by the hypothalamus.

Thyroid hormones T4 and T3 are regulated through a negative feedback loop of the hypothalamic pituitary axis (HPA). The primary point of regulation for this axis occurs at the step of TSH release from the anterior pituitary. The primary factor which stimulates anterior pituitary TSH release is hypothalamic TRH. Negative feedback control is achieved when free, unbound T3 acts on the anterior pituitary to reduce the release of TSH secretion.

1.3.5 Iodine and thyroid health

The health status of the thyroid is determined through thyroid function test in plasma or serum. Levels of TSH, free thyroxine (fT4) and free triiodothyronine (fT3) are easily measurable using commercially available kits. Under normal physiological conditions, plasma concentrations of TSH, fT4 and fT3 are 0.38-5.33 mU/L, 7.9-14.4 pmol/L and 3.8-6.0 pmol/L respectively in humans (NHS, 2023) however there is no standard for diagnosing thyroid function in rodent models for research purposes (Fu et al., 2022).

1.3.5.1 Hypothyroidism

Hypothyroidism is defined as a defect in TH action; it is the most common thyroid function disorder and, in general, the most common endocrine function disorder (Roberts & Ladenson, 2004). A hypothyroid state can be classified based on its time of onset (congenital or acquired) and its severity (overt, i.e., clinical hypothyroidism and subclinical, i.e., mild hypothyroidism. Subclinical hypothyroidism is defined as abnormally high TSH concentrations with fT4 levels within the reference range while overt hypothyroidism refers high TSH concentrations with low fT4 levels (Cappola et al., 2019). Subclinical hypothyroidism is a risk factor for the development of overt hypothyroidism (Farebrother et al., 2019). The most common cause of congenital hypothyroidism remains endemic iodine deficiency (Hetzel, 2002). More than 1000 million people in the world suffer from a condition of chronic iodine deficiency. Low TH in adulthood is associated with increased risk of CVD(Rhee et al., 2013), including risk of hypertension (Saito et al., 1983; Streeten et al., 1988).

1.3.5.2 Hyperthyroidism

Hyperthyroidism (an overactive thyroid gland) is a condition in which excess TH is produced. It is a common disease, with a prevalence of approximately 2-5% among women and 0-6% in men (Bjoro et al., 2000). Subclinical hyperthyroidism is associated with abnormally low TSH concentrations with fT4 and fT3 concentrations within reference range while overt hyperthyroidism refers to low TSH with high levels of fT4 and fT3. Patients with hyperthyroidism have increased risks of various cardiovascular problems, such as atrial fibrillation

(AF), hypertension, coronary artery disease (CAD), stroke and heart failure (HF) (Ryödi et al., 2014). A study by Ryodii et al., demonstrated that hyperthyroidism increases cardiovascular morbidity even in relatively young patients (Ryödi et al., 2014).

1.4 Thyroid hormones and cardiovascular disease

TH are well known for their involvement in neurodevelopment especially in early development and metabolic activities throughout life (Zimmermann et al., 2008), however, they have also been implicated in cardiovascular health later in life (Combet, 2017; Mitchell et al., 2013). TH receptors (TRs) are present in myocardium and vascular endothelial tissues, thereby allowing changes in circulating TH concentration to modulate end organ activity (Figure 1-9). TH have been identified as regulators of cardiac function and cardiovascular hemodynamics. The potential mechanisms that link CVD with thyroid dysfunction are endothelial dysfunction, changes in BP, myocardial systolic and diastolic dysfunction, and dyslipidaemia (Razvi et al., 2018). The regulation of cardiovascular function by TH is described in more detail below.

1.4.1 Thyroid hormones and the heart

TH are known to raise HR and cardiac contractility and improve the systolic and diastolic function of the heart (Klein & Ojamaa, 2001a). T3 binds to nuclear receptor proteins and mediates the expression of several important cardiac genes, inducing transcription of the positively regulated genes including alpha-myosin heavy chain (MHC) and SERCA. Negatively regulated genes include beta-MHC and phospholamban (PLN), which are down regulated in the presence of normal serum levels of TH (Danzi & Klein, 2004).

Hyperthyroidism is known to increase the risk of AF and HF (Ryödi et al., 2014). Moreover, hyperthyroidism increases cardiac preload, body fluid volume and HR and affects both the systolic and diastolic function of the heart (Klein, 1988). Overt hyperthyroidism may thereby worsen the symptoms of underlying, undiagnosed heart disease (Klein, 1988). On the other hand, hypothyroidism weakens the heart muscle and can cause cardiac arrhythmias (Fazio et al., 2004; Kahaly, 2000; Molnár et al., 1998).

1.4.2 Thyroid hormones and peripheral circulation

TH affect peripheral vascular tone (Klein & Ojamaa, 2001b) and has been reported to rapidly reduce peripheral vascular resistance (Klein, 1990). To date, multiple mechanisms by which TH influence the peripheral vasculature have not been fully explained. The endothelium has indeed been indicated to serve as a pressure sensor both by secreting factors with vasodilating action and by modulating responsiveness to counteracting vasoconstrictors (Lervasi & Fommei, 2009). The T3-mediated effect on vascular tone has been reported to exhibit both endothelium-independent and endothelium-dependent components(Park et al., 1997). TH stimulation of endothelial cells (Yu et al., 2020) and VSMC is principally mediated by thyroid receptor alpha (TRα1) and thyroid receptor beta (TRß), regulating transcription of genes including nitric oxide synthase 3 (*NOS3)*, encoding endothelial NO synthase (eNOS) (Cai et al., 2015; Jabbar et al., 2017). T3 also rapidly regulates vascular tone via non-genomic signalling including stimulation of PI3K-Akt signalling leading to phosphorylation and activation of eNOS, thereby stimulating the synthesis of the vasodilator NO (Hiroi et al., 2006; Llévenes et al., 2018; Vicinanza et al., 2013). T3 also induces vasorelaxation through an endothelium-independent pathway (McAllister et al., 1998; McAllister et al., 2000) by stimulating the activation of protein kinase G (PKG)/vasodilator-stimulated phosphoprotein signalling in VSMCs (Samuel et al., 2017). Aortic rings incubated with T3 in the presence of 2 μM KT5823 (a PKG inhibitor) displayed a significant shift of the SNP curve to the right, demonstrating that inhibition of PKG abolishes the effect of T3 (Samuel et al., 2017). TH also increase Ca^{2+} reuptake within arterioles, which leads to smooth muscle relaxation(Park et al., 1997). This decrease in systemic vascular resistance is also a result of the direct repression of PLN expression and the increase in tissue metabolism and thermogenesis induced by THs (Silva, 1995). It is therefore suggested that, if THs have a direct influence on the cardiomyocytes and vasculature, then iodine should also be proposed to have a direct or indirect effect on the CVS since it is a precursor of THs.

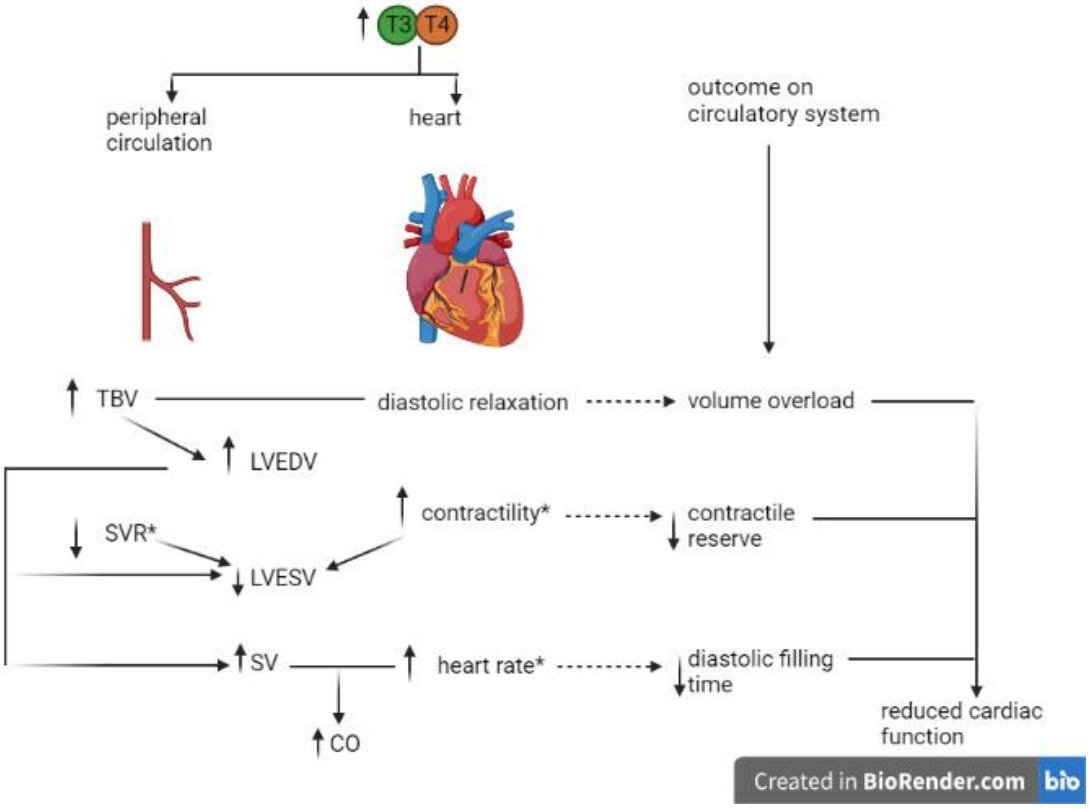

Figure 1-9: Sites of thyroid hormone action on the systemic vasculature and the heart.

T3 which is the biologically active of the thyroid hormones plays a major role in the function of the heart and the vasculature. T3 has both chronotropic and ionotropic effects on the heart also decreases systemic vascular resistance. Total blood volume (TBV), systemic vascular resistance (SVR), left ventricular end diastolic volume (LVEDV), left ventricular end systolic volume (LVESV), cardiac output (CO). * Represent thyroid hormones outcomes on the heart.

1.5 Iodine and cardiovascular function

Even though the majority (67%) of iodine is contained within the thyroid gland, extrathyroidal organs such as the heart, kidney, and liver also contain iodine. Like the thyroid gland, transport in these extrathyroidal tissues involves the expression of SLC5a5 and in some cases SLC26a4 (Cho et al., 2000). Rakoczy et al. showed that Wistar rats fed potassium iodide (KI) biofortified lettuce accumulated iodine in the kidneys, liver, and heart and femoral muscle (22.37 ± 0.09, 5.41 ± 0.08,6.14 ± 0.01 and 2.31 ± 0.05 mg I/kg) respectively, when compared to those fed lettuce not biofortified (Rakoczy et al., 2016). This indicates that dietary iodine can increase iodine in the extra-thyroidal organs, such as the heart, although its direct function in these organs is unknown (Jin et al., 2020; Lee et al., 2016). However, it is suggested that the role of iodine in tissues other than the thyroid include antioxidant, anti-inflammatory, antiproliferative, antibacterial, proapoptotic, and pro-differentiating effects (Jin et al., 2020). Despite the acknowledged importance of iodine for normal growth, maturation, and function in humans via thyroid function, its role in the CVS independent of thyroid function remains unclear. As mentioned, much of the previous research in this area has focused on the indirect effects of iodine mediated through TH. Findings of a direct link between iodine and CVD are limited because previous studies in humans involved participants with thyroid dysfunction and therefore it is difficult to separate the individual effects of iodine from that of thyroid dysfunction.

1.5.1 Iodine deficiency and cardiovascular disease

There is substantial evidence that iodine deficiency is a modifiable risk factor of CVD. Low iodine levels have been associated with several risk factors for CVD, including hyperlipidemia and insulin resistance, in both animal and human studies (Al-Attas et al., 2012; Han et al., 2012; Zhao et al., 2011). In addition, low iodine levels have also been associated with an increased risk of gestational hypertension (Cuellar-Rufino et al., 2017). Atherosclerosis of peripheral arteries is associated with low protein-bound iodine (KIRK et al., 1949). Early studies show that the development of atherosclerotic plaques in cholesterol-fed rabbits was prevented by KI supplementation while the addition of TH did not have a significant effect (8 out of 11 rabbits developed atherosclerotic plaques)

(Turner, 1933). The same study also established that iodine but not potassium was responsible for preventing atherosclerosis since rabbits fed potassium bromide or potassium chloride alongside cholesterol developed gross atherosclerosis (Turner, 1933). Turner concluded that the preventative effect is due to iodine and not potassium and that it is not a general halogen effect as suggested by the inadequacy of both bromide and chloride (Turner, 1933). Iwata et al. showed that infusion of iodide reduces heart damage by as much as 75% when delivered intravenously following the temporary loss of blood flow but before reperfusion of the heart in a mouse model of acute myocardial infarction (AMI) (Iwata et al., 2014). The same study also demonstrated that the benefits are iodide-specific since bromide did not have a similar effect (Iwata et al., 2014).

In a human study, UIC had a negative correlation with age and systolic BP but did not correlate with thyroid volume, thyroid nodularity, fT4, TSH, or TPO levels (Menon et al., 2011). Mean UIC was significantly lower ($p < 0.001$) in people with a history of hypertension (n=101) and in people with hypertension (n=370) when compared to people without a history of hypertension and in people without hypertension respectively (Menon et al., 2011). Menon et al., however suggest that iodine deficiency in people with a history of hypertension may be due to therapeutic salt restriction resulting in insufficient iodine intake, although the history of salt restriction was not assessed in their study (Menon et al., 2011). Their results were similar to the findings of a published study among Caucasian subjects with hypertension in the age range of 20-60 years, where iodine deficiency is more frequent than in the general population, demonstrating that high proportions of men (25%) and women (40%) had iodine deficiency (Tayie & Jourdan, 2010). However, dietary salt restriction may not be the only factor involved in low iodine status, since people without a history of hypertension, but having recently been diagnosed with elevated BP also displayed a similar negative correlation with iodine levels (Tayie & Jourdan, 2010). However, it is important to acknowledge that the above study cannot confirm a direct effect of iodine since thyroid dysfunction was not ruled out. A Spanish study comprising of 4370 individuals with a mean age of 50.4 years (age range 18-93 years) without thyroid dysfunction and monitored during an average follow-up of 7.3 years, showed an association between moderate-severe iodine deficiency and mortality

that remained after the adjustment for multiple potential confounders. The specific analyses by causes of mortality suggest that the association between iodine deficiency and mortality was mainly driven by cardiovascular causes (Table 1-6) (Maldonado-Araque et al., 2021).

Table 1-6 Cox Proportional Hazard Ratios (95% Confidence Intervals) for All-Cause, Cardiovascular, and Cancer Mortality According to Urinary Iodine Categories (World Health Organization–United Nations International Children's Emergency Fund)

	Urinary iodine (µg/L)				
	<50	50-99	100-299	≥300	p *for trend*[a]
Patients (*n*)	4226	1299	2454	191	
All cause-mortality					
Deaths (*n*)	36	84	124	10	
Mortality/1000 person-year [CI]	**11.8 [8.2-16.3]**	8.9 [7.1-11.0]	6.9 [5.8-8.2]	7.2 [3.4-13.2]	
RR crude [CI]	**1.71 [1.18-2.48]**	1.29 [0.97-1.7]	1 (reference)	1.04 [0.54-1.98]	0.004
RR multivariate [CI]	**1.71 [1.12-2.61]**	1.28 [0.94-1.75]	1 (reference)	1.07 [0.54-2.15]	0.01
Cardiovascular mortality					
Deaths (*n*)	11	30	27	3	
Mortality/1000 person-year [CI]	**3.6 [1.8-6.4]**	**3.2 [2.1-4.5]**	1.5 [1.0-2.2]	2.2 [0.4-6.3]	
RR crude [CI]	**2.40 [1.19-4.85]**	**2.10 [1.25-3.54]**	1 (reference)	1.43 [0.43-4.72]	0.002
RR multivariate [CI]	**2.38 [1.05-5.40]**	1.82 [1.00-3.32]	1 (reference)	1.58 [0.46-5.42]	0.011
Cancer mortality					
Deaths (*n*)	11	26	44	4	
Mortality/1000 person-year [CI]	3.6 [1.8-6.4]	2.8 [1.8-4.0]	2.5 [1.8-3.3]	2.9 [0.8-74]	
RR crude [CI]	1.47 [0.76-2.85]	1.12 [0.69-1.82]	1 (reference)	1.17 [0.42-3.25]	0.314
RR multivariate [CI]	1.33 [0.62-2.82]	1.07 [0.63-1.83]	1 (reference)	1.31 [0.46-3.74]	0.443

In bold $p < 0.05$ versus UI 100–299 µg/L (reference).
[a]*p* for trend across categories with UI 100–299 µg/L (reference), 50–99 µg/L, and <50 µg/L.
RR, relative risk; CI, 95% confidence interval; UI, urinary iodine.

Adapted from (Maldonado-Araque et al., 2021)

1.5.2 Excess iodine intake and cardiovascular disease

Contrary to the relationship between low iodine levels and increased incidence of CVD, excess iodine may increase BP, and may increase the risk of hypertension (Liu et al., 2019; Rust & Ekmekcioglu, 2017). Systolic and diastolic BP in iodine-sufficient (221.2 µg/L) and iodine-excess (421.3 µg/L) regions were significantly increased (all $p < 0.01$) when compared to iodine adequate regions (126.6 µg/L) (Table1-6). The same study also reported no significant difference in TSH levels between populations in iodine-sufficient and iodine-excess areas when compared to iodine adequate areas. However, levels of fT3 and fT4 were significantly increased in subjects within iodine-excess regions when compared to iodine adequate regions (fT3 6.1±3.1 pmol/L vs 5.6±0.8 pmol/L and fT4 19.9±2.8 pmol/L vs 16.3±2.1 pmol/L) $p < 0.05$ and $p < 0.01$ respectively(Liu et al., 2019). Data obtained from 51,795 adults (≥ 18 years) without thyroid dysfunction showed that the association of hypertension and UIC produced a U-shaped curve, with a nadir at 300-499 µg/L (Jin et al., 2020). Both men and women showed a similar trend; however male subjects showed a significantly increased prevalence of hypertension at UIC ≥ 800 µg/L when compared to 100-299 µg/L in women ($p < 0.05$). The same study also demonstrated an association of prevalence of metabolic disorders and metabolic syndrome with UIC exhibiting a U-shaped curve, with a nadir at 300-499 µg/L ($p < 0.05$). As UIC increased to ≥ 500 µg/L, the prevalence of metabolic disorders significantly increased in both men and women ($p < 0.05$) (Jin et al., 2020). UIC ≥ 800 µg/L was associated with increased prevalence of hypertriglyceridemia and high LDL-C levels in the overall population and in males, as well as significantly increased prevalence of hypercholesterolemia in the overall population and in females ($p < 0.05$) (Jin et al., 2020). The above studies demonstrated that iodine intake has the potential to influence systolic BP, metabolic disorders, metabolic syndromes, and dyslipidaemia all of which are risk factors for CVD.

Conversely, a study in mice conducted by Zhao et al., demonstrated that TC and triglyceride (TG) decreased in response to excess iodine diet. TG and TC levels were significantly decreased ($p < 0.05$) in iodine excess groups compared to normal iodine groups. However no significant differences in levels of T3, T4, and fT3 between iodine excess and normal iodine groups were observed (Zhao et al., 2011). This study suggests a direct role of iodine in lipid metabolism

independent of THs. These studies suggest a species difference in lipid metabolism between human and mouse. Even though there is limited research on iodine and CVS, there is growing evidence linking iodine status and cardiovascular health independent of thyroid function. These findings, therefore, call for a robust investigation on the direct role of iodine on the CVS.

Table 1-7: Urinary iodine concentration, thyroid function, and blood pressure in three areas with different iodine levels.

Iodine-adequate area[#]		Iodine-sufficient area	Iodine-excess area
N	320	264	241
Urinary iodine (µg/L)			
Median	126.6	221.2**	421.3**
P25-P75	87.7-206.0	147.7-304.8	277.7-620.9
TSH (mIU/L)			
Median	3.0	3.3	3.1
P25-P75	2.2-4.2	2.2-4.9	2.1-4.7
FT_3 (pmol/L)			
Mean	5.6	5.47	6.1**
SD	0.8	0.9	3.1
FT_4 (pmol/L)			
Mean	16.3	16.7	19.9*
SD	2.1	2.8	2.8
Systolic pressure (mmHg)			
Mean	119.0	124.4**	124.2**
SD	19.8	20.6	18.3
Diastolic pressure (mmHg)			
Mean	79.1	82.8**	82.4**
SD	12.8	13.6	12.1

TSH, thyroid-stimulating hormone; fT3, free triiodothyronine; fT4, free thyroxine
Control group; compared with the iodine adequate area, *$p < 0.05$, **$p < 0.01$.
UIC were significantly higher in iodine-sufficient and Iodine-excess areas vs iodine-adequate area ($p < 0.01$). fT3 and fT4 were significantly raised in iodine-sufficient and iodine-excess areas ($p < 0.01$) and ($p < 0.05$) respectively. Systolic and diastolic blood pressures were also significantly high in iodine-sufficient and iodine-excess areas vs iodine adequate areas ($p < 0.01$).

Adapted from (Rust & Ekmekcioglu, 2017)

1.5.3 Mechanisms of iodine action on the cardiovascular system

Iodinated contrast media, a commonly used agent for clinical radiographic imaging, has vasomotor effects on several arterial beds (Limbruno & De Caterina, 2003) and shows vasorelaxation as a prominent side effect(Morcos et al., 1998). The mechanisms responsible for contrast-induced vasomotor changes are not fully elucidated and are likely to be multifactorial. This vasodilation is associated with a decrease in peripheral resistance, increased blood flow, and decreased arterial BP (Uder et al., 2002). A review by Pugh, et al acknowledges that cellular mechanisms underlying the vasodilator effects of iodinated contrast media may include a) effects attributable to hyperosmolality, b) stimulation of the release of endogenous vasoactive mediators, c) direct relaxant effect upon vascular smooth muscle (Pugh et al., 1995). Iodine-induced effects may therefore involve modulating the release of endogenous vasoactive mediators such as prostacyclin, NO, endothelin, adenosine, histamine, serotonin, bradykinin, arterial natriuretic peptide, antidiuretic hormone, and/or through direct effects on vascular smooth muscle cells (Morcos et al., 1998).

Iodine can also positively affect the CVS by acting directly as an antioxidant with reducing power to counteract ROS (Harvey et al., 2017). Figure 1-10 gives a summary of the direct and indirect effects of iodine on CVS. Iodine has been proposed as a primitive antioxidant, with algae having an effective and perhaps necessary evolutionary role in quenching free radicals from the atmosphere (Venturi & Venturi, 1999). A low concentration of iodine (15 μM) has the same antioxidant capacity as ascorbic acid (Smyth, 2003). It is an antioxidant at low or moderate (≤ 3506 mg/L) levels but has the potential to act as a potent free radical at high concentrations (4076 to 7512 mg/L) (Joanta et al., 2006; Smyth, 2003; Vitale et al., 2000; Zhang et al., 2015). Iodide can catalytically convert hydrogen peroxide (H_2O_2) to water and O_2 (Blackstone et al., 2005; Blackstone & Roth, 2007) and when added to plasma, iodide increases peroxidase activity (Tatzber et al., 2003). Dugrillon also argued that possible functions of trapped and organified iodide in extrathyroidal tissue may include antiproliferative and antioxidant effects (Dugrillon, 1996). A study on AMI in rats and pigs by Morrison et al. measured peroxidase activity in blood after AMI and iodide administration and found that compared with saline-treated animals, iodide treated animals had higher peroxidase activity (iodide : 32 μM/mg/min vs saline: 23 μM

/mg/min; $p < 0.05$) (Morrison et al., 2018). The increased formation of ROS (reduced antioxidant activity) is generally associated with oxidative stress and subsequent cardiovascular tissue injury (Dhalla et al., 2000). Morrison et al. concluded that sodium iodide (NaI) improves outcome in both rat and pig models of AMI by reducing the effects induced by ROS (Morrison et al., 2018).

Even though iodine is alleged to have beneficial effects through its vasodilatory and antioxidant activities, there appears to be a balance between good and bad effects of iodine on physiological systems. Zhang et al., demonstrated that high levels of iodine (4076-7512 mg/L) increased the apoptosis rate and the expression of intercellular adhesion molecule-1 (ICAM-1), vascular cell adhesion molecule-1 (VCAM-1) and inducible nitric oxide (iNOS) and decreased the activity of eNOS of endothelial cells (Zhang et al., 2015). Excessive iodine intake can cause damage to vascular endothelial cells and alter the expression of adhesion molecules and the activity of NOS (Yu et al., 2020). A high iodine intake in rats can lead to endothelial cell activation, injury, and hyperplasia, thereby increasing the subendothelial extracellular matrix, promoting intimal thickening, thickening of the inferior vena cava wall, and stenosis (Zhang et al., 2015). Results from this study indicate a dose-response relationship between iodine and endothelial cell damage. Experiments using rat endothelial cells from the aorta have shown that high amounts of iodine (4076 to 7512 mg/L) cause endothelial cell damage by inhibiting cell proliferation and destroying the cell's antioxidant capacity (Zhang et al., 2015).

Despite the suggested effect of iodine on vascular cells, the molecular mechanisms underlying iodine action remain unclear (Morrison et al., 2018).

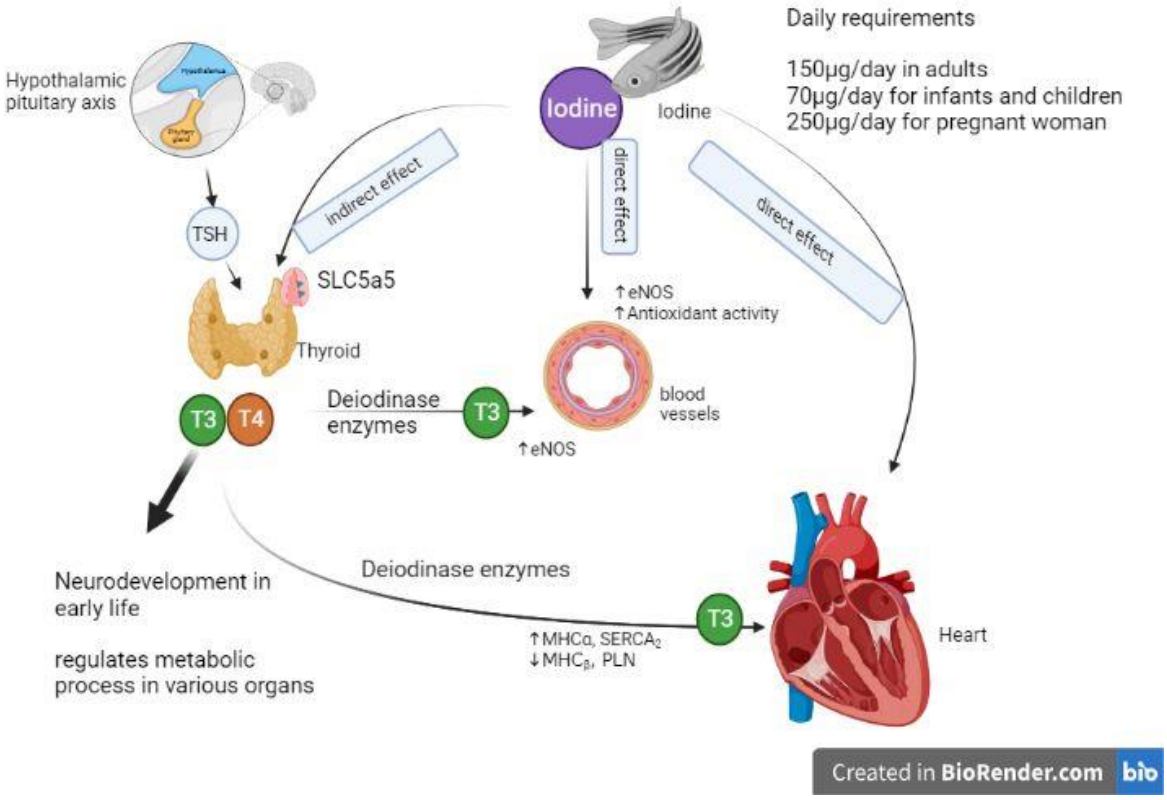

Figure 1-10: The direct and indirect effect of iodine on heart and blood vessels.

Iodine has both direct and indirect effect on the heart and blood vessels. Iodine acquired from food sources is either taken up by the thyroid for thyroid hormone production or utilised directly by the heart and blood vessels. Thyroid stimulating hormone (TSH), endothelial nitric oxide (eNOS), myosin heavy chain alpha (MHCα), myosin heavy chain beta (MHCβ) phospholamban (PLN), sarcoendoplasmic reticulum Ca^{2+} ATPase ($SERCA_2$) Triiodothyronine (T3), Thyroxine (T4).

1.5.4 Table salt, dietary iodine, and cardiovascular disease

Iodine intake has been shown to decline in subjects on sodium-reduced diets, which is recommended as a lifestyle change intervention for CVD (Hoption Cann, 2006). High dietary salt causes increased sympathetic nerve activity (SNA), a major trigger of vasoconstriction (Blaustein et al., 2012), and alters sodium balance causing altered kidney function and reduced fluid excretion (Ohta et al., 2013) leading to elevated BP. WHO strongly recommend reductions in dietary salt intake as one of the top priority actions to tackle non-communicable disease crisis and has advised member states to take action to reduce population wide dietary salt intake to decrease the number of deaths from hypertension, CVD and stroke (Ha, 2014). On the other hand, salt iodisation has been the preferred strategy to control and eliminate IDD and is implemented in more than 120 countries around the globe ("Sustainable elimination of iodine deficiency," 2008). Sodium and potassium are essential electrolytes that play crucial roles in maintaining various bodily functions, however sodium enriched salt is preferred over potassium enriched salt. This is mainly because potassium salt has a bitter taste, especially when heated, making it less appealing for widespread use in cooking (Braschi et al., 2009). Nevertheless, some potassium-enriched salts containing iodine are available as alternatives to regular iodized table salt. Over the past decade, intensive efforts have been made by the governments of IDD-affected countries to implement salt iodisation programmes. Salt is considered an appropriate vehicle for fortification for a number of reasons: (i) it is widely consumed in all countries with little seasonal variation in consumption patterns; (ii) in many countries, salt production is limited to a few centres thereby facilitating quality control; (iii) the technology needed for salt iodization is well established and relatively inexpensive (Zimmermann et al., 2008). Each gram of iodized salt contains about 77μg of iodine (100μg potassium iodide) at the production level (Dunn, 2002; Hetzel, 2005), and therefore reduced salt intake can compromise iodine intake (Hoption Cann, 2006). However, it is possible that the concentration of iodine in salt can easily be adjusted to meet policies aimed at reducing the consumption of salt in order to prevent CVD (Network, 2013).

1.6 Animal models of cardiovascular disease

Experimental animal models are essential to obtain basic knowledge of the underlying biological mechanisms in human diseases (Schughart et al., 2013). They have many advantages for studying complex traits, including control over variables such as genetic background, diet, stress, bacterial and viral load, and chemical and toxin exposures. Inbreeding provides a level of genetic control not possible in humans. Detailed phenotyping can be undertaken in time-course studies. Cells, tissues, and organs can be assessed that are not available in humans (Buchner & Nadeau, 2015). Several models have been developed to address human cardiovascular complications, including hypertension, atherothrombotic and cardiac diseases, and similar pathology has been successfully recreated in different species, including small and large animal models of disease (Zaragoza et al., 2011).

1.6.1 Rodent models of cardiovascular disease

Rodent models of CVD are important for studying and enhancing knowledge on biomedical and cardiovascular research. Rats and mice share a high degree of homology to the human genome, with approximately 23,000 and 22,000 protein coding genes in rats and mice compared to approximately 20,000 protein coding genes in humans (Breschi et al., 2017; de Jong et al., 2022). Rat models have dominated research into CVD and heart damage because, while rats share many of the benefits of mice (low cost, ease of handling, etc.), their larger size greatly facilitates surgical and postsurgical procedures and are more similar in cardiovascular function and disease to humans than mice (Zaragoza et al., 2011). Laboratory rats originate from Rattus Norvegicus.

1.6.1.1 The spontaneously hypertensive rat model

The SHR is a well-established model for hypertension research (Okamoto, 1972). This rodent strain originated in Kyoto, Japan, from the cross of an outbred Wistar male rat, which exhibited spontaneously elevated BP, and a female with slightly elevated BP (Okamoto & Aoki, 1963). Subsequent brother-sister mating was continued with selection for animals with systolic BP >150 mm Hg. The inbred strain was subsequently established in the United States in the late 1960s after 20 generations of inbreeding at the National Institutes of Health (NIH) and

spontaneously develops hypertension as adult animals. The SHR BP increases spontaneously from 4 weeks of age reaching SBP of 180-200 mmHg in males compared to 130 mmHg in sex and age matched WKY (Dickhout & Lee, 1998). The SHR animals develop many features of hypertensive end organ damage including cardiac hypertrophy and renal dysfunction (Pinto et al., 1998). It is extensively used in different studies as a rat model of primary or essential hypertension.

1.6.1.2 The stroke-prone spontaneously hypertensive rat model

Subsequently the stroke prone spontaneously hypertensive rat (SHRSP) was established from a sub strain of SHR under the following conditions (i) the selection started with the 24th generation of SHR, (ii) only after 3 generations of selection was the high stroke susceptibility fixed, (iii) the severe hypertension and stroke was fixed simultaneously (Figure 1-11) (Pinto et al., 1998; Yamori & Okamoto, 1974). The SHRSP have even higher BP levels which range from 220-240 mmHg versus 180-200 mmHg in the SHR and just like in humans, male SHRSP rats exhibits higher BP than age match females (Nabika et al., 2012; Olson et al., 2019). Moreover, they exhibit a frequency of spontaneous strokes, when fed a high salt diet, and increased sensitivity to experimental stroke compared with the SHR and WKY rats (Coyle & Jokelainen, 1983; Jeffs et al., 1997; Yamori & Okamoto, 1974). The SHRSP is useful animal model of human CVD as it exhibits spontaneous onset of hypertension between 8-12 weeks of age (Ishikawa et al., 2008; Nabika et al., 2012). In addition, the SHRSP develops several other cardiovascular complications such as cardiac hypertrophy, endothelial dysfunction and chronic kidney disease if administered salt. It has also been demonstrated that the SHRSP exhibit a significant increase in LVMI compared to that of WKY at 5 weeks of age, before the onset of hypertension.

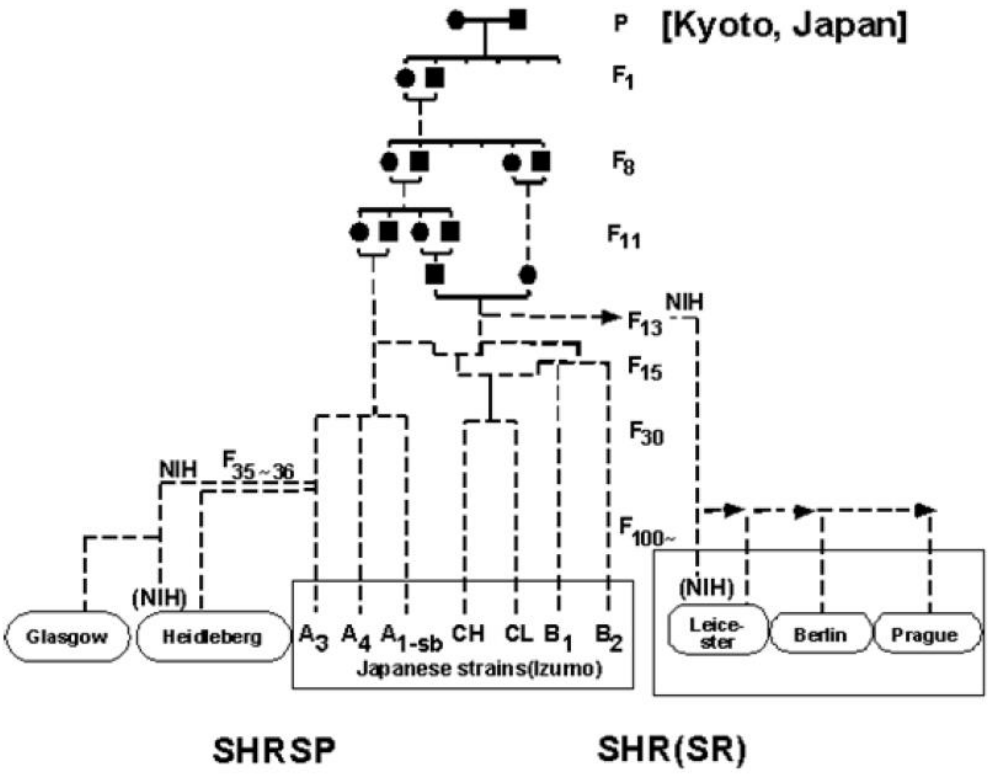

Figure 1-11: Establishment of the Stroke-Prone Spontaneously Hypertensive Rat.

The SHR was developed from selective breeding of hypertensive WKY in Kyoto, Japan through parental (P) stock. Subsequent generations (F) were then bred in many institutes and locations leading to the current strains available detailed at the base of the above diagram. NIH: National Institute of Health.

1.6.1.3 The stroke-prone spontaneously hypertensive rat and dietary studies

Hypertension in SHRSP is multifactorial just like in the human condition and is worsened by elevated dietary salt and reduced potassium, which can damage the CVS; resulting in ischemic stroke, cardiac hypertrophy and renal disease (Di Castro et al., 2013; Takeda et al., 2001). SHRSP has been used in various nutritional experiments including feeding high protein diets and altering Ca^{2+} and magnesium (Mg) levels (Nara et al., 1978; Yamori et al., 1986; Yamori et al., 2022). This rat strain has been used to observe the effect of various diets on stroke and hypertension. For example, SHRSP given 1% salt in drinking water developed severe hypertension and stroke, however hypertension was attenuated by increasing K^+ intake (Yamori, 1984). The adverse effect of salt was attenuated by alginic acid rich in dietary fibers of seaweed, which absorbed Na^+ to decrease its uptake in the intestine (Yamori et al., 1986). It has also been demonstrated that SHRSP fed on a soy protein diet or Mg-rich diet survived significantly longer (200 days longer) compared to those fed control diet and 1% salt in drinking water (Yamori et al., 2022). This study provided scientific evidence that soy protein, Mg^+ and Ca^{2+} rich diets were preventative against hypertension and stroke. Even though SHRSP have not been used to study the effects of dietary iodine on CVD, previous studies utilising SHRSP suggest that this rat strain can be a suitable model to study the effect of dietary iodine on CVD.

1.6.2 Thyroid function in spontaneously hypertensive rats and stroke-prone spontaneously hypertensive rats

Just like in humans, TH in rats are synthesised in the thyroid gland and regulated similarly to human through a negative feedback system involving the hypothalamic pituitary (HPA) axis (Fekete & Lechan, 2007). Little information regarding TH levels in rats is provided in the literature. However, serum levels of T3 and T4 have been widely reported in the untreated Sprague Dawley rat (Christianson et al., 1981; Tang, 1985) but not the SHR and SHRSP rats. A common way of assessing thyroid status of an organism is by measuring serum levels of TH (T4 and T3) and TSH as well as; rT3 which is normally measured for special situations to confirm abnormalities in the TH metabolism. Serum TH levels may vary substantially according to sex, age, and strain of the rat (Bianco

et al., 2014). As mentioned previously elevated levels usually indicate thyrotoxicosis or hyperthyroidism, while decreased serum levels are indicative of hypothyroidism. Typical standard curves are prepared over the range 2.5–240 ng/mL for T4 and 0.1–6 ng/mL for T3. It has been reported that plasma levels of T3 does not differ between the WKY and SHR, however it is also reported that SHR does not respond adequately to TSH stimulation mainly due to defects in synthesis of TH (Krupp et al., 1977).

1.7 Hypothesis

This PhD project has been divided into four main hypotheses:

- Short term dietary intervention to alter iodine intake will not have an influence on thyroid function in WKY and SHRSP males and females.

- Altering iodine level intake will directly influence cardiovascular function; low dietary iodine will cause blood pressure elevation, left ventricular hypertrophy and increased peripheral vascular resistance.

- Low iodine diet will change the vascular transcriptome in WKY and SHRSP rats.

- Modifying iodine levels in cell culture media will affect cell signalling pathways in mesenteric artery VSMCs from WKY and SHRSP rats.

1.8 Aims

- To assess plasma thyroid-stimulating hormone (TSH), free thyroxine (fT4), free triiodothyronine (fT3) and thyroglobulin (Tg) and compare UIC in WKY and SHRSP under normal and low iodine dietary conditions.

- To assess cardiovascular parameters including haemodynamic and vascular function changes to low iodine diet in WKY and SHRSP rats.

- To perform a transcriptomic analysis and generate a differential expressed gene (DEG) profile of the thoracic aorta of WKY and SHRSP

male rats fed low iodine diet versus those fed normal iodine diet and to uncover the biology related to the DEGs.

- To investigate the signalling pathways involved in iodine induced disease process, using cell based mechanistic assessments.

Chapter 2 General Materials and Methods

2.1 General laboratory practice

Laboratory equipment and reagents used in this study were of the highest possible grade commercially available. All substances deemed hazardous were handled and dealt with in accordance with Control of Substances Hazardous to Health regulations. Details of the preparation of all laboratory solutions that were not commercially acquired are given in Appendix III. Reagents were weighed using an Ohaus Portable Advanced balance (sensitive to 0.01 g) or a Mettler HK160 balance (sensitive to 0.00001 g). Sterile disposable plastic ware or standard laboratory glassware was used to prepare reagents. Glassware was washed using Decon 75 detergent (Decon Laboratories Ltd, UK), rinsed with distilled H_2O (dH_2O), and placed in a 37ºC drying cabinet. RNase-free disposable plastic ware (Thermo Fisher, Paisley, UK) was used when appropriate. Volumes from 1 µL to 1 mL were measured using calibrated Gilson® pipettes (Woodside Estate Dunstable, UK) and disposable tips or RNase-free filter tips (Thermo Fisher, Paisley, UK) when appropriate. For volumes larger than 25mL clean measuring cylinders were used. dH_2O was used to prepare all aqueous solutions unless otherwise stated in Appendix III. To dissolve solutions, a Jenway 1000 hotplate/stirrer was utilized. A mini vortex 2800 rpm Lab Dancer (Fisher Scientific, Loughborough, UK) was used to mix solutions. Heraeus™ Pico™ benchtop microcentrifuge (Thermo Fisher, Paisley, UK) was used to centrifuge <2mL sample volumes while Sorvall™ Legend™ Centrifuge (Thermo Fisher, Paisley, UK) was used to centrifuge larger samples. Incubations at 37ºC to 95ºC were done in a Julabo TW8 water bath equipped with a thermometer while for experiments requiring 95ºC to 100ºC an Eppendorf ThermoMixer® was used. The pH of solutions was measured using a Mettler Toledo pH meter calibrated with pH 4.0, 7.0 and 10.0 standards (Sigma-Aldrich, Dorset, UK).

2.2 In vivo studies

2.2.1 Animal ethical approval and personal license

All animal procedures were approved by the Home Office according to the Animals (Scientific Procedures) Act of 1986 and ARRIVE (Animal Research:

Reporting of *In Vivo* Experiments) guidelines and assigned project license number PP0895181 held by Dr. Delyth Graham. In addition, I was trained and awarded a personal license number I48155713 which allowed me to perform minor / minimally invasive procedures involving sedation, analgesia, or brief general anaesthesia, plus surgical procedures conducted under brief non-recovery general anaesthesia.

2.2.2 Animal strains

The inbred strain of SHRSP rats and its reference strain WKY have been maintained at the University of Glasgow since December 1991(Jeffs et al., 2000). These strains are recognized as $SHRSP_{Gla}$ and WKY_{Gla}.

2.2.3 Animal housing

All animals were housed under controlled conditions, 12 hrs light and 12 hrs darkness, and an average temperature of 21 ± 3ºC. Prior to putting them on procedure animals were maintained on a standard rodent diet (rat and mouse No1 maintenance diet, Special Diet Services) and given tap water ad libitum.

2.3 Animal procedures

2.3.1 Blood pressure measurement by tail-cuff plethysmography

Systolic blood pressure (SBP) was measured at the beginning of the experiment (pre-diet) and weekly for 4 weeks (wks) by tail-cuff plethysmography. Animals were briefly, placed in heated incubation boxes with heat lamps at approximately 30ºC to induce tail vasodilation for approximately 10 min. The behavior and physical appearance of the rats were carefully observed to prevent overheating. Rats were restrained and wrapped in a soft, dry cloth with the tail exposed and placed on a heat mat to maintain body temperature. A blood pressure occlusion cuff was placed at the base of the tail alongside a piezoceramic transducer cuff to detect the pulse. A programmed electro-sphygmomanometer was connected to these to ensure consistent inflation-deflation rates of 1mmHg per sec and register pressure changes detected by the transducer (NHS Greater Glasgow and Clyde). Upon inflation, peak SBP was measured and on deflation base SBP was measured. On average, six readings per

animal were taken to estimate mean SBP. Measurements were generally made in the morning between 09:00 and 11:00 to minimise diurnal variation.

2.3.2 Transthoracic echocardiography

Rats were lightly anaesthetised throughout the procedure (2% isoflurane in 1.5L/min O_2). The thoracic fur was removed by shaving and the area cleaned of stray hair. Ultrasound gel was applied to exposed skin as an ultrasound coupling medium. Rats were imaged trans-thoracically using an Acuson Sequoia C256 imager fitted with a 15 MHz linear array transducer (Siemans, Surrey, UK). The heart was imaged along a para-sternal short-axis view to obtain M-mode images for 6-7 cardiac cycles. During the procedure tibial length and body weight were also measured to standardize measurements.

Analysis of the echocardiographic images was carried out using ImageJ software (Schneider et al., 2012). Distance (in mm) between M-mode waveform peaks and troughs was measured (shown in Figure 2-1B) and used to calculate SV, CO, left ventricular mass index (LVMI), ejection fraction (EF), fractional shortening (FS) and relative wall thickness (RWT). Two modes (B-mode and M- mode) are used for echocardiography analysis. The B-mode is used to visualize the two-dimensional structure of the heart and the M-mode to visualise the left ventricle and calculate functional parameters respectively. Formulas for calculations can be found in Table 2-1.

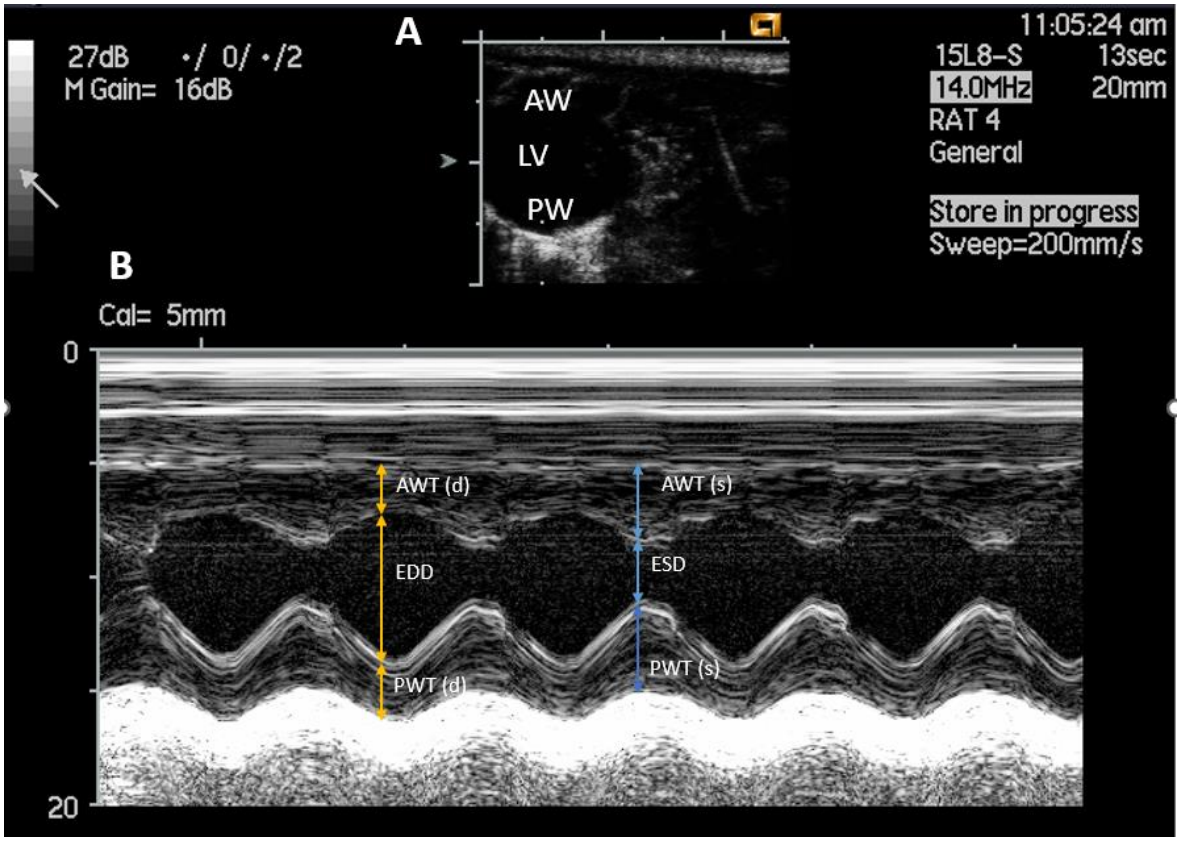

Figure 2-1: A representative of echocardiography image

Echocardiography was performed on short axis which can visualises cross section of the left ventricle (LV). (**A**) B-mode (**B**) M-mode. M-mode images were analyzed by measuring the left ventricular anterior wall thickness (AWT) and the left ventricular posterior wall thickness (PWT), as well as the left ventricular internal diameter for diastole (EDD) and for systole (ESD).

Table 2-1: Calculations of cardiac function from echocardiography images.

Cardiac function	Calculation
Stroke volume (mL)	= EDV/ESV
Cardiac output (mL/min)	= $SV \times HR$
Ejection Fraction (%)	(%) = ($SV/EDVol$) × 100
Fractional shortening (%)	= ($EDD-ESD/EDD$) × 100
Left ventricular mass (g)	= (0.8 × $ASEcube$) + 0.6/1000
Where ASEcube	= 1.04 × ($IVSTd + LVIDd + PWTd$)^3 $-LVIDd^3$
LVIDd	= average EDD x 10
IVSTd	= average AWTd x 10
APWTd	= average PWTd x 10
EDVol	= 1.047 × $LVIDd^3$
ESV	= 1.047 × ($Average\ EDDs$)^3

Formulas for cardiac function parameters generated from the M mode of the echocardiography.

2.3.3 Metabolic cage measurements

Water intake, food intake, and urine output were determined via metabolic cage measurements. Percentage (%) BW change per wk was determined by subtracting the previous wk BW from the current wk BW/current wk BW then multiplying by 100. Animals were first acclimatised to the metabolic cages for 2 hrs with no urine collection or water or food consumption determination, one wk prior to the actual collection period. On the day of metabolic cage measurement, animals were placed into individual stainless steel metabolic collection cages and given access to 200 mL water and the respective rodent diet, which was weighed but enough to ensure ad libitum consumption over the 24-hr period. After 24 hrs rats were removed from cages and final water volume remaining and urine produced were recorded. Per animal, volume of liquid consumed, and volume of urine excreted were obtained as metrics, whilst the urine was aliquoted into 1.5 mL Eppendorf tubes and stored at -80ºC until use. The amount of food consumed was determined by subtracting the feed remaining from the amount given. The BW of the individual rats was measured using an analytical balance and recorded.

2.4 Sacrifice and tissue harvesting

On completion of the study, animals were anesthetized with 5% isoflurane in 1.5L/min O_2 in an induction chamber. Animals were then carefully moved to an operating table in a supine position and attached to a face mask to maintain general anaesthesia. To confirm deep anaesthesia pressure was applied forcefully to the tip of the tail or toes until non-responsiveness. Blunt forceps were used to raise the skin above the diaphragm before cutting off the skin covering the area that's, leaving muscle tissue overlaying the chest exposed. A blunt incision was made into the peritoneum before the tissue was cut away on either side of the Xiphoid process of the sternum, exposing the diaphragm. A second blunt incision was made into the diaphragm before this was cut away. Following this, the rib cage 5mm on either side of the sternum was cut, exposing the organs of the chest. A 23G needle (Terumo, leuven, Belgium) fitted to a 2mL syringe (Sigma-Aldrich, Manchester, UK) was inserted into the apex of the heart, targeting the LV to exsanguinate the animal by collecting blood as the LV filled. Following exsanguination, watchmakers' forceps were used to lift and hold the

aorta from the posterior wall of the thoracic cavity before this was cut away from the base of the spine upward toward the heart until it was cut away completely at the aortic arch. The aortic section was divided into two equal halves (superior and inferior), with the superior half placed in 10% (v/v) neutral buffered formalin solution (CellPath, Powys, UK) with the other half snap frozen in liquid nitrogen. The whole heart was then dissected, and the connective tissue was cleaned off before it could be weighed using an analytical balance. The atria and RV were dissected off then the remaining LV plus septum was weighed. The apex was cut off and placed in 10% (v/v) neutral buffered formalin while the remaining LV plus septum was dissected into two sections and transferred into a 1.5 mL Eppendorf tube before snap freezing them in liquid nitrogen. With the thoracic aorta and heart removed, the abdomen wall was then cut to expose the organs of the abdomen. Both the right and left kidneys were removed and weighed and then one kidney was cut vertically into two halves while the other was cut into 4 equal sections. One half of the kidney was placed in 10% (v/v) neutral buffered formalin while the other six sections were snap frozen in liquid nitrogen. The thyroid was also harvested and cleaned of connective tissue before being weighed. It was then cut into 3 sections, with one section going into 10 % (v/v) buffered formalin and the other 2 sections snap-frozen in liquid nitrogen. The liver and lungs were removed and weighed; but not stored.

2.5 Mesenteric artery dissection

Rats were sacrificed under deep terminal (isoflurane) anaesthesia and the intestines with intact mesenteric vasculature were removed after incision of the abdominal cavity to expose and open the overlying peritoneum. The mesenteric was removed and transferred to a 50 mL Falcon tube (Corning, Arizona AZ, USA) containing 1X phosphate buffered saline (PBS) (Gibco™, ThermoFisher, Paisley, UK) which was placed on a sealed cooler box and transported to the myography laboratory. The intestine and the mesentery were then pinned out on a clean slygard-coated plate in ice-cold in Ca^{2+} free Phosphate saline solution (PSS) so that the mesentery was spread out and first order mesenteric artery was visualised. The orientation was such that the artery was on top of the vein. The first-order arteries were located with a Zeiss Stemi 2000-C dissection microscope (Carl Ziess Ltd, Cambridge, UK) and identified as those branching directly from

the superior mesenteric artery. The third-order mesenteric vessels were located as those between the gut wall and the second-order vessels in the arcade. They were cleaned of surrounding fat with ultra-fine forceps and removed with small spring scissors.

2.6 Wire myography

Vascular functional studies to assess vascular reactivity to various agonists were performed using a four-chamber wire myograph (Danish Myo Technology, Aarhus, Denmark). Wire myography is an in vitro technique employed to examine the vascular function of isolated small resistance arteries (Mulvany & Halpern, 1977).

2.6.1 Vessel mounting

Two short segments (≈ 4 cm) of a 40 μm tungsten-free stainless-steel wire (Danish Myo Technology, Aarhus, Denmark) were cut with fine forceps and inserted into the lumen of each artery (approximately 2mm in length) from the central portion of each dissected artery placed in a slygard-coated plate containing Ca^{2+} free PSS taking care not to damage the endothelium. The myograph chamber (620M, Danish Myo Technology, Aarhus, Denmark) was filled with PSS containing Ca^{2+} [120mM NaCl, 4.7mM KCl, 1.2mM MgSO4, 25mM NaHCO3, 1.2mM KH2PO4, 10mM glucose,2.5mM CaCl2] at 37ºC and using forceps the threaded vessel segment was carefully transferred from the petri dish into the myography chamber and secured using the fixing screws. Figure 2-2 shows a schematic diagram of a wire myography. 3 vessels were mounted per rat per in each treatement group and their responses averaged to represent n=1. Table 2-2 gives a summary of number of animals used and the total number of vessels used to generate dose response curves per treatment group. Full details of vessel dissection and mounting procedure are included in Appendix II.

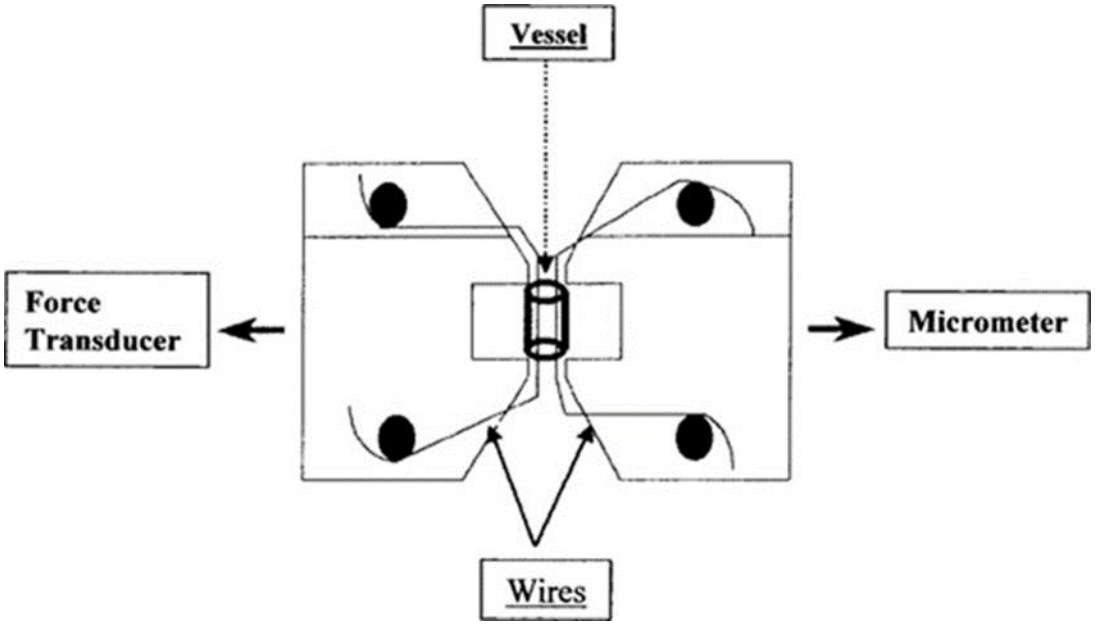

Figure 2-2 Schematic diagram of wire myograph as viewed from above(Spiers & Padmanabhan, 2005).

LabChart software (ADInstruments, Oxford, UK) was utilized for recording and analysing vessel tension response. Vessels were equilibrated for 30 min at 30 ºC and gassed with 95% O_2 and 5% CO_2 before normalization using the DMT normalization protocol (see Appendix II for full details of normalization protocol).

Table 2-2: Number of vessels mounted per rat to make an average response of n=1 and the total number of rats used per treatment group.

Experimental groups	Number of vessels mounted per rat (vessel responses averaged to n=1)	Number of rats used per an experimental group	Total number of vessels mounted per an experimental group
Males			
WKY_NID	3	6	18
WKY_LID	3	6	18
SHRSP_NID	3	6	18
SHRSP_LID	3	7	21
Females			
WKY_NID	3	6	18
WKY_LID	3	6	18
SHRSP_NID	3	7	21
SHRSP_LID	3	7	21

Six to seven rats were sacrificed and 3 vessels per rat were mounted on myograph. An average cumulative response of the 3 vessels was used to represent n=1 per an treatment group.

2.6.2 Cumulative concentration response curves

Cumulative concentration-response curves were obtained by adding concentrations of agonist to the bath in half-log molar increments. The contractile response of the vessel was assessed by adding U46619 (Enzo life sciences, UK) to the bath in 2-min intervals or when a response is observed to give final concentrations of $1x10^{-10}$M, $3x10^{-10}$M, $1x10^{-9}$M, $3x10^{-9}$M, $1x10^{-8}$M, $3x10^{8}$M, $1x10^{-7}$M, $3x10^{-7}$M, $1x10^{-6}$M and $3x10^{-6}$M. The vessels were then washed (see Appendix II) and returned to baseline before pre-constricting vessels with $3x10^{8}$M U46619. After 2-5 min (once the vessel reached a steady tension) vessels were subjected to varying doses of acetylcholine (Ach) (Sigma-Aldrich, UK), in 2-min increments at the following final concentrations: $1x10^{-10}$M, $3x10^{-10}$M, $1x10^{-9}$M, $3x10^{-9}$M, $1x10^{-8}$M, $3x10^{-8}$M, $1x10^{-7}$M, $3x10^{-7}$M, $1x10^{-6}$M $3x10^{-6}$M, $1x10^{-5}$M, and $3x10^{-5}$M. Vessels were subjected to washing as before and a relaxation response was then repeated using sodium nitroprusside (SNP) (Sigma-Aldrich, UK), a NO donator, at the following final concentrations: $1x10^{-10}$M, $3x10^{-10}$M, $1x10^{-9}$M, $3x10^{-9}$M, $1x10^{-8}$M, $3x10^{-8}$M, $1x10^{-7}$M, $3x10^{-7}$M, $1x10^{-6}$M, $3x10^{-6}$M, $1x10^{-5}$M, and $3x10^{-5}$M. At the final step, vessels were washed again and 5mL KPSS replaced the PSS in the bath to ensure vessels still exhibited a contractile response that signified they were alive. This procedure was followed as a standard protocol to assess the response to an agonist since a maximal response could be determined from this data. Also, it was possible to calculate the half maximal effective concentration (EC50) by means of spreadsheet calculations and so give an indication of the sensitivity of the tissue to the agonist. Figure 2-3 show an example of raw data trace generated from wire myography protocol using rat mesenteric arteries. Vascular function of the mesenteric arteries was assessed by using U46619 at different concentrations for contraction of the vessels and acetylcholine (Ach) for relaxation.

Data analysis was conducted using LabChart Reader (ADInstruments, Oxford, UK). Mean baseline tension prior to each dose response curve, maximal contractile responses and mean relaxation responses were measured for each agonist concentration. The following equations were used to determine constriction response to U46619:

Normalised diameter (μm) = $\frac{Internal\ circumference\ (IC1)}{\pi}$

Wall tension (mN/mm) = $\frac{Force\ change\ (mN)}{2\ x\ vessel\ length\ (mm)}$

Active Effective Pressure (KPa) = $\frac{Wall\ tension\ (mN/mm)}{(Normalised\ diameter \mu m/2) x\ 100}$

Vasodilation response was expressed as a percentage of KPSS constriction, where 100% was fully constricted. Each dose response curve was also used to determine the EC50. The active effective pressure curves for constriction response were normalised and the relaxation responses were inverted to produce a sigmoidal curve ranging from 0 (100% constriction) to 100 (0% constriction), all response curves were then transformed so that X=log(X) and a non-linear regression analysis conducted. The EC50 values were then subject to further statistical analysis.

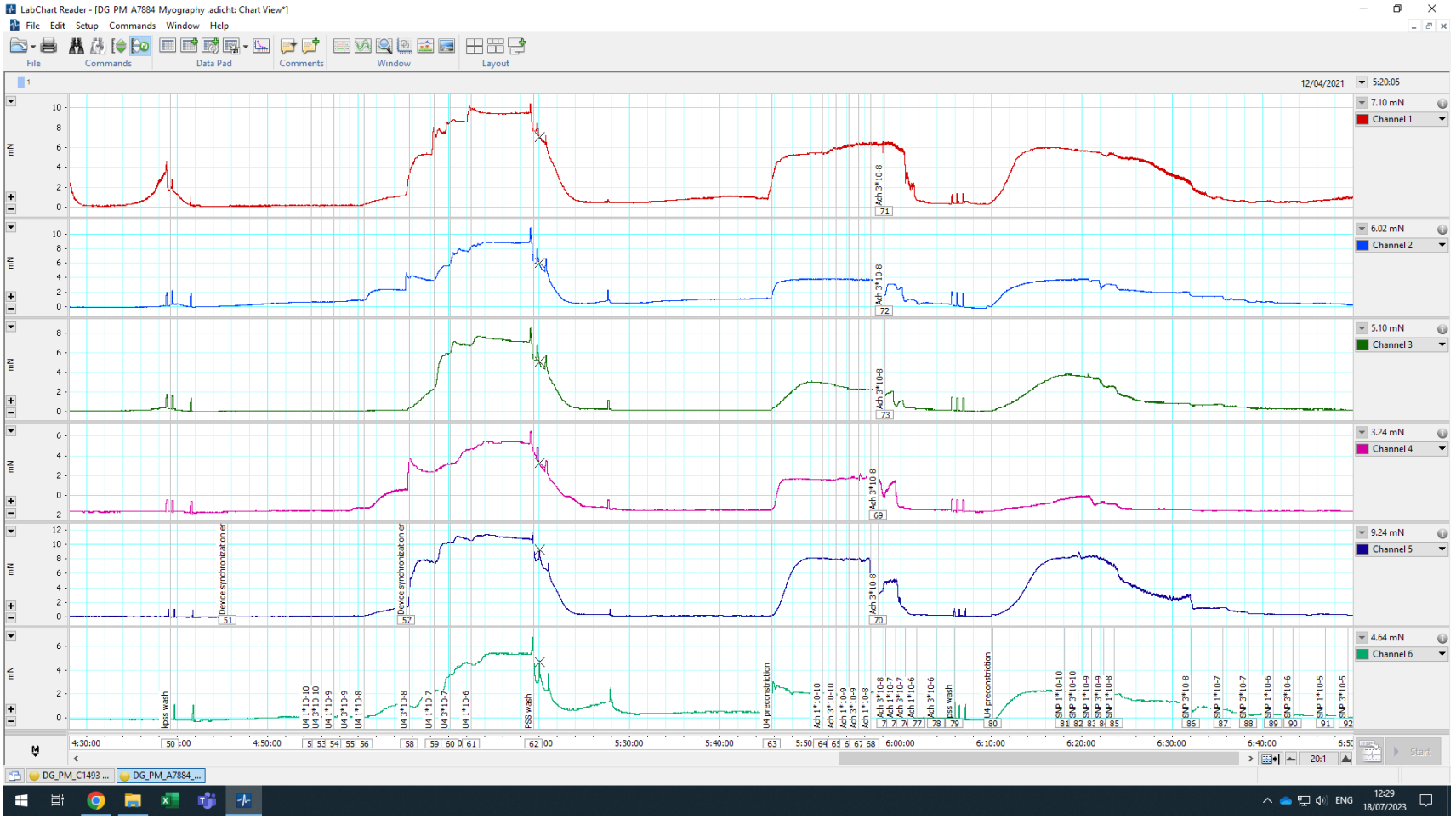

Figure 2-3: A representative of raw trace from wire myography protocol using rat mesenteric resistant arteries.

Six mesenteric arteries were mounted (3 vessels per rat), and their vascular response was challenged twice with KPSS followed by U46619 and relaxation by Ach and SNP.

2.7 Assessment of dietary iodine intake and thyroid hormone profiles

2.7.1 Urinary iodine concentration

Urine samples were collected as described in section 2.3.3.The measurement of UIC was derived from the Sandell- Kolthtoff reaction (Pino et al., 1996). Urine was oxidized with ammonium persulfate. Iodine is the catalyst in the reduction of ceric ammonium sulfate (yellow) to the cerous form (colourless) and is detected by the rate of colour disappearance (Sandell-Kolthoff reaction). A stock of potassium iodate (Sigma-Aldrich® Brand) was used to make serial dilutions of 500 µg/L to 3.9 µg/L in the first set of calibrators while the second set of calibrators was from 300 µg/L to 2.34 µg/L. The two sets of calibrators were preferred to provide a more accurate correction of the sensor output by re-scaling it at two points instead of one. Urine samples (stored at -80^{o}C) were thawed in ice and centrifuged for 1 min at 1000 rpm using a bench top refrigerated centrifuge (VWR international Ltd, UK). 50 µL of calibrators were added to columns 1,2 and 12 of a 96 well heat-resistant polypropylene plate while 50 µL of urine samples and quality controls were added in triplicate to the rest of the wells and their position noted. 100 µL 1.31 mol/L ammonium persulfate (Sigma-Aldrich® Brand) was added to each well before securely sealing the plate with an aluminium plate seal film. The plate was then placed in a heat cassette arranged such that there is a foil at the top and bottom of the plate and placed in an oven set at 100^{o}C for 60 min. The plate was then cooled on ice for 10 min. 50 µL per sample was transferred to 2 clean 96 well plates. The first plate was covered with film and set aside while the second plate had 100 µL 0.875mol/L arsenic acid added before being gently mixed by swirling for approximately 15-20 sec. 50 µL 0.1M ceric ammonium sulfate solution was added within 1 min. 75 sec after the addition of ceric ammonium sulfate the absorbance at 405nm was assessed using a multiscan plate reader (Thermo Fisher, Paisley, UK) every minute for 15 min. The iodine concentration of the unknown samples was determined from standard curve generated from iodine concentration of the calibrators.

2.7.2 Determination of thyroid hormone levels

Animals were sacrificed as described in section 2.4. Following exsanguination, blood was collected into VACUETTE® heparin and EDTA-lined tubes (Greiner Bio-One, Stonehouse, UK) and kept on ice until centrifugation at 3000 rpm for 15 min at 4ºC. Plasma was carefully separated from the red blood cell layer into a 1.5 mL microcentrifuge tubes (STARLAB, Milton Keynes, UK) and stored at -80ºC until use. TH levels were determined using commercially available kits following manufacturers instruction. Briefly, 50 µL fT3, fT4 TSH and Tg standards and plasma samples were added to anti-fT3, fT4, TSH and Tg coated wells. 50 µL of detection reagent A was added to each well and the plate incubated at 37 ºC for 1 hr. The plate was washed 3 times with washing buffer before adding 100 µL of detection reagent B. The plate was then incubated at 37 ºC for 30 mins before washing 5 times. 90 µL substrate was then added to each well and the plate was incubated at 37 ºC for 20 mins before adding stop solution. Absorbance was the determined using a plate reader set at 450 nm. The TH levels in each sample were extrapolated from the standard curve and were expressed as pmol/L, ng/mL and pg/mL for fT3, fT4, TSH and Tg respectively.

2.8 General molecular techniques

2.8.1 Ribonucleic acid (RNA) extraction

RNA extraction was performed on animal tissues snap-frozen at time of sacrifice using Qiagen miRNeasy Mini Kit (Qiagen; Manchester, UK). RWT and RPE buffers were prepared before use by addition of 100% ethanol as per manufacturer's instructions. Tissue was disrupted in liquid nitrogen using mortar and pestle and <30g was homogenized in 700µL QIAzol Lysis Reagent using bead-milling in a Polytron PT2100 Benchtop Homogeniser (KINEMATICA, Luzern, Switzerland) set to 30Hz cycling period for 30 sec repeated twice, placing samples on ice between lysis periods. The tissue homogenate was incubated at room temperature (15-25ºC) for 5 min. Homogenates were shaken with 140µL chloroform then incubated for 2-3 min at room temperature and centrifuged at 12,000xg for 15 min at 4ºC. The upper aqueous phase containing the RNA was transferred to separate tube and mixed with a 1.5x volume of 100% ethanol (aqueous phase was approximately 400µL therefore 600µL ethanol was used).

700µL of the sample was placed onto RNeasy Mini spin column in a 2mL collection tube and centrifuged at 8000xg for 15 sec at room temperature. The flow through was discarded and this step was repeated with the reminder of the sample. DNA digest step was performed using 80µL of DNase I stock solution diluted 1:7 with RDD buffer incubated for 15 min at room temperature. 700µL RWT buffer was added, and samples were centrifuged at 8000xg for 15 sec. Samples were then centrifuged with 500µL RPE buffer at 8000xg for 15 sec, then again with 500µL RPE buffer at 8000xg for 2 min. Membranes were further dried by spinning columns at 13,000xg for 1 min. RNA was eluted from membrane using 40µL RNase-free water and centrifuging at 8000xg for 1 min. RNA concentration and purity were determined using a Nanodrop spectrophotometer (ThermoFisher Scientific, Paisley, UK). Absorbance was read at 260nm (A260) to detect nucleic acids, at 280nm (A280) which identifies protein contaminants, and at 230nm to detect any organic or solvent contamination from the extraction process. A260/A280 ratios of between 1.9 and 2.1 signified appropriate sample purity and samples were stored at -80ºC until needed.

2.8.2 Reverse transcription polymerase chain reaction (RT-PCR)

Complementary DNA (cDNA) was prepared using an input of between 400ng-1000ng RNA using the Super Script II Reverse Transcription kit (ThermoFisher Scientific, Paisley, UK). The RNA sample was diluted to 500ng/µL to a total volume of 20 µL using nuclease free water. 2 µL of the RNA sample was transferred to a labelled 96 well PCR plate (Starlab, Milton Keynes, UK). A negative control (2 µL of nuclease free water) was included. Plates were covered with adhesive PCR plate seal (ThermoFisher Scientific, Paisley, UK). The PCR conditions were set as follows; 70ºC for 10 min (RNA denaturation), 4ºC for 10 min (to allow addition of RT master mix), 42ºC for 1 hr (elongation/strand transfer/RNaseH activity), 72ºC for 15 min (enzyme inactivation) and 4ºC forever. A PCR must mix was prepared as outlined in Table 2-2; 4 µL of 5X superscript II (SSII) buffer, 1 µL of 10mM dNTPs, 1 µL of random hexamers primers (invitrogen N8080127), 1 µL of dTT, 0.5 µL RNAse out ribonuclease INH-(Invitrogen10777.019), 1 µL Superscript II RT and 9.5 µL of nuclease free water. The total volume of the master mix was 18 µL per well. During the 4ºC 10-min step, the plate was removed from the block and 18 µL of RT master mix was added to each well. Following completion of the PCR conditions samples were

then cooled to 4ºC and diluted to an approximate final concentration of 50ng/µL cDNA. Samples were stored at -20ºC until use. End-point PCR reactions were amplified on a MJ Research PTC 225 Tetrad thermal cycler (Marshall Scientific, Hampton NH, USA) using 96-well PCR plates (Starlab, Milton Keynes, UK).

2.8.3 Quantitative real time polymerase chain reaction (qRT-PCR)

The Taqman® assay used a fluorogenic probe, labeled with FAMTM or VICTM dye, specific for the target gene and unlabelled target-specific primers. The assay allowed for the probe to incorporate the double-strand DNA during the PCR. The dye was cleaved in the next cycle and separated from a non-fluorescent quencher. The intensity of fluorescence increased proportionally to the amount of PCR product produced. Assays were prepared in a MicroAmp™ Optical 384-Well Reaction Plate (ThermoFisher Scientific, Paisley, UK) with 2µL cDNA (produced in section 2.8.2 with a final amount of 50ng cDNA per well). Assays utilized a duplex reaction, using a FAMTM-labeled probe for the gene of interest and a VICTM-labeled housekeeper probe (glyceraldehyde-3-phosphate dehydrogenase (GAPDH) (0.25µL of each probe was added to the wells). The final volume was made up of 1x Taqman® Universal Master Mix II to give a total volume of 5µL per well. Table 2-3 gives a summary of qRT-PCR reagents and their volumes. Each assay plate also contained RT control from cDNA synthesis in section 2.8.2 and no RT control which is nuclease-free water added to the qRT-PCR 384 plate. All samples and controls were run in triplicate. Plates were sealed with self-adhesive Advanced Polyolefin StarSeal (STARLAB, Milton Keynes, UK) and centrifuged at 1,000xg for 2 min to ensure reaction components were mixed and in the base of each well. The qRT-PCR reactions were conducted using a QuantStudio 12K Flex Real-Time PCR System (ThermoFisher Scientific, Paisley, UK). mRNA levels were normalized concerning glyceraldehyde-3-phosphate dehydrogenase (GAPDH) and expression levels were calculated using double delta Ct (ΔΔCT) method.

ΔCt = Ct (gene of interest) – Ct (housekeeping gene)

ΔΔCt = ΔCt (Sample) – ΔCt (Control average)

Fold gene expression = 2^-(ΔΔCt)

Table 2-3 RT-PCR master mix reagents and volumes (µL)

Reagent	1 sample	10 samples	20 samples
5X superscript II (SSII) buffer	4µL	40µL	80µL
10mM dNTPs	1µL	10µL	20µL
Random Hexamers primers (invitrogen N8080127)	1µL	10µL	20µL
dTT (comes with SSII)	1µL	10µL	20µL
RNAse out ribonuclease INH-Invitrogen10777.019	0.5µL	5µL	10µL
Superscript II RT (Invitrogen 18064022)	1µL	10µL	20µL
Nuclease free water	9.5µL	95µL	190µL
Total	18µL	80µL	360µL

Reagents and volume for each RT-PCR component is listed for 1, 10 and 20 samples.

Table 2-4: Tagman® master mix reagents and volumes (µL)

Reagent	Volume per sample per well (µL)
Tagman® master cat No 4440040	2.5
SLC5a5 or SLC26a4 probe assay ID Rn01420254_g1 Rn01469208_m1 respectively	0.25
GAPDH probe assay ID Rn01462661_g1	0.25
cDNA	2
Total	5

Reagents and volume for each RT-qPCR component for a single reaction.

2.9 Next generation RNA sequencing (RNA-Seq)

2.9.1 Preparation of samples for next generation RNA sequencing

Rat thoracic aorta total RNA was extracted using same procedure as stated in 2.8.1 above.

2.9.2 Bulk RNA sequencing on thoracic aortas from WKY and SHRSP males fed NID and LID

Following RNA extraction and quantification, 30 µL (250-500 ng/µL) of thoracic aorta, total RNA was labelled and shipped on dry ice to Glasgow Polyomics (Garscube, Glasgow, UK). Following delivery, an operator fragmented RNA to approximately 300 base pair fragments and libraries were prepared using Illumina Truseq Stranded mRNA Sample preparation Kit adapters (Illumina, SanDiego CA, USA). The prepared library was then sequenced on the NextSeq2000 platform in paired end mode 1 at Glasgow Polyomics (Illumina, SanDiego CA, USA).

2.9.3 RNA sequencing data processing steps

Raw sequence reads were trimmed for contaminating sequence adapters and poor-quality bases using the program FastP (Version 0.20.0). Bases with an average Phred score lower than 15 were trimmed. Reads that were trimmed to less than 54 bases were discarded. The quality of the reads was checked using the FastQC program (http://www.bioinformatics.babraham.ac.uk/projects/fastqc/) before and after trimming. The sequenced reads were checked for other species contamination using the Fastq-Screen program (Version 0.13.0), which selects a sample of the reads and aligns them to a selection of reference genomes that are routinely sequenced at Glasgow Polyomics. The quality trimmed reads were aligned to the reference genome using the program Hisat2 (Version 2.1.0) and the read counts using HtSeq Count. The quality control and alignment reports were combined for all samples and presented in one report using the program MultiQC.

The differential expression for the analysis groups was assessed using the Bioconductor package DESeq2. Base mean of gene and transcript expressions

across all groups were determined. Comparisons were made between the strains and treatments for gene level analysis, as illustrated in Figure 4-2.

2.9.4 Ingenuity pathway analysis

Qiagen Ingenuity® Pathway Analysis (IPA) (Qiagen, Manchester, UK) was used to understand the biology in our data set. More details can be found in Chapter 4 section 4.3.2.

2.10 General primary cell culture methods

All cell culture was performed under sterile conditions in a biological safety class II vertical laminar flow hood (Thermofisher Scientific, Paisley, UK). Cells were cultured in a T75 culture flask with vented cups (Corning, Arizona AZ, USA) and were maintained in suitable media at 37^{o}C in a 5% CO_2 and 95% O_2 humidified incubator (Thermofisher Scientific, Paisley, UK). Rat VSMCs were cultured in sterile Corning 6 well plates (Corning, Arizona AZ, USA) for experimentation. Cell culture media was replaced every other day.

2.10.1 Isolation of rat mesenteric artery primary VSMCs

Primary VSMCs derived from mesenteric arteries of 12-week-old male WKY and SHRSP were isolated by collagenase/elastase enzymatic digestion method which is based on a modified version of the protocol described by Yogi and colleagues(Yogi et al., 2011). In brief 3-4 animals were sacrificed as described in section 2.4 and their mesenteric vascular beds were excised and pooled in ice-cold 50 mL falcon tubes containing F12 media (Invitrogen Ltd, Paisley, UK) supplemented with Hepes 25 mM, 100 IU/mL penicillin, 100 µg/mL streptomycin and 10% (v/v) foetal bovine serum (FBS) (Sigma-Aldrich Company Ltd, Dorset, UK). Maximum storage time was 1 hr on ice. Mesenteric beds were gently washed off the remaining blood in cold Dulbecco's phosphate buffered saline (DPBS) in a safety class II vertical laminar flow cabinet and incubated in pre-digestion media (F12 media plus 3 mg/mL collagenase) for 15 min, at 37^{o}C under agitation using a Biometra rotating incubator. The mesentery was placed in a petri dish containing F12 media and cleaned by removing fat, connective tissue, and adventitia. Cleaned mesenteric vascular beds were incubated in digestion media (F12 media supplemented with 10% (v/v) FBS, 3 mg/mL collagenase,

elastase, and 0.72 mg/mL soybean trypsin inhibitor) (7mL/mesenterium) for 60-90 min, at 37°C under agitation using a Biometra rotating incubator. The digested vessel fragments were subsequently passed in progression from 16, 18 to 21-gauge needles to obtain a homogenized solution and filtered through a 100nm nylon filter to remove debris. The filtrate was centrifuged for 5 min at 2000 rpm at room temperature and re-suspended in 5 mL of complete growth media, then 2 mL distributed in a T75 flask containing 10 mL of Dulbecco's modified Eagle medium (DMEM) (Gibco®-Life technologies, U.K.) supplemented with 10% (v/v) FBS. The flasks were then kept in a 5% CO_2 humidified incubator at 37°C (passage 0). Media was replaced after 24 hrs. Cells were cultured up to passage 7.

2.10.2 Culture and passage of rat mesenteric artery VSMCs

VSMCs were maintained in DMEM medium (Gibco®-Life technologies, U.K.) supplemented with 10% FBS (Invitrogen, U.K.), 100 IU/mL pencillin and 100 µg/mL streptomycin (Sigma Aldrich, U.K.) and used for experiments at passage 1 to 4. Cultured cells were passaged at approximately 80-90% confluency, ensuring they were not subject to stress by over or under-confluency. Media was aspirated and cells were washed in DPBS. Cells were incubated in 10% trypsin-EDTA in PBS (700 µL/ 25cm^2), (Thermofisher Scientific, UK) at 37°C for 5 min or until > 90% of cells were detached. The trypsin-EDTA enzymatic reaction was subsequently stopped by the addition of twice the volume of pre-warmed complete culture media. Cells were transferred to a sterile 50 mL conical tube and centrifuged at 1500 rpm for 5 min and at room temperature. The supernatant was removed, and cells were resuspended in complete cell culture media and transferred to a T75 flask containing 10 mL of complete cell culture media or in 6 well plates containing 2mL per well of cell culture media and incubated in a 5% CO_2 humidified incubator at 37°C until the next passage.

2.10.3 Characterization of rat mesenteric artery passaged VSMC

For verification and purity of VSMC phenotype positive immunofluorescent staining (ICC) for SMC specific marker SMC α-actin (ACTA2, polyclonal rabbit-anti rat antibodies; ab5694) was used. Cells at passage 4 were harvested and seeded

onto sterile coverslips in 6 well plates and allowed to attach overnight. The following morning media was removed, and cells were rinsed twice with sterile DPBS and then fixed in 4% (w/v) PFA for 15 min at room temperature and washed 3 times for 5 min each in DPBS. Cells were permeabilized with Triton X-100 (0.1% (v/v) in DPBS) at room temperature for 15 min followed by three 5 min washes. Coverslips were then incubated with 20% (v/v) goat serum/DPBS for 30 min at room temperature followed by a single DPBS wash. Cells were then incubated with the primary antibodies (1:50 anti-ACTA2 in 20% goat serum/DPBS) for 1hr at room temperature. Excess primary antibodies were removed by three 5 min washes in DPBS. Cells were then incubated with secondary FITC-conjugated antibodies (1:200 goat anti-rabbit IgG antibodies in 20% goat serum/DPBS) for 45 min at room temperature. Coverslips were then kept in the dark to prevent photobleaching of samples. Excess secondary antibodies were removed by washing 3 times for 5 min in DPBS. Coverslips were then mounted on a glass slide using Vectashield supplemented with propidium iodide (PI) for nuclei counterstaining. The coverslips were sealed with nail varnish and left to dry overnight at room temperature and stored at 4^{o}C. Cells were then imaged under a Zeiss LSM 510 Meta confocal microscope (Carl Zeiss Ltd, Hertfordshire, UK) with compatible objectives, at 40x and 100x magnifications.

2.10.4 Cryo-preservation of rat passaged VSMCs

Cells were harvested as described above (2.10.2) and resuspended in complete growth medium supplemented with 10% DMSO (Thermo Fisher Scientific, Loughborough, UK) to prevent formation of ice crystals. The cell suspension was aliquoted into sterile 1 mL cryogenic vials and cooled at a constant -1^{o}C /min down to -80^{o}C, using isopropanol in a MrFrosty container (Thermofisher Scientific, Loughborough, UK) kept in a -80^{o}C ultra freezer. After 24 hrs vials were stored in liquid nitrogen tanks until required.

2.10.5 Preparation of whole cell lysates

Following cell treatment and on ice, the cell medium was removed, and cells were washed twice with cold DPBS before adding 100 µL per well of ice-cold cell RIPA lysis buffer (Sigma-Aldrich, Dorset, UK). The cells were scrapped off

vigorously using a plastic cell lifter (Corning, Arizona AZ, USA) and transferred into a labelled pre-cooled 1.5 mL microcentrifuge tubes, then incubated on ice for 30 min. Cells were then sonicated (Thermofisher Scientific, UK) in ice for 30 sec allowing a 30-sec break in between sonication. The cell extracts were centrifuged at 12000 rpm for 12 min at 4^{o}C (Thermo Fisher, Paisley, UK). The supernatants were transferred to fresh microcentrifuge tubes and stored at -80^{o}C until required.

2.11 General protein methods

2.11.1 Determination of protein concentration

Protein concentrations were determined using a Pierce bicinchoninic acid (BCA) protein assay kit following the manufacturer's instructions (Thermo Scientific, UK). Serial dilutions of the provided albumin protein standard, ranging from 20 to 2000 µg/mL, were prepared (in BCA reagent) to generate a concentration standard curve for each assay. BCA working reagent (WR) was prepared by mixing reagents A and B (provided) at a ratio of 50:1. 10 µL of the albumin standards/protein samples / BCA reagent (blank) were added to a 96-well plate, in duplicate. 200 µL of BCA reagent (copper sulphate and bicinchoninic acid) was then added to each well and the plate was thoroughly mixed on a Stuart mini orbital plate shaker set at 60 rpm for 30 sec. Plates were subsequently covered and incubated in Hybaid mini oven at 37^{o}C for 30 min. At this temperature, protein peptide bonds reduce copper ions in the BCA reagent ($Cu^{2+} \rightarrow Cu^{1+}$). Each Cu^{1+} reacts with 2 molecules of BCA to produce a purple-coloured product detectable at 562nm. The colour's optical density (OD) is directly proportional to the amount of protein in a sample. Following incubation, the plate was cooled to room temperature. Absorbance at 562nm was determined using a Spark Tecan microplate reader (Tecan, Männedorf Switzerland). An average value of the two replicates was calculated. The concentration of protein in each sample was calculated from the linear equation of the standard curve by GainData arigo laboratories (https://www.arigobio.com/elisa-analysis).

2.11.2 SDS-PAGE

For each experiment, equal amounts of cell lysate protein (10 µg) (as determined by the BCA Protein Assay) were resolved by SDS-polyacrylamide gel electrophoresis (SDS-PAGE). SDS-PAGE was performed using 1.5 mm thick vertical slab gels containing 12% acrylamide (Seven Biotech Ltd, Kidderminster, Hereford, UK). A 30% acrylamide / bis-acrylamide mixture, 1.5M Tris buffer (pH 8.8) and 10% (w/v) SDS were used to form the gels, which were polymerized by the addition of APS and TEMED (Sigma-Aldrich, Dorset, UK). Slab gels were prepared using Bio-Rad Mini-Protean III gel units (Bio-Rad Laboratories, UK) with a stacking gel approximately 2 cm deep. Cell lysates were mixed with 4X complete sample buffer (New England Biolabs, USA) and heated to 95^{0}C for 5 min in a heating block (VWR International Ltd, Leicestershire, UK) before separation by SDS-PAGE. Bio-Rad Rainbow molecular weight markers were resolved alongside protein samples to allow size estimation of immunoreactive protein bands. Electrophoresis was performed at a constant voltage of 80 V for stacking and up to 150 V through the separating gel for approximately 1 hr or until the tracking dye had migrated to the bottom of the gel and good resolution of the molecular mass markers had been obtained.

2.11.3 Wet protein transfer

Proteins separated by SDS-PAGE (section 2.11.2) were subsequently electro-transferred from the gel onto a Protran nitrocellulose membrane (0.2 µm pore size) (Pall Life Sciences, USA) by a wet transfer. Briefly, sponge, filter paper (GE Healthcare Buckinghamshire, UK), and nitrocellulose membrane were equilibrated in transfer buffer for 10min. Then, they were placed on a transfer apparatus in the following order at the cathode side: sponge, 2 layers of filter paper, then the nitrocellulose membrane, followed by the gel and a further 2 layers of filter paper and a sponge. Air bubbles from in-between the layers were removed; the apparatus lid was placed on before taking the apparatus to the transfer tank containing the transfer buffer and a constant current of 40 mA was applied overnight at room temperature. The nitrocellulose membranes were then removed from the transfer cassette, and the transfer efficiency was determined by the presence and intensity of pre-stained molecular weight

standards. The membranes were then washed with Tris-Buffered saline (TBS) and rinsed with dH_2O.

2.11.4 Revert total protein staining/De-staining.

Total protein was determined by incubating the membranes with a Revert protein stain (LI-COR Odyssey, Lincoln, NE, USA) for 5 min in a shaker and then washed with a revert stain wash solution two times for 30 sec each. The membranes were visualized at a 700 nm channel using an Odyssey Sa infrared imaging system (Li-Cor Biosciences UK Ltd, Cambridge, U.K). The nitrocellulose membranes were rinsed in dH_2O before incubation with destain for 10 min for complete removal of the revert stain. Following the destain stage, nitrocellulose membranes were washed with dH_2O before washing with TBS 3 times for 5 min each.

2.11.5 Membrane blocking and antibody incubation.

To prevent non-specific binding, nitrocellulose membranes were blocked by incubation with shaking in TBS supplemented with 5% (w/v) milk protein (Premier International Food, Cheshire, UK) for 30 min at room temperature. Nitrocellulose membranes were washed with TBST (3 x 5 min) before incubation with primary antibody diluted in TBST containing 5% (w/v) BSA (Sigma-Aldrich Ltd, Dorset, UK) or milk proteins with shaking, at 4^{0}C overnight. Following primary antibody overnight incubation, membranes were washed (3 x 5 min) in TBST, before the appropriate IRDye®-conjugated secondary antibody (diluted the same way as in the primary antibody) was added (Table 2-4), and incubated at RT for 1 hr, in the dark, with shaking. The membranes were then washed (3 x 5 min) in TBST followed by (1 x 5 min) TBS. Immunolabelled proteins were visualized using infrared dye-labeled secondary antibodies (Table 2-5) and an Odyssey Sa infrared imaging system (Li-Cor Biosciences UK Ltd, Cambridge, U.K.).

Table 2-5: Primary antibodies for western blotting

Epitope (Clone)	Host species	Dilution	Supplier (Cat NO)
MLC2	Rabbit	1:1000	Cell Signalling technology, Massachusetts, USA (#8505)
Phospho-MLC2	Rabbit	1:1000	Cell Signalling technology, Massachusetts, USA (#95777)
TBXA2R	Rabbit	1:2000	Proteintech, 6 Atherton, Manchester, UK (#27159-1-AP)
SLC5a5	Rabbit	1:1000	Proteintech, 6 Atherton, Manchester, UK (#224324-1-AP)

Table 2-6: Secondary antibody for western blotting

Conjugate	Epitope	Host species	Dilution	Supplier (Cat NO)
IRDye® 800CW	Rabbit	Donkey	1:5000	LI-COR Biosciences, Lincoln, NE, USA (#926-32213)

2.11.6 Stripping nitrocellulose membrane for re-probing

Nitrocellulose membranes were stripped by incubating in a stripping solution (0.2 M NaOH) for 15 min at room temperature with shaking. Membranes were then washed 3 times for 5 min washes in TBST followed by 1 time 5 min wash in TBS so they could be re-blocked and re-probed.

2.11.7 Densitometric quantification of protein bands

Images were exported from the LI-COR Odyssey® Sa imaging program to Empiria Studio® Software (LI-COR Bio Sciences, Lincoln, NE, USA). Densitometric quantification of protein bands was expressed as a ratio of phospho-specific immunoreactivity/total immunoreactivity as indicated.

2.12 Statistical analysis

Animals were randomly assigned to treatment groups and ARRIVE guidelines were followed for all *in vivo* studies. Results are presented as a mean ± standard deviation (SD) unless stated otherwise. In general, statistical analyses were performed using one way and two-way ANOVA followed by Tukey post-hoc test (GraphPad Software Inc. San Diego. CA, USA). $P< 0.05$ was considered as statistically significant. The actual statistics used for each set of analysis are provided in the relevant chapter.

Chapter 3 Impact of short-term low dietary iodine on cardiovascular disease parameters in the SHRSP rat independent of thyroid hormone.

3.1 Introduction

Understanding the role of nutrition in the fight against CVD continues to be an important area of research, and evidence shows the effectiveness of healthy dietary patterns and lifestyle for the prevention of CVD. Low-salt and low-fat diets are among the lifestyle modifications recommended for people at high risk of CVD. Even though scientific evidence supports the association between high salt intake and high cholesterol diet in CVD, the polygenic nature of hypertension requires a holistic understanding of potential causes and risk factors, some of which might have been overlooked. Iodine deficiency may be one of these risk factors. It is difficult to distinguish the individual effects of iodine and TH on the CVS and CVD outcomes since the two are closely related. The role of TH on cardiovascular function is well researched and understood, however, there is limited literature on the direct effect of iodine on the CVS independent of TH.

Over two billion people live in areas with iodine insufficiency (Andersson et al., 2012). In spite of remarkable progress in the control of iodine deficiency , with many countries adopting strategies such as universal salt iodization, it remains a significant global problem in vulnerable populations, such as those diagnosed with hypertension (Tayie & Jourdan, 2010). Iodine is an essential microelement used for synthesizing TH. Thyroid iodide uptake through the SLC5a5 and SLC26a4 is regulated by TSH which is secreted by the anterior pituitary gland in response to feedback from circulating TH (Chiamolera & Wondisford, 2009). Iodine deficiency has multiple adverse effects in humans, termed IDD, due to inadequate TH production (Zimmermann, 2009). IDD are frequently reported in CVD and alongside cardiovascular risk factors such as hypertension, obesity, and atherosclerosis suggesting a strong correlation with cardiovascular health (Harvey et al., 2017; Morcos et al., 1998). Iodine deficiency and excess cause thyroid dysfunction such as hypothyroidism and hyperthyroidism which are both associated with increased CVD risk factors. Given that iodine deficiency is the leading cause of hypothyroidism (Zimmermann & Boelaert, 2015), iodine

deficiency could be an independent risk factor of hypertension especially in settings where iodine intake is insufficient

Despite our knowledge of the role of iodine in TH synthesis and its significant antioxidant and anti-inflammatory effects, little is known about its effects on cardiovascular function independent of TH. As mentioned, much of the previous research in this area has focused on the indirect effects of iodine mediated through TH. Findings of a direct link between iodine and cardiovascular function are limited because previous studies in humans involved participants with thyroid dysfunction and therefore it is difficult to separate the direct effects of iodine from that of thyroid dysfunction. However, emerging evidence suggests that iodine can directly affect cardiovascular function and impact on disease outcomes independent of TH profiles (Menon et al., 2011; Tran et al., 2017; Zhao et al., 2011). In support of this, SLC5a5 expression has been discovered in extrathyroidal organs such as the heart and kidney suggesting roles for iodine in non-thyroid tissues/organs (Rakoczy et al., 2016). Circulating low iodine levels have been associated with several risk factors for CVD, including hyperlipidemia and insulin resistance, in both animal and human studies (Al-Attas et al., 2012; Lee et al., 2016; Zhao et al., 2011). In addition, low iodine levels have also been associated with an increased risk of gestational hypertension (Cuellar-Rufino et al., 2017). Furthermore, human population studies have concluded that lower levels of UIC are associated with higher SBP levels independent of thyroid function (Song et al., 2022). Suggested mechanisms of iodine action on CVS include stimulation of nitric oxide (NO) from endothelial cells (Morcos et al., 1998) and acting as an antioxidant counteracting ROS (Harvey et al., 2017).

While the association between iodine deficiency and cardiovascular function has been suggested, it lacks supportive evident in terms of the molecular mechanisms underlying CVD. However, due to ethical restrictions in humans, investigations of the mechanisms underlying the effects of iodine on the CVS require to be carried out in pre-clinical models. Inbred rodent models, and particularly rat models of hypertension, which have very well characterised cardiovascular parameters are ideal for such investigations. The SHR and SHRSP are well-characterized experimental models for human primary hypertension and endothelial dysfunction (Small et al., 2016). These rat strains have proved

useful in studies of stroke, vascular function, autonomic regulation, renal function, therapeutic interventions, and the genetics of primary hypertension (Nabika et al., 2012). However, both the SHR and SHRSP have not been utilised for dietary iodine manipulation and thyroid function studies and therefore literature is limited in these areas. Little is known about TH profiles in SHRSP rats however it has been reported that the plasma T3 levels between the SHR and WKY males are not significantly different (Krupp et al., 1977). It has also been reported that no sex differences exist in levels of TSH, fT3 and Ft4 in WKY rats (Zabka et al., 2011). Despite both SHR and SHRSP being suitable for this study, SHRSP rat strain was chosen since it was readily available in the University of Glasgow, it is characterized in detail and shows more severe cardiovascular disease phenotype than the SHR strain.Although the SHRSP is a well-established model of primary hypertension, it is necessary to establish baseline levels of thyroid function in this model before commencing to modulate dietary iodine studies. To elucidate the involvement of LID in the development of CVD, we measured cardiac and hemodynamic parameters in addition to vascular function in male and female WKY and SHRSP fed NID and compared them to male and female WKY and SHRSP fed LID. To determine whether the effect of low dietary iodine is sex dependent, both male and female WKY and SHRSP were included in this study. The Home Office and local ethics committee also encourages investigations to be conducted in both sexes. The findings of this research will shed light on the individual effect of iodine on CVD outcomes independent of TH profiles.

3.2 Hypothesis and Aims

3.2.1 Hypothesis

Short-term dietary intervention to alter iodine intake will not influence thyroid function but will alter cardiovascular function. In WKY and SHRSP rats, low dietary iodine will cause BP elevation, left ventricular hypertrophy and vascular dysfunction. Low dietary iodine will result in exacerbated CVD outcomes in both males and female SHRSP when compared to WKY rats.

3.2.2 Aims

1. To establish baseline levels of plasma TSH, fT4, fT3 and Tg and UIC in WKY and SHRSP male and female rats.

2. To assess plasma TSH, fT4, fT3 and Tg and UIC in WKY and SHRSP males and females under normal and low iodine dietary conditions.

3. To assess vascular function and cardiac parameters including haemodynamic changes to LID in WKY and SHRSP male and female rats.

4. To determine SLC5a5 and SLC26a4 expression in thyroid, thoracic aorta, and heart tissues of WKY and SHRSP males and females under normal and low iodine dietary conditions.

3.3 Materials and methods

3.3.1 Experimental animals

Male and female WKY and SHRSP from the University of Glasgow colonies were started on a LID or maintained on NID from 5 wks of age (n=7-8 rats per strain, sex, and diet). The rats were started on their respective diet at 5 to 9 weeks of age to determine the effect of low dietary iodine on cardiovascular parameters during developmental stages into early adult life. NID consisted of Rat and Mouse No. 1 Maintenance Diet 10mm compressed, (Special Dietary Services) (see Appendix I, Supplementary Table 1 for details of dietary composition). LID was a modified version of Rat and Mouse No. 1 Maintenance Diet 10mm compressed (Special Diet Services), which was modified by the manufacturer to remove as much of the iodine content as possible (See Appendix I, supplementary Table 2 for details of dietary composition). Iodine content assessed by the manufacturer for our three batches of diet was 0.211, 0.029 and 0.097 mg/kg in the LID and 1.2 mg/kg in the NID (see Appendix 1, Supplementary Figure 1 to Figure 3). The diets were the same colour, form, and texture. Animals were housed as described in section 2.2.3. Water consumption and urine collection was done at pre-diet (5 wks of age), 2 wks of diet (7 wks of age) and 4 wks of diet (9 wks of age) using metabolic cage as outlined section 2.3.3. BW was recorded weekly from pre-diet to 4 wks of diet. Percentage (%) BW change per wk was determined by subtracting the previous wk BW from the current wk BW/current wk BW then multiplying by 100. SBP measurements were done at pre-diet (5 wks) and weekly through the 4-wk dietary period as described in section 2.3.1. Echocardiography was conducted as described in section 2.3.2.

3.3.2 Urinary iodine concentration

Urine samples were collected as described in section 2.3.3. UIC was determined at pre-diet and 4 wks post diet as described in section 2.7.1.

3.3.3 Tissue harvesting

Animals were sacrificed and tissues harvested as described in section 2.4. Plasma samples were prepared as described in section 2.7.2.

3.3.4 Measurement of thyroid hormone levels

Plasma samples from WKY and SHRSP male and female rats were prepared as described in section 2.7.2. TSH assay was carried out using a rat thyroid stimulating hormone (TSH) ELISA kit (Catalog No: abx055103, Abbexa Ltd, Cambridge, UK) as described in the manufacturer's instructions for use. fT4, fT3 and Tg measurements were done using a rat free thyroxine ELISA kit (Novus Biologicals NBP2-60000), a rat free tri-iodothyronine ELISA kit (Novus Biologicals NBP-60011) and a rat thyroglobulin ELISA kit (Novus Biologicals NBP3-08184) respectively according to the manufacturer's instructions for use. The concentration of TSH, fT3, fT4 and Tg was estimated from the linear equation of the standard curve by GainData arigo laboratories (https://www.arigobio.com/elisa-analysis).

3.3.5 SLC5a5 and SLC26a4 gene expressions

Thyroid, thoracic aorta and heart (left ventricle) were harvested as described in section 2.4. RNA extraction and cDNA synthesis were as described in section 2.8.1 and 2.8.2 respectively while quantitative polymerase chain reactions (qPCR) were performed as described in section 2.8.3.

3.3.6 Statistical analysis

All data are reported as the mean ± SD. Statistical comparisons of parameters between and within groups were determined using student t-tests or 1-way or 2-way ANOVA followed by Tukey's post-hoc-test, as appropriate. $P < 0.05$ was considered significant. U46619 dose response curves were constructed using nonlinear regression and analysed using area under the curve (AUC). Descriptive data analysis and graphical representation was completed using GraphPad Prism 9 software (GraphPad Software Inc. San Diego. CA, USA).

3.4 Results

3.4.1 Assessment of thyroid hormone profiles and urinary iodine concentration in male and female WKY and SHRSP fed normal and low iodine diet.

3.4.1.1 Baseline thyroid hormone profile and urinary iodine concentration

Baseline TSH in males and females (Figure 3-1 A and B respectively), fT4 (Figure 3-1 C), fT3 (Figure 3-1 D) and Tg Figure 3-1 E) showed no significant differences between SHRSP and WKY males and females respectively. We could not compare TSH levels between males and females because they were done on different ELISA plates and at different times, however baseline TSH, fT4. fT3 and Tg were not significantly different between the strains (Figure 3-1 A-E).

There was no significant difference in UIC at pre diet (baseline) in male and female WKY and SHRSP, however females have slightly higher UIC compared to males (Figure 3-2 A and B).

3.4.1.2 Thyroid hormone profile and urinary iodine concentration at 4 weeks of diet

Following feeding of the respective diets for 4 wks, rats that were fed LID had a significantly reduced UIC compared to those fed NID irrespective of rat strain and sex (Figure 3-2 A and B).

At 4 wks of diet, TSH levels significantly increased in SHRSP males (Figure 3-3 A 3.4.1)($p < 0.001$) and females (Figure 3-3 B) ($p < 0.05$) fed LID but not in WKY when compared to strain, sex- and age-matched rats fed NID. fT3 and fT4 were not significantly influenced by LID in male and female WKY and SHRSP rats (Figure 3-3 C-F). Tg levels were not significantly different between the treatment groups in male and female WKY and SHRSP rats, however there is a trend which suggests possible strain differences in both male and females (Figure 3-4 A and B respectively).

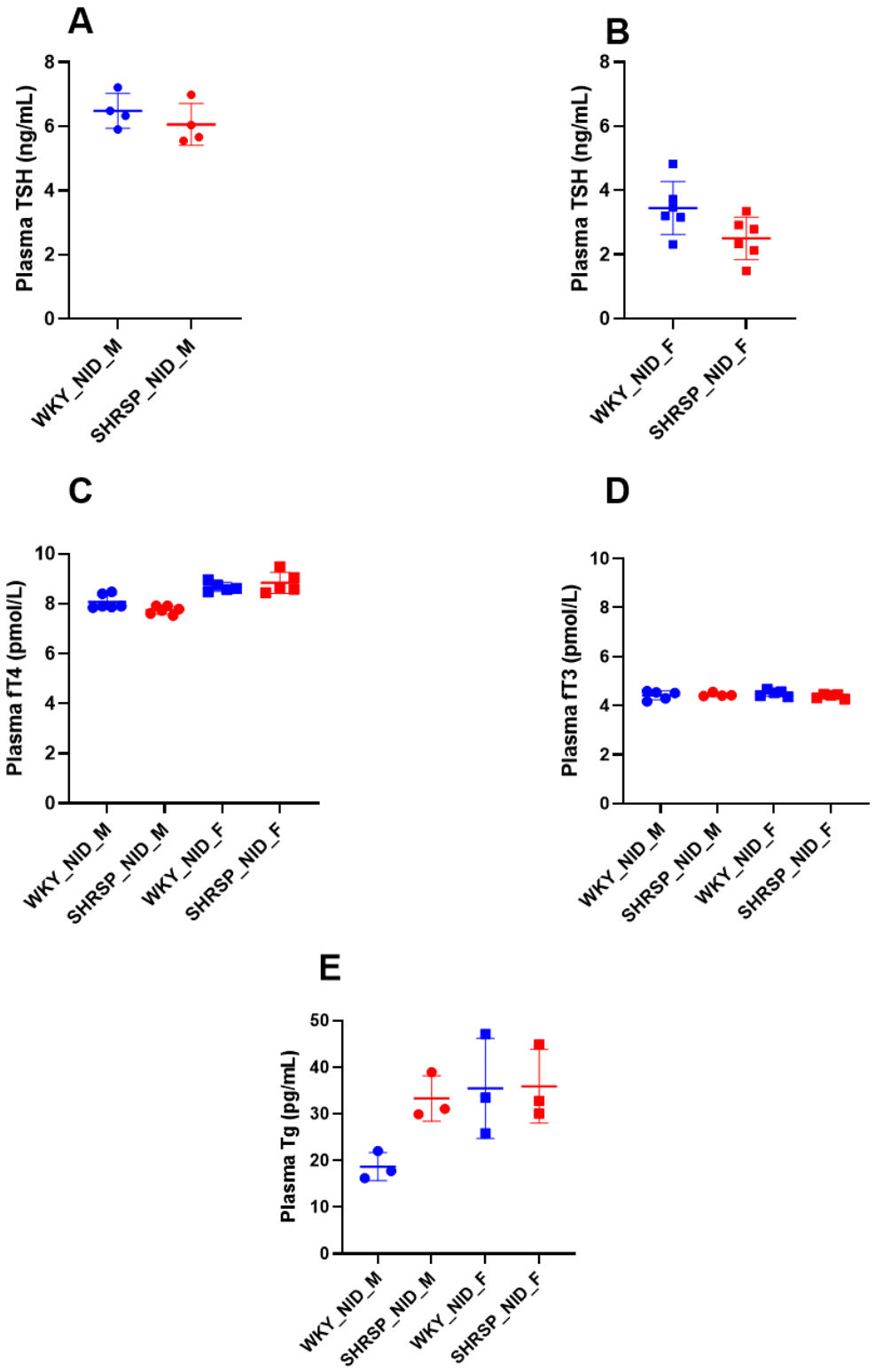

Figure 3-1: Baseline thyroid hormones profiles.

Thyroid stimulating hormone (TSH) in males (**A**) and females (**B**), free thyroxine (fT4) (**C**), and free-triiodothyronine (fT3) (**D**) and thyroglobulin (Tg) (**E**) in male and female WKY and SHRSP rats fed a normal iodine (NID) at 5 wks of age. Data was generated using ELISA kit. All values are reported as mean ± SD (n=3-6 per group).

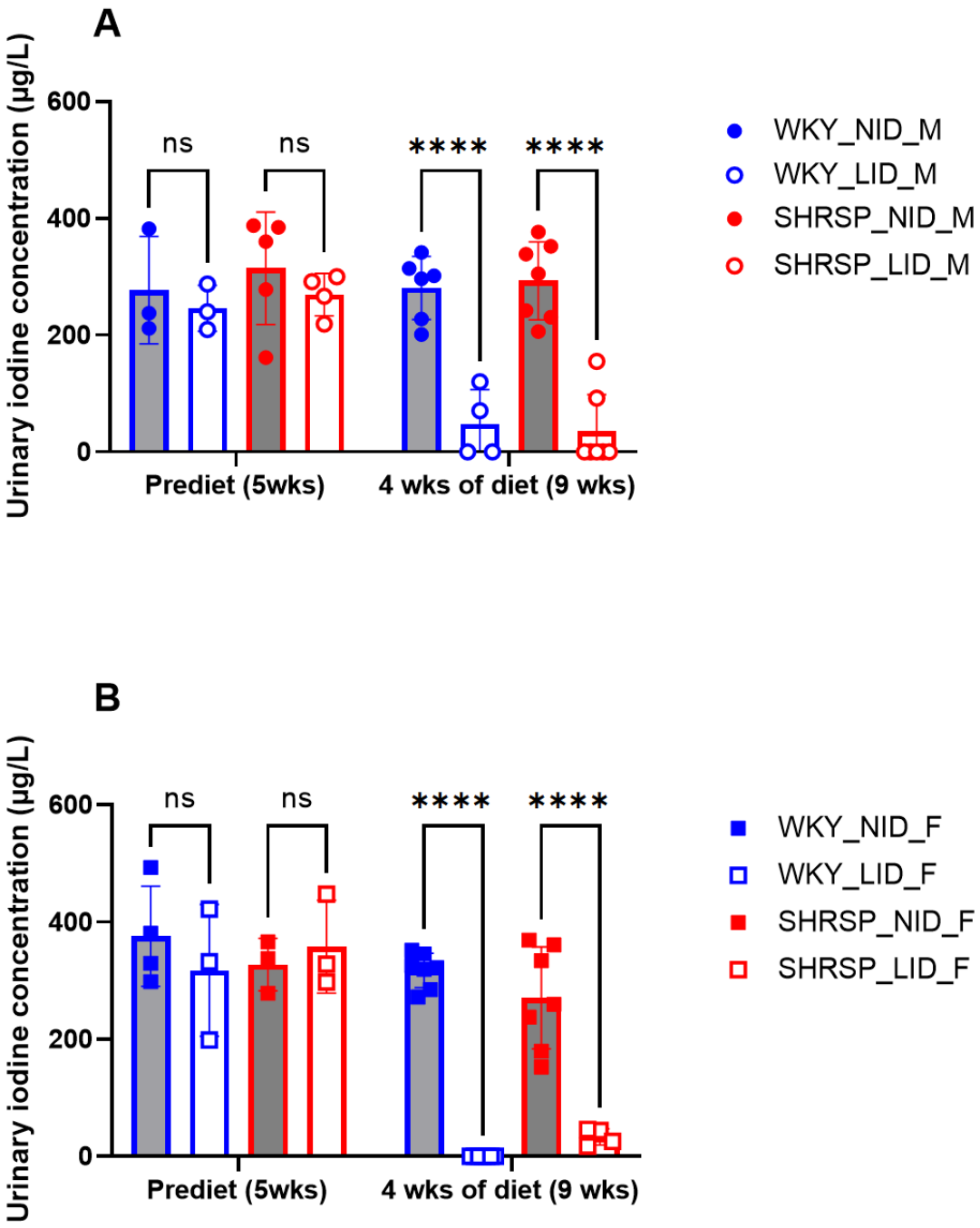

Figure 3-2: Urinary iodine concentration (UIC).

UIC in male (**A**), female (**B**), WKY and SHRSP rats fed normal iodine diet (NID) or low iodine diet (LID) at prediet and 4 wks of diet. UIC were determined using a modification of the Sandell-Kolthtoff reaction. All values are reported as mean ± SD (n=3-7 per group). Two-way ANOVA followed by Tukey's multiple comparison were used to determine significance. ****$p < 0.0001$.

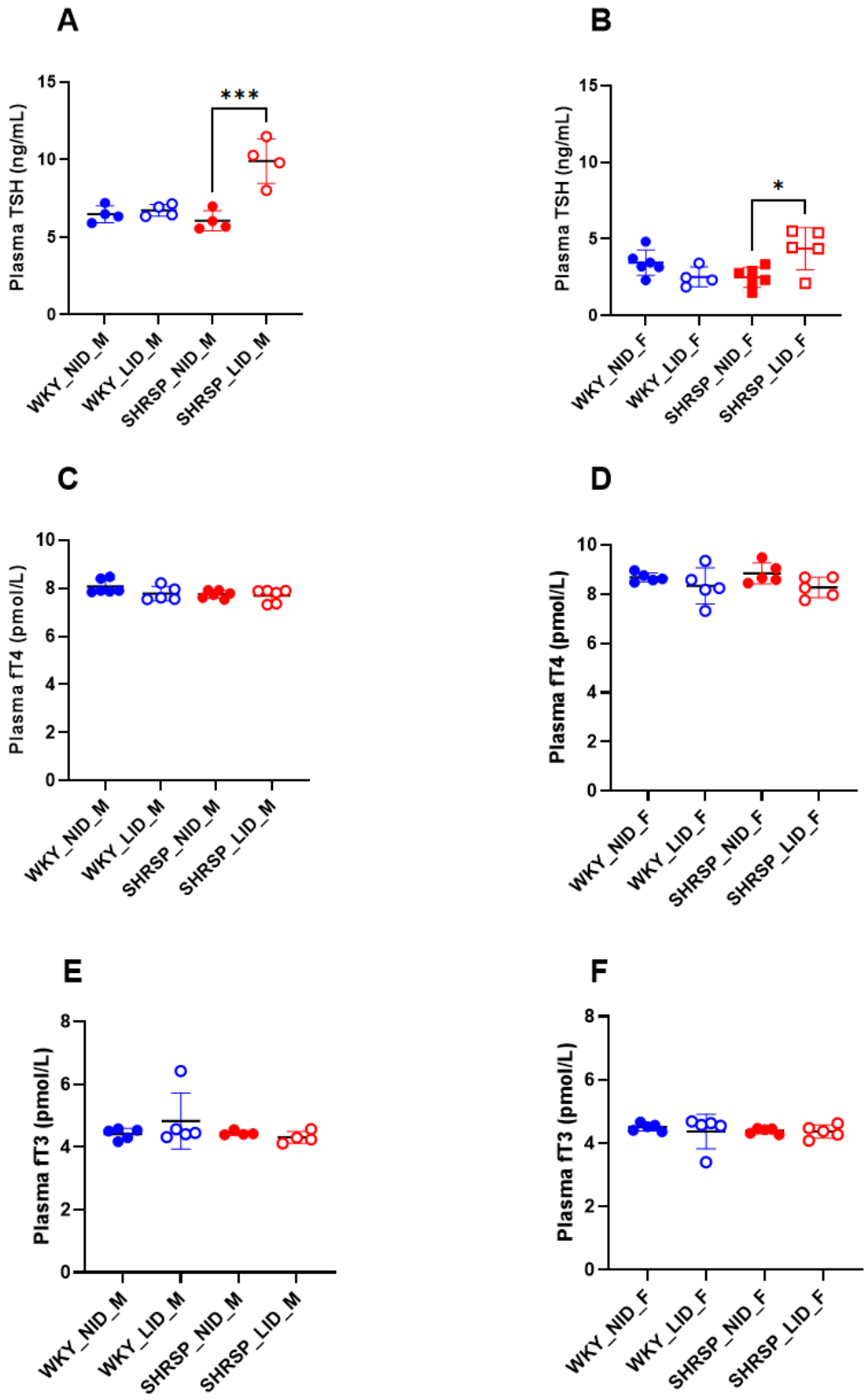

Figure 3-3: Thyroid hormone levels at 4 weeks of diet.

Plasma levels of thyroid stimulating hormone (TSH) in males (**A**) and females (**B**), free thyroxine (fT4) in males (**C**) and females (**D**) and free-triiodothyronine (fT3) in males (**E**) and female (**F**) WKY and SHRSP rats fed a normal iodine (NID) or low iodine diets (LID) at 4 wks of diet. Data was generated using ELISA kits**.** All values are reported as mean ± SD (n=4-6 per group). Ordinary one-way ANOVA followed by Tukey's multiple comparison were used to determine significance. *$p < 0.05$, ***$p < 0.001$**.**

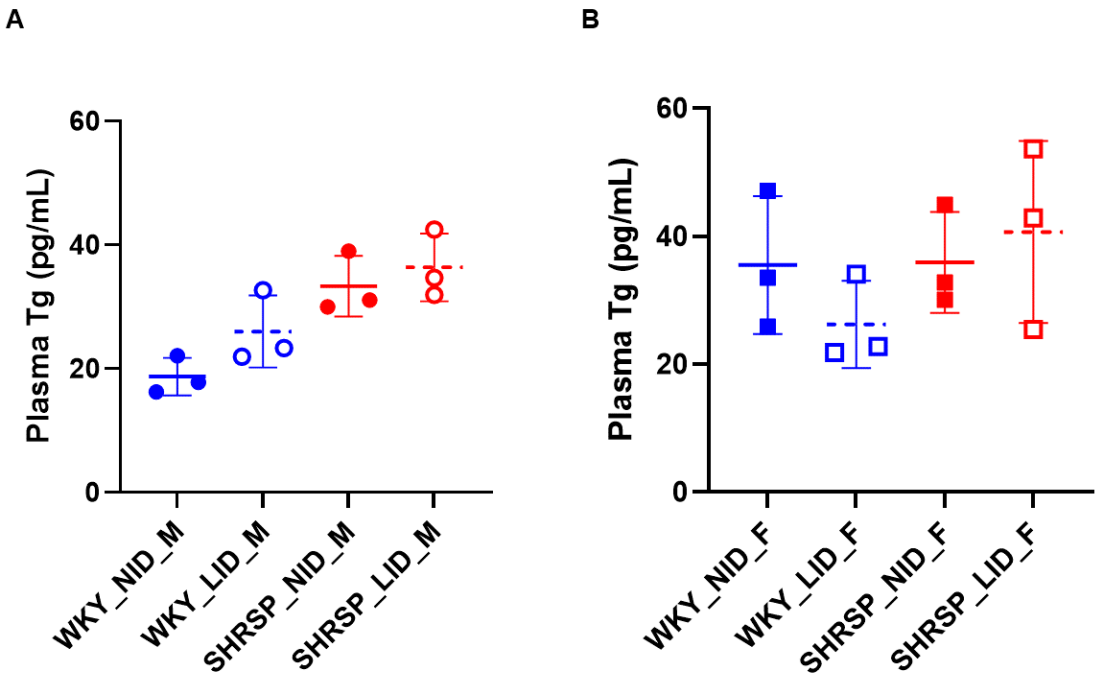

Figure 3-4: Plasma thyroglobulin (Tg) levels.

Tg levels in males (**A**) and female (**B**) WKY and SHRSP rats fed a normal iodine (NID) and low iodine diet (LID). Data was generated using ELISA kit. All values are reported as mean ± SD (n=3 per group).

3.4.2 Impact of dietary iodine manipulation on metabolic parameters in WKY and SHRSP rats

3.4.2.1 Impact of low iodine diet on food consumption and body weight

LID did not influence 24-hr food consumption (Figure 3-5 A and B), BW changes (Figure 3-5 C and D) and % BW gain (Figure 3-5 E and F) in male and female WKY and SHRSP rats. SHRSP males tended to eat less at 5 wks of age (pre-diet stage) although this was not significantly different when compared to WKY males of same age (Figure 3-5 A). WKY males and females had a significantly increased BW compared to sex and age matched SHRSP irrespective of diet (Figure 3-5 C and D) ($p < 0.0001$).

3.4.2.2 Impact of low iodine diet on fluid homeostasis

Water intake increased steadily in males and females irrespective of rat strain and diet (Figure 3-6 A and B). WKY males and females fed LID had a significantly increased urine output when compared to sex matched SHRSP fed LID (Figure 3-6 C and D, $p < 0.05$ and $p < 0.001$ respectively). A trend towards decreased 24-hr urine output was observed at 4 wks of diet in SHRSP females fed LID when compared to SHRSP females fed NID ($p = 0.3309$) (Figure 3-6 D). The difference between SHRSP females on NID and LID was further illustrated, though not significant, when fluid balance was expressed as a ratio of water intake/urine output ($p = 0.1355$) (Figure 3-6 F).

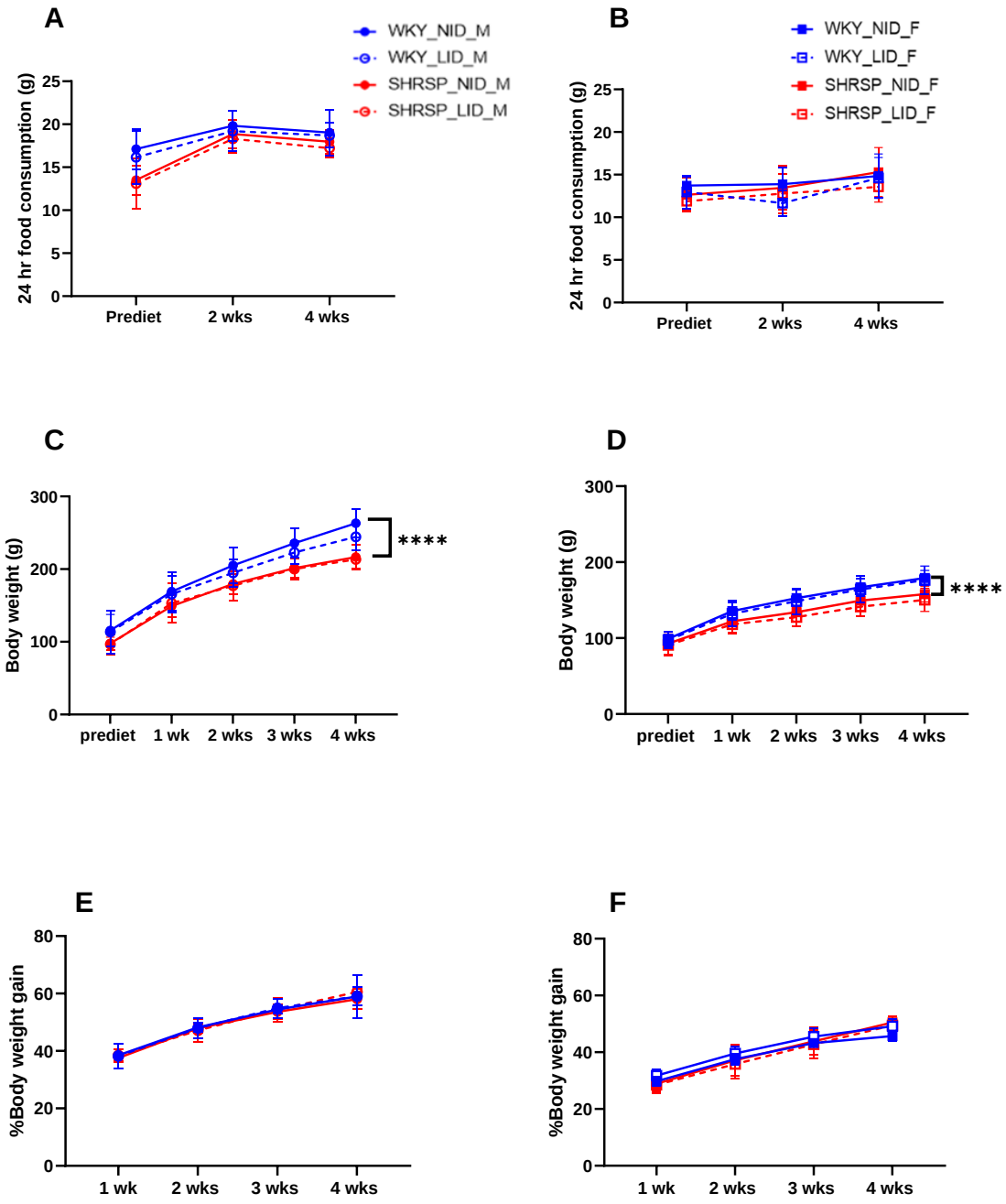

Figure 3-5: Food consumption and body weight (BW) changes in WKY and SHRSP rats.

Food consumption (g) in males (**A**) and females (**B**), BW (g) in males (**C**) and females (**D**) and % BW gain in males (**E**) and (**F**) in WKY and SHRSP fed a normal (NID) or low iodine diet (LID) at prediet, 1,2 ,3 and 4 wks of diet. All values are reported as mean ± SD (n=6-8 per group). Two-way repeated ANOVA followed by Tukey's multiple comparison were used to determine significance. ****$p < 0.0001$.

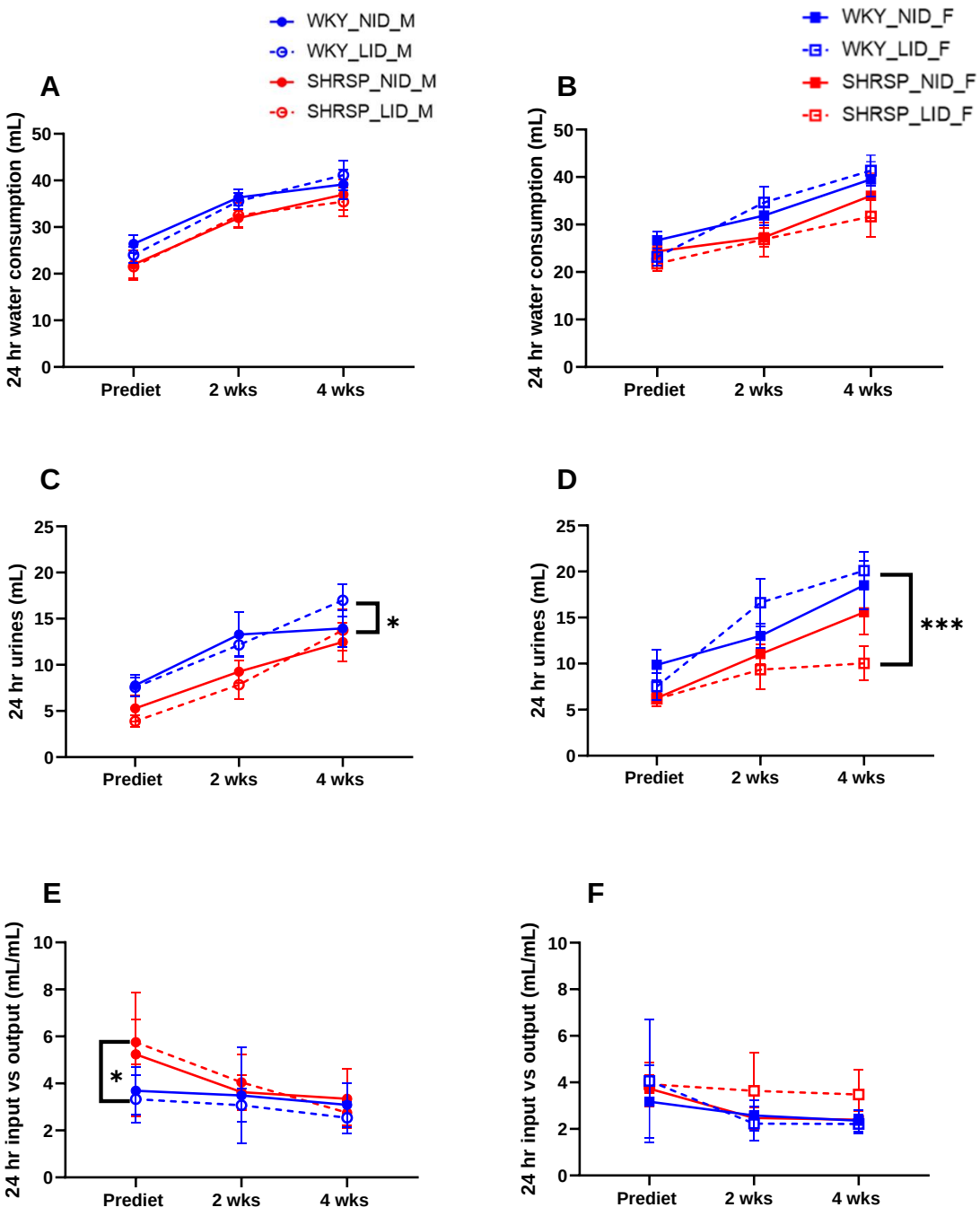

Figure 3-6: Fluid balance in WKY and SHRSP rats.

24-hr water consumption (mL) in males (**A**) and females (**B**), urine production (mL) in males (**C**) and females (**D**) and water intake vs urine output (mL/mL) in males (**E**) and females (**F**) WKY and SHRSP fed a normal (NID) or a low iodine (LID) diet at prediet,2 and 4 wks of diet. All values are reported as mean ± SD (n=5-7 per group). Two-way repeated ANOVA followed by Tukey's multiple comparison were used to determine significance. *$p < 0.05$, ***$p < 0.001$.

3.4.3 Effect of low iodine diet on cardiovascular parameters and hemodynamic changes

3.4.3.1 Influence of low dietary iodine on systolic blood pressure

Both WKY and SHRSP males and females were normotensive at 5 wks of age (pre-diet) (Figure 3-7 A and B) and BP started increasing 2 wks post diet (7 wks of age) in SHRSP males and females. BP increased significantly in the SHRSP males and females irrespective of diet when compared to sex matched WKY (Figure 3-7 A and B) ($p< 0.0001$). Diet did not influence BP in WKY and SHRSP males and females.

3.4.3.2 Cardiac function in response to low iodine diet

WKY males had significantly increased SV ($p< 0.05$) and CO ($p< 0.05$) when compared to SHRSP irrespective of diet (Figure 3-8 A and C respectively). The same observation was made in females where WKY females had a significantly increased SV ($p < 0.001$) and CO ($p< 0.0001$) when compared to SHRSP (Figure 3-8 B and D) irrespective of diet. LID did not significantly influence SV and CO in any of the strain/sex groups. A trend towards reduced SV and CO was observed in males fed LID irrespective of rat strain ($p = 0.7884$) (Figure 3-8 A and C).

There were no significant differences in %EF (Figure 3-9 A and B) and %FS (Figure 3-9 C and D) in male and female WKY and SHRSP rats in response to LID. Strain and diet did not influence RWT and LVMI in male and female WKY and SHRSP rats (Figure 3-10 A-D respectively). However, SHRSP males had a slightly increased RWT and LVMI when compared to WKY irrespective of diet after 4 wks of treatment (Figure 3-10 A and C).

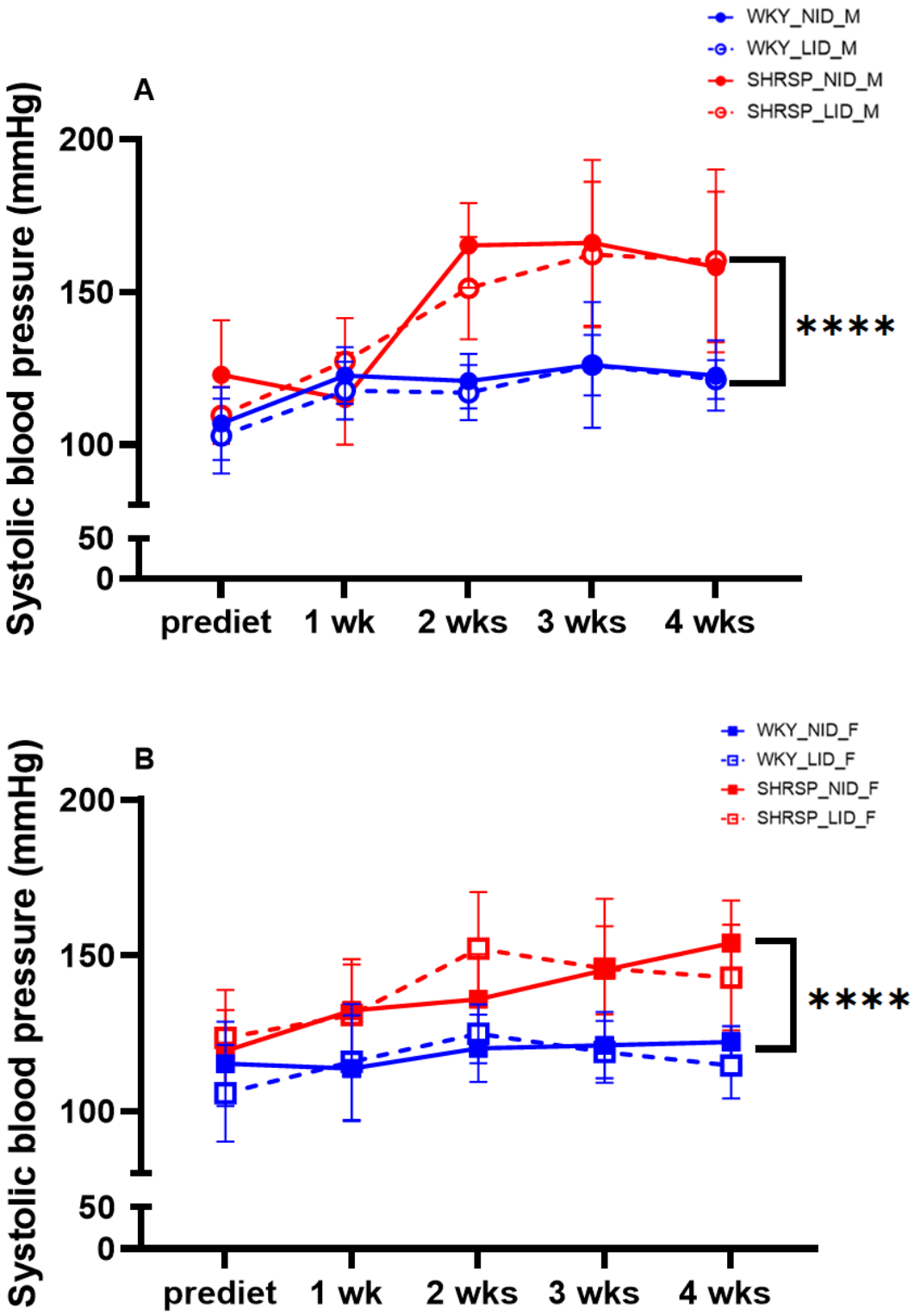

Figure 3-7: Systolic blood pressure (SBP) by tail cuff plethysmography.

SBP in males (**A**) and female (**B**) WKY and SHRSP rats fed normal (NID) or low iodine diet (LID) at pre-diet, 1, 2,3 and 4 wks of diet. All values are reported as mean ± SD (n=4-6 per group). Two-way repeated ANOVA followed by Tukey's multiple comparison were used to determine significance. ****$p < 0.0001$

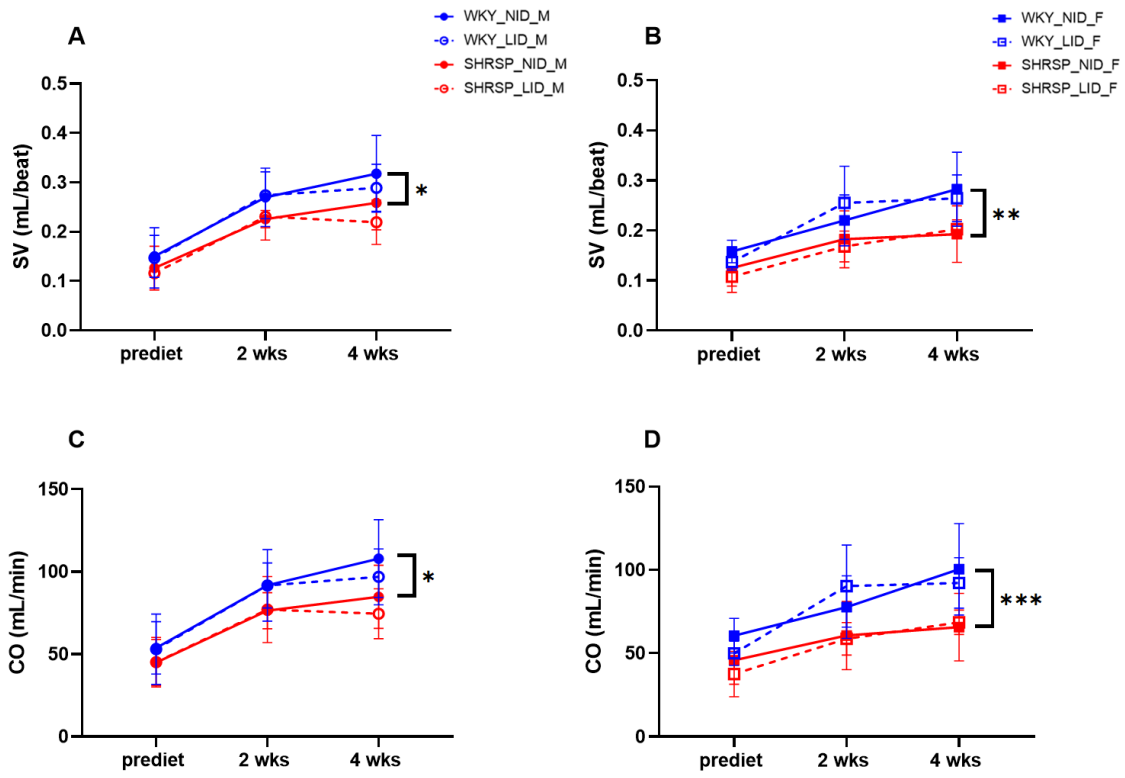

Figure 3-8: Cardiac function by echocardiography.

Stroke volume (SV) in males (**A**) and female (**B**) and cardiac output (CO) in males (**C**) and female (**D**) WKY and SHRSP rats fed a normal (NID) and a low iodine diet (LID) at prediet, 2 and 4 wks of diet. All values are reported as mean ± SD (n=6-8 per group). Two-way repeated ANOVA followed by Tukey's multiple comparison were used to determine significance. *$p < 0.05$, **$p < 0.01$, ***$p < 0.001$.

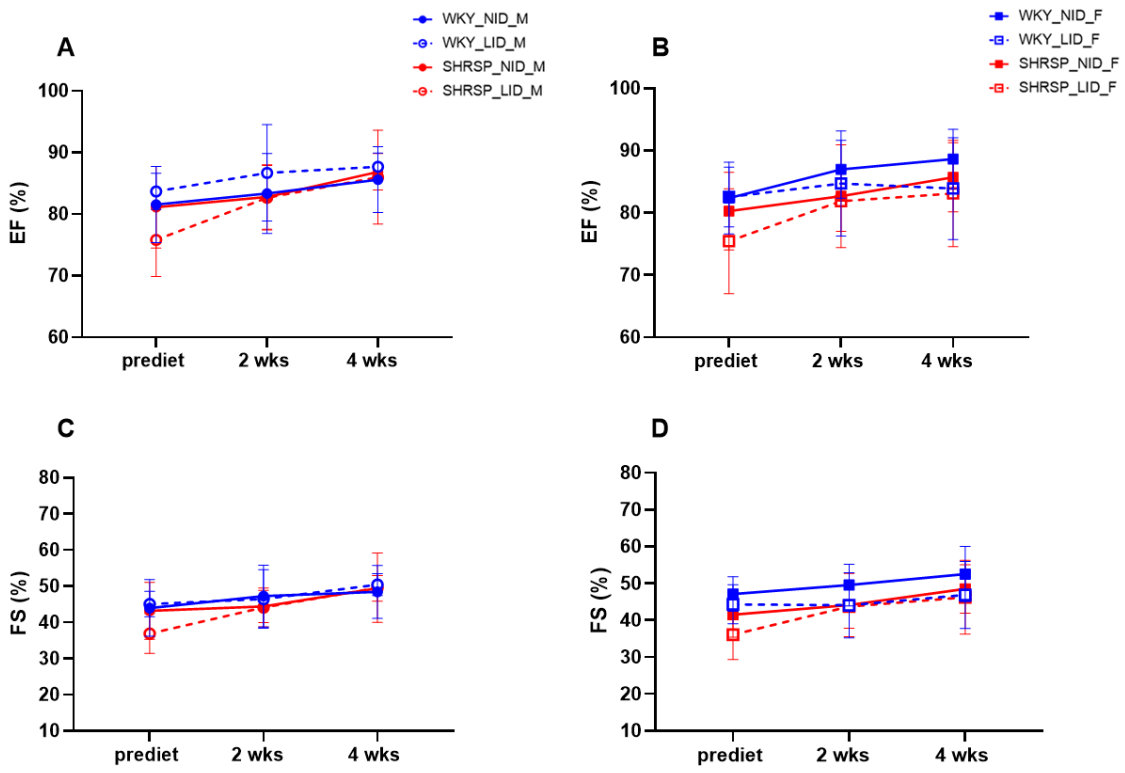

Figure 3-9: Ejection fraction (EF%) and fractional shortening (FS%) by echocardiography.

EF% in males (**A**) and female (**B**) and FS% in males (**C**) and female (**D**) WKY and SHRSP rats fed a normal (NID) and a low iodine diet (LID) at prediet, 2 and 4 wks of diet. All values are reported as mean ± SD (n=6-8 per group).

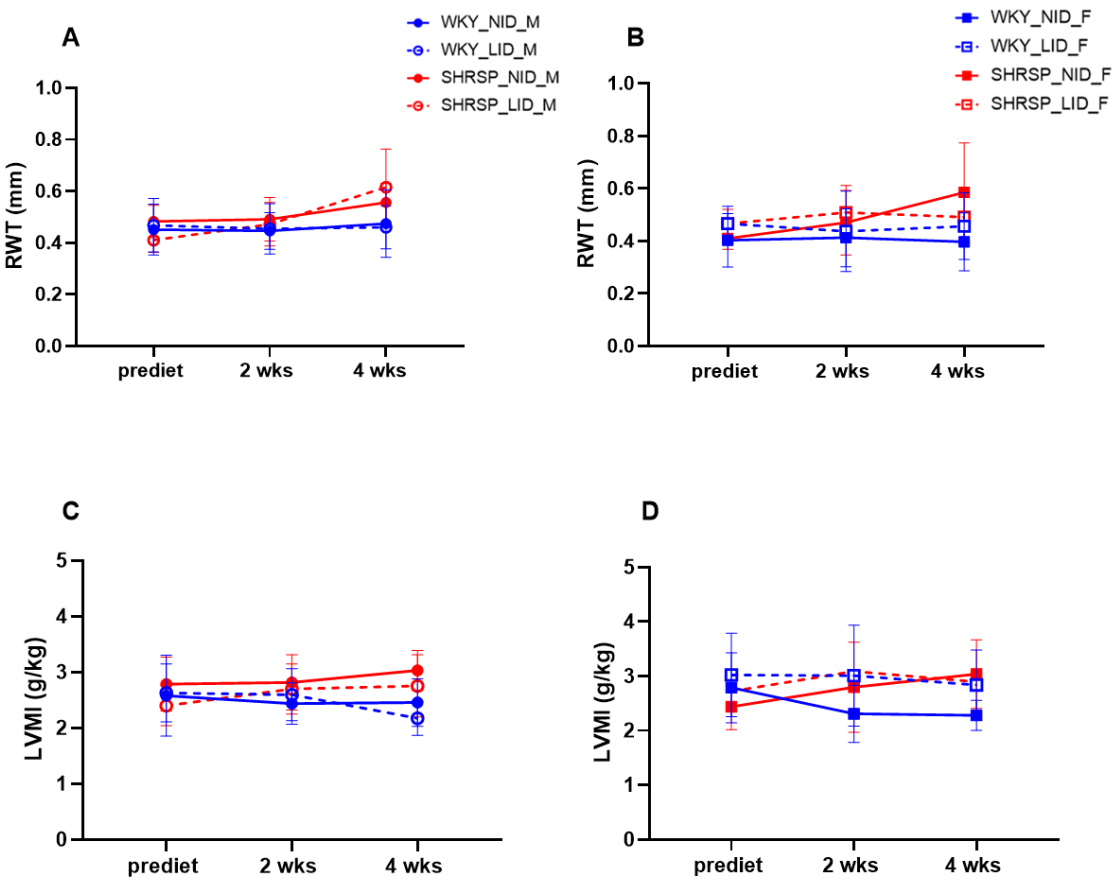

Figure 3-10: Relative wall thickness (RWT) and left ventricular mass index (LVMI) by echocardiography.

RWT in males (**A**) and females (**B**), and LVMI in male (**C**) and female (**D**) WKY and SHRSP rats fed a normal (NID) or a low iodine diet (LID) at prediet, 2 and 4 wks of diet. All values are reported as mean ± SD (n=4-6 per group).

3.4.4 Effect of low iodine diet on tissue weights

At sacrifice the thyroid was carefully dissected and weighed and its weight normalised to BW of the rat. Diet did not influence size of the thyroid in male and female WKY and SHRSP rats (Figure 3-11 A-D); however, sex differences are observed in WKY and SHRSP rats (Figure 3-11 A and B). WKY and SHRSP females had significantly increased thyroid/BW ratio compared with WKY and SHRSP males respectively ($p< 0.0001$).

Diet did not influence whole heart mass index in male WKY and SHRSP rats (Figure 3-12 A), however whole heart mass index was significantly increased ($p < 0.05$) in SHRSP females fed LID compared to SHRSP females fed NID (Figure 3-12 B). Left LVMI was not significantly influenced by diet in both male and female WKY and SHRSP rats (Figure 3-12 C and D). Whole heart mass index was significantly increased in SHRSP male and female rats compared to WKY male and female respectively at 9 wks of age (Figure 3-12 A and B) ($p< 0.0001$). The same observation was also evident for LVMI between SHRSP and WKY males and females (Figure 3-12 C and D) ($p < 0.001$ and $p < 0.0001$ respectively).

Kidney mass index was significantly increased in SHRSP males and females (Figure 3-13 A and B) when compared to WKY males and females irrespective of diet ($p < 0.0001$). Diet, sex, and rat strain did not influence liver and lungs mass indexes in males and female WKY and SHRSP rats (Figure 3-13 C, D and Figure 3-13 E, F respectively).

Gonadal fat mass index was significantly increased in SHRSP males ($p < 0.001$) and females ($p < 0.05$) when compared to WKY males and females irrespective of diet (Figure 3-14 A and B respectively). Retroperitoneal fat was not significantly influenced by diet, sex, and rat strain (Figure 3-14 C and D).

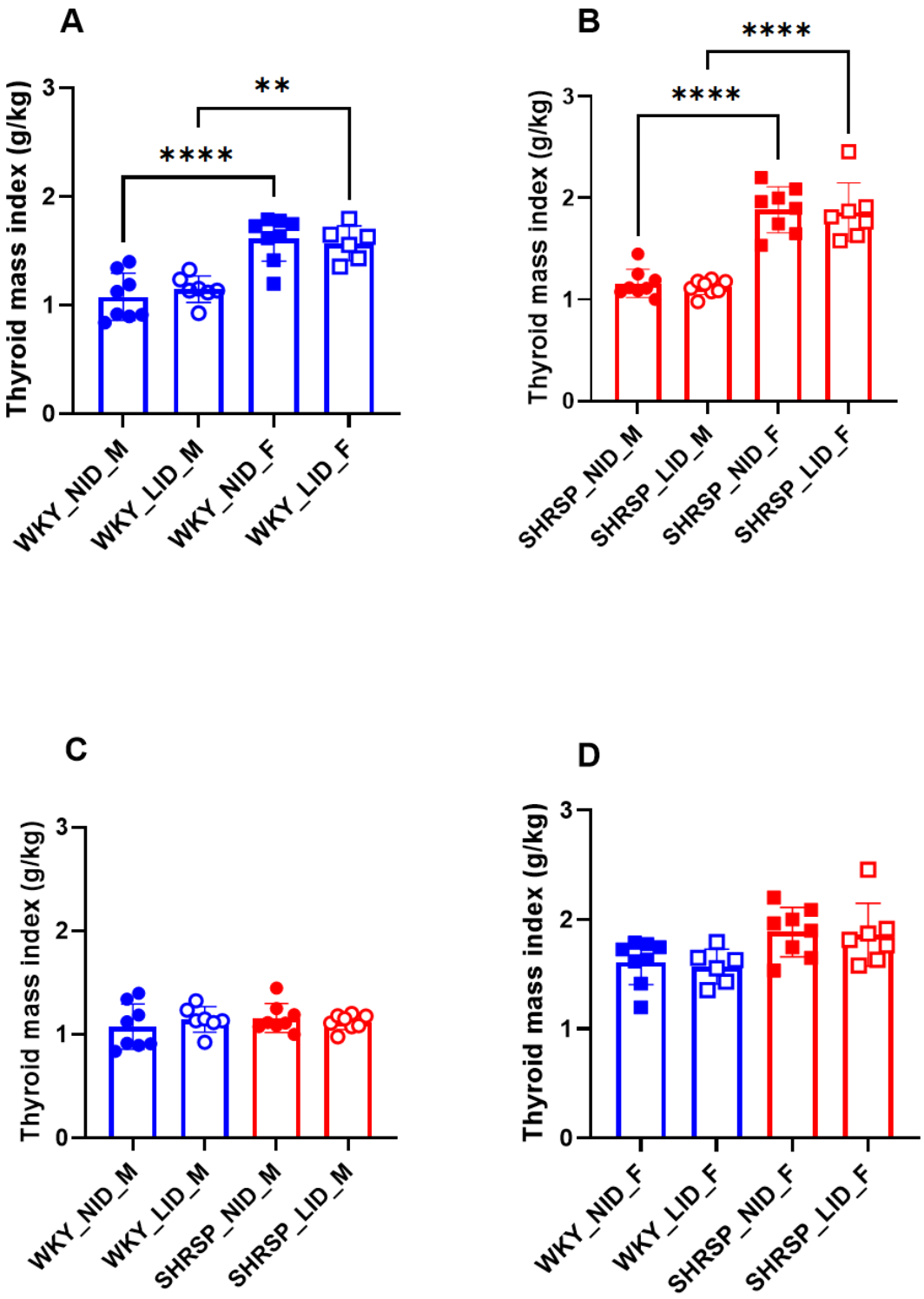

Figure 3-11: Thyroid mass index at 4 weeks of diet.

Thyroid mass index of WKY (**A**), SHRSP (**B**) and males (**C**) and females (**D**) fed a normal (NID) or a low iodine diet (LID) at 4 wks post diet. All values are reported as mean ± SD (n=7-8 per group). Ordinary one-way ANOVA followed by Tukey's multiple comparison were used to determine significance. $^{**}p < 0.01$, $^{****}p < 0.0001$.

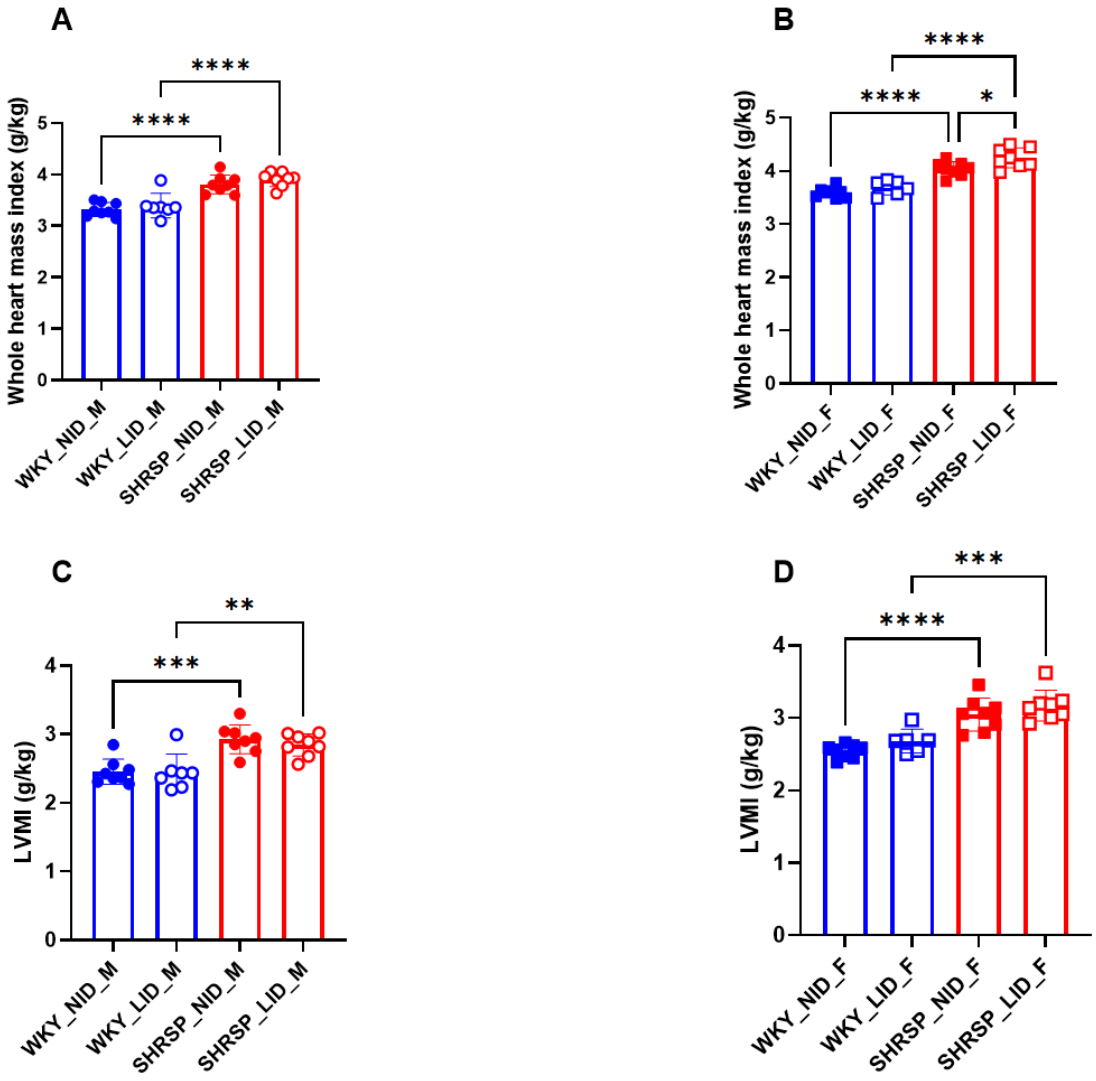

Figure 3-12: Whole heart mass index and left ventricular mass index (LVMI) at 4 weeks of diet.

Whole heart index in males (**A**) and female (**B**) and LVMI in males (**C**) and females (**D**) WKY and SHRSP rats fed a normal (NID) or low iodine diet (LID) at 4 wks of diet. All values are reported as mean ± SD (n=7-8 per group). Ordinary one-way ANOVA followed by Tukey's multiple comparison were used to determine significance. *$p < 0.05$, **$p < 0.01$, ***$p < 0.001$, ****$p < 0.0001$.

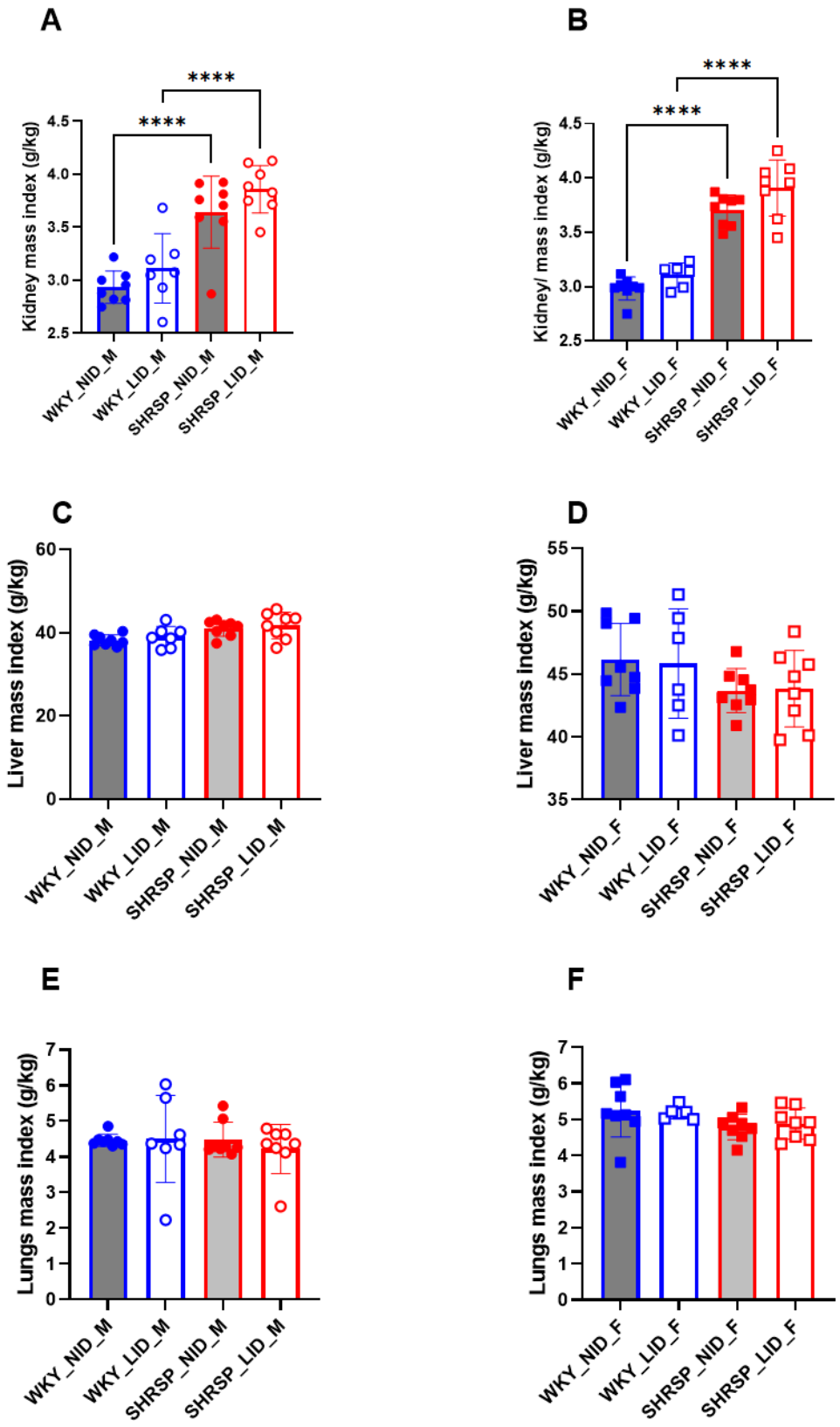

Figure 3-13: Kidney, liver and lungs mass indexes at 4 weeks of diet.

Kidney mass index in males (**A**) and female (**B**), liver mass index in males (**C**) and females (**D**) and lungs mass index in males (E) and females (F) WKY and SHRSP rats fed a normal (NID) or low iodine diet (LID) at 4 wks of diet. All values are reported as mean ± SD (n=5-8 per group). Ordinary one-way ANOVA followed by Tukey's multiple comparison were used to determine significance. ****$p < 0.0001$.

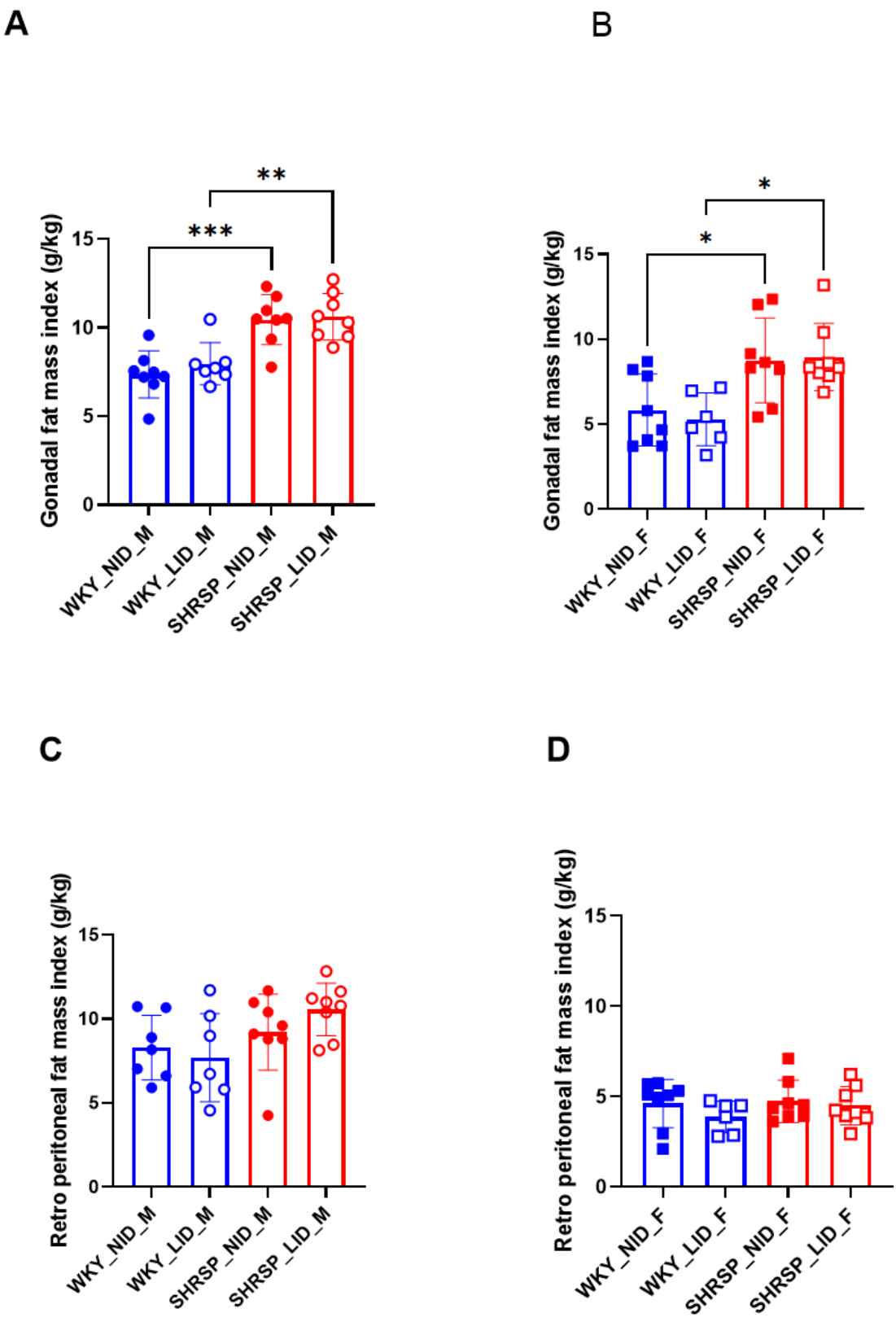

Figure 3-14: Gonadal and retroperitoneal fat mass indexes at 4 weeks of diet.

Gonadal fat mass index in males (**A**) and female (**B**) and retroperitoneal fat mass index in males (**C**) and females (**D**) WKY and SHRSP rats fed a normal (NID) or low iodine diet (LID) at 4 wks of diet. All values are reported as mean ± SD (n=6-8 per group). Ordinary one-way ANOVA followed by Tukey's multiple comparison were used to determine significance. *$p < 0.05$, **$p < 0.01$, ***$p < 0.001$.

3.4.5 SLC5a5 and SLC26a4 gene expression in thyroid, thoracic aorta, and heart of WKY and SHRSP fed normal iodine and low iodine diet.

SLC5a5 gene expression was significantly increased in thyroid tissue from WKY males but not SHRSP males fed LID when compared to WKY and SHRSP males fed NID ($p < 0.01$) (Figure 3-15 A). A similar trend is observed in WKY females fed LID compared with WKY females fed NID ($p = 0.1637$) (Figure 3-15 B). A trend towards reduced SLC5a5 gene expression is observed in SHRSP males fed LID compared to SHRSP males fed NID ($p = 0.8530$) (Figure 3-15 A).

LID did not influence SLC26a4 gene expression in thoracic aorta of male and female WKY and SHRSP rats (Figure 3-16 A and B). SLC5a5 and SLC26a4 gene expression were not influenced by LID in thoracic aorta (Figure 3-17 A-D) of male and female WKY and SHRSP rats while no expression of SLC5a5 and SLC26a4 was observed in the heart (left ventricle) regardless of diet, sex, and strain (Figure not shown).

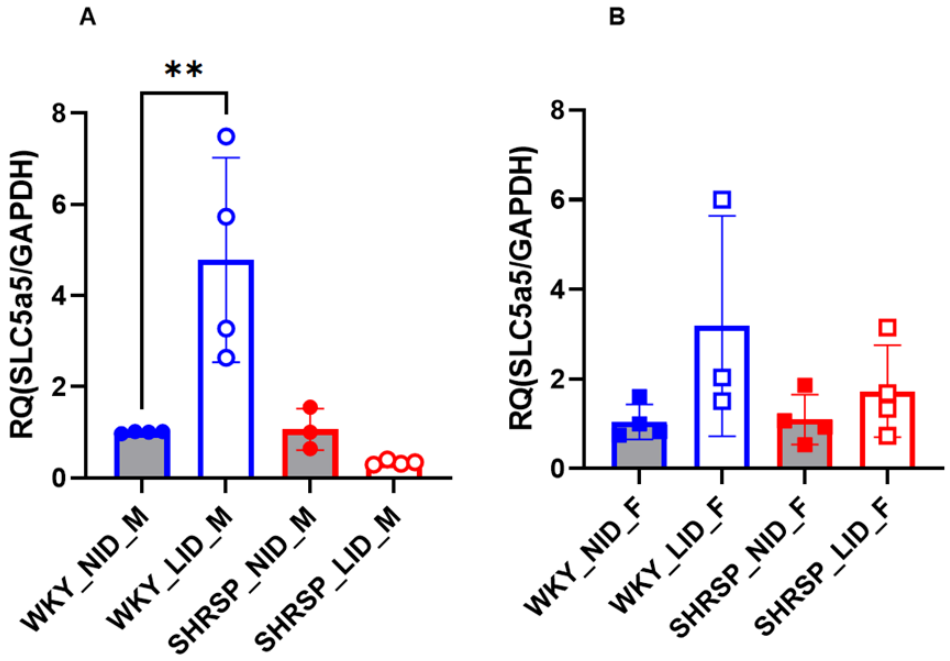

Figure 3-15: Effect of low iodine diet (LID) on SLC5a5 gene expression in thyroid gland.

SLC5a5 gene expression in males (**A**) and female (**B**) WKY and SHRSP rats fed normal iodine (NID) and low iodine (LID) diet at 4 wks post diet. All values are reported as mean ± SD (n=4 per group). Ordinary one-way ANOVA followed by Tukey's multiple comparison were used to determine significance. $^{**}p < 0.01$.

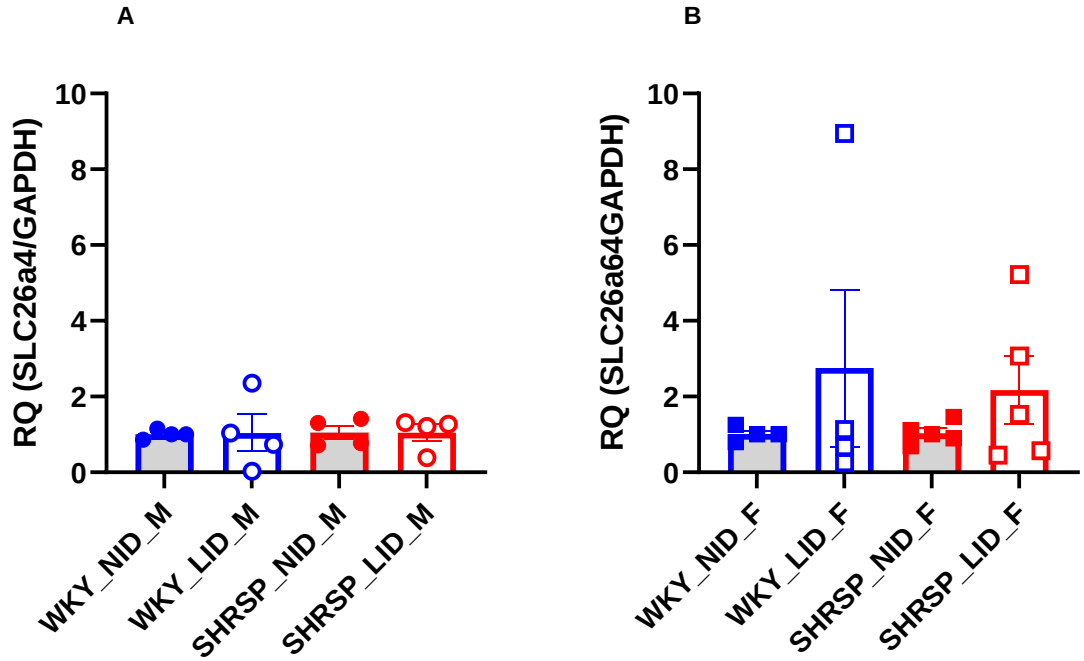

Figure 3-16: Effect of low iodine diet (LID) on SLC26a4 gene expression in thyroid gland.

SLC26a4 gene expression in males (**A**) and female (**B**) WKY and SHRSP rats fed normal iodine (NID) and low iodine (LID) diet at 4 wks post diet. All values are reported as mean ± SD (n=4-5 per group).

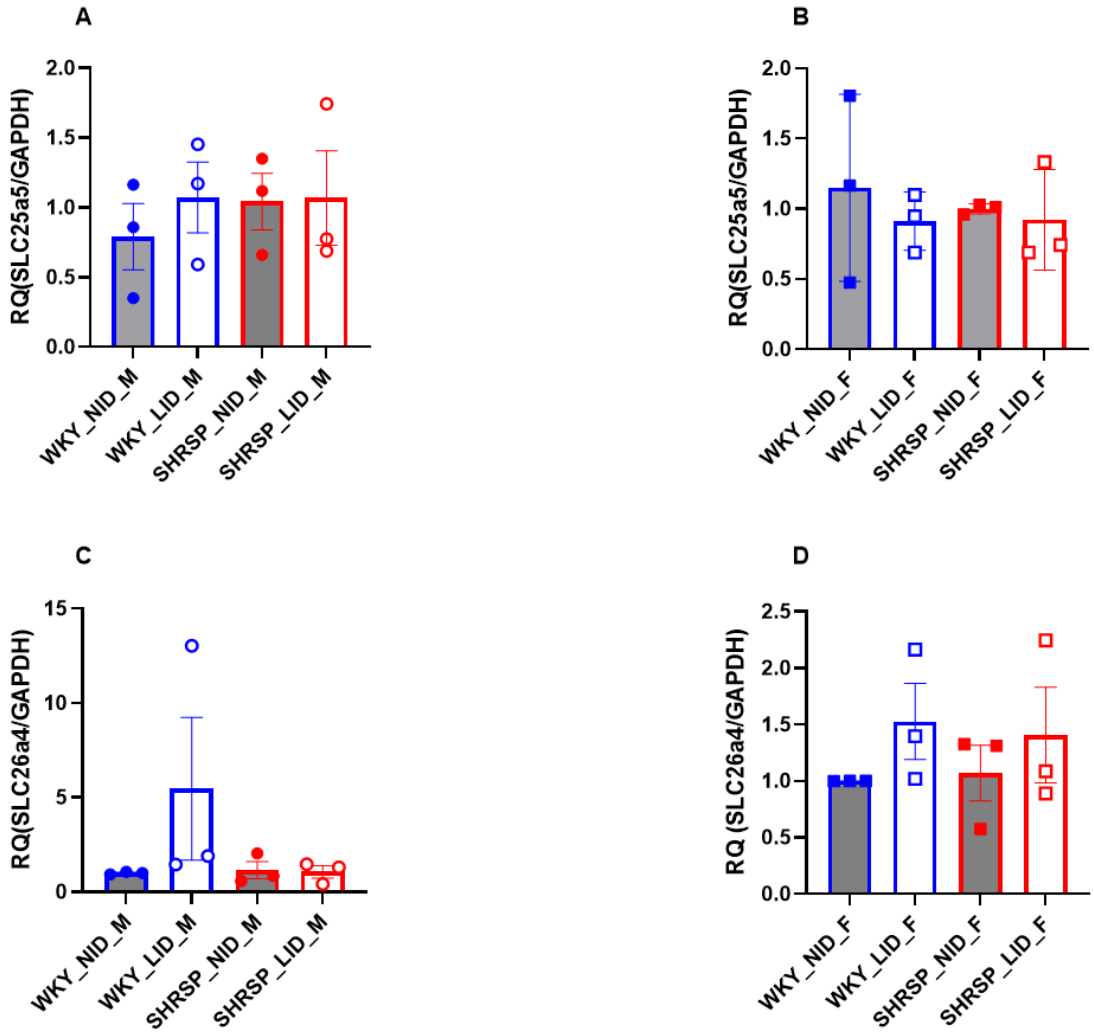

Figure 3-17: Effect of low iodine diet (LID) in SLC5a5 and SLC26a4 gene expressions in thoracic aorta.

SLC5a5 gene expression in males (**A**) and females (**B**), and SLC26a4 gene expression in males (**C**) and females (**D**) WKY and SHRSP rats fed normal iodine (NID) and low iodine (LID) diet at 4 wks post diet. All values are reported as mean ± SD (n=4-5 per group).

3.4.6 Low dietary iodine and vasculature

U46619 (10^{-10}–10^{-5} M) induced a concentration-dependent contraction of the mesenteric artery. LID fed WKY and SHRSP males had a significantly increased contractile response to U46619 when compared to sex and strain matched rats fed NID ($p < 0.05$ and $p < 0.0001$ respectively) (Figure 3-18 A). However, LID had an opposing effect in female WKY fed LID when compared to WKY fed NID which demonstrated significantly reduced reactivity to U46619 ($p < 0.05$) (Figure 3-18 B). SHRSP females fed LID had significantly increased contractile response to U46619 ($p > 0.001$) when compared to WKY females fed LID while no strain differences are observed under NID (Figure 3-18 B). The difference between SHRSP males on NID and LID was further illustrated with maximal vascular reactivity to U46619 and area under the curve (AUC) graphs which were significantly increased in SHRSP males fed LID compared to SHRSP males fed NID ($p < 001$ and $p < 0.1$ respectively) (Figure 3-19 A and C respectively). LID did not influence maximal vascular reactivity and AUC in females regardless of strain and diet (Figure 3-19 B and D). Similarly, half maximal effective concentration (EC50) was not significantly influence by LID in male and female WKY and SHRSP rats (Figure 3-19 E and F respectively).

LID did not have a significant effect on relaxation responses to Ach (Figure 3-20 A and B) and SNP (Figure 3-20 C and D).

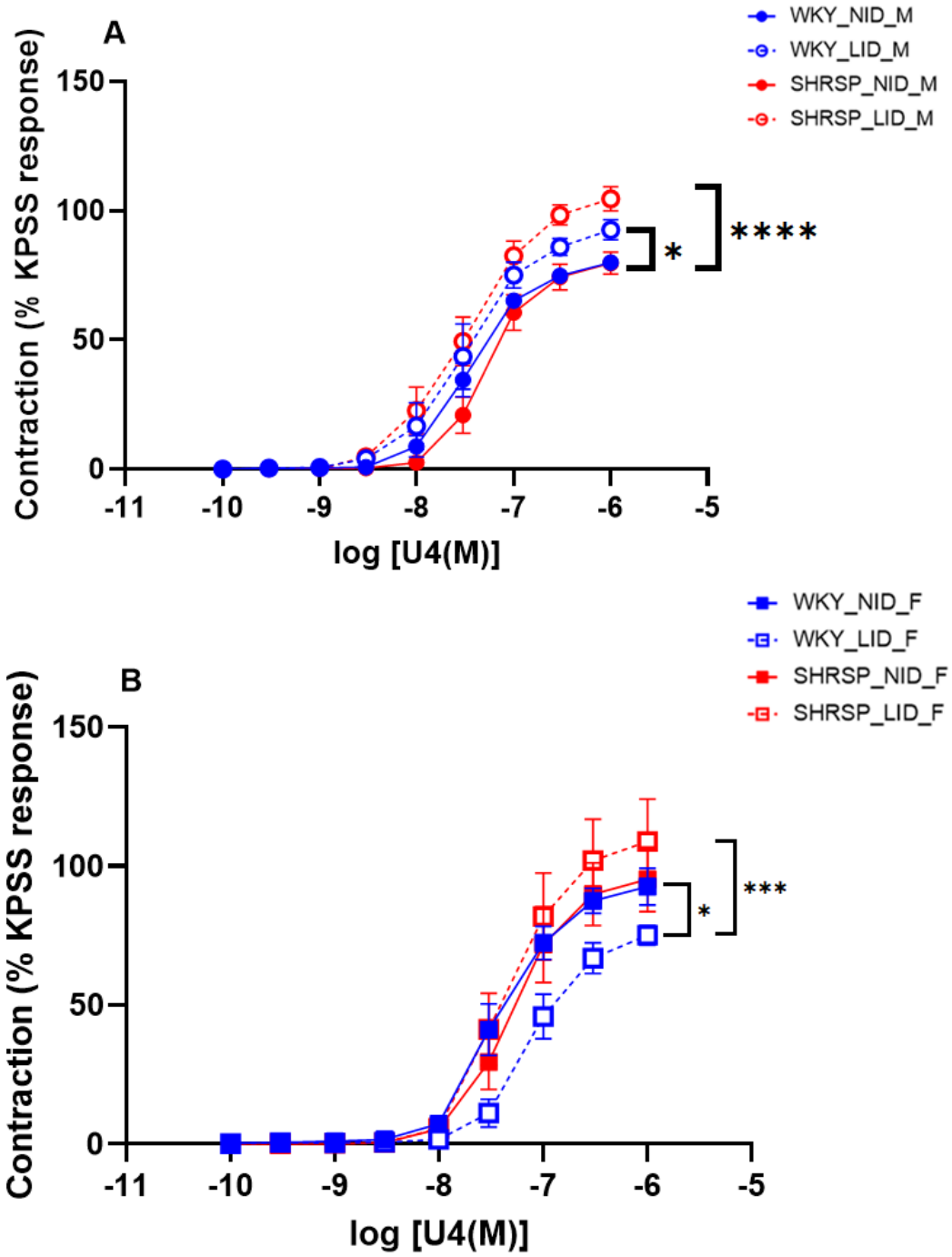

Figure 3-18: Effect of low iodine diet (LID) on mesenteric arteries contractile response to U46619.

Concentration response curve to U46619 (1×10^{-10}- 3×10^{-6}) in males (**A**) and females (**B**) on isolated third order mesenteric artery of WKY and SHRSP rats fed a normal (NID) or low iodine (LID) diet. All values are reported as mean ± SD (n=6-7 per group). Two-way ANOVA followed by Tukey's multiple comparison were used to determine significance. *$p < 0.05$, ***0.001****$p <$ 0.0001**.**

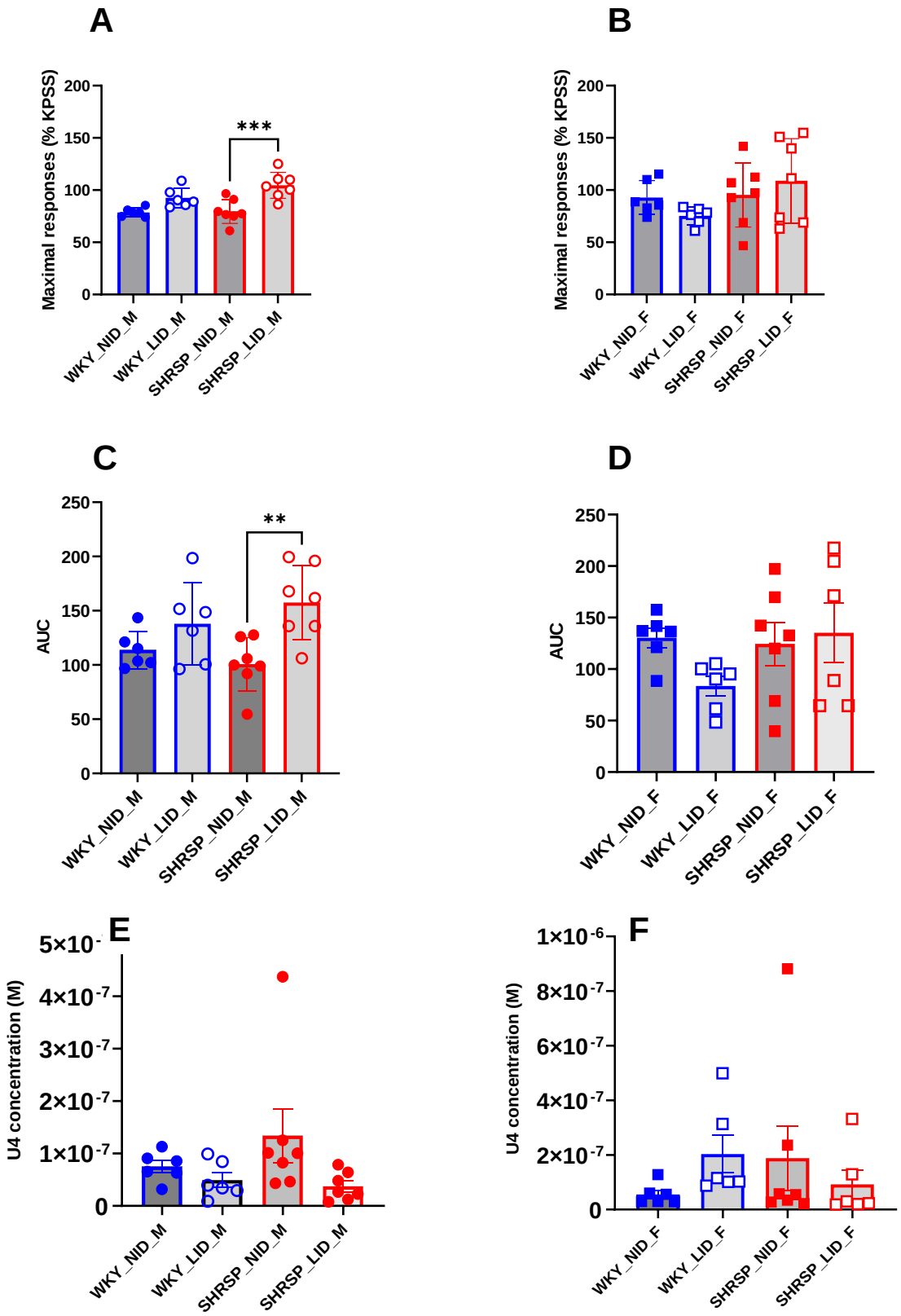

Figure 3-19: Maximal responses, area under the curve (AUC) and EC50 of mesenteric arteries response to U46619.

Maximal responses to U46619 in males (**A**) and females (**B**), Area under curve (AUC) in males (**C**) and females (**D**) and EC50 in males (**E**) and females (**F**) on isolated third order mesenteric artery of WKY and SHRSP rats fed a normal (NID) or low iodine (LID) diet. All values are reported as mean ± SD (n=6-7 per group). Ordinary one-way ANOVA followed by Tukey's multiple comparison were used to determine significance. $^{**}p < 0.01$$^{***}p < 0.001$.

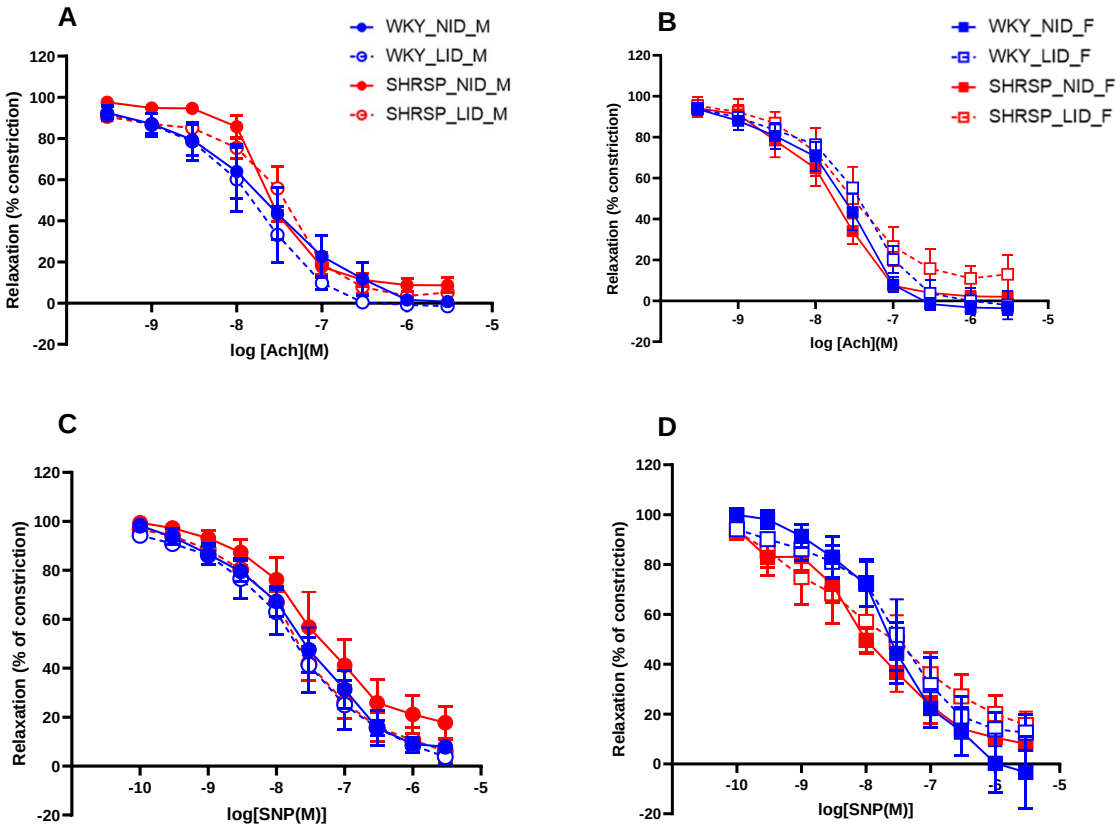

Figure 3-20: Effect of low iodine diet (LID) on mesenteric arteries relaxation response to Acetylcholine (Ach) and sodium nitroprusside (SNP).

Concentration response curve to Ach (1×10^{-10}- 3×10^{-6}) in males (**A**) and females (**B**), SNP (1×10^{-10}- 3×10^{-6}) in males (**C**) and females (**D**) on isolated third order mesenteric artery of WKY and SHRSP rats fed a normal (NID) or low iodine (LID) diet. All values are reported as mean ± SD (n=6-7 per group).

3.5 Discussion

This chapter aimed to investigate the individual effect of LID on cardiac, hemodynamic parameters and vascular function in addition to UIC and TH profiles in young male and female WKY and SHRSP rats. Baseline thyroid function is similar in WKY and SHRSP rats, however WKY and SHRSP rats responded differently to LID. Specifically, these rats demonstrated differences in thyroid function homeostatic mechanisms and vascular reactivity to U46619. Little is known about the individual effect of dietary iodine on CVD and to our knowledge, the present study is the first to investigate the link between short-term dietary iodine intake and CVD independent of thyroid dysfunction using WKY and SHRSP rat models.

Identifying a suitable animal model to study iodine deficiency and CVD allows scientific enquiry which could lead to a translational application. In this chapter we demonstrated that at baseline TH profiles (TSH, fT4, fT3 and Tg) in SHRSP are comparable to WKY rats. Little is known about TH profiles in SHRSP, however a study conducted by Bruhn and Jackson is in contrast with our findings since this study reported a two-fold increase in plasma TSH concentration in euthyroid SHR compared to WKY control while fT3 and fT4 levels were within normal range under NID (Bruhn & Jackson, 1992). The reason for discrepant TSH results could be due difference in age (17 wks compared to 9 wks in our study) and rat strains used. The assessment of UIC at baseline showed no significant differences between male and female WKY and SHRSP rats. Taken together these results indicate that SHRSP and WKY rats are suitable models for examining dietary iodine manipulation since they show similar TH levels prior to the start of LID i.e., they show no thyroid dysfunction at baseline.

Following 4 wks LID feeding, TSH but not fT4, fT3 and Tg levels were significantly increased in male and female SHRSP, but no changes were observed in WKY rats. The significant increase in TSH with normal levels of fT4 and fT3 observed in our study are consistent with subclinical hypothyroidism. However, it should be noted that there is no standard for diagnosing thyroid function in rats (Fu et al., 2022). Normal fT3 levels in moderately iodine deficient adult rats has long been known (Abrams & Larsen, 1973). Our results are consistent with findings by Min et al., who reported no significant difference in plasma TSH, fT3

and fT4 levels between iodine deficient and control groups in pregnant female Wistar rats at gestational day 0 to 28 (Min et al., 2017). Fu et al., reported no significant differences in TSH, fT4 and fT3 in lactating Wistar rats fed NID compared to those fed LID at 14 days of lactation (Fu et al., 2022). Similarly our results are supported by Marković et al., who reported no significant differences in fT4 and fT3 and TSH in male Wistar rat treated with a low KI solution compared to a normal KI solution administrated daily intraperitoneally for 26 days (Marković et al., 2010). As mentioned previously, information on thyroid hormone profiles in SHRSP rats is limited, therefore we could not find studies to directly compare our thyroid function results in this rat strain.

UIC is the World Health Organization gold standard for assessment of iodine intake. It is used as a biomarker of iodine status since it reflects very recent iodine intake in epidemiological studies (Zhang et al., 2016). From our data a LID led to low dietary iodine intake as demonstrated by significantly reduced UIC in rats fed LID diet compared to those fed NID irrespective of strain and sex. Significantly reduced UIC in rats fed LID was a confirmation of the dietary analysis report from the supplier and the assurance of the intended use of the diet for this study.

As stated previously production of TH begins with active iodide accumulation in the thyroid follicular cells mediated by SLC5a5 (Dai et al., 1996). Accumulation of iodide in the thyroid is regulated by TSH, which is secreted from the pituitary gland in response to changes in circulating TH, through a negative feedback mechanism involving the HPT axis (Farebrother et al., 2019). Based on our results WKY but not SHRSP males significantly increased the expression of SLC5a5 in response to LID when compared to strain and sex matched rats fed NID and this increase was independent of TSH levels. A similar trend was observed in WKY but not SHRSP females fed LID when compared to WKY and SHRSP females fed NID. SLC26a4 was not significantly affected by LID in both male and female WKY and SHRSP rats. The inability of the SHRSP male rat thyroid gland to increase SLC5a5 expression in response to LID is an important finding. These discoveries point to a difference in thyroid function homeostatic mechanism between WKY and SHRSP male rats and suggests that SHRSP males are likely to progress into overt hypothyroidism at an earlier stage than WKY males fed LID.

The ability of WKY males to increase SLC5a5 expression in response to LID reflects their capacity to maintain normal thyroid function despite receiving LID.

Alterations of the structure and/or expression of SLC5a5 gene are implicated in various thyroid disorders including congenital hypothyroidism and iodine deficiency (Matsuda & Kosugi, 1997; Uyttersprot et al., 1997). ADP-ribosylation factor 4 (ARF4) and valosin-containing protein (VCP)-control SLC5a5 trafficking. ARF4 enhances SLC5a5 vesicular trafficking from the Golgi to the plasma membrane, whereas VCP, a principal component of endoplasmic reticulum (ER), is associated with degradation governed SLC5a5 proteolysis (Fletcher et al., 2020). A proposed mechanism for the inability of the SHRSP rats to increase SLC5a5 expression in response to LID could be an over expression of VCP leading to degradation of SLC5a5 reducing its localization to the basal membrane and thus affecting iodide transport (Fletcher et al., 2020). It can also be suggested that SHRSP males lack sensitivity to LID because they don't increase their SLC5a5 expression levels as a result of low iodine, so they are unable to respond to low levels of dietary iodine. To compensate for the lack of increase in SLC5a5, male and female SHRSP rats responded by increasing the secretion of TSH to stimulate the thyroid to produce more TH. Further studies are required to understand why SLC5a5 is unable to respond to low dietary iodine in SHRSP rats. This includes assessing genetic differences between SHRSP and WKY by employing high through put technologies like RNA-Seq and function of the SLC5a5 protein. It would also be meaningful in future to place WKY rats on a long-term LID to determine how long they can maintain normal thyroid function before they become hypothyroid.

Short-term LID did not influence size of the thyroid corrected to BW in any of the experimental groups; however, the current study is reporting for the first time, a significant difference in the size of the thyroid gland between male and female WKY and SHRSP rats. Our results agree with Yoshida et al who showed that male Wistar rats subjected to more than 3 mg/day of KI over 4 wks didn't show thyroid weight variation (Yoshida et al., 2014). By contrast Zhao reported a significant increase in thyroid weights and relative thyroid weight in LID compared to NID fed female Wistar rats after 12 wks of feeding (Zhao et al., 2021). These results are supported by Pedraza et al., who reported significantly

increased thyroid weight in response to moderate and severe iodine deficiency after 3 months of feeding (Pedraza et al., 2006). This result contrasts with the findings reported in our study and the reason could be duration of the treatment period since, in the previous study, rats were on diet for 12 wks and 3 months respectively while our rats were on diet for only 4 wks. The second reason could point to the difference in the rat strains used. TH have multiple roles in cardiovascular function and disease outcomes exerting profound effects on the heart and peripheral circulatory system. They are known to decrease peripheral vascular resistance, influence the renin-angiotensin system (RAS), and increase blood volume and erythropoietin secretion with subsequent increased preload and cardiac output (Klein, 1990). The relationship between TH functional abnormalities and CVD has long been established. Despite the known relationship, none of the studies have compared the size of the thyroid gland in rodent models of CVD. In future studies it would be pertinent to explore the changes in thyroid size and thyroid function in a longer-term LID study. Results from such studies will provide a theoretical basis for understanding long term effect of LID on thyroid weight and TH homeostasis in WKY and SHRSP and their association with CVD.

The use of diet to study nutritional elements is often a challenge since diet manipulation can affect the palatability of the food leading to differences in food intakes and weight gain in rodent studies. However, the rodent diet used in our study was of the same form and texture as the control diet. LID diet did not influence food consumption, BW or % BW changes. Under LID male and female WKY rats showed a significantly increased urine output when compared to sex matched SHRSP fed LID. In males this was further illustrated with water intake/urine output ratio significantly increased in SHRSP fed LID compared to WKY fed LID. There was also a trend towards increased water intake vs urine output in SHRSP females fed LID when compared to SHRSP females fed NID. These results indicate that despite lack of significant differences in fluid homeostasis between the strains under NID, LID has the potential to encourage fluid retention in SHRSP males and females.

LID diet did not influence BP in either WKY or SHRSP irrespective of sex. WKY and SHRSP were within normal BP ranges at 5 wks of age, and SHRSP developed

hypertension from 7 wks of age. This finding is in line with previous publications from this rat colony (McBride et al., 2005; Rajani et al., 2018), and are also supported by Chen et al. who also reported that systolic BP of young WKY and SHRSP rats was in the normotensive range (Chen et al., 2009). It is important to note that in the current study, rats were recruited at 5 wks of age because we wanted to determine the effects of iodine on CVD from early development stage (between 5-9 wks of age). The reasons for lack of significant differences in BP because of LID diet could be due to age and duration of the dietary period induction. It might be beneficial to maintain the animals on diet for longer, into early adulthood and beyond (e.g., 16 wks of age). These results suggest that hypertension occurs before any signs of thyroid dysfunction in the SHRSP model, but even with short-term treatment, LID is inducing a subclinical hypothyroid state in this model. Thyroid dysfunction, both hypo and hyperthyroidism increase the risk of hypertension (Cappola & Ladenson, 2003), and therefore it has been suggested that the correction of thyroid dysfunction may normalize BP in most cases (Berta et al., 2019). Despite the acknowledged effect of thyroid dysfunction on BP, little is known about the effect of hypertension on thyroid function. It could therefore be beneficial to carry out a long-term study to determine the association between LID, TH levels and hypertension.

Echocardiography measurements demonstrate that SV and CO were significantly increased in WKY compared to SHRSP rats irrespective of diet in both males and females. Similar results have been reported in other studies on these rat strains (Chen et al., 2000; Olson et al., 2019). This corresponds to the larger BW and hence larger hearts in WKY rats compared to SHRSP rats. Even though LID did not significantly influence SV and CO, we observed trends toward reduced SV and CO in males fed LID irrespective of strain. Reduced SV and CO are markers of reduced cardiac function, and their effects are typically counterbalanced by left ventricular hypertrophy which is also an adaptive response to increased BP (Johnson & Ahrens, 2015) and a risk factor for CVD. However, when measured by echocardiography LID did not significantly influence LVMI in our study.

In contrast to the echocardiography results above, whole heart mass index but not LVMI was significantly increased in SHRSP females fed LID when compared to SHRSP females fed NID. LID did not influence whole heart mass index and LVMI in

SHRSP males or WKY males and females, however typical strain related differences were observed whereby both whole heart mass index and LVMI were significantly increased in male and female SHRSP versus age matched WKY rats at 9 wks of age. These changes in whole heart mass index and LVMI occurred in parallel with the observed elevations in BP in the SHRSP rats that occurred from wk 7 of age. These results are in line with what is currently known about this rat strain. Left ventricular hypertrophy is well established in SHRSP males and females as an adaption to raised BP which can become pathological in older animals (Graham et al., 2004). Although whole heart mass index was significantly increased in SHRSP females fed LID, it is important to note that there was no significant difference in %EF and %FS between rats fed NID and LID regardless of rat strain and sex indicating normal functioning of the heart. However, the significant increase in whole heart mass index observed in SHRSP females fed LID could potentially indicate hypertrophic development in the heart of the females which could eventually lead to functional deterioration (i.e., early signs of heart disease).

Visceral adipose tissue (VAT) (i.e., gonadal, and retro-peritoneal fat) were significantly increased in SHRSP males and females compared to sex matched WKY rats. These results are in line with what has already been shown in this model (Small et al., 2019; Strahorn et al., 2005). Increased adiposity is associated with reduced vascular function and increased vascular disease (Small et al., 2019). However, LID did not influence VAT in any of the experimental groups.

Small resistant arteries (lumen diameter < 300 μm) are responsible for regional distribution of vascular tone and blood flow and play an important role in the regulation of BP, through effects on vascular resistance (Christensen & Mulvany, 2001). The endothelium is crucial for the maintenance of vascular tone by releasing several vasoactive substances, including NO. VSMC cell activity is regulated through the release of endothelial-derived relaxing and constricting factors, and these secretions are maintained in balance while the vascular endothelium is healthy (Kang, 2014). Although we didn’t see any effects on endothelium dependent or independent vasorelaxation in response to LID, we do see changes in contractile response to U46619.

Mesenteric arteries of WKY and SHRSP male rats fed LID were hypercontractile to U46619 while an opposite response was observed in WKY females fed LID when compared to those fed NID. Despite lack of strain differences in contractile responses to U46619 under NID conditions, LID significantly increased vascular reactivity in SHRSP females fed LID when compared to WKY females fed LID. This clearly demonstrated that under LID, female WKY and SHRSP mesenteric arteries respond differently to U46619. LID did not produce significant differences in EC50 in any of the experimental groups, however, AUC, and maximal tensions were significantly increased in SHRSP males fed LID compared to SHRSP males fed NID and this was independent of fT4, fT3 and Tg levels. It is important however to note that increase in vascular reactivity in WKY and SHRSP males fed LID was independent of lack of significant difference in BP. Vascular changes characterized by endothelial dysfunction, increased vascular contraction and arterial remodelling are generally associated with hypertension (Savoia et al., 2011), and therefore LID has the potential to worsen hypertension in male and female SHRSP rats fed LID and has the potential to cause elevated BP in WKY males. As previously mentioned, the lack of significant differences in BP between SHRSP males fed LID and those fed NID could have been that the rats were still young and had not attained mature hypertensive state. It will be beneficial in future to conduct a longer-term study in these rats. Increased contractility of mesenteric arteries could be the result of increased expression of thromboxane A2 receptor (TP) which binds U46619 (an analogue of thromboxane A2) therefore leading to increased contractility of mesenteric arteries. A previous study demonstrated that U46619 induces contraction through activation of TP, depending on Ca^{2+} influx through L-type and non-L-type Ca^{2+} channels, while the intracellular stores do not appear to contribute to these contractions (Grann et al., 2016). In support of the above results Zhang et al., reported that the response of mesenteric vessels to U46619 was significantly increased in hypertension and was associated with increase of TP (Zhang et al., 2022). We did not find studies to directly compare our vascular function results, however hypothyroidism was not associated with alterations in arterial vessel response to endothelin-1 (ET-1) in Sprague Dawley rats (McAllister et al., 2000). In contrast to enhanced expression of TP in hypercontractility, the decreased contractile response to U46619 observed in female WKY fed LID could have been due to decreased TP. Zhang et al., found that mesenteric vasoconstriction

response induced by U46619 was diminished remarkably in old WKY and old SHR rats (Zhang et al., 2022) therefore LID has the potential to accelerate vascular aging in WKY females. It is known that aging can be associated with an increase in cardiovascular morbidity and mortality, even in the absence of known cardiovascular risk factors (Lakatta & Levy, 2003). Zhang et al. further demonstrated that the expression of TP membrane proteins in mesenteric vessels was decreased, and the endogenous TP competitor, 8,9-Epoxyeicosatrienoic acid (8, 9-EET), in serum was increased, which was partly responsible for the decreased vascular reactivity of U46619 (Zhang et al., 2022).

Nutritional dietary elements such as iodine are increasingly recognised as important lifestyle modifications in the control of CVD. It is therefore becoming crucial to understand the individual role of iodine in cardiovascular function in addition to its indirect effect through TH synthesis. In this study rat models of CVD have been utilised in a 4-wk dietary intervention study to reduce iodine intake. This study has confirmed that LID can have an impact on cardiovascular function, in the absence of changes in circulating levels of TH. Whilst we did not observe any significant effect on BP or any major impact on cardiac hypertrophy, we observed significantly elevated vascular reactivity in SHRSP and WKY males fed LID. These changes were observed despite no significant alteration in TH levels. This indicates that iodine has direct effects on the vascular system independent of thyroid functional changes.

In order to understand the underlying molecular mechanisms and signalling pathways involved in LID induced hypercontractility, we performed RNA-Seq in vascular tissue isolated from NID and LID fed WKY and SHRSP male rats. Moreover, mesenteric artery VSMC from WKY and SHRSP males were isolated and cultured in cell medium with or without iodide before stimulation with U46619. Details of these studies will be covered in chapter 4 and 5 respectively.

Chapter 4 Transcriptome profiling of thoracic aorta of normal and low iodine diet fed WKY and SHRSP males.

4.1 Introduction

In the previous Chapter, a significant effect of LID was observed when mesenteric arteries from male WKY and SHRSP fed LID were shown to be hypercontractile to U46619 when compared to sex and strain-matched rats fed NID. This was an important discovery and prompted an investigation to uncover the molecular mechanisms underpinning the hypercontractility of mesenteric arteries from LID fed rats. Therefore, in this chapter, we aimed at understanding the effect of LID at the transcriptome level in vascular tissue isolated from WKY and SHRSP male rats.

Tissue-specific gene transcriptome profiles can offer insight into expression pathways underlying functional differences during physiological and pathophysiological conditions. Vascular transcriptome analysis may lead to a better understanding of the molecular mechanisms underpinning enhanced vascular reactivity in LID fed WKY and SHRSP male rats. In addition, identifying implicated gene networks may contribute to establishing a risk profile for the pathology process of CVD.

Early high-throughput methods for gene expression analysis, like microarrays of cDNA and serial analysis of gene expression (SAGE) provided powerful tools for large-scale transcriptome studies in the 1990s(Lockhart et al., 1996; Velculescu et al., 1995). These techniques proved useful to characterize gene expression patterns under multiple experimental conditions, however, both methods have limitations. The microarray-based analysis is limited in that it uses a panel of pre-selected genes and has a limited ability to accurately quantify lowly expressed and very highly expressed genes.(Casneuf et al., 2007; Shendure, 2008). On the other hand, SAGE generates a simultaneous quantitative and qualitative analysis of thousands of genes, (Zhang et al., 1997) but nonetheless this assay is insensitive to measuring expression levels of splice isoforms and cannot be used for novel gene discovery (Kukurba & Montgomery, 2015; Zhang et al., 2015).

The innovation of high-throughput next-generation sequencing (NGS) analysis through sequencing of complementary DNA (cDNA) has revolutionized transcriptomics (Wang et al., 2009). There are several distinct advantages of RNA sequencing (RNA-Seq) over previous approaches, and these have revolutionized our understanding of the complex and dynamic nature of the transcriptome (Kukurba & Montgomery, 2015). RNA-Seq uses next generation sequencing to estimate the quantity of RNA in biological samples of given transcripts (Rutter et al., 2019). RNA-Seq provides a more detailed and quantitative view of gene expression, and allele-specific expression(Han et al., 2015). Recent advances in the RNA-Seq workflow, from sample preparation to sequencing platforms to bioinformatic data analysis, have enabled deep profiling of the transcriptome and the opportunity to elucidate different physiological and pathological conditions (Kukurba & Montgomery, 2015).

Ex vivo and in vitro experimental models have been very useful in investigating the mechanisms involved in vascular contractility, however little has been done at the transcriptome level. While the effect of iodine deficiency on vascular transcriptomics has not been extensively investigated, it has been shown that when facing short periods of acute iodine deficiency, the level of reactive oxygen species (ROS) increases in thyrocytes, which increases local blood flow via a VEGF-dependent pathway. This occurs independently of changes in TSH production and is probably a response to rapidly improve iodide supply (Gérard et al., 2009; Gérard et al., 2008). In rats, the transcriptome profile of the follicular cell lineage PCCl3 under untreated and treated conditions with 10^{-3}M NaI revealed 84 transcripts differentially expressed in response to iodide (Leoni et al., 2008). Moreover, they showed that iodide excess inhibits the expression of essential genes for thyroid differentiation(Leoni et al., 2008). Several other researchers have shown that basal diet supplemented with potassium iodide (KI) influences the transcriptome in sheep and cow whole blood and that biological processes associated with the differentially expressed genes (DEGs) were associated with cell growth regulation, immune response and oxidative stress (Iannaccone et al., 2020; Iannaccone et al., 2019). These studies demonstrate that iodine has the potential to modulate gene transcripts in blood and thyroid follicular cell lines independent of TH and could potentially influence the transcriptome in the vasculature of LID fed rats.

In this study we utilised RNA-Seq to perform a DEGs profile of the thoracic aorta of WKY and SHRSP male rats fed LID versus those fed NID. In addition, we utilised Ingenuity® Pathway Analysis (IPA) to uncover biological pathways and biological functions and disease processes associated with DEGs. Thoracic aorta rather than mesenteric arteries was used because of the necessary time taken to prepare the mesenteric vessels for myography, which could impact the quality of the RNA because RNA quality rapidly deteriorates if the tissue is not immediately snap frozen. For accurate transcriptome analysis it is critically important that high quality mRNA is utilised (Sheng et al., 2017).

4.2 Hypothesis and Aims

4.2.1 Hypothesis

Low iodine diet changes the vascular transcriptome of male WKY and SHRSP rats leading to exacerbated vascular reactivity.

4.2.2 Aims

1. To determine the effect of LID on protein coding gene expression in thoracic aorta of WKY and SHRSP rats.

2. To determine biological functions, significant canonical pathways and diseases and functions influenced by most significant DEGs in thoracic aorta of NID and LID fed male WKY and SHRSP male rats.

3. To validate several significantly DEGs in key pathways.

4. To determine the relationship between SLC5a5 and DEGs within the most affected canonical pathway in LID fed SHRSP versus NID-fed male SHRSP.

4.3 Materials and methods

Thoracic aorta from WKY and SHRSP males fed NID and LID were dissected as mentioned in the general materials and methods (section 2.4). RNA extraction and quantification was done as in materials and methods (section 2.8.1). 30 µl (250-500 ng/µL) of the RNA sample was sent for RNA-Seq while the remaining 10 µL was used for validation of genes. RNA-Seq was carried out as explained in materials and methods (section 2.9). A summary of the RNA-Seq workflow is illustrated in figure 4-1.

4.3.1 Identification of differentially expressed genes based on Deseq2.

DESeq2 integrates methodological advances with several novel features to facilitate a more quantitative analysis of comparative RNA-Seq data using shrinkage estimators for dispersion and fold change(Love et al., 2014). DESeq2 performs an internal normalization where geometric mean is calculated for each gene across all samples. The counts for a gene in each sample is then divided by this mean. The median of these ratios in a sample is the size factor for that sample. This procedure corrects for library size and RNA composition bias, which can arise for example when only a small number of genes are very highly expressed in one experiment condition but not in the other. As small number of replicates make it impossible to estimate within-group variance reliably, DESeq2 uses shrinkage estimation for dispersions and fold changes. A dispersion value is estimated for each gene through a model fit procedure. Biological replicates of each experiment condition are required to estimate dispersion properly. DESeq2 fits negative binomial generalized linear models for each gene and uses the Wald test for significance testing. DESeq2 automatically detects count outliers using Cooks's distance and removes these genes from analysis. It also automatically removes genes whose mean of normalized counts is below a threshold determined by an optimization procedure. Removing these genes with low counts improves the detection power by making the multiple testing adjustment of the *p*-values less severe. The analysis output consists of; de-list-deseq2.tsv: Table containing the significantly DEGs (Love et al., 2014).

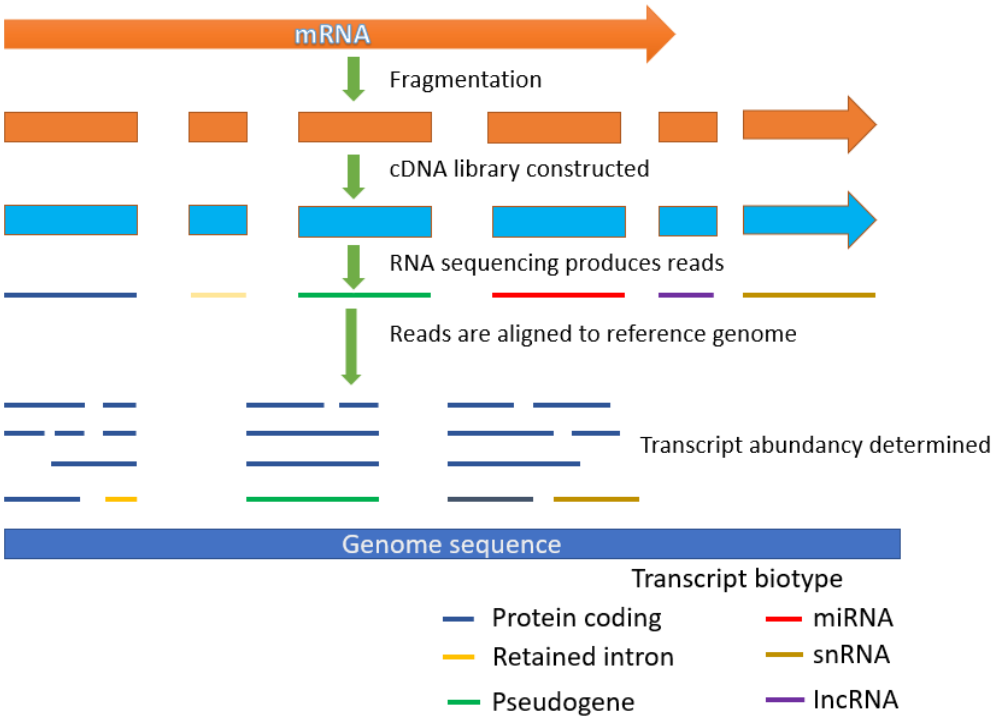

Figure 4-1: Schematic illustration summary of the RNA sequencing process.

Following total RNA extraction and fragmentation, cDNA library is prepared using paired end sequencing. The library is then sequenced, and the quality trimmed reads are aligned to the reference genome using the program Hisat2 (Version 2.1.0). The reads are then quantified using HtSeq count. miRNA = microRNA, snRNA = small nuclear RNA, lncRNA = long non-coding RNA.

4.3.2 Data handling and analysis

DEGs list was generated by p adjusted values (which determines the significance of expression changes) restricted to (padj) < 0.05. There were less than 1000 changes and therefore no further restrictions were applied for analysis. Differential gene expression was examined using pair wise comparison between WKY fed LID versus WKY fed NID and SHRSP fed LID versus SHRSP fed NID, and comparison between SHRSP fed NID versus WKY fed NID and SHRSP fed LID versus WKY fed LID (Figure 4-2). These comparisons generated several significantly DEGs between comparison groups and those that were common. The were no DEGs between WKY fed LID versus WKY fed NID, however there were 438 DEGs between SHRSP fed LID versus SHRSP fed NID. Moreover, DEGs were observed between strains under NID versus LID conditions (285 versus 81). In terms of direction, expression increased or decreased relative to the second group; for example, if the comparison was A versus B, expression differences are expressed

relative to B, i.e., a positive fold changed would mean an increase in A relative to B.

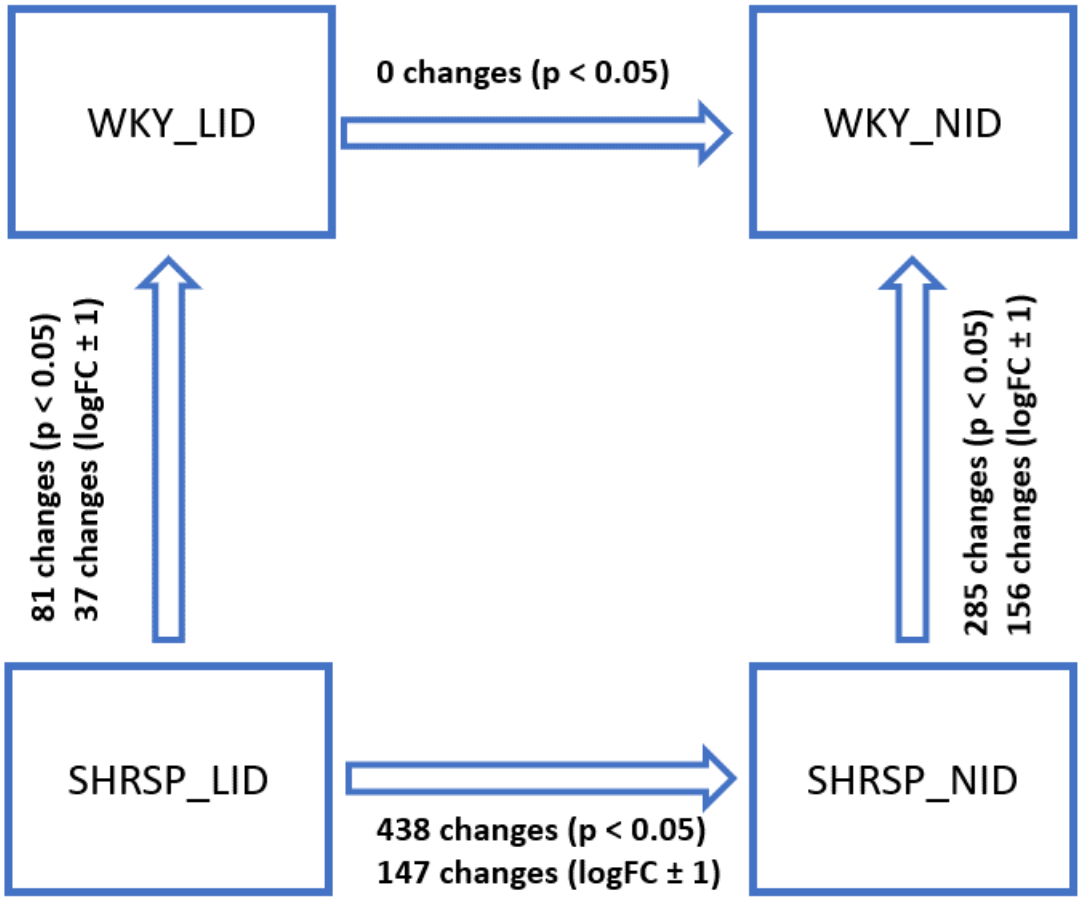

Figure 4-2: Pairwise comparison groups for DESeq2 analysis of reads.

Thoracic aorta RNA samples were compared between diet (LID versus NID) within strain and between strains (SHRSP versus WKY). Arrows indicate direction of comparison (n; = 3 per group).

Heatmaps and principal component analysis (PCA) plots were generated for post RNA-Seq quality control assessment. Most significantly DEGs (padj < 0.1 or less) were used to make heatmaps for all comparison groups and to generate heatmaps for each pairwise comparison. Volcano plots were used to analyse DEGs, in which orange spots and blue spots represent upregulated and downregulated genes respectively.

Qiagen Ingenuity® Pathway Analysis (IPA) was used to understand the biological context of our expression analysis profiles and to identify the most significant pathway changes to protein coding gene expression. IPA was also used to

discover potential novel regulatory networks and causal relationships associated with our experimental data. Datasets used in IPA were loaded into the application in comma-separated-values 'csv' format, filtered with adjusted p-value of (<0.05). Core IPA analysis was used to predict pathways and regulators that were changing based on gene expression in addition to the effected biology (cellular processes, biological functions). Activation z-scores were assigned for each comparison group. The z-score provides predictions about upstream or downstream processes inferred from observed gene expression. It considers the directional effect of one molecule on another molecule or on a process, and the direction of change of molecules in the dataset. Inhibition is reflected with a negative z-score while a positive value suggests activation.

4.3.3 Validation of some of the differentially expressed genes in key pathways.

Validation by TaqMan® quantitative PCR (q-PCR) was carried out on the original RNA samples plus additional samples as previously described in the general materials and methods (section 2.8.3).

4.4 Results

4.4.1 RNA-Seq pipeline

Analysis of clustering of samples via PCA plots for all detected genes in the thoracic aorta samples largely reveal distinct cluster groups except C1642 and A8198 (Figure 4-3), thus implying large differences in gene expression between diet (PC1=60% variance) and across strain (PC2=13% variance). Large variation across diet suggest that diet had a greater impact on gene expression in the thoracic aorta than strain differences. Visualisation of the RNA-Seq data through a heat map shows an overall consistency among replicates of WKY and SHRSP fed NID, however there is inconsistency with regards, to diet especially with samples A8198 and C1375 (Figure 4-4). However, clustering within the pairwise comparison group shows consistency among replicates between the NID and LID WKY and SHRSP respectively (Figure 4-5A and B respectively). Clustering of pairwise comparison is consistent in the NID fed WKY versus SHRSP but not in the LID fed WKY versus SHRSP, with one SHRSP LID sample clustering with WKY LID (Figure 4-6A and B respectively).

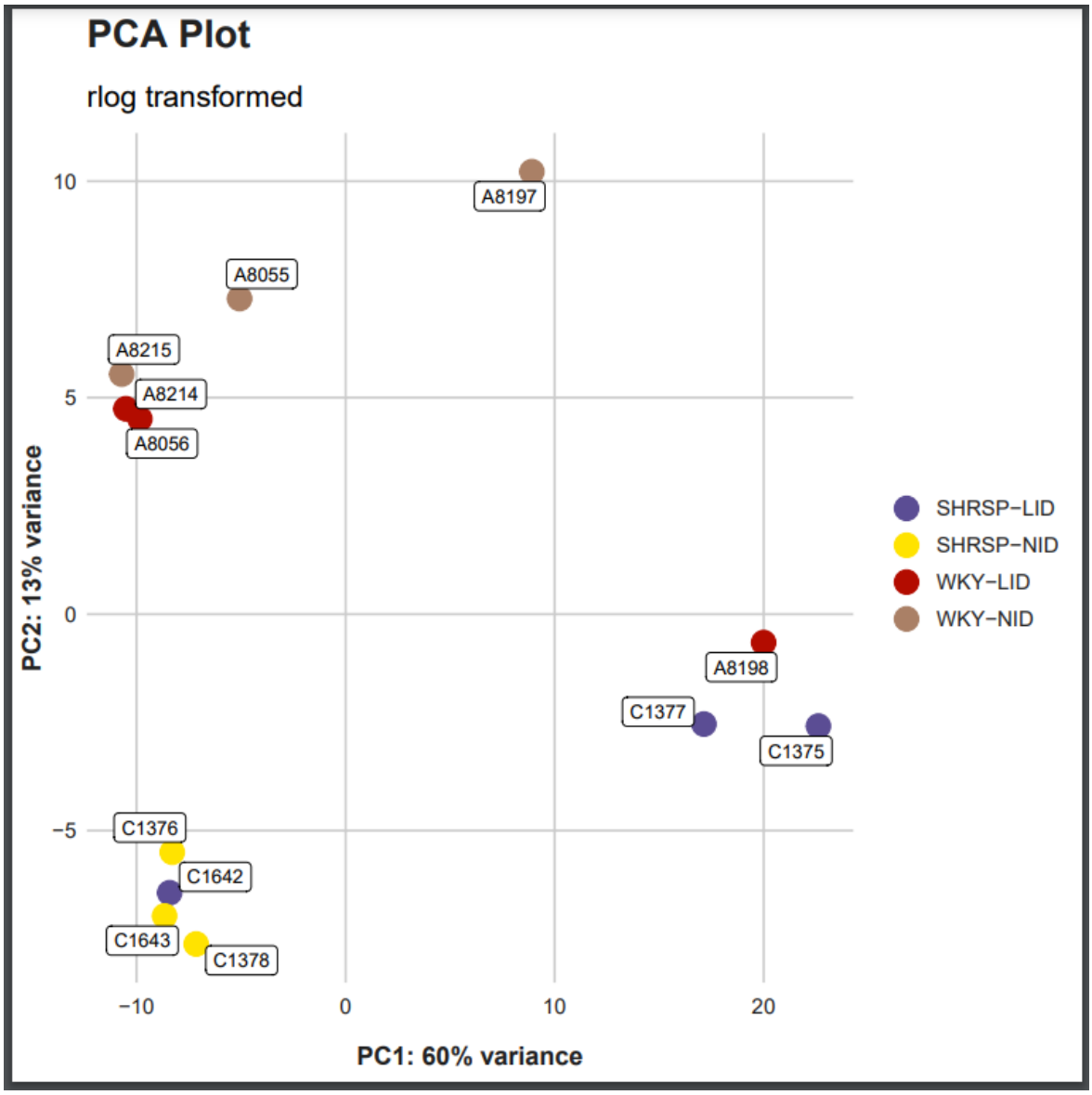

Figure 4-3: Principal component analysis (PCA) of each individual thoracic aorta gene expression.

The plot shows that the gene expressions of each sample cluster between diet (NID and LID and strain (WKY and SHRSP) except A8198 and C1642. Principal component 1 was attributed to diet and demonstrated the largest variance (60%). Principal component 2 was the strain variance between WKY and SHRSP, accounting for 13% variance.

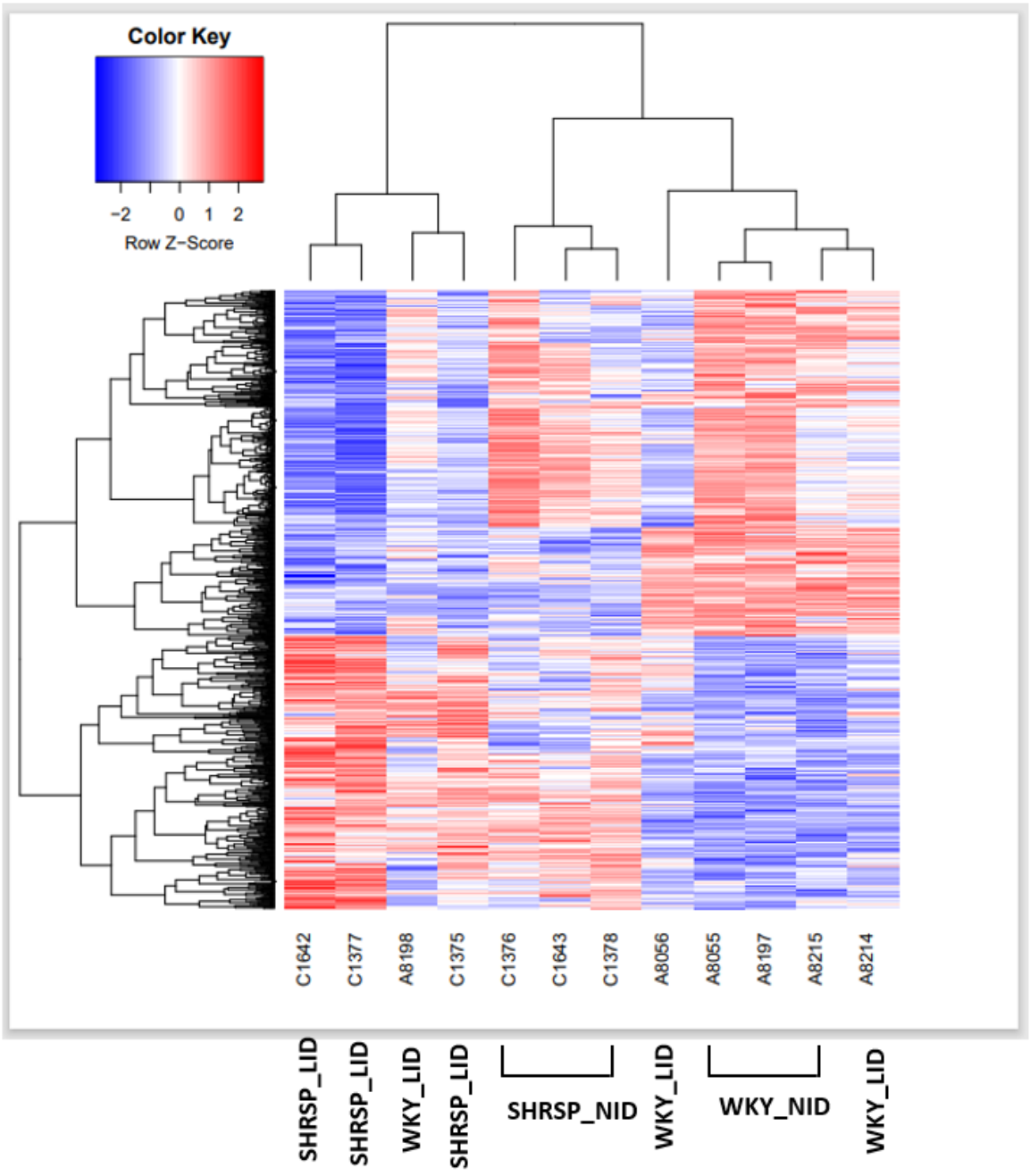

Figure 4-4: Heatmap of the individual intensity of the significant differentially expressed genes.

The heatmap demonstrates the individual intensities of significant DEGs (padj < 0.1 or less) from each comparison group. Hierarchical centroid linkage clustering was applied for each individual thoracic aorta (labelled with animal ID). Row z-score indicates the intensity change of samples for DEGs. The dendrogram at the top show gene expression clusters with strain and diet except A8198, A8056 and A8214 and dendrogram to the left of the heatmap represents hierarchical clustering within and between up and downregulated genes.

.

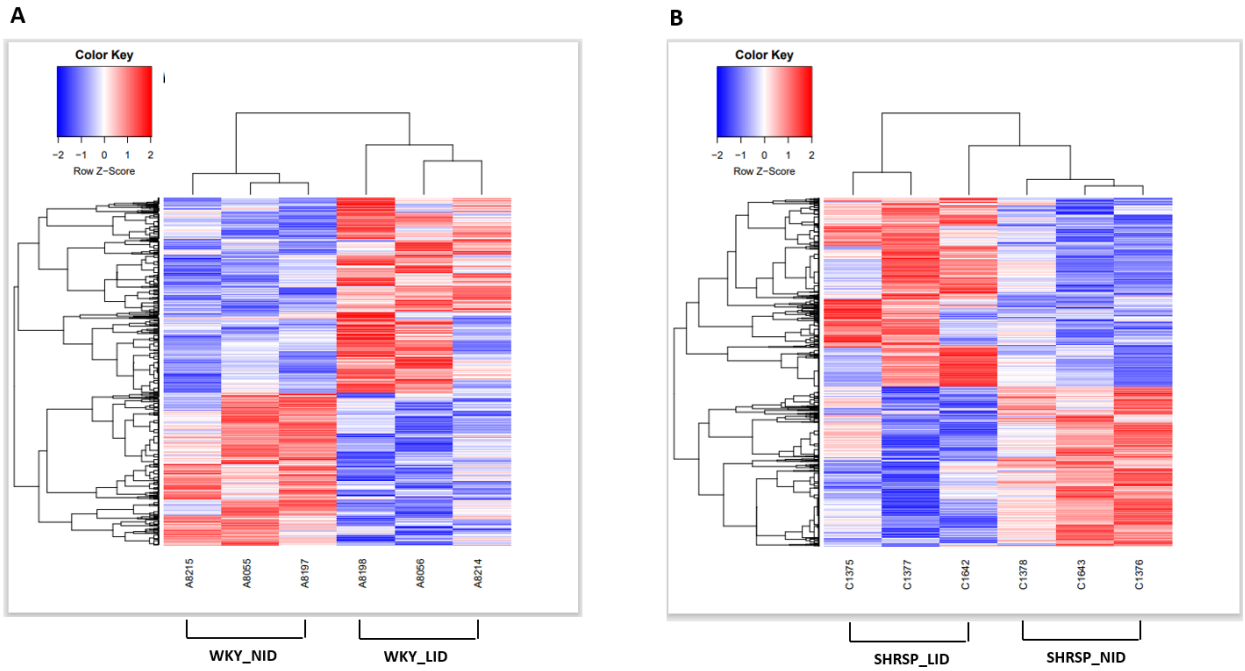

Figure 4-5: Heatmap of the individual intensity of the significant differentially expressed genes in WKY (A) and SHRSP (B) fed normal iodine (NID) or low iodine (LID) diet.

The heatmap demonstrates the individual intensities of most significant DEGs (padj < 0.1 or less) from WKY_LID versus WKY_NID (**A**) and SHRSP_LID versus SHRSP_NID (**B**). Hierarchical centroid linkage clustering was applied for each individual thoracic aorta (labelled with animal ID). Row z-score indicates the intensity change of samples for DEGs. The dendrogram at the top show gene expression clusters with strain and diet and dendrogram to the left of the heatmap represents hierarchical clustering within and between up and downregulated genes.

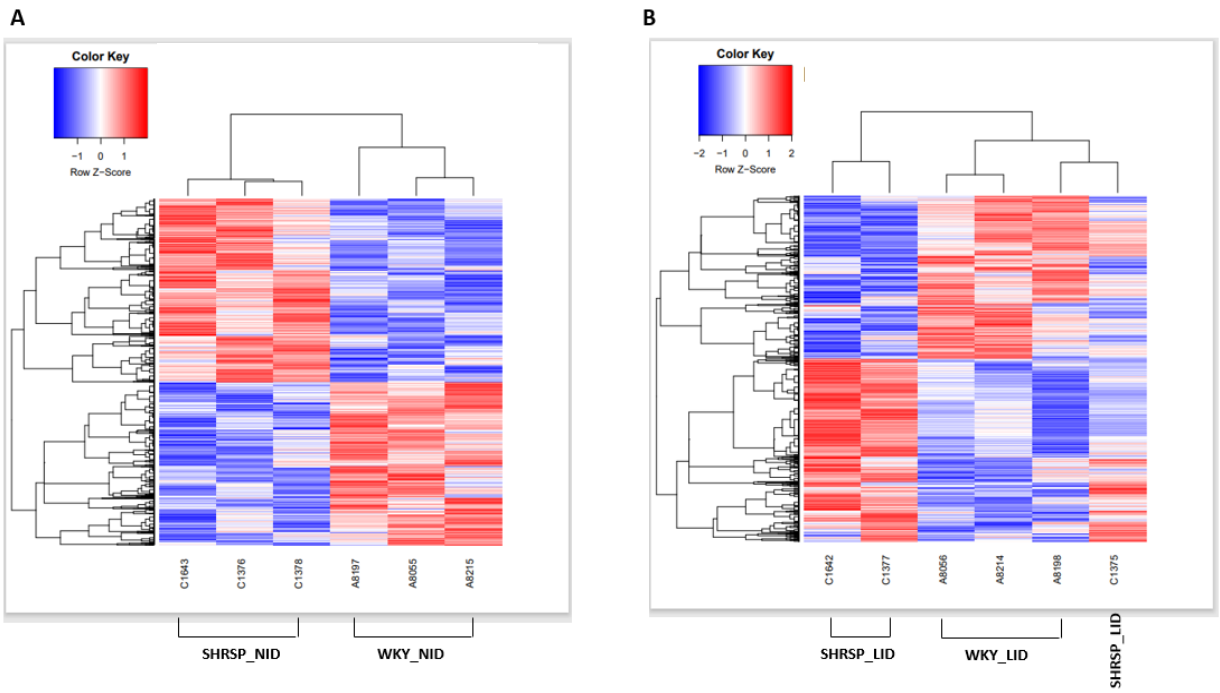

Figure 4-6: Heatmap of the individual intensity of the significant differentially genes in SHRSP and WKY fed normal iodine diet (NID) (A) and SHRSP and WKY fed low iodine diet (LID) (B).

The heatmap demonstrates the individual intensities of most significant DEGs (padj < 0.1 or less) from SHRSP fed NID versus WKY fed NID (**A**) and SHRSP fed LID versus WKY fed NID (**B**). Hierarchical centroid linkage clustering was applied for each individual thoracic aorta (labelled with animal ID). Row z-score indicates the intensity change of samples for DEGs. The dendrogram at the top show gene expression clusters with strain and diet and dendrogram to the left of the heatmap represents hierarchical clustering within and between up and downregulated genes.

.

4.4.2 Summary of differentially expressed genes.

The Mean Average (MA) and volcano plots were constructed to show global distribution of DEGs in each pairwise comparison (Figure 4-7 Figure 4-8 respectively). It distributes each gene based on the log2 fold change (y-axis) and the normalised log 10 Base mean (x-axis). Each DEG is represented on the plot, with the blue dots indicating significantly DEGs that have a padj < 0.05 and log 2-fold change. The MA plots for each of the pairwise comparison groups indicate that each has a sizeable number of significant DEGs except for MA plot A (WKY fed LID versus WKY fed NID) (Figure 4-7 A).

Table 4-1 shows the number of significantly DEGs for each pairwise comparison group. The number of DEGs was greater in the SHRSP pairwise comparison than the WKY with majority downregulated in the SHRSP fed LID group. There were no DEGs in the WKY fed LID versus WKY fed NID group. This suggests that LID negatively impacts thoracic aorta transcriptome in SHRSP but not in WKY male rats.

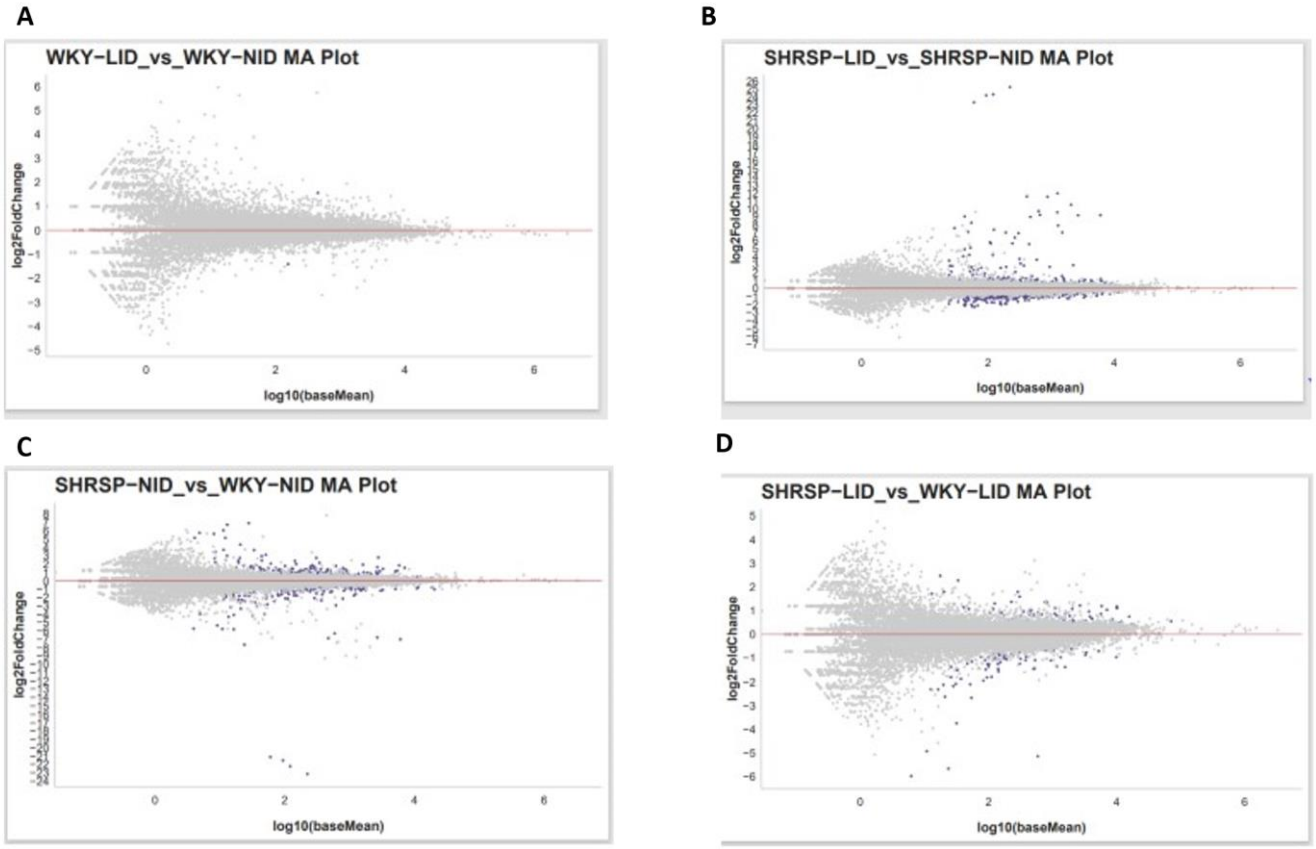

Figure 4-7: Mean-Average (MA) plots for each comparison group.

An MA plot was constructed for each comparison group to visualise the transcriptomic expression differences. Each DEG is represented by one dot and the plots illustrate the distribution of the log 2-fold change verses log 10 base Mean. **A** and **B** are changes induced by low iodine diet (LID) in WKY and SHRSP respectively while **C** and **D** are changes induced by strain in the NID and LID respectively.

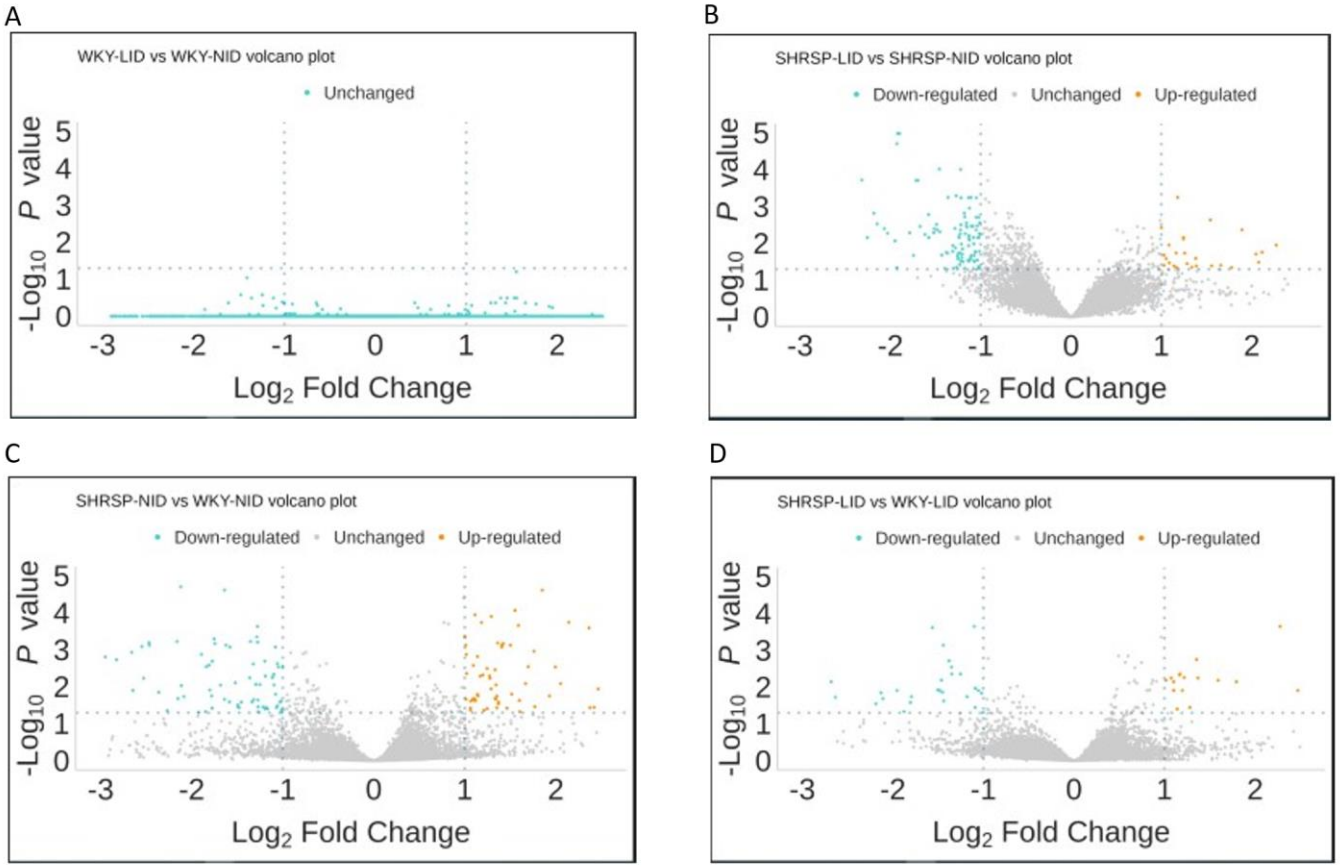

Figure 4-8: Volcano plots for each comparison group.

A volcano plot was constructed for each comparison group to visualise the transcriptomic expression profiles. Each DEG is represented by one dot and the plots illustrate the distribution of the log 10 p value versus Log2-fold change. **A** and **B** are changes induced by low iodine diet (LID) in WKY and SHRSP respectively while **C** and **D** are changes induced by strain in the NID and LID respectively**.**

Table 4-1: Number of significantly upregulated and downregulated genes in each group and the number common between LID and NID and between the SHRSP and WKY rats.

	LID versus NID			SHRSP versus WKY		
	WKY	SHRSP	Common	NID	LID	Common
Upregulated	0	107	0	146	34	11
Downregulated	0	331	0	139	47	24
Total	0	438	0	285	81	35

The DEGs between the groups were limited to padj < 0.05 to determine the total number of significantly DEGs and the number of common genes. These DEGs were further subdivided into the number of upregulated and downregulated genes per pairwise comparison.

4.4.3 Biological functions and pathways associated with differentially expressed genes.

The main aim of this chapter was to determine the effect of LID on gene expression in WKY and SHRSP thoracic aorta. The pairwise comparison between the WKY fed LID versus WKY fed NID did not yield significant DEGs and therefore this chapter focuses on the comparison between LID and NID fed SHRSP male thoracic aorta gene expression differences. This comparison had the highest number of DEGs which allowed investigation on changes in gene expression because of LID. The 438 DEGs that were revealed to be LID dependent were uploaded to QIAGEN Ingenuity® Pathway Analysis (IPA®, QIAGEN Redwood City, www.qiagen.com/ingenuity) to determine their predicted involvement in biological functions and molecular pathways. Figure 4-9 shows a bubble plot for the biological functions predicted to be under influence of this subset of DEGs. The most significant enriched canonical pathway is the dilated cardiomyopathy signalling pathway with a $p < 5.54 \times 10^{-8}$, and z-score -2.138.

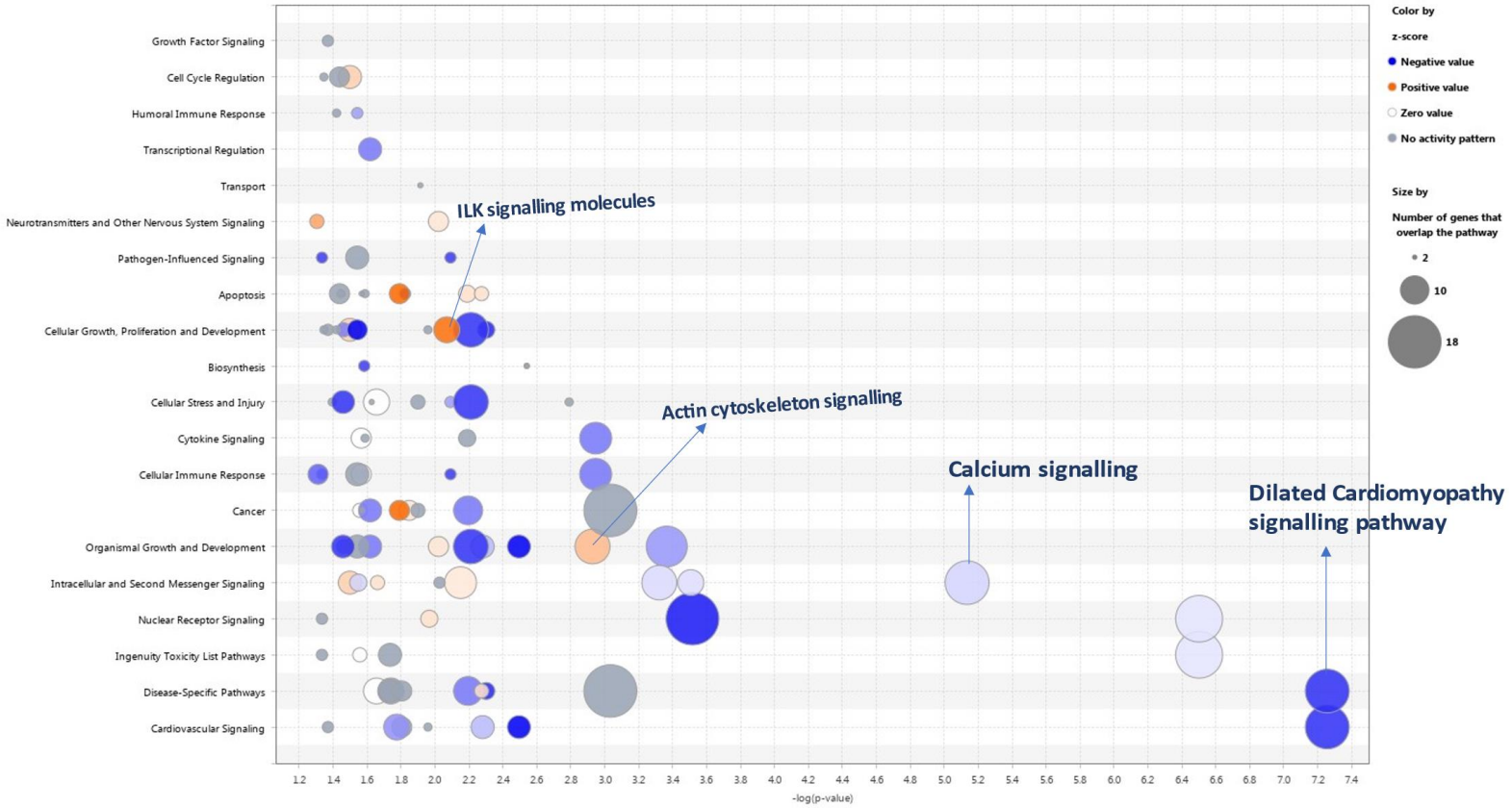

Figure 4-9: Top biological functions and critical pathways altered due to low iodine diet (LID) in SHRSP thoracic aorta predicted by IPA®.

The 438 DEGs found to be common to LID in SHRSP were predicted to have the most significant influences on these biological functions. The colour is predicted by the z score and colour intensity represent degree of activation (Orange) or inhibition (Blue). Darker shades represent lower p-values and more statistically significant**.**

4.4.4 Genes associated with critcial pathways under low iodine diet

The most significant canonical pathways were identified (Benjamini-Hochberg (BH) adjusted p < 0.05, z-score great than 2). Pathway analysis revealed the most perturbed pathways to be dilated cardiomyopathy signalling pathway (15 molecule, z-score -2.138 and p value = 5.54×10^{-08}). Muscle contractile and regulatory proteins (Actin alpha cardiac muscle 1 (Actc1), Myosin heavy chain 6 (Mhy6), Myosin heavy chain 7 (Mhy7), Troponin C1, slow skeletal and cardiac type (Tnnc1), Troponin I3, cardiac type (Tnni3), Troponin T2, cardiac type (Tnnt2) and titin (Ttn) were significantly increased in this pathway (Figure 4-10 and 4-11). Actc1, Mhy6, Mhy7, Tnnc1, Tnni3, Tnnt2 were also found to be significantly increased in Ca^{2+} and integrin-linked kinase (ILK) signalling pathways, (Figure 4-12 and Figure 4-13-14 respectively) while Actc1, Mhy6, Mhy7 and Ttn were also significantly increased in actin cytoskeleton (Figure 4-15-16). Table 4-2, 4-3, 4-4, and 4-5 summarises the top 10 DEGs in dilted cardiomyopathy, Ca^{2+}, ILK and actin cytoskeleton signalling pathways respectively (padj < 0.05).

4.4.5 Upstream transcription regulators

The upstream regulator analysis (URA) tool is a novel function in IPA which can, identify potential upstream regulators including transcription factors (TFs) and any gene or small molecule that has been observed experimentally to affect gene expression by analysing linkage to DEGs through coordinated expression (Krämer et al., 2014). IPA identified activated potential upstream regulators (Bonferroni corrected p value < 0.05). The most significant upstream activated regulator is predicted to be Myocardin (MYOCD) acting through serum response factor (SRF). Its target molecules were found to be Actc1, DES, Myh6, Myl7, SCN5A, Tnnt2 and Ttn (Figure 4-17).

4.4.6 Diseases and functions associated with differentially expressed genes under low iodine diet.

IPA predicted the activation (or inhibition) state of associated diseases and biological function influenced by DEGs under LID (Figure 4-18). Twenty nine diseases and biological functions were predicted according to padj-value and z-

score. Seventeen diseases or functions were predicted to be increased while 11 diseases or functions were predicted to be decreased. The DEGs were mostly linked to increased chances of organisimal death, growth failure or short stature, hypoplasia and decreased possibility of infection with HIV-1 and infection by RNA virus. Table 4-7 summaries the diseases or functions increased or diseased in response to LID according to padj-value and z-score. IPA revealed that a total of 43 genes contributed to growth failure or short stature and out of the 43 genes, 35 genes were downregulated while 8 were upregulated (Figure 4-19).

4.4.7 Ingenuity pathway analysis upstream regulator effects and downstream biology.

IPA identified Micro RNA (miRNA) as some of the top predicted upstream regulators in connection to the DEGs in the dataset and their influcence on the top diseases and biological funtions, likely to be affected by LID. miR-124-3p, miR-155-5p, miR-17HG and miR-17 were activated in SHRSP fed LID and were associated with predicated increase in growth failure or short sature, hypoplasia, bleeding, midline brain anormally and organismal death. The upstream regulators were also linked to predicted decrease in size of the body, export of molecule and autophagy of cells (Figure 4-20).

4.4.8 Verification of differentially expressed genes by RT q-PCR.

To verify the reliability of the RNA-Seq results, 4 DEGs linked with muscle contraction were quantified using TaqMan q-PCR. Two out of the 4 genes agreed with the RNA-Seq data while the other two showed a trend towards increased expression under LID. These validation results imply that the our RNA-Seq data seem to be of high reliability. Nonetheless, it would be still necessary to conduct more single gene experiments using RT-qPCR as a method to get a better estimate of the reliability of the implemented RNA-Seq results. The expression of Myh6 and Actc1 in the thoracic aorta were significantly increased in LID fed SHRSP males when compared to NID fed SHRSP males, while Myh7 and Tnni3 were not significantly different between the NID and LID thoracic aorta (Figure 4-21).

4.4.9 Potential connections of sodium iodide , sodium iodide symporter (SLC5a5) and vascular disease with significantly increased genes in dilated cardiomyopathy signalling pathway.

Exploring potential connections between sodium iodide, SLC5a5, genes enriched from the dilated cardiomyopathy signalling and vascular disease pathways demonstrated indirect interaction between sodium iodide and SLC5a5. A direct interaction was demonstrated between SLC5a5, Actn2 and Ttn while an indirect interaction was established between SLC5a5, Tnni3 and Myh7. Moreover, indirect interaction between Tnnc1, Tnnt2, Myh6, Myh7, Ttn, Tnni3 and vascular disease was observed while there was no established connection between Actc1 and SLC5a5 or vascular disease (Figure 4-22).

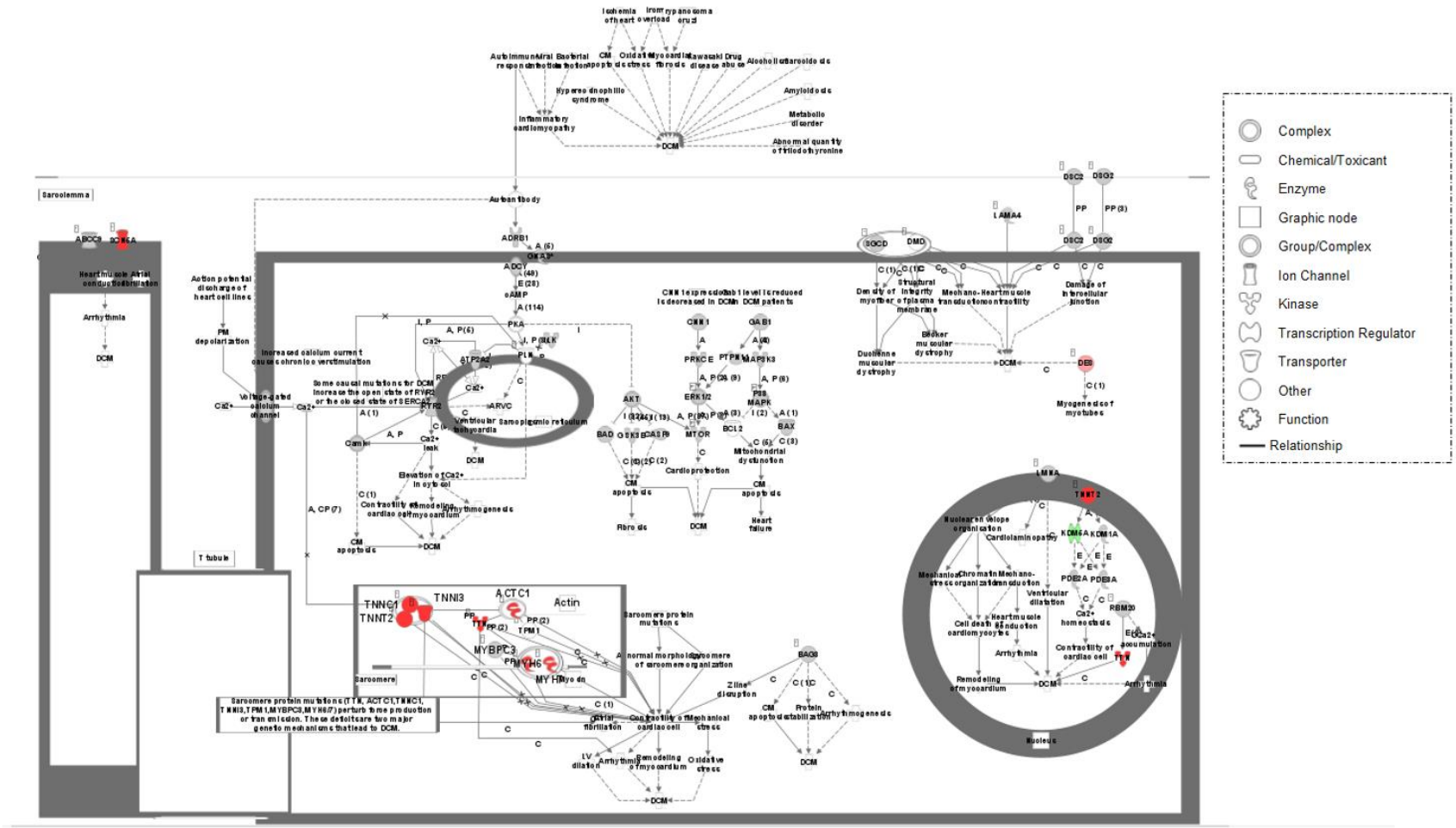

Figure 4-10: The network of genes involved with dilated cardiomyopathy signalling pathway.

Gene interaction network created from IPA shows that there is differential expression of genes involved in muscle contraction. 7 subunits associated with muscle contraction were significantly increased (padj < 0.05) in the SHRSP fed LID compared to those fed NID. Red = increased expression and green =reduced expression.

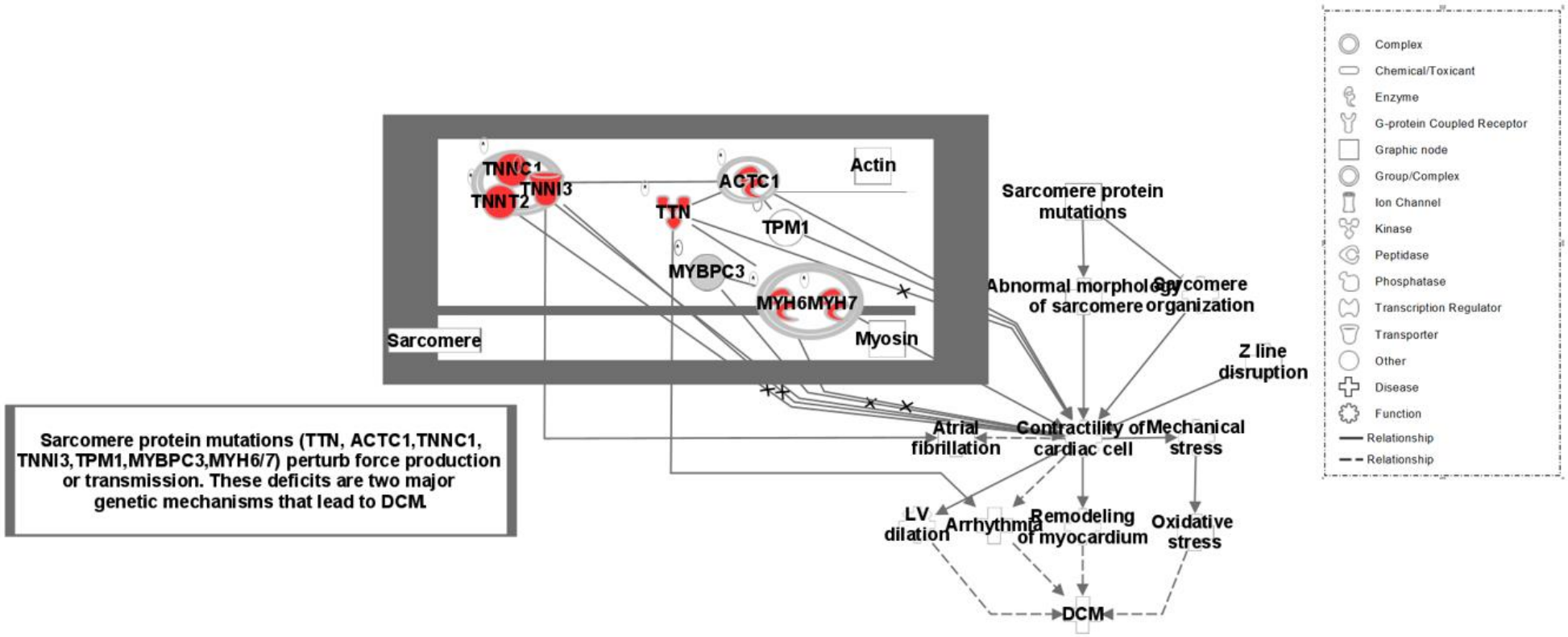

Figure 4-11: An expansion of dilated cardiomyopathy signalling pathway highlighting significantly altered genes.

The pathway was highlighted by IPA and further investigation revealed that 7 subunits involved in muscle contraction where significantly increased (padj < 0.05) in SHRSP fed LID compared to those fed NID. Red = increased expression and green is reduced expression.

Table 4-2: A list of Top 10 genes significantly expressed in dilated cardiomyopathy signalling pathway.

Symbol	Ensembl gene ID	padj p-value	Log2Fold Change	BaseMean
MYH6	ENSRNOG00000025757	0.0055	9.17	6056.63
ACTC1	ENSRNOG00000008536	0.007	9.15	2679.77
TNNT2	ENSRNOG00000033734	0.0137	9.53	1256.82
TNNI3	ENSRNOG00000018250	0.0138	11.47	878.68
TTN	ENSRNOG00000069271	0.0142	9.2	666.65
TNNC1	ENSRNOG00000018943	0.0181	5.55	449.26
DES	ENSRNOG00000019810	0.0184	1.26	1578.80
MYH7	ENSRNOG00000016983	0.026	11.91	1266.06
KDM5A	ENSRNOG00000010591	0.0367	-0.61	591.55
SCN5A	ENSRNOG00000015049	0.0461	7.35	124.12

The above genes had a significantly altered expression in SHRSP male fed LID (padj < 0.05)

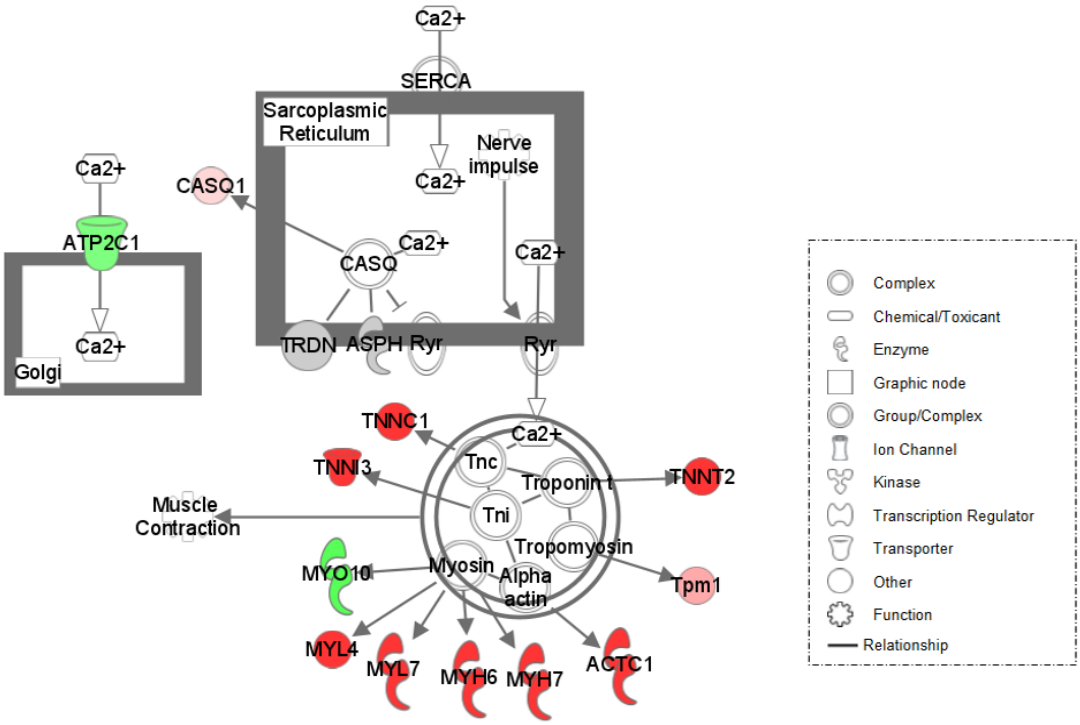

Figure 4-12: The network of genes involved in Ca^{2+} signalling pathway.

The pathway was highlighted by IPA and further investigation revealed that 8 subunits involved in muscle contraction where significantly increased while 1 was significantly reduced (padj < 0.05) in SHRSP fed LID compared to those fed NID. Red = increased expression and green is reduced expression.

Table 4-3: A list of top 10 genes significantly expressed in Ca2+ signalling pathway.

Symbol	Ebsembl gene ID	padj p-value	Log2Fold Change	BaseMean
ATP2C1	ENSRNOG00000013305	0.0015	-0.7	1087.68
MYO10	ENSRNOG00000010161	0.0045	-0.91	929.95
MYH6	ENSRNOG00000025757	0.0055	9.17	6056.63
MYL4	ENSRNOG00000050675	0.0069	7.87	1290.30
ACTC1	ENSRNOG00000008536	0.007	9.15	2679.77
TNNT2	ENSRNOG00000033734	0.0137	9.53	1256.82
TNNI3	ENSRNOG00000018250	0.0138	11.47	878.68
MYL7	ENSRNOG00000014409	0.0181	10.47	2068.51
TNNC1	ENSRNOG00000018943	0.0181	5.55	449.26
MYH7	ENSRNOG00000016983	0.026	11.91	1266.06

The above genes had a significantly altered expression in SHRSP male fed LID (padj < 0.05).

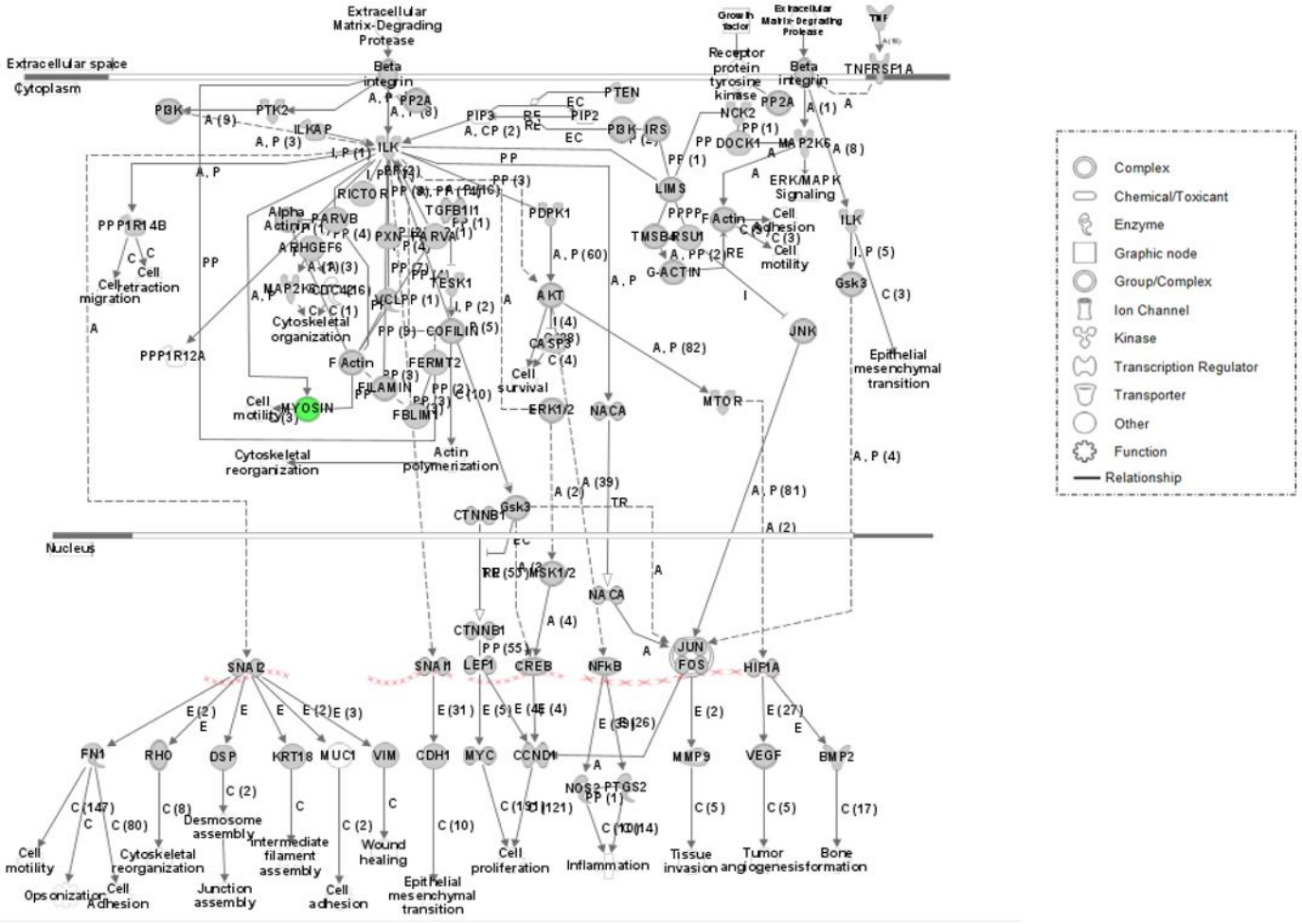

Figure 4-13: A network of genes involved in ILK signalling pathway.

The pathway was highlighted by IPA and further investigation revealed gene expression changes in the SHRSP fed LID compared to those fed NID. Red = increased expression and green is reduced expression (padj < 0.05).

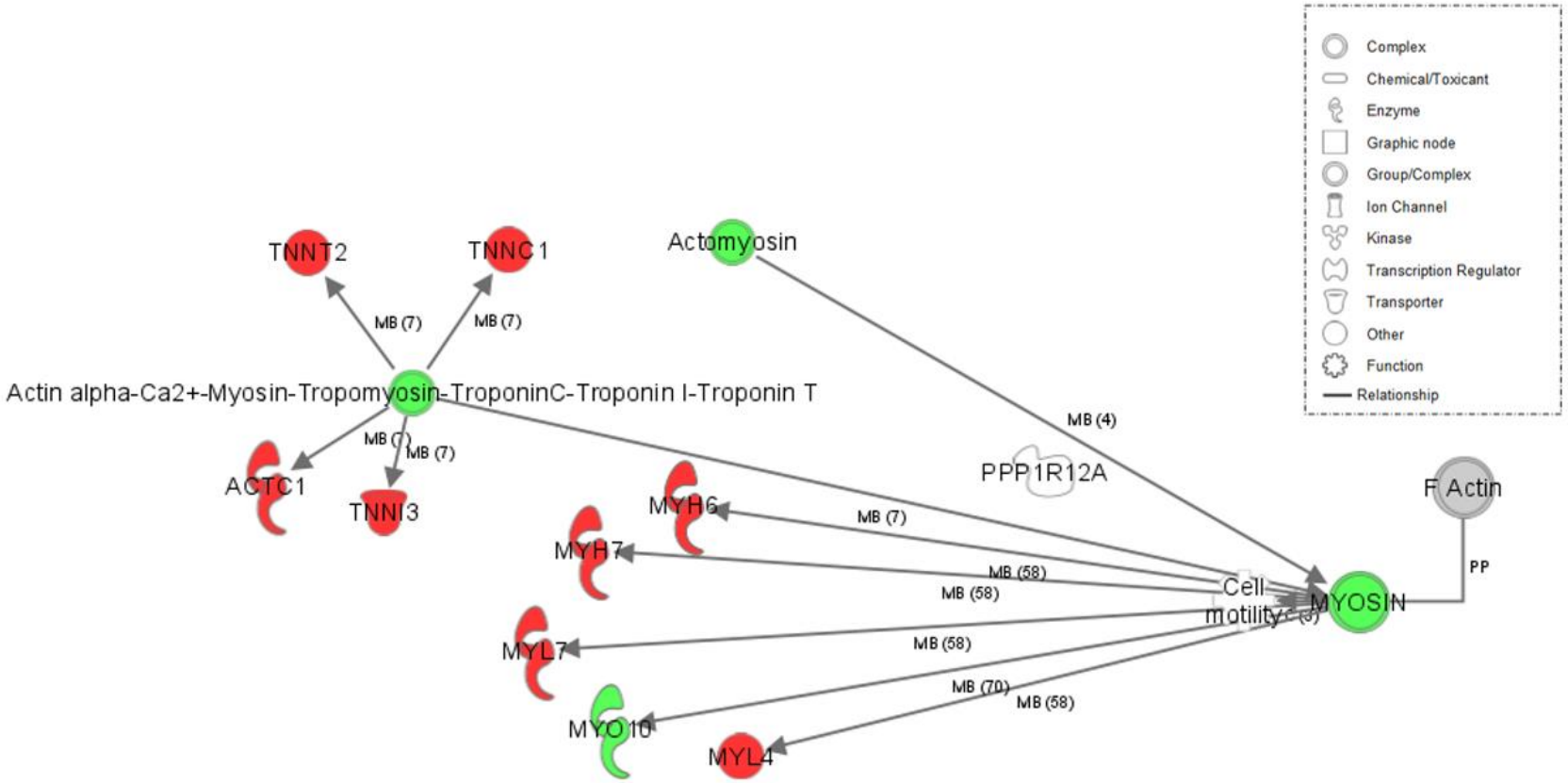

Figure 4-14: An expansion of ILK signalling pathway highlighting a network of genes significantly altered by LID.

The pathway was highlighted by IPA and further investigation revealed 8 subunits involved in muscle contraction where significantly increased while 1 was significantly reduced (adj $p < 0.05$) in SHRSP fed LID compared to those fed NID. Red = increased expression and green is reduced expression

Table 4-4: A list of top 10 genes significantly expressed in ILK signalling pathway.

Symbol	Ensembl gene ID	padj p-value	Log2Fold Change	BaseMean
MYO10	ENSRNOG00000010161	0.0044	-0.91	929.95
MYH6	ENSRNOG00000025757	0.0055	9.17	6056.63
MYL4	ENSRNOG00000050675	0.0069	7.87	1290.30
ACTC1	ENSRNOG00000008536	0.007	9.15	2679.77
TNNT2	ENSRNOG00000033734	0.0137	9.53	1256.82
TNNI3	ENSRNOG00000018250	0.0138	11.47	878.68
MYL7	ENSRNOG00000014409	0.0181	10.47	2068.51
TNNC1	ENSRNOG00000018943	0.0181	5.55	449.26
MYH7	ENSRNOG00000016983	0.026	11.91	1266.06

The above genes had a significantly altered expression in SHRSP male fed LID (padj < 0.05).

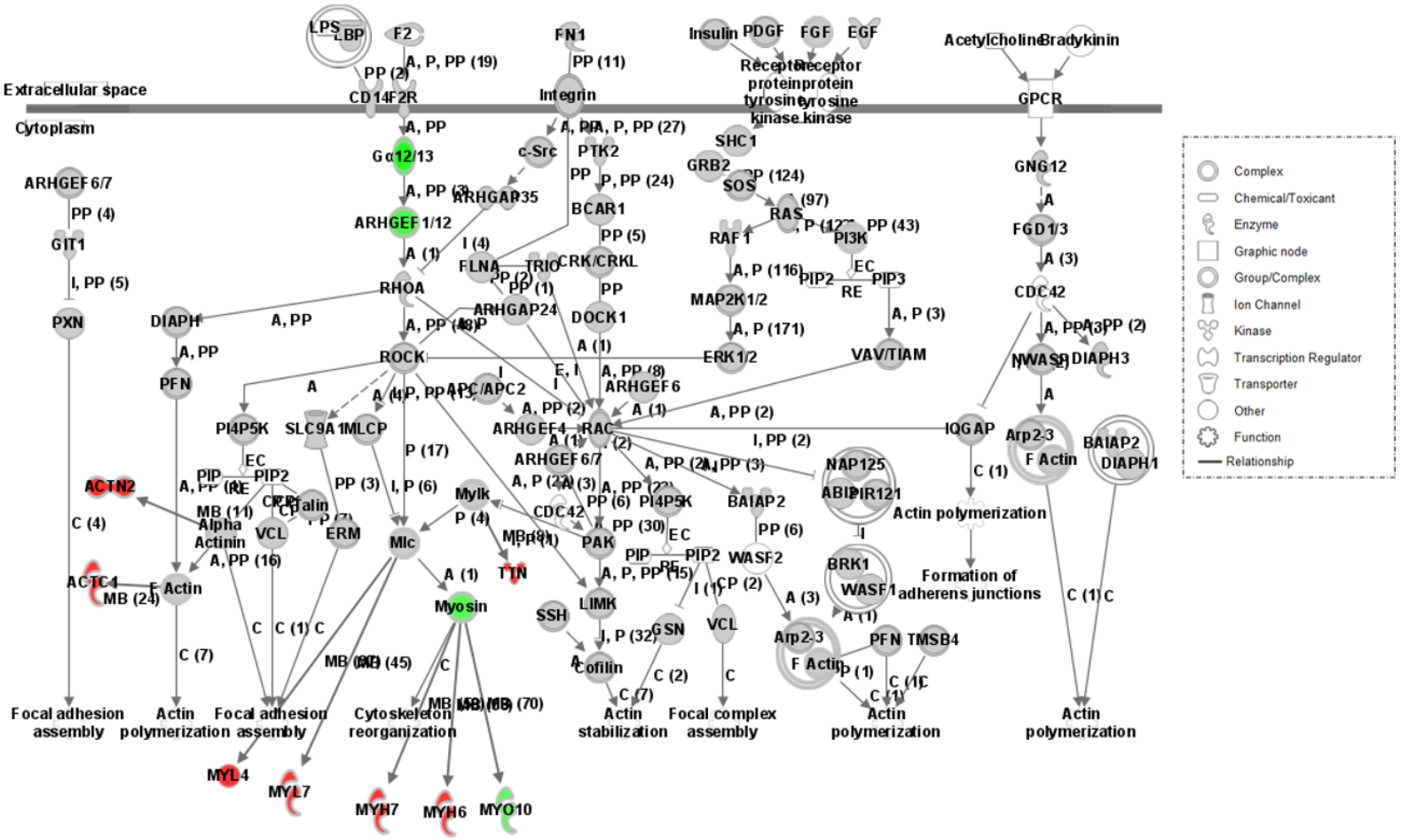

Figure 4-15: A network of genes involved in actin cytoskeleton signalling pathway.

The pathway was highlighted by IPA and further investigation revealed gene expression changes in the SHRSP fed LID compared to those fed NID Red = increased expression and green is reduced expression.

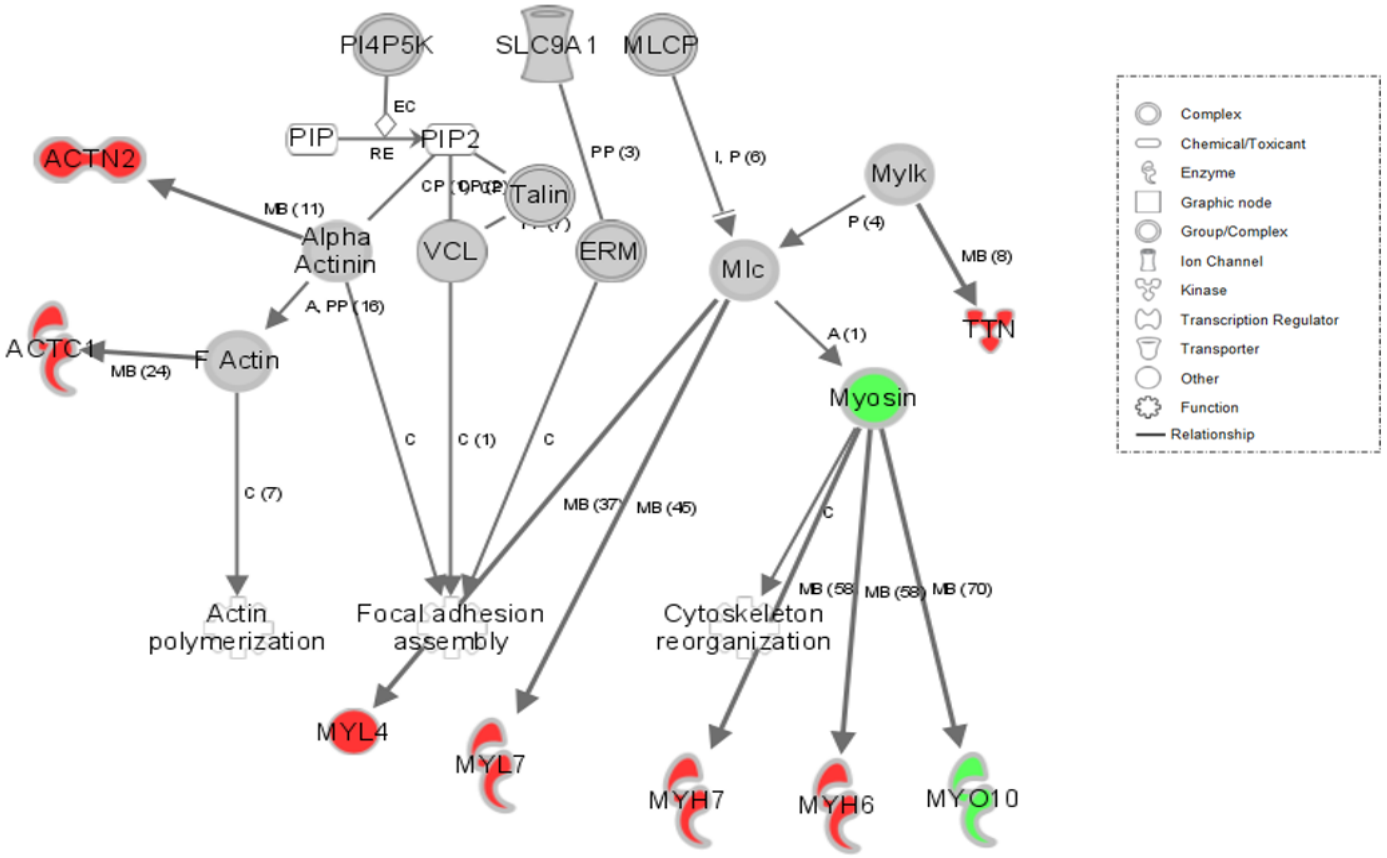

Figure 4-16: An expansion of the actin cytoskeleton signalling pathway highlighting a network of genes significantly altered by LID.

The pathway was highlighted by IPA and further investigation revealed 7 subunits involved in muscle contraction where significantly increased while 1 was significantly reduced (adj $p < 0.05$) in SHRSP fed LID compared to those fed NID. Red = increased expression and green is reduced expression.

Table 4-5: A list of top 10 genes significantly expressed in actin cytoskeleton signalling pathway.

Symbol	Ensembl gene ID	padj p-value	Log2Fold change	BaseMean
MYO10	ENSRNOG00000010161	0.0045	-0.91	929.95
MYH6	ENSRNOG00000025757	0.0055	9.17	6056.63
MYL4	ENSRNOG00000050675	0.0069	7.87	1290.30
ACTC1	ENSRNOG00000008536	0.007	9.15	2679.77
TTN	ENSRNOG00000069271	0.0142	9.2	666.65
MYL7	ENSRNOG00000014409	0.0181	10.47	2068.51
MYH7	ENSRNOG00000016983	0.026	11.91	1266.06
ACTN2	ENSRNOG00000017833	0.0437	3.59	594.69
DOCK1	ENSRNOG00000018683	0.0509	-0.46	761.32
LBP	ENSRNOG00000014532	0.1362	0.76	160.18

The above genes had a significantly altered expression in SHRSP male fed LID (padj < 0.05).

.

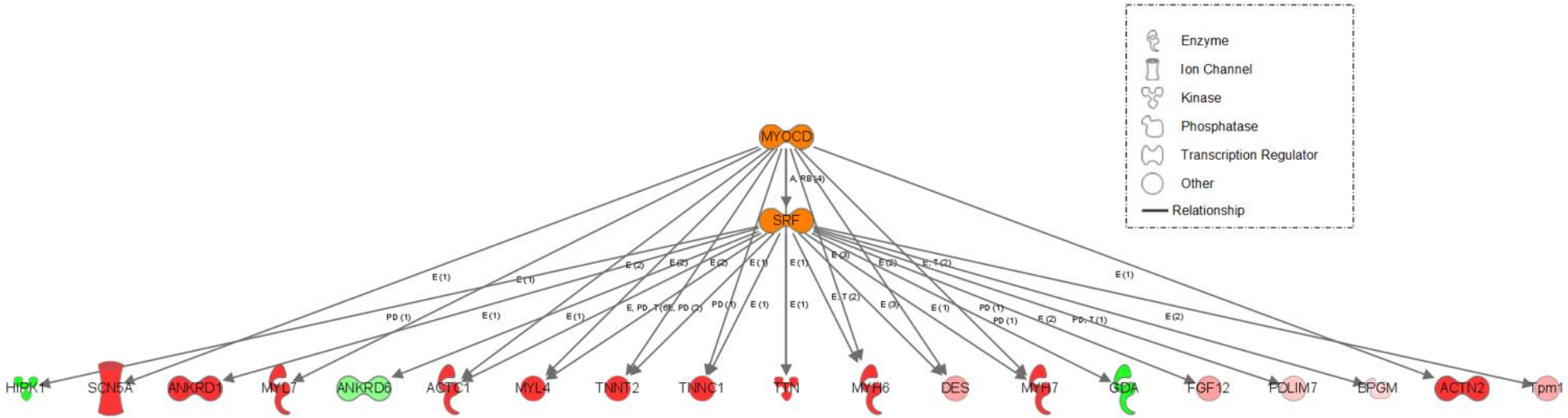

Figure 4-17:Ingenuity pathway analysis mechanistic network of upstream potential regulators.

Interaction between MYOCD SRF and differentially expressed genes (DEGs) is shown. An increased measurement (red) indicates that gene was more highly expressed in the LID thoracic aorta, and thus reduced over normal iodine (NID) and vice versa for a decreased measurement (green). Orange represents activation state. The filled lines indicate published connections, dashed lines indicated *in silico* inferred connections. An arrow indicates a regulatory vector. (E) represents expression while a number in brackets represent number of publications related to MYOCD/SRF and a particular gene.

Table 4-6: List of Top 10 genes significantly expressed in upstream interaction between MYOCD and SRF.

Symbol	Ensembl gene ID	padj p-value	Log2Fold Change	BaseMean
HIPK1	ENSRNOG00000019333	0.0035	-1.67	298.32
BPGM	ENSRNOG00000010133	0.0049	0.58	587.96
MYH6	ENSRNOG00000025757	0.0056	9.17	6056.63
GDA	ENSRNOG00000018282	0.0055	-1.23	219.32
MYL4	ENSRNOG00000050675	0.0076	7.87	1290.30
ACTC1	ENSRNOG00000008536	0.007	9.15	2679.77
TNNT2	ENSRNOG00000033734	0.0137	9.53	1256.82
TTN	ENSRNOG00000069271	0.0142	9.2	666.65
MYL7	ENSRNOG00000014409	0.0181	10.47	2068.51
TNNC1	ENSRNOG00000018943	0.0181	5.55	449.26

The above genes had a significantly altered expression in SHRSP male fed LID (padj < 0.05).

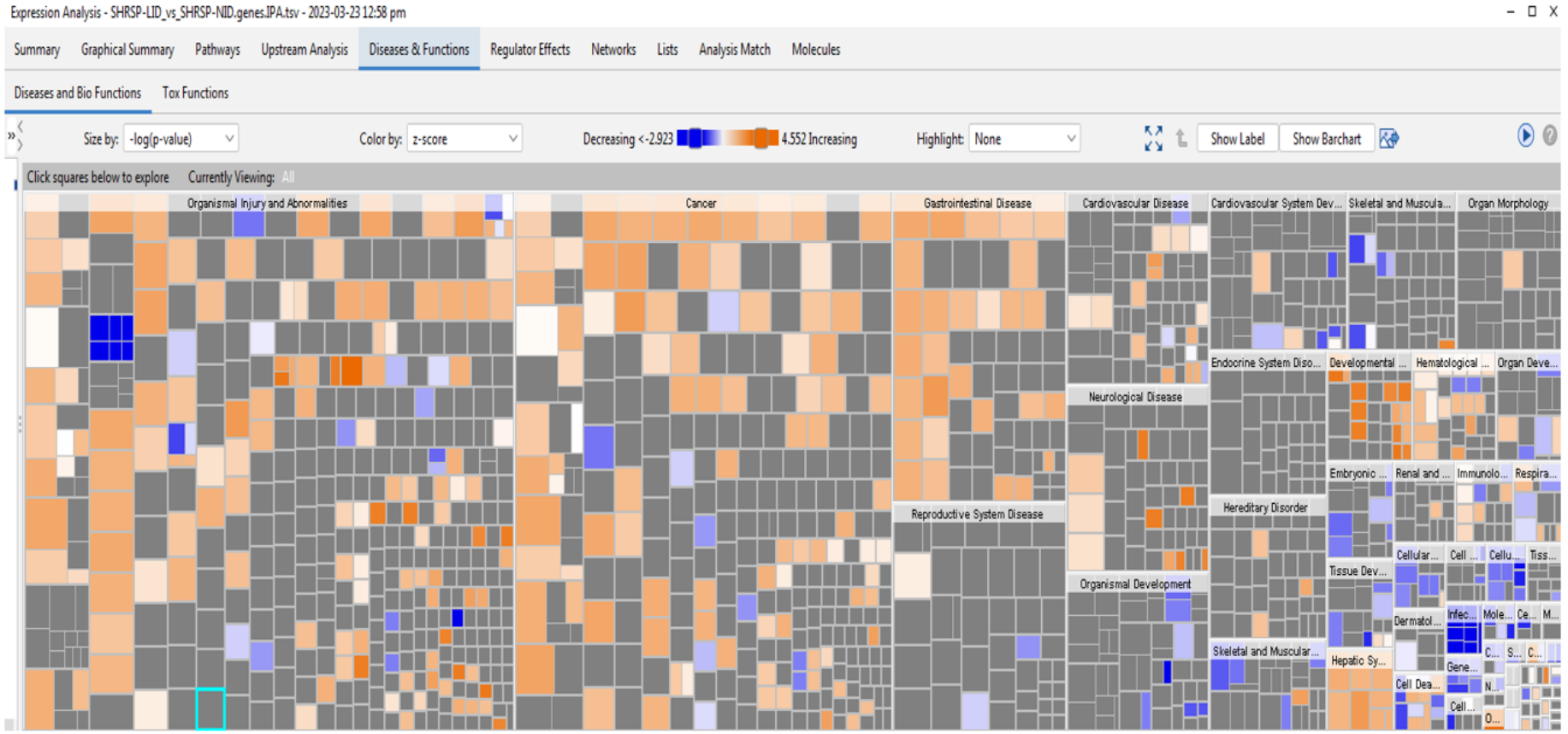

Figure 4-18: Ingenuity pathway analysis downstream effect analysis demonstrating upregulated and downregulated biological processes.

Predicted effected biology based on differentially expressed genes (DEGs) in response to low iodine diet (LID). Each box represents a biological process or disease. The size of the box represents gene enrichment. The orange colour denotes upregulation, blue denotes down regulation while grey shows no change to the cellular process and biological functions.

Table 4-7: List of Disease and functions predicted activation state in response to LID in SHRSP thoracic aorta.

Diseases or Functions Annotation	p-value	Predicted Activation State	Activation z-score	# Molecules
Organismal death	2.64E-11	Increased	6.154	132
Hypoplasia	0.000361	Increased	3.732	29
Aplasia or hypoplasia	0.00059	Increased	3.668	30
Bleeding	0.000347	Increased	3.478	25
Early-onset encephalopathy	1.15E-05	Increased	3.422	41
Congenital encephalopathy	1.53E-05	Increased	3.422	35
Congenital neurological disorder	9.7E-07	Increased	3.411	50
Growth failure or short stature	1.28E-06	Increased	3.335	43
Growth Failure	1.92E-06	Increased	3.335	37
Midline brain anomaly	0.000235	Increased	3.148	10
Exencephaly	0.000717	Increased	2.985	9
Thoracic hypoplasia	1.31E-05	Increased	2.853	15
Sensitivity of cells	2.63E-06	Increased	2.672	33
Liver lesion	2.89E-15	Increased	2.181	231
Hypoplasia of heart	0.000132	Increased	2.138	8
Intraabdominal organ tumor	1.11E-20	Increased	2.107	375
Apoptosis	2.11E-06	Increased	2.05	119
Development of neural cells	0.000455	Decreased	-2.155	48
Export of molecule	0.000753	Decreased	-2.255	17
Cellular homeostasis	5.84E-05	Decreased	-2.296	79
Autophagy of cells	0.000667	Decreased	-2.696	24
Size of body	0.00016	Decreased	-3.42	41
Infection of cervical cancer cell lines	4.87E-05	Decreased	-3.536	25
Viral Infection	2.28E-07	Decreased	-3.792	92
Infection of tumor cell lines	2.32E-05	Decreased	-3.811	30
Infection of cells	9.44E-06	Decreased	-4.25	42
HIV infection	0.000176	Decreased	-4.333	35
Infection by RNA virus	7.34E-06	Decreased	-4.336	60
Infection by HIV-1	0.00019	Decreased	-4.525	30

The above diseases and function activation status was predicted as increased or decreased based on p-value ($p < 0.05$) and activation z-score (±2).

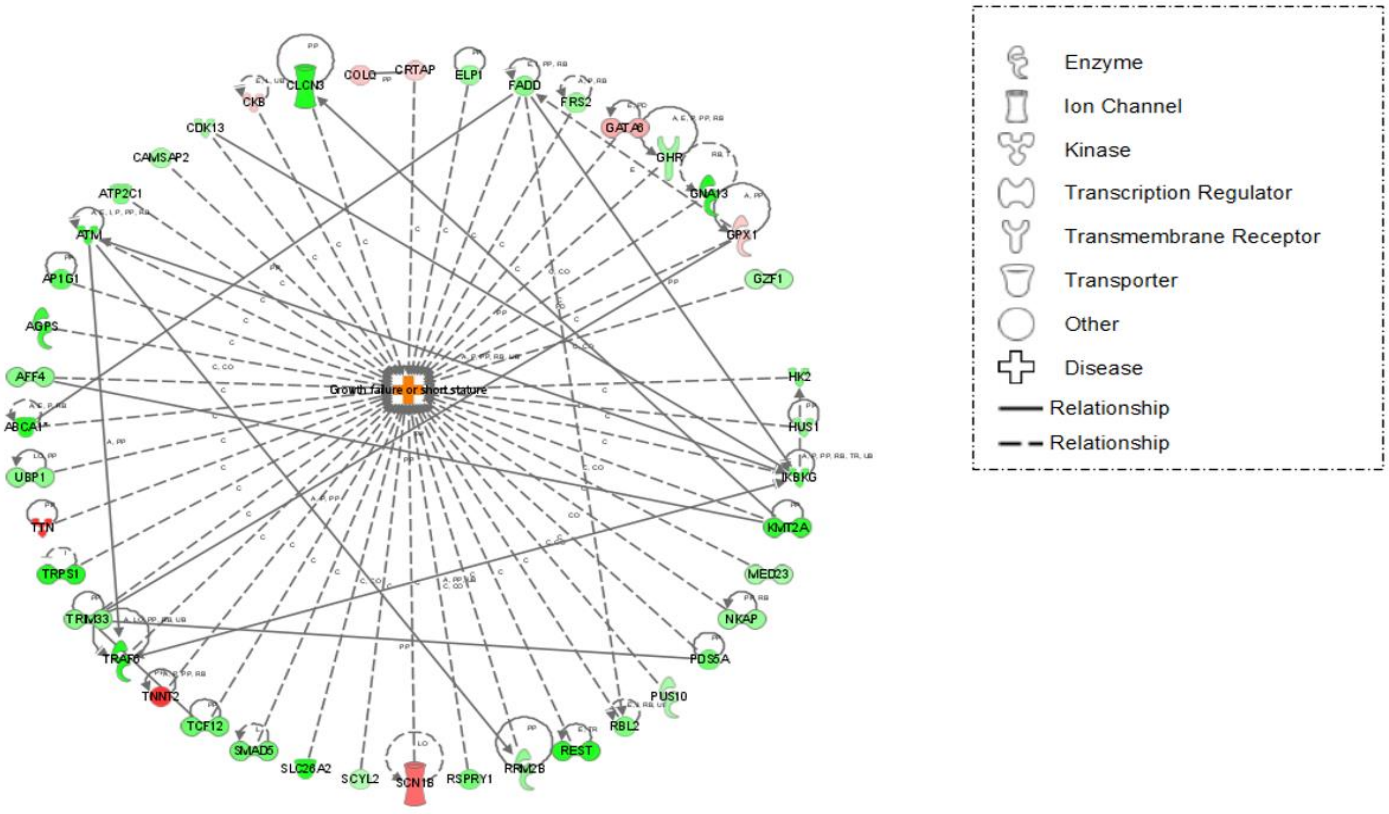

Figure 4-19: Genes predicted to encourage growth failure and short stature in thoracic aorta of SHRSP males fed LID.

The male SHRSP thoracic aorta gene expression profile predicated growth failure and short stature as one of the top disease or function in response to LID. A total of 43 genes contributed to this prediction. 35 of these genes were downregulated while 8 were upregulated. An increased measurement (red) indicates that gene was more highly expressed in the LID thoracic aorta, and thus reduced over normal iodine (NID) and vice versa for a decreased measurement (green). Orange is the activated stated. The filled lines indicate published connections, dashed lines indicated *in silico* inferred connections. An arrow indicates a regulatory vector.

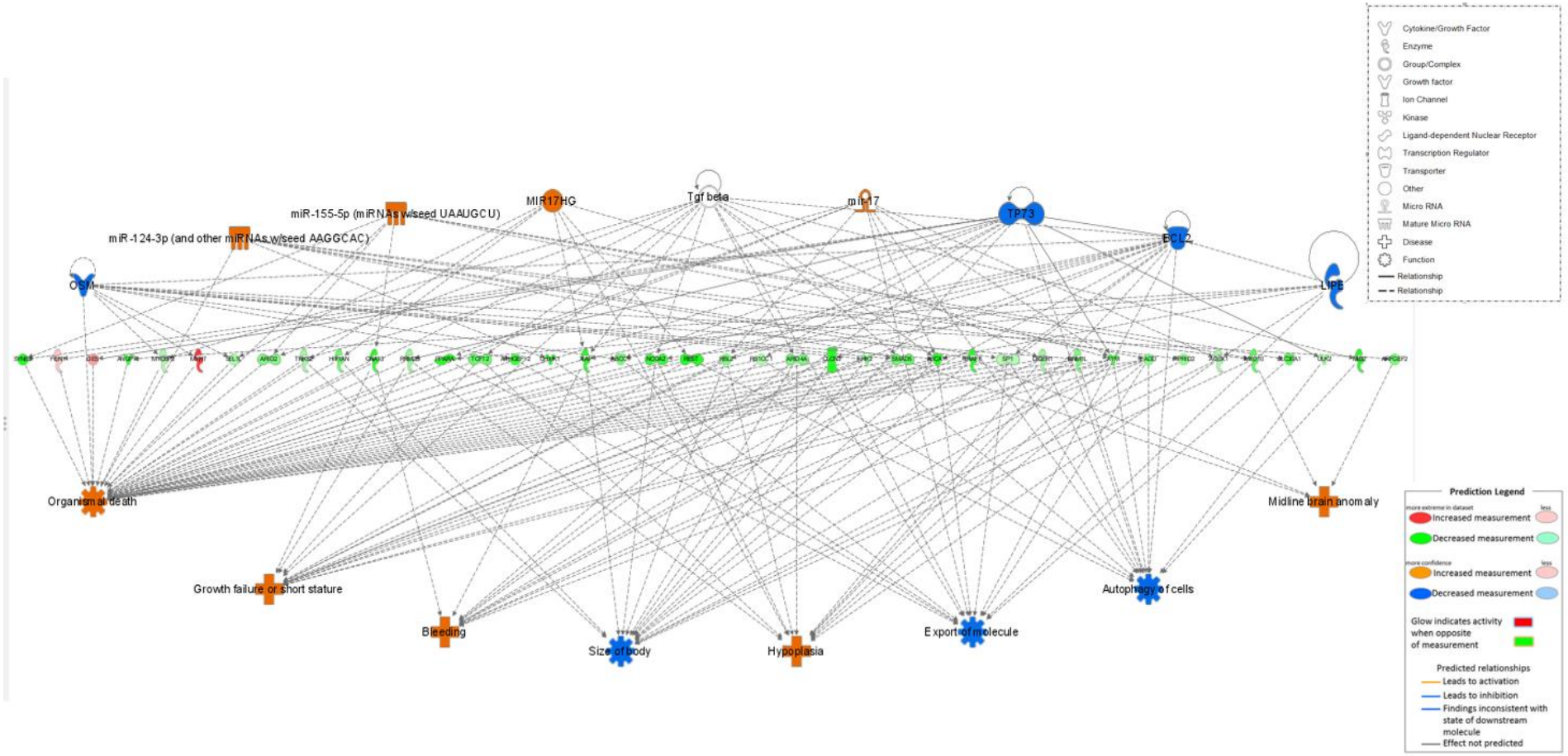

Figure 4-20: Ingenuity pathway analysis regulator effects highlighting the relevant phenotypes.

miR -124-3p, miR -155, MIR 17 HG were predicted as some of the upstream regulators of downstream biology using DEGs in low iodine diet (LID). Orange = predicted activation, blue = predicted inhibition, red = increased expression and green = reduced expression**.**

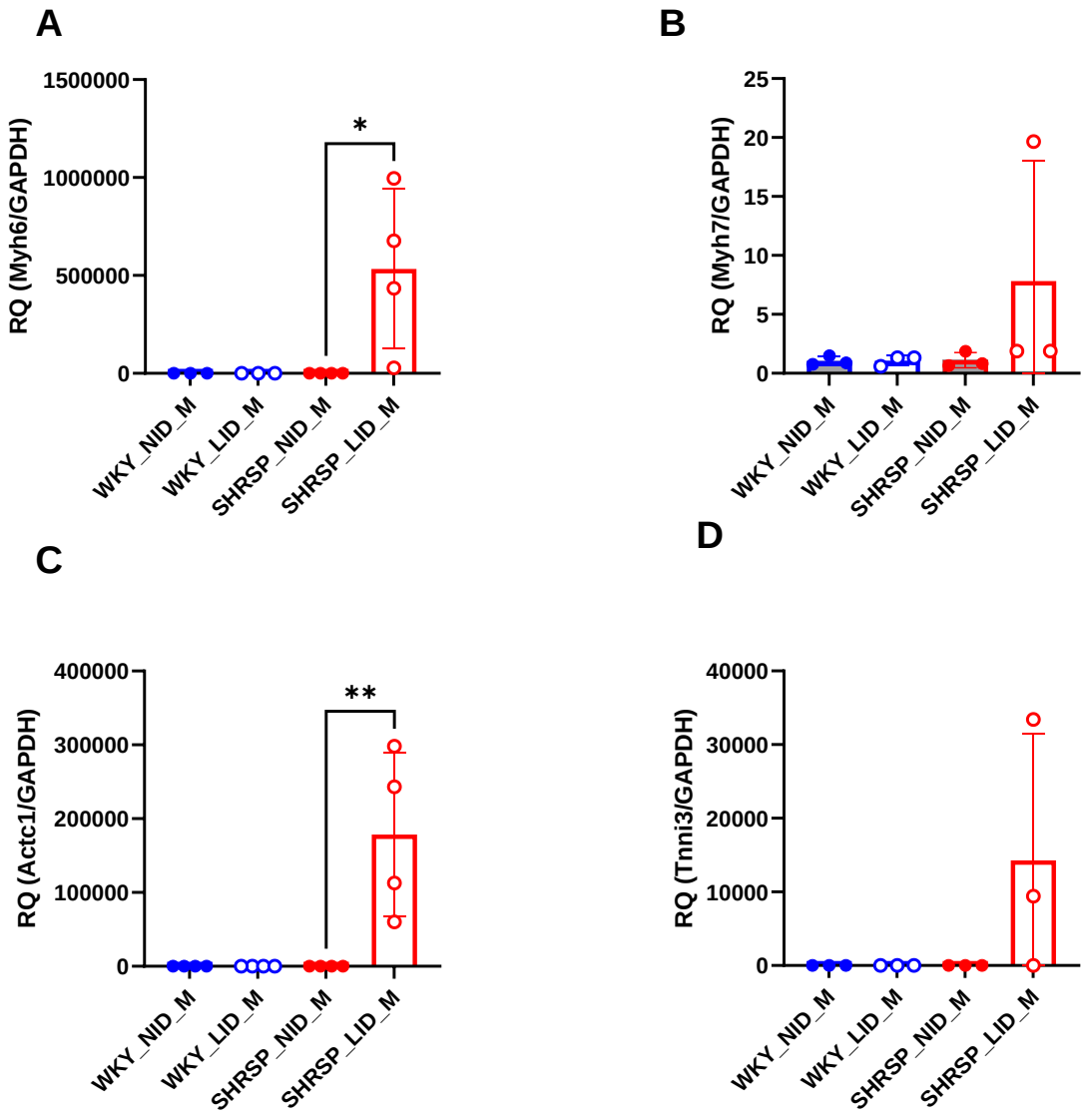

Figure 4-21: Validation of DEGs by RT-qPCR.

RT-qPCR was used to validate RNA-Seq data in thoracic aorta of WKY and SHRSP rats fed NID and LID at 4 weeks of diet. (**A**) myosin heavy chain 6 (Myh6), (**B**) myosin heavy chain 7 (Myh7), (**C**) actin alpha cardiac muscle 1 (Actc1) and (**D**) and troponini3 (Tnni3). Gene expression levels were quantified relative to GAPDH. All values are reported as mean ± SD (n=4 per group). Ordinary one-way ANOVA followed by Tukey's multiple comparison were used to determine significance. *p < 0.05, **p < 0.01.

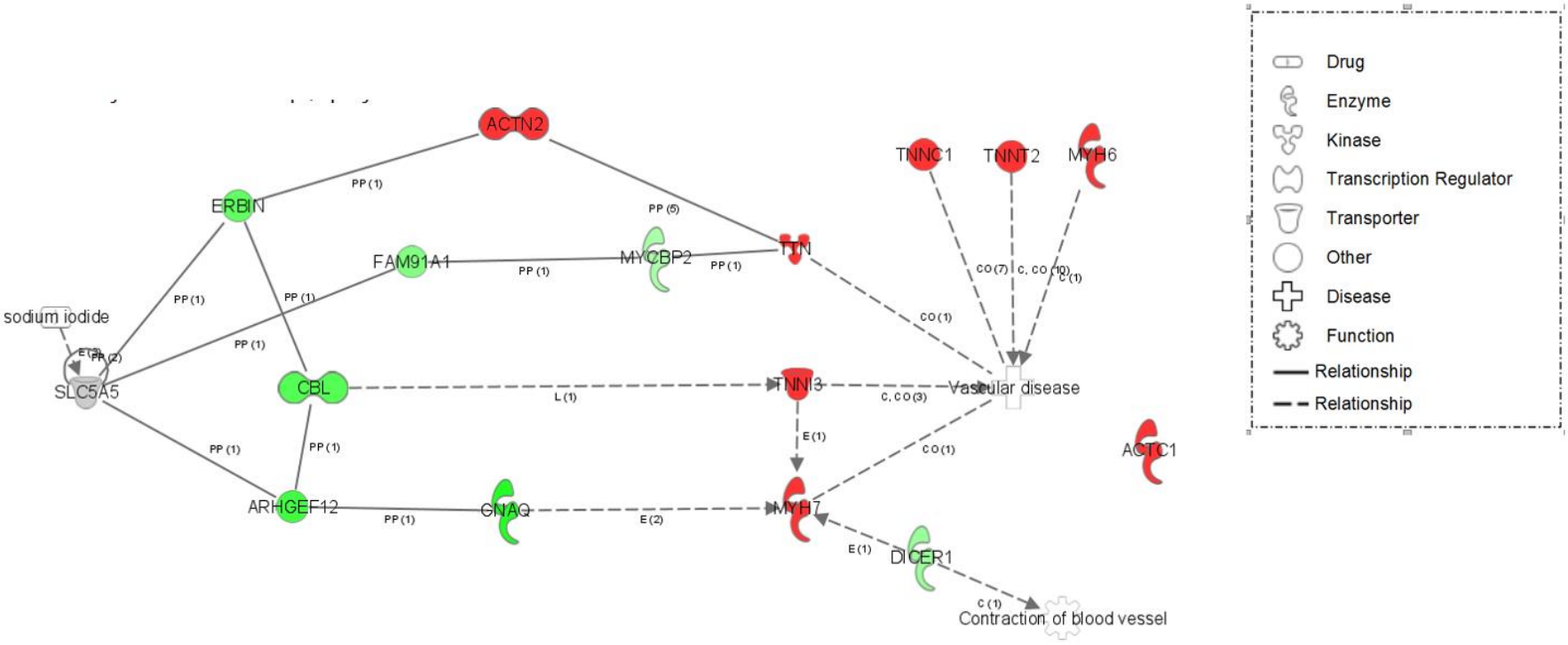

Figure 4-22: Ingenuity pathway analysis of data-mined potential connections between differentially expressed genes, and their interaction with sodium iodide, SLC5a5 and vascular disease.

An increased measurement (red) indicates that gene was more highly expressed in the LID thoracic aorta and reduced over normal iodine (NID) and vice versa for a decreased measurement (green). The filled lines indicate published connections, dashed lines indicated *in silico* inferred connections. An arrow indicates a regulatory vector.

4.5 Discussion

To the best of our knowledge, this is the first study that employed RNA-Seq analysis to characterize the transcriptomic response of rat thoracic aorta to LID. In the previous chapter we demonstrated that mesenteric arteries from WKY and SHRSP males fed LID were hypercontractile to U46619. To elucidate the molecular mechanisms leading to hypercontractility of vascular tissue we performed RNA-Seq with an aim to transcriptionally profile thoracic aorta gene expression in WKY and SHRSP male rats fed NID and LID. There were no DEGs between the NID and LID WKY males hence the focus of this chapter is based on LID and the transcriptome in SHRSP males. A total of 438 DEGs were significantly different between NID and LID fed SHRSP males, potentially contributing to the diet-induced phenotypic differences observed. The results provide insight into the strain differences between WKY and SHRSP males in response to LID as initially evidenced in chapter 3.

The novel findings of this study are that LID significantly affects SHRSP but not WKY male thoracic aorta transcriptome. Previously, it was demonstrated that the largest number of DEGs in the brain occurred in salt-loaded SHRSP compared to non-salt loaded SHRSP as opposed to salt loading changes in WKY(Bailey et al., 2018). This could potentially mean that gene expression is more easily altered by stressors in SHRSP rats. The DEGs in the current study were mostly associated with muscle contraction, actin filament-based processes, and various cytoskeletal structures suggesting a unique contribution of LID to these biological functions. Dysregulation of all these biological functions have been linked to vascular injury and disease (Daniel et al., 2010; Karki et al., 2013; Touré et al., 2012). A subset of DEGs were linked to growth failure or short stature, organismal death, bleeding, and hypoplasia. Therefore, our data confirms known molecular pathways that would be expected to be altered as a result of LID. It is known that iodine deficiency leads to stunted growth, hypoplasia, and bleeding (Hernández-Cassis et al., 1995; Kapil, 2007; Sievert et al., 1996; Zimmermann, 2012).

In general, molecules associated with muscle contraction were upregulated in dilated cardiomyopathy, Ca^{2+}, ILK, and actin cytoskeleton signalling pathways. Overwhelmingly our results indicate up regulation of troponin isoforms (Tnnc1,

Tnnt2, Tnni3), Tnn, Actc1 and Myh6, Myh7 and Ttn potentially through enhanced MYOCD, and SRF upstream regulators. This suggest that SHRSP males but not WKY fed LID may have vascular dysfunction because of increased expression of genes that code for contractile machinery proteins.

To confirm the reliability of the RNA-Seq results, several DEGs, such as Myh6, Myh7, Tnni3, and Actc1 were selected and tested by RT-q-PCR, and the results demonstrated that 2 out 4 of the tested genes show significantly increased expression in line with the RNA-Seq data. Even though the other 2 genes were not significant, they showed a trend toward increased expression in the LID fed SHRSP group compared to the NID fed rats. The reason for the lack of significance in the other 2 genes may be due to variation in gene expression between the sample biological replicates.

RNA-Seq data revealed the presence of troponin complexes in thoracic aorta. All troponin complex genes were significantly increased in thoracic aorta of SHRSP males fed LID. Even though it is generally understood that proteins of the troponin complex are not expressed in SMCs, studies have reported their expression in rat and mouse thoracic aorta (Moran et al., 2008) and bladder smooth muscle (Wang, Reiter, et al., 2001). Moran et al., further suggested that troponin proteins are associated with actin filaments within smooth muscle tissues and places them in a position to play a functional role in regulation of smooth muscle contraction (Moran et al., 2008). Elevated serum levels of Tnni3 and Tnnt2 are markers of cardiac muscle injury (Babuin & Jaffe, 2005; Newby et al., 2012), therefore if they are suggested to play a similar role in SMCs, this could imply that increased expression of these genes could be associated with muscle injury of resistance arteries as in cardiac muscles.

In addition to troponin gene complexes, contractile machinery protein coding genes such as Myh6 and Myh7 Myl4 and Myl7 were significantly increased in thoracic aorta of SHRSP males fed LID. All these genes are classically known to be expressed in sarcomere of cardiac cells (England & Loughna, 2013). We could not find reports about these genes or their translated protein function in thoracic aorta. However, the presence of cardiac genes in rat thoracic aorta perivascular tissue (PVAT) has also been reported by Contreras *et al.*, although their function is currently unknown in vascular tissue (Contreras et al., 2020). In

rodents, Myh6 is predominantly expressed to the atrial region during embryogenesis, and its presence is also demonstrated in the ventricle, and it becomes the dominant myosin heavy-chain isoform after birth in both the atrial and ventricular chambers (Franco et al., 1998; Lyons et al., 1990). Myh7 becomes ventricular-specific during embryogenesis in rodents however it is downregulated postnatally, so that in the adult rodent heart Myh6 is the dominant myosin heavy chain gene expressed in both the atrial and ventricular chambers (Franco et al., 1998; Lyons et al., 1990).

In the literature, Myh6 and Myh7 genes are involved in cardiac muscle contractile machinery and their mutation is associated with a number myopathies including dilated cardiac myopathy (DCM) and hypertrophic myopathy (HCM) (Tardiff, 2005). The presence of these genes in thoracic aorta suggest that they might play a role in maintaining the structural integrity of the vascular smooth muscle contractile machinery like in cardiac and skeletal muscle. Therefore, their increased expression in LID fed SHRSP male rats might suggest a vascular dysfunction related to contractile machinery. One possible explanation for enrichment of cardiac genes was through cross contamination of thoracic aorta with cardiac tissue during tissue harvesting, however we were careful to prevent cross contamination. We therefore believe the findings are novel and might suggest the involvement of these genes in vascular muscle cell contraction when SHRSP male rats are subjected to iodine deficiency.

In addition to regulatory and contractile protein coding genes, the structural gene Ttn was also significantly increased in all significant canonical pathways. Ttn is anchored to the Z-discs at its N-terminus, and the M-line at its C-terminus, and is thought to be important for the assembly of the sarcomeric proteins (Fürst et al., 1988). Again, expression of this gene is not typically observed in vascular tissue, however LID might have triggered its expression in thoracic aorta.

Smooth muscle contraction is influenced by factors that regulate actin cytoskeleton re-organisation and contractile apparatus assembly; mediated by RhoA/Rho-kinase, in part via inhibitory phosphorylation (Arber et al., 1998; Leduc et al., 2016; Vardouli et al., 2005). Cytoskeleton remodelling occurs over time, with actin polymerization increasing as vasoconstriction persists (Martinez-

Lemus et al., 2009). Although LID did not alter the expression of RhoA kinase it seems to increase the expression of F actin via the decreased expression of Arhgef1/12 suggesting actin polymerisation by LID. It was previously reported that dysregulation of Rho guanine nucleotide exchange factors (Rho-GEFs) was implicated in RhoA-Rho kinase (ROCK) hyperactivation in hypertension (Komers et al., 2011), however it is important to note that LID did not significantly influence ROCK in our study. In contrast Xiang et al., reported that Arhgef1 promotes F-actin polymerization in neurons (Xiang et al., 2016), however our results show that a decrease in Arhgef1 expression results in increased expression of F actin.

Expression of Myh6 and Myh7 is regulated by transcription factors including MYOCD, Gata4, Mefc2 (Dai et al., 2002). Our results revealed that LID increased the expression of MYOCD Gata4, Mefc2, and SRF. This could be a potential mechanism that leads to the upregulation of Myh6 Myh7 Myl4 and Myl7 and troponin isoform expression. MYOCD plays an important role in cardiac and smooth muscle differentiation. MYOCD has been reported to have two tissue-specific isoforms of myocardin-856 in SMCs (smooth muscle MYOCD) and myocardin-935 in cardiac cells (cardiac MYOCD). It plays a critical role in cardiovascular development (Wang, Chang, et al., 2001) and also plays important physiological and pathological roles in the human CVS(Morita & Hayashi, 2023). MYOCD lacks the ability to bind directly to DNA; therefore, it is recruited indirectly to its target loci by interacting with SRF and can activate the expression of smooth muscle specific genes (Wang et al., 2007). Our results are consistent with similar studies where the expression of VSMC contractile genes was reported to be upregulated primarily by SRF-MYOCD(Chen et al., 2002; Wang et al., 2003). It has been stated that MYOCD expression represents a contractile and differentiated SMC phenotype while a deletion of MYOCD, represents a synthetic and dedifferentiated phenotype, a hallmark of atherosclerosis (Xia et al., 2017). Our results demonstrated increased expression of MYOCD-SRF, with increased expression of contractile genes which could suggest hypercontractile phenotype in SHRSP fed LID compared to those fed NID.

Micro RNA (miRNA) are short non-coding RNAs that are known to regulate mRNA stability and protein translation by binding to their target mRNA(Bartel, 2004).

Long and short noncoding RNAs are implicated to regulate SMC phenotype (Ballantyne et al., 2016; Bell et al., 2014). The regulation of miRNA is combinatorial in nature since an individual miRNA may target hundreds of different mRNAs, and conversely, each mRNA may be regulated by multiple miRNAs (Friedman et al., 2009). Furthermore, miRNAs are important regulators of a variety of cellular processes involving development, differentiation, and signalling (Ambros, 2004; Bagga & Pasquinelli, 2006). Dysregulation of specific miRNAs leads to various human diseases, including cancer, metabolic disorders, CVDs, liver disease, and immune dysfunction (Blenkiron & Miska, 2007; Poy et al., 2004; Poy et al., 2007). miR-124-3p, miR-155-5p, miR-17HG and miR-17 were activated in SHRSP fed LID. This indicates that these miRNAs may be differentially regulated post transcriptionally by iodine in thoracic aorta of male SHRSP but not WKY. Dysregulation of these miRNAs is associated with organismal death, growth failure or short stature, hypoplasia, and bleeding. It is an interesting discovery that our RNA-Seq data revealed growth failure or short stature as one of the disease and functions associated with DEGs, however we did not expect significant differences in BW since our study was short term and did not significantly affect TH production. Nevertheless, BW might not have been a suitable measure to detect short stature, and for future studies it might be ideal to measure femur length or the entire body length of the rat. Low-level of TH in the blood is the principal factor responsible for the series of functional and developmental abnormalities, collectively referred to as IDD (Kapil, 2007), however in our studies LID did not significantly affect TH and these suggest that development abnormalities might occur independent of TH.

The discovery of genes whose expression is considered specific to cardiac tissue is an important finding and should provide a basis for further research to probe the functions of these subset of genes in VSMC. Historically, VSMC within the vessel wall were identified by markers, including myosin heavy chain 11 (MYH11), calponin 2 (CNN2), smooth muscle 22a/taglin (SM22a/taglin) and smooth muscle cell actin (ACTA2) (Sorokin et al., 2020). Advanced technologies tracing cell origin developed in recent years have raised questions about studies of VSMC based only on marker identity (Wang et al., 2015). For instance, VSMC-specific lineage tracing studies have revealed that previous results based on markers might have produced incorrect or inaccurate identification of VSMC

(Wang et al., 2015). This finding explains by fact that VSMC in different environments can downregulate contractile markers such as SM22a, and upregulate other markers, including CD68 and ATP-binding cassette transporter 1 (ABCA1) (Rong et al., 2003). Therefore, LID might have triggered thoracic aorta VSMCs in SHRSP males to express genes formally known to be cardiac genes.

In cardiac and skeleton muscles, contraction occurs when myosin binds to actin which is primarily regulated by Ca^{2+}, via the thin filament–associated proteins tropomyosin (Tm) and troponin (Tn). The troponin complex is made up of three components (Greaser & Gergely, 1973; Schaub & Perry, 1969) being the Ca^{2+} binding subunit, troponin C (TnC); the inhibitory subunit, troponin I (TnI); and an elongated protein, troponin T (TnT), that binds both TnC and TnI and anchors the entire complex to tropomyosin (Li & Hwang, 2015). However unlike in cardiac and skeletal muscle, SMCs lack troponins; once Ca^{2+} has entered the cell, it is free to bind calmodulin, which transforms into activated calmodulin. Calmodulin then activates the enzyme myosin light chain kinase (MLCK), MLCK then phosphorylates a regulatory light chain on myosin with consequent rapid vasoconstriction (Kim et al., 2008).

The RNA-Seq performed in this chapter generated a vast gene expression dataset and only genes that appeared in the most significant pathways were investigated. This data could also be utilised to identify biological functions, major pathways and diseases and functions associated with short term LID. The RNA-Seq analysis provided information on hundreds of significantly differentially expressed transcribed RNAs and only a small subset was investigated during this study. In terms of generating data for public knowledge, there is a limitation since research questions are limited to the hypothesis of this PhD work. However, these RNA-Seq data set will be made available to allow an in-depth analysis and examination by third parties.

A major limitation of this study was that thoracic aorta instead of mesenteric artery was used for our RNA-Seq analysis. This chapter was a follow up study from our vascular functional studies in chapter 3. Myography procedures normally take time, and this would have compromised the quality of RNA from mesenteric arteries by the time we finished the vascular dissection procedures, hence we decided to use thoracic aorta which was snap frozen immediately

following sacrifice. However, it is important to acknowledge that SMCs from conduit artery like thoracic aorta may fundamentally respond differently to those of small resistant arteries like mesenteric arteries. Constituents of mRNAs expressed in each tissue depend on the biochemical and physiological roles of the target organ in the body (Ikawa et al., 2019). Secondly the sample size was restricted to n=3 tissues per experimental group mainly because of the expensive nature of RNA-Seq. It would be beneficial in future to include more samples per group to allow exclusion of outliers if in any case they are identified.

In summary, the present study provided evidence that the transcriptome of thoracic aorta of WKY and SHRSP respond differently to LID resulting in significant changes to the transcriptome of SHRSP but not in WKY males. The cellular pool of SRF/MYOCD-dependent genes that determine the VSMC contractile phenotype were increased in thoracic aorta of SHRSP males fed LID suggesting hypercontractile phenotype in the vessels in these rats. Some of the DEGs in SHRSP fed LID were also linked to growth failure or short stature, bleeding, and hypoplasia, which are known to occur in severe iodine deficiency. The results agree with the vascular functional studies in SHRSP, which showed that mesenteric arteries from SHRSP males fed LID were hypercontractile to U46619. This raises the possibility that LID may worsen CVD in SHRSP rats by altering the expression of genes involved in contractile machinery. Data presented in this chapter provides further evidence for translational studies that could lead to dietary iodine being established as a modifiable risk factor for CVD.

Chapter 5 Effect of low iodine on WKY and SHRSP vascular smooth muscle cell contractility.

5.1 Introduction

We previously demonstrated that LID significantly affects vascular contractility but not endothelial-dependent and independent relaxation in mesenteric arteries of WKY and SHRSP male rats. Moreover, our RNA-Seq data also established that expression of genes that code for contractile proteins were significantly increased in the thoracic aorta of SHRSP male rats fed LID compared to those fed NID. To investigate further whether differences in vascular responses between the NID and LID fed males are represented at the molecular level, mesenteric primary VSMC from 12 wks WKY and SHRSP rats were isolated and cultured in cell medium with and without iodide supplementation.

It is appreciated that functional changes, in the form of altered vascular reactivity, occur at the earliest stages of hypertension, and contribute to the development and reinforcement of the condition (Wilson et al., 2019). Our vascular functional studies have demonstrated that LID has the potential to worsen this condition as mesenteric arteries from WKY and SHRSP fed LID were hypercontractile to U46619. However, the precise mechanism underlying altered vascular reactivity is not well understood. The alterations in signalling pathways in VSMC and endothelial cells are known to be the key molecular mechanisms underlying vascular dysfunction and hypertension development (Ma et al., 2023). VSMC are specialized for maintaining vascular homeostasis through active contraction and relaxation under physiological conditions. Under normal circumstances, they express genes and proteins important for contraction/dilation, allowing them to control systemic and local pressure by regulating vascular tone (Coll-Bonfill et al., 2016). However, in the early stage of hypertension, VSMC in conduit arteries may undergo a transition from a contractile phenotype to a more synthetic phenotype, including the production of both contractile and secreted proteins (Delbosc et al., 2008).

Contractile activity is controlled by the Ca^{2+}-dependent phosphorylation state of the myosin light chain (MLC) and other associated calponins and caldesmon that

allow the interaction of actin and myosin to generate tonic contraction (Carrillo-Sepúlveda & Barreto-Chaves, 2010). In disease states such as hypertension, many of the mechanisms regulating intracellular Ca^{2+} homeostasis are perturbed, with experimental models and hypertensive patients demonstrating abnormal vascular Ca^{2+} handling and high intracellular Ca^{2+} in red blood cells and SMC (Gonzalez & Suki, 1995; Touyz et al., 2018). In addition to Ca^{2+}-dependent mechanisms, Ca^{2+}-independent processes regulate vascular smooth muscle contraction, by influencing the sensitivity of MLC to Ca^{2+}. Following the initial Ca^{2+} sensitization process force generation is maintained. There are two major signalling pathways implicated in Ca^{2+} sensitization, which include the DAG-PLC-PKC pathway and the RhoA-Rho kinase (ROCK) pathway (Guzik et al., 2017; Loirand & Pacaud, 2010). In addition, other kinases such as the integrin-linked kinase (ILK), p21-activated protein kinase and zipper-interacting protein kinase (ZIPK) also play a role (Endo et al., 2004). The Ca^{2+} sensitization mechanism regulates the phosphorylation state of MLC20 independently of Ca^{2+}–calmodulin–MLCK signalling (Touyz et al., 2018). Our RNA-Seq data demonstrated enrichment of genes linked to ILK and Ca^{2+} signalling pathways. These pathways could potentially explain the hypercontractility phenotype observed in mesenteric arteries of SHRSP fed LID.

Dietary iodine continues to get attention as potential remedy to control hypertension through its antioxidant, anti-inflammatory and antiproliferative properties. Iodine is known as a vasodilator that acts directly on VSMC to cause relaxation on several arterial beds (Limbruno & De Caterina, 2003). Iodinated contrast media demonstrated vasorelaxation as a prominent side effect in vascular beds (Morcos et al., 1998; Uder et al., 2002). However, the mechanisms responsible for contrast-induced vasomotor changes were not fully elucidated and are thought to be multifactorial. It was thought that iodine modulates the release of endogenous vasoactive mediators such as prostacyclin, NO, endothelin, adenosine, histamine, serotonin, bradykinin, arterial natriuretic peptide, antidiuretic hormone, and/or through direct effects on VSMC (Morcos et al., 1998). Moreover, iodine can act as an antioxidant neutralizing hydrogen peroxide in a two-step process, by converting it first to hypoiodous acid and then to water, thereby preventing the formation of a hydroxyl radical (Küpper et al., 2008). Therefore, LID may promote oxidative stress in VSMC which may help

explain mechanisms underlying LID-induced vascular hypercontractility observed in WKY and SHRSP male rats.

Despite the evidence for a direct effect of iodine on vascular beds, this evidence is relatively weak as the few references that relate to this used iodide contrast media on intact arterial beds instead of isolated VSMC. This study therefore sought to understand the effect of iodide on contractile signalling in mesenteric artery VSMC from 12 wk old WKY and SHRSP male rats following stimulation with U46619. Specifically, this study assessed the potential effect of iodide on VSMC MLC phosphorylation. The study also aimed to establish the effect of iodide on SLC5a5 protein levels in mesenteric VSMC from 12 wk old WKY and SHRSP rats. 12 wk old rather than 9 wk old WKY and SHRSP rats were used because the protocol for VSMCs preparation had previously been optimized in 12 wk old rats.

5.2 Hypothesis and Aims

5.2.1 Hypothesis

Addition of iodide to cell media will reduce MLC levels and agonist stimulated MLC phosphorylation in mesenteric artery VSMC from WKY and SHRSP rats. Iodide will reduce SLC5a5 protein levels in VSMC from WKY and SHRSP rats.

5.2.2 Aims

1. To determine the optimum concentration of U46619 required to stimulate MLC phosphorylation in mesenteric artery VSMC of WKY and SHRSP rats.

2. To determine the effect of iodide supplementation on MLC in VSMC of WKY and SHRSP rats.

3. To determine the effect of iodide supplementation on phospho-MLC following U46619 stimulation in VSMC of WKY and SHRSP rats.

4. To determine the effect of iodide supplementation on SLC5a5 protein levels in VSMC of WKY and SHRSP rats.

5.3 Materials and methods

Primary VSMC from mesenteric from 12 wk old WKY and SHRSP male rats were isolated and cultured as described in general materials and methods (section 2.10.1 and 2.10.2). Purity of the primary VSMC cultures was assessed as described in section 2.10.3.

5.3.1 Iodide treatment and drug stimulation of rat mesenteric primary VSMC

This part of the experiment utilized cells at passage 1-4 and it was carried out in 6 well plates as illustrated in Figure 5-1. When cell growth reached 80-90% confluence, the growth medium was aspirated, and cells were washed twice with warm DPBS before replacing with growth media containing 10 μM NaCl (control) or 10 μM NaI (treatment) and incubated in a 5% CO_2 humidified incubator at 37^{o}C for 48 hrs. Following 48 hrs, media was aspirated, and cells were washed with warm DPBS before replacing with low serum growth media (DMEM supplemented with 0.5% FBS) inoculated with 10 μM NaCl or 10 μM NaI for 24 hrs to quiesce the cells prior to drug treatment. Media was aspirated and cells were washed twice with warm DPBS before replacing with respective media as above. Cells were then treated with 0.1%DMSO, 0.1 μM U46619, and 0.1 μM ionomycin and incubated in a 5% CO_2 humidified incubator at 37^{o}C for 10 min. Whole cell lysates were the prepared as described in general materials and methods section 2.10.5.

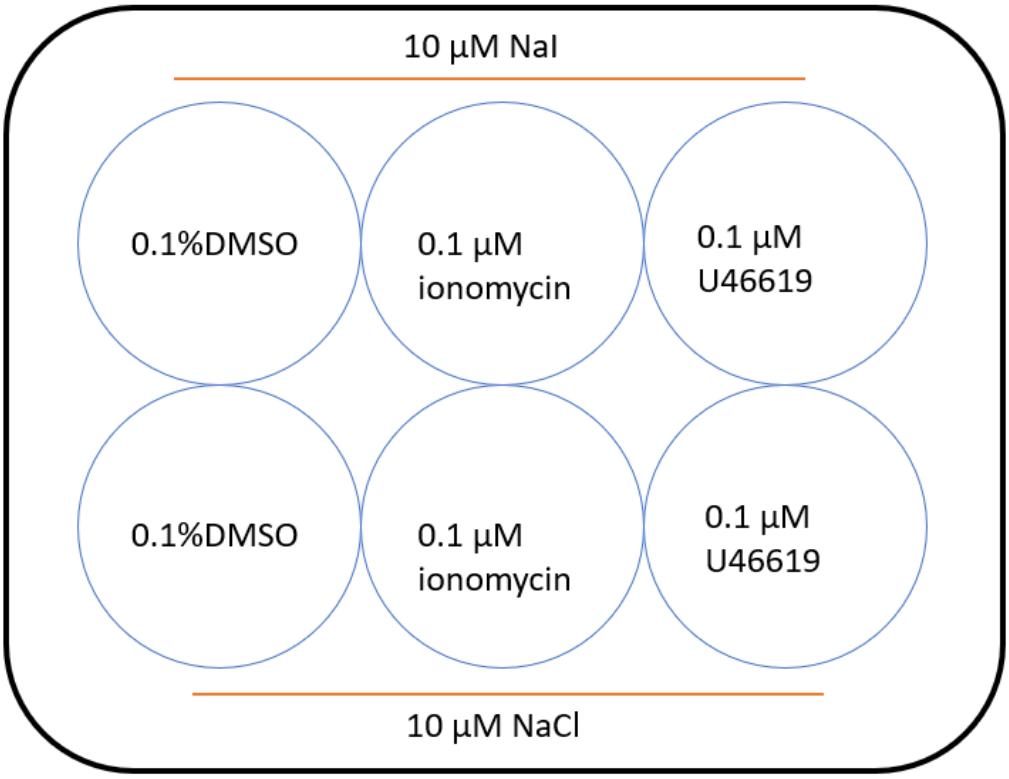

Figure 5-1: Diagrammatic illustration of the cell treatment experimental design

Cells were cultured until 80-90% confluency in growth media before incubation with media supplemented with 10 µM NaI or 10 µM NaCl for 48 hrs. After 48 hrs cells were washed and media replaced with low serum media before treatment with 0.1 % DMSO, 0.1 µM ionomycin or 0.1 µM U46619.

5.3.2 General protein methods

Protein concentration determination, SDS-polyacrylamide gel electrophoresis and western blotting were done as described in general materials and methods section 2.11.

5.3.3 Densitometric quantification of protein bands

Western blots were scanned and quantified by densitometry using Empiria Studio® Software (LI-COR Bio Sciences, Lincoln, NE, USA). Densitometric quantification of protein bands was expressed as a ratio of phospho-MLC to MLC specific immunoreactivity or total immunoreactivity as indicated.

5.4 Statistical analysis

Results are presented as a mean ± standard error of the mean (SEM). Statistical analyses were performed using two-way ANOVA followed by Tukey post-hoc test (GraphPad Software Inc. San Diego. CA, USA). $P< 0.05$ was considered as statistically significant.

5.5 Results

5.5.1 Quality of the mesenteric VSMC

Purity of the cultured VSMC cultures was assessed by a positive immunofluorescent staining (ICC) for the SMC-specific marker SMC α-actin (ACTA2), at passage 4 as described in section 2.10.3. A micrograph of VSMC demonstrated a spindle shape. Fluorescent staining of α-actin microfilaments further confirmed that majority (determined by subjective impression of appearance) of isolated cells were VSMCs (Figure 5-2).

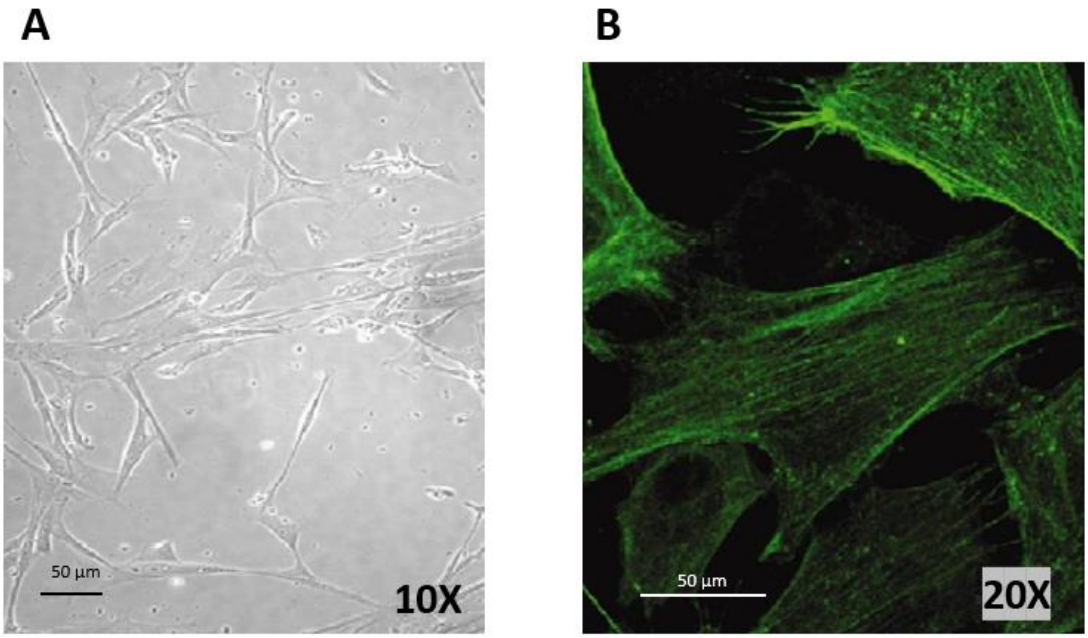

Figure 5-2: Representative images of mesenteric artery VSMC cultures from 12 week old WKY rats.

A Representative phase contrast image of VSMC cell culture at passage 4 (Scale bar = 50µm) and **B** Representative immunofluorescent micrograph of VSMCs stained with anti-ACTA2 antibodies (polyclonal rabbit-anti rat, 1/100, ab5694). (Scale bar = 50µm).

5.5.2 Determination of iodine levels in cell culture media

The ammonium persulfate digestion method of iodine concentration was used to determine the level of iodine in DMEM cell culture media as described in section 2.7.1. DMEM containing either 10% or 0.5% FBS did not contain measurable concentrations of iodine. Spiking either the DMEM containing 10% or 0.5% FBS with 10000 µM NaI significantly increased the iodine concentration to 3000-4000 µM, indicating that the assay was saturated at this concentration. Dilution of the spiked media 1:10 with water resulted in the expected iodine concentrations of ~1000 µM iodide in both cases (Figure 5-3). This clearly demonstrated that DMEM +FBS did not contain iodine and that iodide can be added to cell culture media at specified concentrations.

5.5.3 Concentration dependence of U46619 on mesenteric VSMC myosin light chain phosphorylation.

The concentration of U46619 and incubation time required to stimulate MLC phosphorylation was determined in mesenteric VSMC from 12 wk old WKY male rats. 1% DMSO was used as a vehicle control while the Ca^{2+} ionophore ionomycin (0.1 µM) was used as a positive control. Both 1% DMSO and 0.1 µM ionomycin did not stimulate MLC phosphorylation after 10 min. Stimulation with 1µM U46619 for 10 min produced the highest MLC phosphorylation followed by 0.1 µM U46619 for 10 min (Figure 5-4). 0.1 µM U46619 for 10 min was chosen for further experiments because it allows the assessment of hyperphosphorylation or hypo phosphorylation in the presence of or lack of iodine.

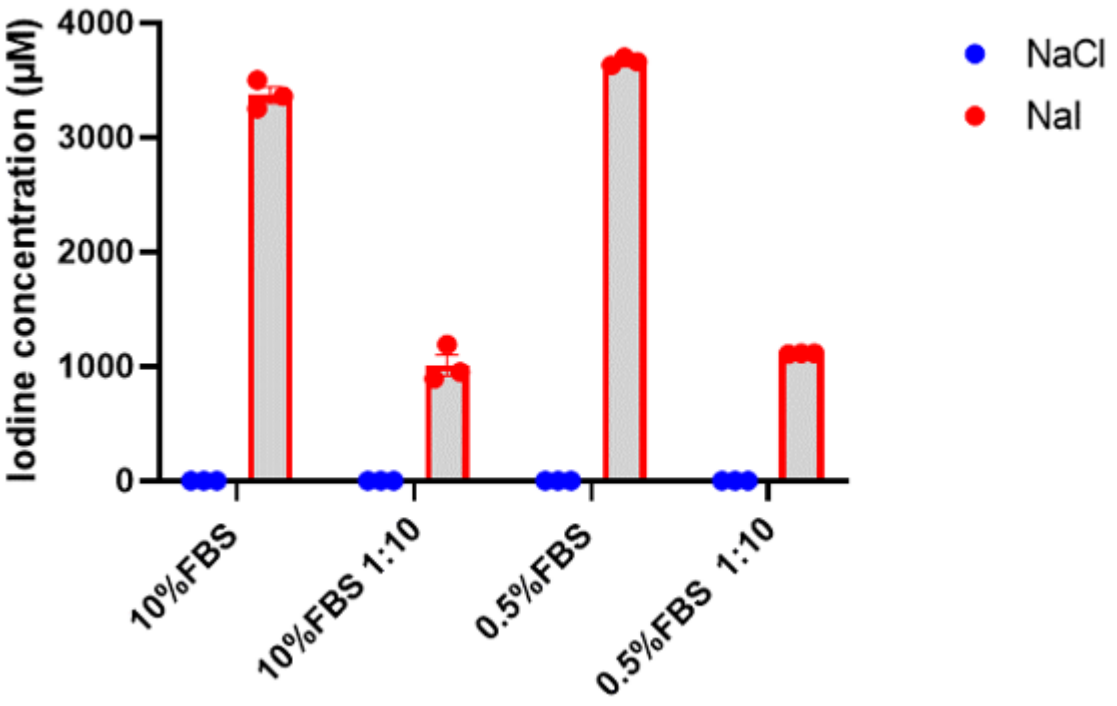

Figure 5-3: Iodine concentration levels in DMEM cell culture media.

Cell growth media (10% FBS) and starvation media (0.5% FBS) was supplemented with 10000 µM NaCl or 10000 µM NaI. To avoid assay saturation, media supplemented with 10000 µM NaCl or 10000 µM NaI was diluted 10 times (1:10). Iodine concentration was determined by the ammonium persulfate digestion method. (Technical replicates n= 3).

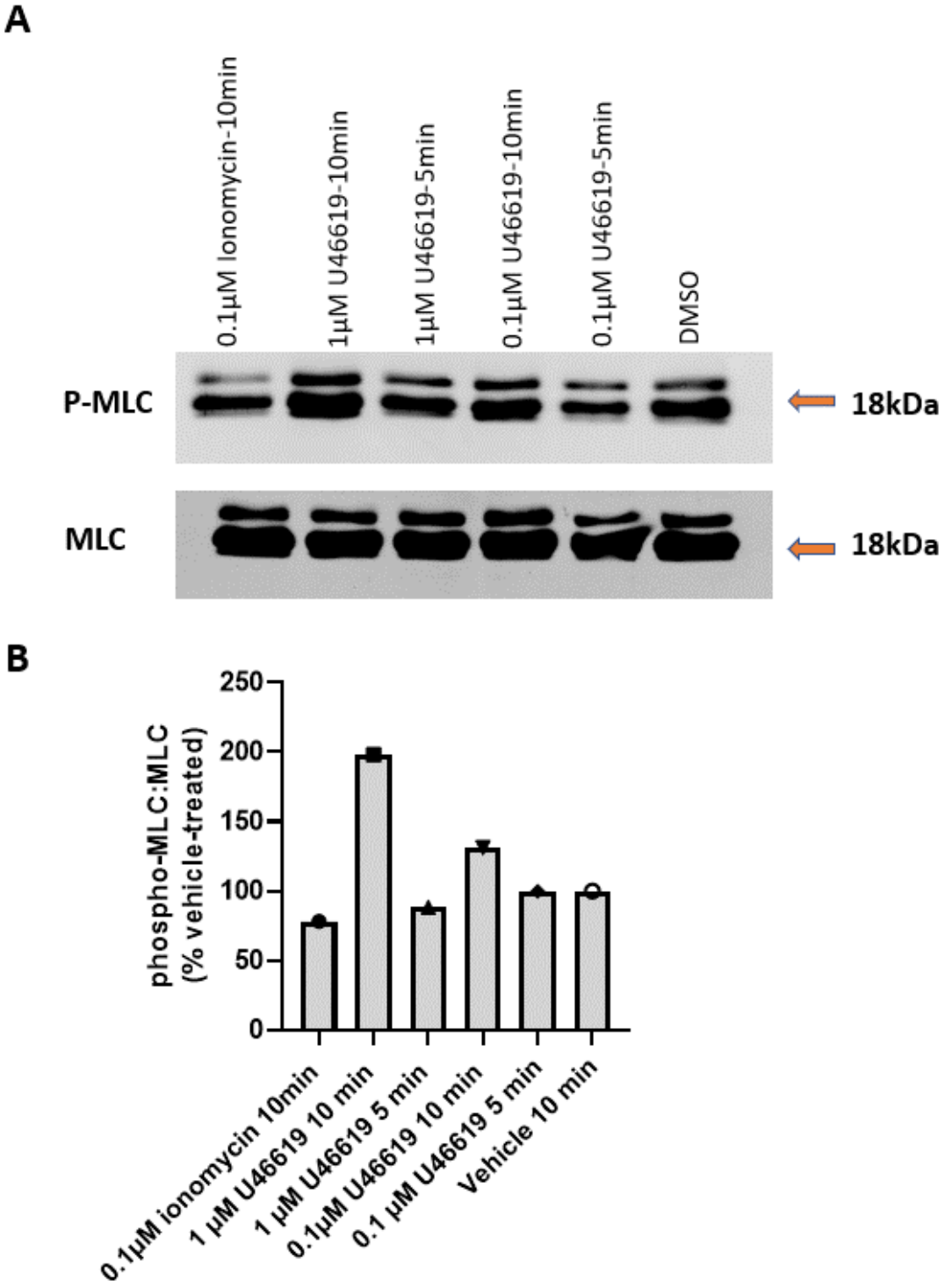

Figure 5-4: Time and concentration dependence of U46619-stimulated MLC phosphorylation in 12-week-old WKY mesenteric artery VSMC.

Mesenteric VSMCs from WKY rats were incubated in the presence or absence of ionomycin and U46619 at the concentrations and for the durations indicated. Cell lysates were prepared, and phospho-MLC and total MLC levels assessed by immunoblotting. (**A)** Representative immunoblots for phospho-MLC (top) and MLC (bottom) with molecular mass of the protein indicated on the right from a single experiment. Protein loaded= 10 µg. (**B)** Quantification of MLC phosphorylation relative to total MLC levels. (Pilot study n=1).

5.5.4 Effect of iodide supplementation on myosin light chain in mesenteric VSMC from WKY and SHRSP rats.

MLC protein levels in mesenteric VSMC of 12 wk old WKY and SHRSP rats were determined following 48 hours incubation in 10 μM NaCl or 10 μM NaI cell culture media. MLC protein levels did not differ between mesenteric VSMC of WKY rats cultured in media supplemented with 10 μM NaCl or 10 μM NaI. However, MLC protein levels were significantly increased in mesenteric VSMC of SHRSP rats supplemented with 10 μM NaI compared to those supplemented with 10 μM NaCl (Figure 5-5).

5.5.5 Effect of iodide supplementation on myosin light chain phosphorylation in mesenteric VSMC from WKY and SHRSP rats.

To understand the molecular effect of iodide on vascular contractile signalling, mesenteric VSMC from 12 wk old WKY and SHRSP rats were incubated for 48 hr in media supplemented with 10 μM NaCl or 10 μM NaI and then stimulated with 1% DMSO, 0.1 μM U46619 or 0.1 μM ionomycin for 10 min. The ratio of phospho-MLC to total MLC was determined. Neither ionomycin or U46619 treatment stimulated MLC phosphorylation in VSMCs from WKY rats after culture in medium supplemented with NaI or NaCl (Figure 5-6). In contrast, stimulation with 0.1 μM U46619 significantly increased phospho-MLC in mesenteric VSMC of SHRSP rats cultured in media supplemented with 10 μM NaCl when compared to strain matched mesenteric VSMC cultured in media supplemented with 10 μM NaI (Figure 5-7).

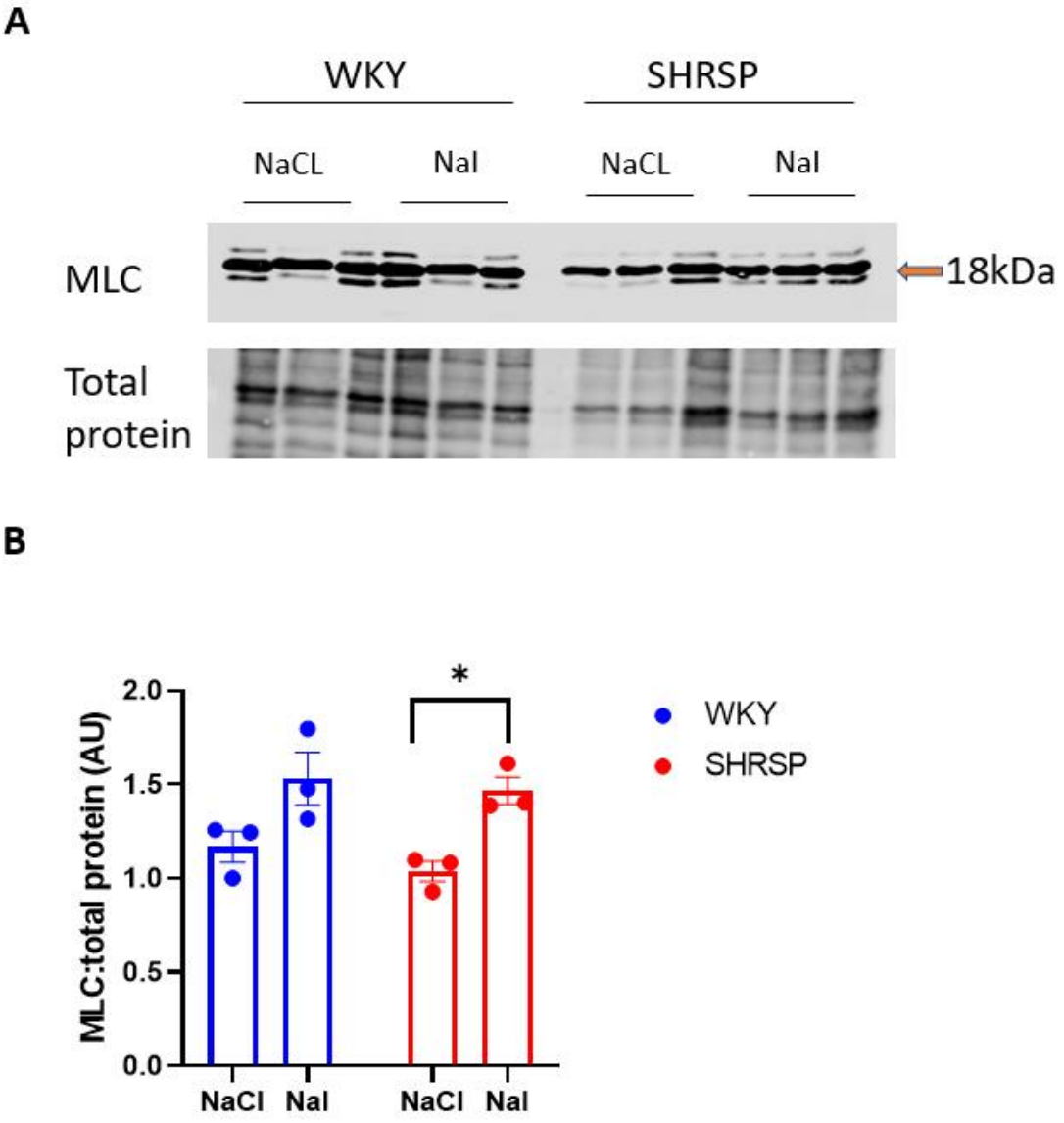

Figure 5-5: Effect of iodide on MLC levels in mesenteric artery VSMC from 12-week-old WKY and SHRSP rats.

VSMC were cultured in media supplemented with 10 µM NaCl or 10 µM NaI and incubated with 1% DMSO for 10 min. The ratio of MLC to total protein stain was assessed by immunoblotting in VSMC lysates. (**A)** Representative immunoblots for MLC (top) and total protein (bottom) with molecular mass of MLC indicated on the right. Protein loaded = 10 µg. (**B)** Quantification of MLC levels relative to total protein stain. All values are reported as mean ± SEM (n=3 per group). Two-way ANOVA followed by Tukey post-hoc test was used to determine significance. * $p < 0.05$.

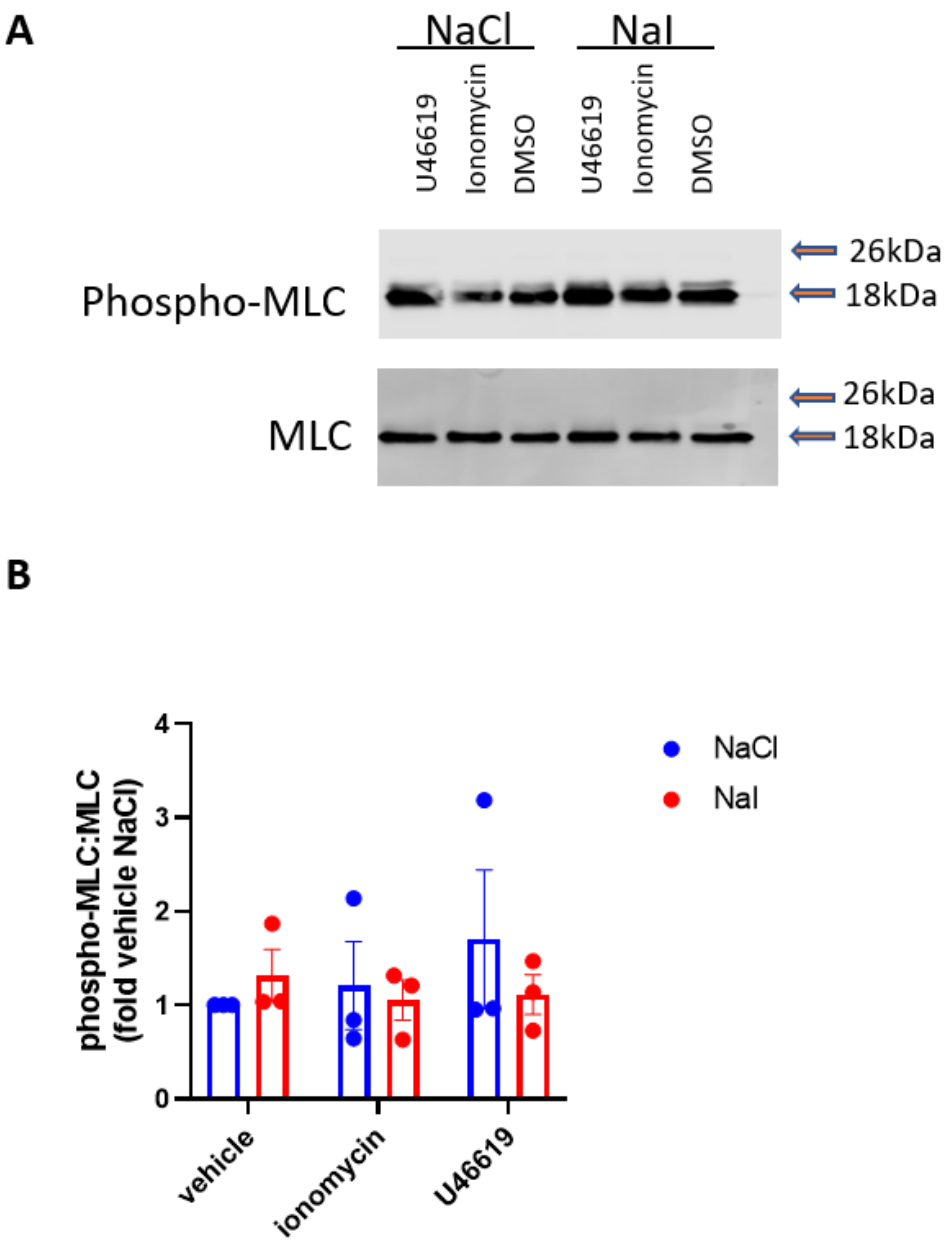

Figure 5-6: Effect of iodide on agonist-stimulated phospho-MLC in mesenteric artery VSMC from 12-week-old WKY rats.

VSMC were cultured in media supplemented with 10 µM NaCl or 10 µM NaI and stimulated with 0.1 µM U46619 or ionomycin for 10 min. The ratio of phospho-MLC to total MLC was assessed in VSMC lysates by immunoblotting. (**A)** Representative immunoblots for phospho-MLC (top) and total MLC (bottom) with molecular mass of the marker and protein indicated on the right from a single experiment. Protein loaded = 10 µg. (**B)** Quantification of phospho-MLC relative to total MLC. All values are reported as mean ± SEM (n=3 per group).

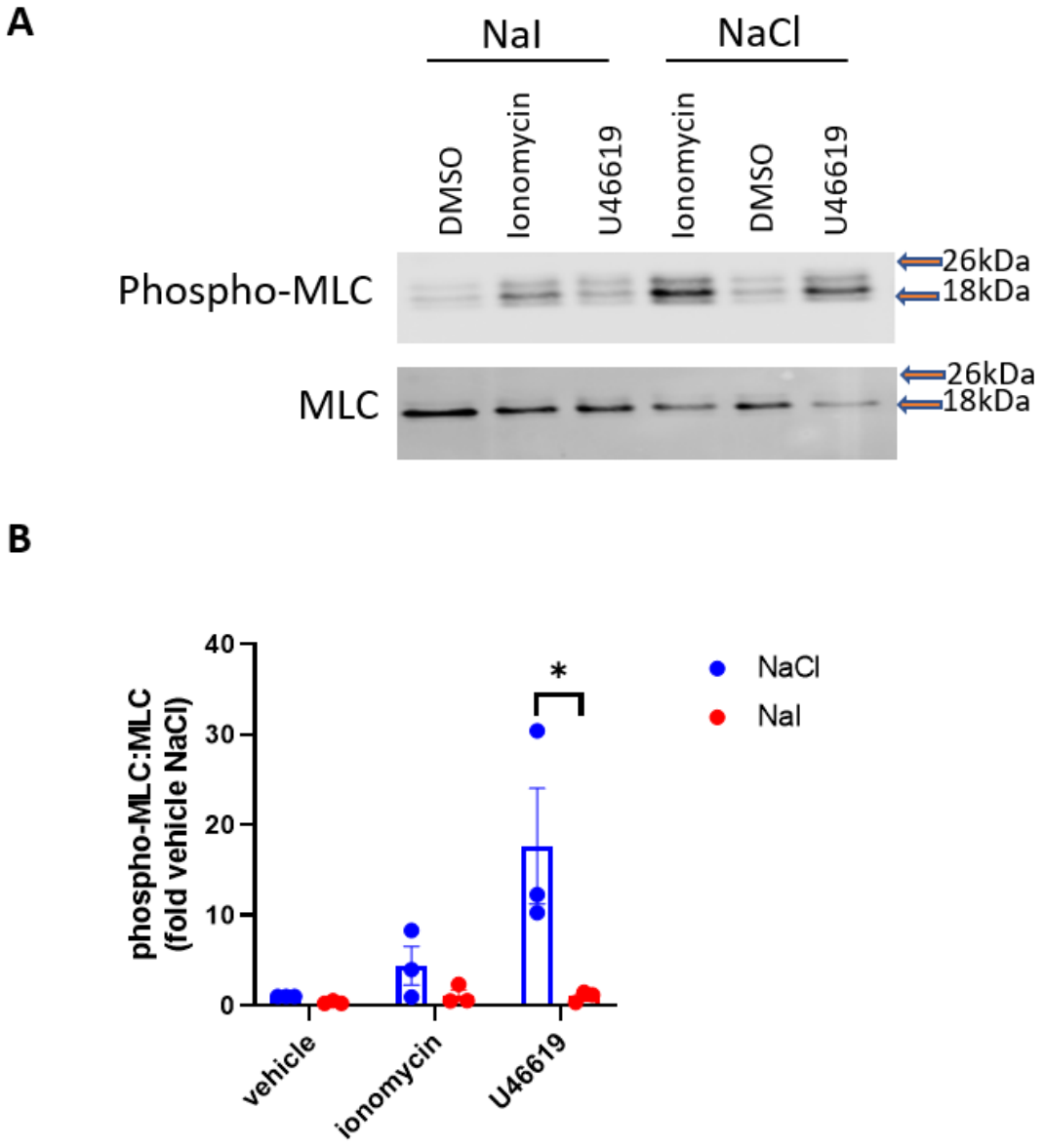

Figure 5-7: Effect of iodide on agonist-stimulated phospho-MLC in mesenteric artery VSMC from 12-week-old SHRSP rats.

VSMC were cultured in media supplemented with 10 µM NaCl or 10 µM NaI and stimulated with 0.1 µM U46619 or ionomycin for 10 min. The ratio of phospho-MLC to total MLC was assessed in VSMC lysates by immunoblotting. (**A**) Representative immunoblots for phospho-MLC (top) and total MLC (bottom) with molecular mass of the marker and protein indicated on the right from a single experiment. Protein loaded = 10 µg. (**B**) Quantification of phospho-MLC relative to total MLC. All values are reported as mean ± SEM (n=3 per group). Two-way ANOVA followed by Tukey post-hoc test was used to determine significance. * $p < 0.05$.

5.5.6 Effect of iodide supplementation on SLC5a5 protein levels in mesenteric artery VSMC from WKY and SHRSP rats.

The uptake of iodine into cells involves the SLC5a5 protein. We determined the SLC5a5 protein levels in VSMC from WKY and SHRSP rats cultured in media supplemented with either 10 μM NaCl or 10 μM NaI for 48 hrs and incubated with 1% DMSO for 10 min. Neither iodide nor strain of the mesenteric VSMC influenced SLC5a5 protein levels (Figure 5-8). Moreover, stimulating VSMC with 0.1 μM U46619 or 0.1 μM ionomycin did not significantly affect SLC5a5 protein levels in WKY and SHRSP mesenteric artery VSMC cultured in media supplemented with either 10 μM NaCl or 10 μM NaI (Figure 5-9 and Figure 5-10 respectively).

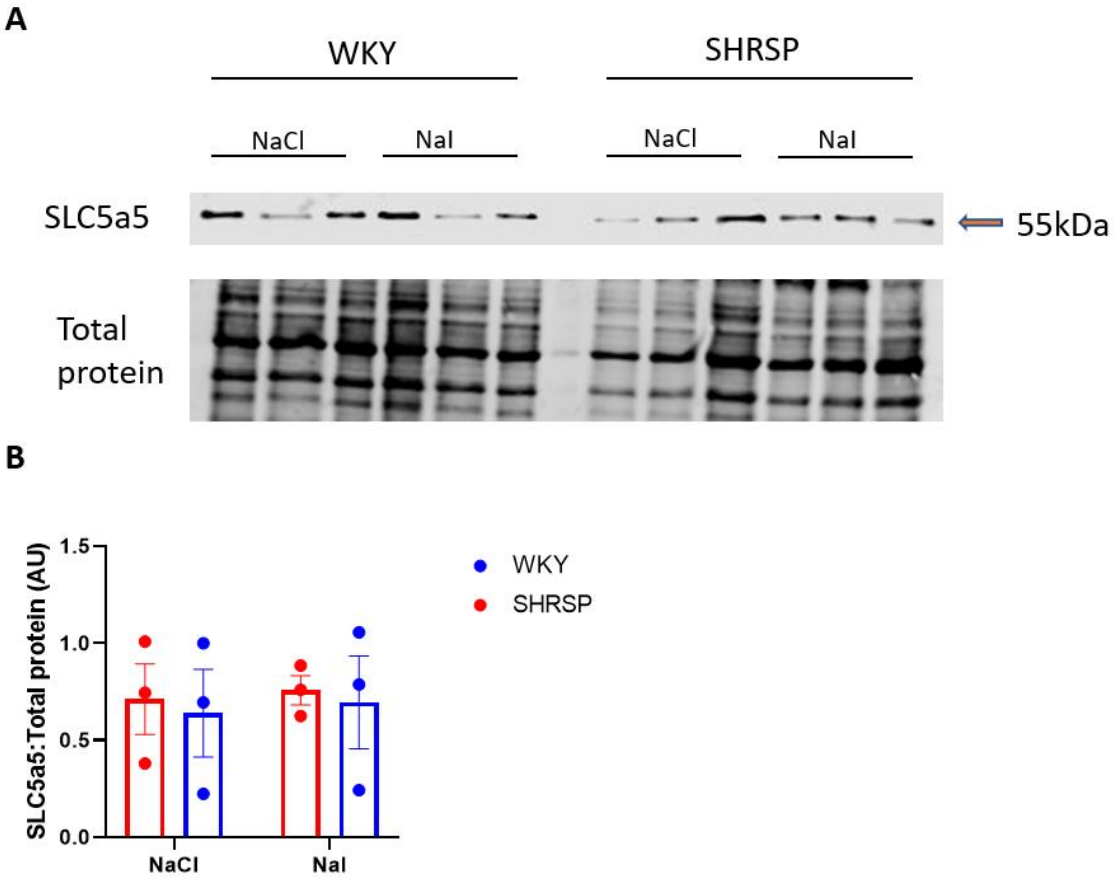

Figure 5-8: Effect of iodide SLC5a5 protein levels in mesenteric artery VSMC from 12-week-old WKY and SHRSP rats.

VSMC were cultured in media supplemented with 10 µM NaCl or 10 µM NaI and incubated with 1% DMSO for 10 min. The ratio of SLC5a5 to total protein stain was assessed by immunoblotting in VSMC lysates. (**A**) Representative immunoblots for SLC5a5 (top) and total protein (bottom) with molecular mass of SLC5a5 indicated on the right. Protein loaded = 10 µg. (**B**) Quantification of SLC5a5 levels relative to total protein stain. All values are reported as mean ± SEM (n=3 per group).

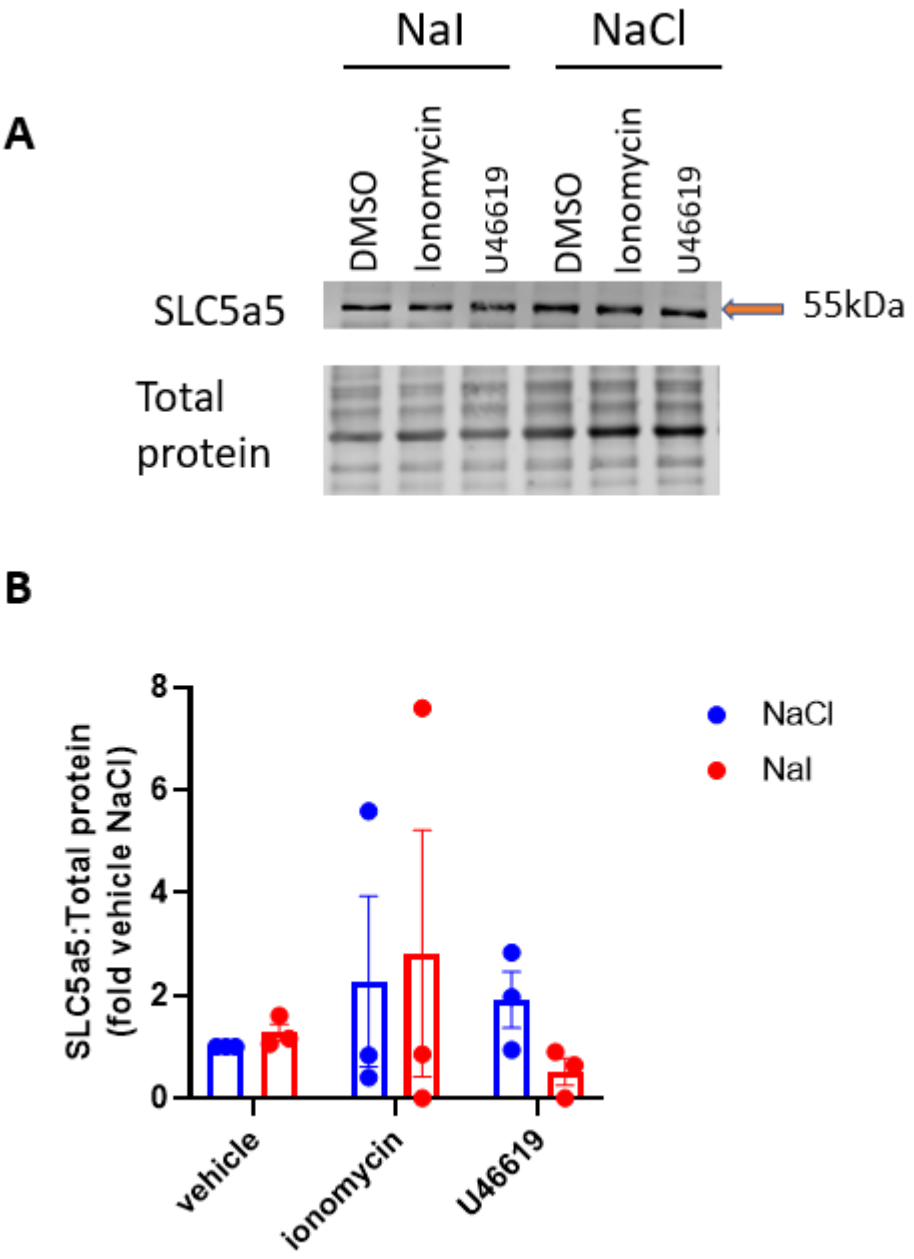

Figure 5-9: Effect of iodide on agonist stimulated SLC5a5 levels in mesenteric artery VSMC from 12 week old WKY rats.

VSMC were cultured in media supplemented with 10 µM NaCl or 10 µM NaI and stimulated with 0.1 µM U46619 or ionomycin for 10 min. The ratio of SLC5a5 to total protein stain was assessed in VSMC lysates by immunoblotting. (**A**) Representative immunoblots for SLC5a5 (top) and total protein (bottom) with molecular mass of SLC5a5 indicated on the right from a single experiment. Protein loaded = 10 µg. (**B**) Quantification of SLC5a5 relative to total protein stain. All values are reported as mean ± SEM (n=3 per group).

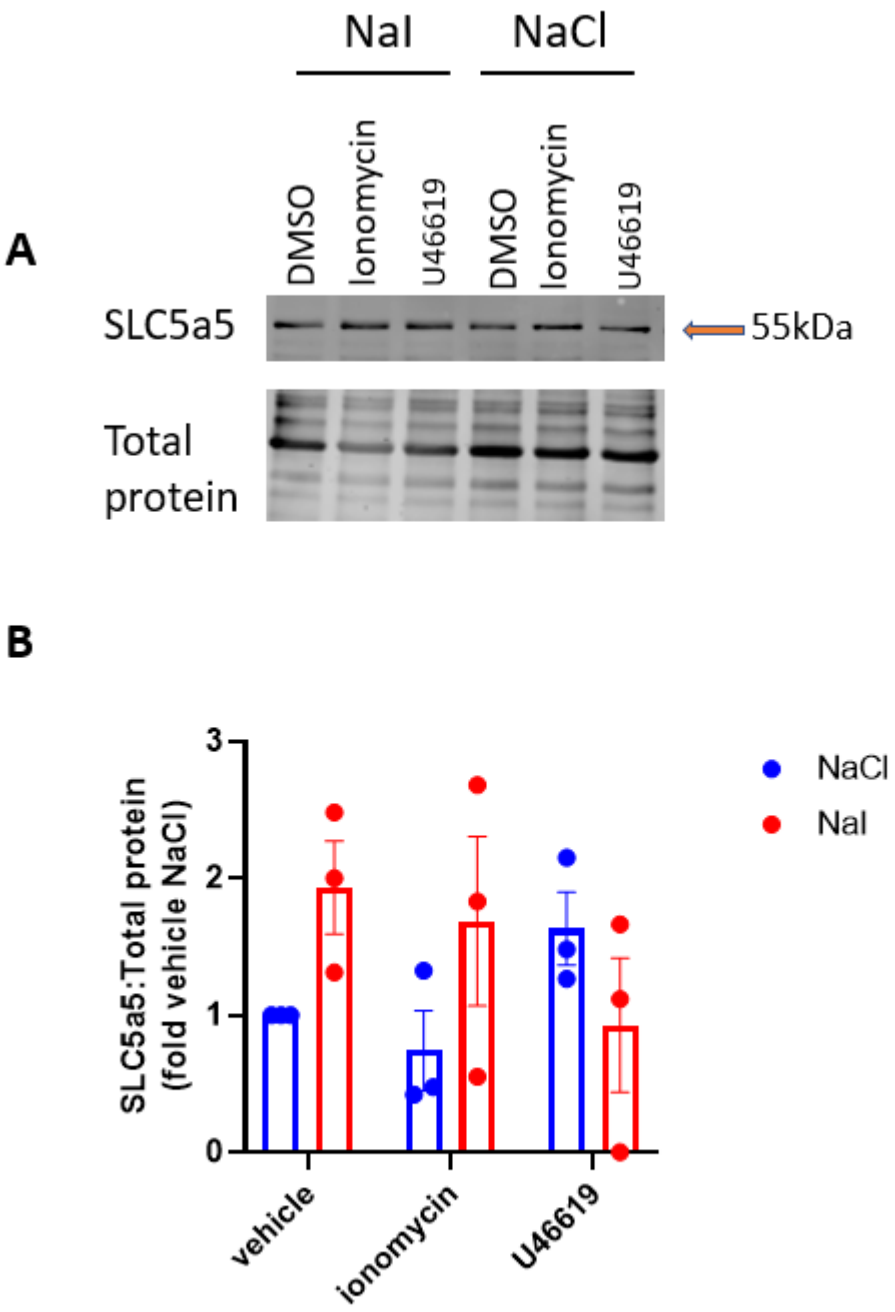

Figure 5-10: Effect of iodide on agonist stimulated SLC5a5 levels in mesenteric artery VSMC from 12 week old SHRSP rats.

VSMC were cultured in media supplemented with 10 µM NaCl or 10 µM NaI and stimulated with 0.1 µM U46619 or ionomycin for 10 min. The ratio of SLC5a5 to total protein stain was assessed in VSMC lysates by immunoblotting. (**A**) Representative immunoblots for SLC5a5 (top) and total protein (bottom) with molecular mass of SLC5a5 indicated on the right from a single experiment. Protein loaded = 10 µg. (**B**) Quantification of SLC5a5 relative to total protein stain. All values are reported as mean ± SEM (n=3 per group).

5.6 Discussion

In this chapter, we aimed to understand the molecular effect of iodide on vascular contractile signalling in mesenteric artery VSMC from WKY and SHRSP male rats. We measured protein markers typically thought to indicate a contractile phenotype in VSMC to determine how iodide influences these proteins. In addition, we also determined the effect of iodide on the levels of proteins involved in iodine uptake. We demonstrated that iodide in cell culture media significantly affects SHRSP but not WKY male mesenteric artery VSMC MLC-phosphorylation. We also showed that SLC5a5 protein is present in WKY and SHRSP male mesenteric artery VSMC and its levels were not significantly affected by iodide supplementation of cell culture media. The changes in MLC-phosphorylation as a result of iodide supplementation may be part of the mechanisms involved in the hypercontractility of mesenteric arteries isolated from SHRSP and WKY male rats fed LID.

In line with our vascular function data, VSMC cultured in media supplemented with 10 μM NaI significantly reduced contractile signalling response concomitant with decreased level of phospho-MLC in SHRSP but not WKY mesenteric VSMC following 0.1 μM U46619. Ionomycin stimulation did not have a significant effect on phospho-MLC in both WKY and SHRSP VSMC. This clearly demonstrates that iodide decreased sensitivity of SHRSP but not WKY VSMC to U46619. Mechanisms are unknown but some potential hypothesis can explain this action. Several studies have shown iodine to be a potent antioxidant and able to act as reducing agent (Elstner et al., 1985; Winkler et al., 2000). Therefore, Iodide could be acting directly as an electron donor that quenches free radicals such as OH^- or H_2O_2. Alternatively, it may act as a free radical that readily iodinates tyrosine, histidine, and double bonds of some polyunsaturated fatty acids in cellular membranes, making them less reactive with oxygen radicals (Smyth, 2003). In contrast, it has been demonstrated that iodine deficiency induces a significant release of ROS in mice thyrocytes and MCF12A breast cell lines (Gérard et al., 2008; Vanderstraeten et al., 2020). Iodine deficiency could rapidly induce a shift in the redox state of VSMC leading to a shift in the redox state of mitochondria Ca^{2+} signalling and VSMC contraction. Moreover, it has been reported that O_2^- enhances IP_3-induced Ca^{2+} release from fractioned VSMC sarcoplasmic reticulum (Suzuki & Ford, 1992). Mitochondrial-derived ROS have been implicated in

regulation of vasomotor tone (pulmonary artery vaso-constriction and cerebral artery vasodilation) (Beardsley et al., 2005; Schumacker, 2003). Contraction and relaxation of VSMC are regulated by phosphorylation and dephosphorylation of the 18-kDa light chain of myosin (Carrillo-Sepúlveda & Barreto-Chaves, 2010; Haeberle et al., 1985). Phosphorylation of myosin is initiated primarily by an increase in the intracellular concentration of free cytoplasmic Ca^{2+} which results in the activation of MLCK (Carrillo-Sepúlveda & Barreto-Chaves, 2010). MLCK catalyses phosphorylation of the regulatory 18-kDa light chain subunit of myosin. The presence of iodide in media supplemented with NaI could have potentially increased the antioxidant capacity of VSMC and therefore prevented the release of Ca^{2+}. Moreover, reduced MLC phosphorylation in iodide supplemented cell media might also have resulted from activation of MLC phosphatase because of increased iodide. Further investigations are needed to clarify the relationship between free radicals, intracellular Ca^{2+} levels and MLC phosphorylation in order to confirm this hypothesis.

We sought to determine if changes in the phospho-MLC in VSMC cultured in iodide supplemented media were due to alterations in the content of pro contractile protein MLC. Contrary to phospho-MLC, MLC protein levels were significantly increased in mesenteric VSMC from SHRSP but not WKY males incubated in 10 μM NaI when compared to 10 μM NaCl. The significance of this finding is not clear given that iodine is associated with vasodilation, antioxidant, and anti-inflammatory properties both which are inhibitory to vascular contraction. Therefore, the significant increase in MLC protein levels cannot account for the decreased levels of phospho-MLC in VSMC from SHRSP rats cultured in media supplemented with iodide. The extent of phosphorylation of smooth muscle myosin is regulated by the relative activities of MLCK and MLC-phosphatase and therefore the decreased levels of phospho-MLC in VSMC from SHRSP rats cultured in media supplemented with iodide maybe be due to lower concentration of free cytoplasmic Ca^{2+} compared to high cytosolic Ca^{2+} concentration in low iodine media. Although the content of MLCK was not determined in this study, alterations in the activation properties of MLCK during contraction may also have contributed to different levels of light chain phosphorylation in these VSMC. Furthermore, in pursuit to find mechanisms for reduced protein levels of phospho- MLC in VSMC cultured in iodide media, we

determined the protein levels of thromboxane A2 receptor, which binds U46619, however the antibody used was nonspecific therefore the data was inconclusive. U46619 is an analogue of thromboxane A2 and contracts VSMC by binding to specific G-protein-coupled receptors (TP receptors) that may increase cytosolic free Ca^{2+} by releasing stored Ca^{2+}, mainly from the sarcoplasmic reticulum (SR), or by causing entry of extracellular Ca^{2+} through activation of channels in the plasma membrane (McKenzie et al., 2009).

Contrary to expectations ionomycin did not stimulate MLC phosphorylation. The main reason for failure of ionomycin to phosphorylate MLC in VSMC of WKY and SHRSP rats might be attributed to a low concentration used (0.1 μM). Other studies have reported failure of ionomycin to phosphorylate MLC at a concentration of 1 μM in chicken embryo fibroblasts (Kolodney et al., 1999). It might be beneficial in future to increase the concentration of ionomycin. The lack of significant difference in phospho-MLC in VSMC from WKY incubated in cell culture media supplemented with NaI or NaCl could be due to decreased sensitivity of VSMC from WKY to U46619. Furthermore, our RNA-Seq data also demonstrated no DEGs in thoracic aorta of WKY male fed NID when compared to those fed LID. This clearly demonstrates that iodide significantly affects SHRSP but not the WKY rat strain. However, it might be beneficial in future to use a higher concentration of U46619 to stimulate contractile signalling in VSMC from WKY which would enable us to establish the effect of iodide in these cells. Moreover, it will be beneficial to determine how iodide affects contractile signalling in VSMC isolated from other CVD rat models such as the SHR strain. Further studies are required to elucidate the involvement of iodide on reduced VSMC contractile signalling response and its effect of on SLCa5 protein levels. This includes determination of intracellular Ca^{2+} concentration and the protein levels of thromboxane A2 receptor in VSMC from WKY and SHRSP rats cultured in media supplemented with iodide.

In addition to MLC and phospho-MLC, we wanted to establish if SLC5a5 was expressed in mesenteric VSMC. Our results indicate that SLC5a5 protein was expressed in mesenteric VSMC from WKY and SHRSP male rats. Moreover, short term stimulation with U46619 does did not affect SLC5a5 levels in VSMC from WKY and SHRSP rats cultured in media supplemented with iodide. The results

were not unexpected since the duration of U46619 stimulation was only 10 min. The synthesis of most protein molecules takes between 20 sec to several min or hours depending on abundance and size of the target protein, duration, and intensity of stimulus (Ben-Ari et al., 2010). This observation suggests that SLC5a5 is expressed in VSMC from WKY and SHRSP male rats, however short-term stimulation with agonist does not affect SLC5a5 protein levels. To our knowledge, this study is the first to show SLC5a5 protein in mesenteric artery VSMC from WKY and SHRSP rats. SLC5a5 is known to be expressed in the basolateral membrane of the thyroid follicular cell, however its expression is also reported in extrathyroidal cells and tissues including the salivary glands and lactating mammary gland (Dohán et al., 2003; Riesco-Eizaguirre et al., 2021). The role of SLC5a5 expression in the extrathyroidal tissues is not known, however is it suggested that it is involved in iodine uptake in these tissues (Cho et al., 2000; Tazebay et al., 2000).

In summary, the present results demonstrated that iodide supplementation in cell culture media decreases contractile signalling response in mesenteric artery VSMC from SHRSP but not WKY male rats. This result is attributed to VSMC from SHRSP being more sensitive to U46619 than VSMC from the WKY strain. Moreover, the concentration of ionomycin used might have not been sufficient to elicit contractile signalling response in both WKY and SHRSP VSMC. The study also confirms the presence of SLC5a5 protein in mesenteric VSMC from WKY and SHRSP male rats. Thus, iodide might play a protective role against agonist stimulated contraction in SHRSP VSMC and this may open novel perspectives on the role of iodine on cardiovascular function and CVD.

Chapter 6 General Discussion

IDD and CVDs have been the subject of considerable medical attention since the early twentieth century(Dalen et al., 2014; Pearce, 2007). CVD remains the leading cause of death in developed and developing countries. Although recent advances in BP control have decreased the incidence of CVD, it is still a major cause of death. On the other hand, there has been a decline in IDD as more countries have become iodine sufficient, from 16 countries in 2004 to 102 countries in 2019(Ahad & Ganie, 2010; Network, 2020). Iodine is used for the synthesis of TH, and these hormones are reported to have a direct effect on CVS and CVD outcomes. Moreover, historically iodine has been used for the treatment and control of CVD. In Europe, iodine regimes such as iodine brine baths in spas were used in the early 1960s to treat CVD (Klieber et al., 1982; Vinogradova et al., 1990) and in China and Japan iodine-rich seaweed has been used as a traditional treatment for CVD and control of hypertension (Cardoso et al., 2015; Hitzenberger, 1961). Iodine's essential role in TH formation and function has overshadowed its independent physiological effects. Despite the known indirect effects of iodine on CVS through TH, its antioxidant properties, and its historic use for treatment of CVD, there are no studies that have utilised animal models to study its direct effects on CVD independently of TH. This PhD work is the first to investigate the link between short-term dietary iodine modification and CVD independent of thyroid dysfunction using WKY and SHRSP rat models. Moreover, the investigations into gene expression in thoracic aorta and protein levels in mesenteric artery VSMC from hypertensive and normotensive rat models sought to account for difference in vascular reactivity observed between NID and LID fed rats.

Animal models have been used to gain insights into the mechanisms causing diseases in order to help identify novel therapeutic strategies for the future. The SHRSP rat is a well characterised model of primary hypertension and mimics many of the traits observed in humans. However, thyroid function in rats is not well characterised and there are no standards for diagnosing thyroid dysfunction in rats. Nevertheless, the studies described in this thesis demonstrated that there were no strain differences in TSH, fT3 fT4 and Tg between the WKY and SHRSP rats at baseline. Contrary to our findings, others also using rat models

reported conflicting results which might be attributed to the use of different strains of rats or the different ages of the rats used (Takami et al., 1991). The findings observed at baseline in this study confirmed the suitability of the two rat models used for studying the effect of iodine on CVD independent of TH.

In Chapter 3, 5 wk old WKY and SHRSP male and female rats were assigned NID or LID for 4 wks. We showed that LID did not significantly influence food consumption and BW in any of the experimental groups and therefore this suggests that LID did not compromise the welfare of the rats during this period. We observed a trend towards reduced SV and CO in male rats fed LID suggesting that iodine deficiency over a longer time period is likely to affect cardiac function in these rats. However, LID did not significantly influence %EF and %FS, in any of the experimental groups. In contrast we demonstrated that mesenteric arteries isolated from WKY and SHRSP male rats fed LID for 4 weeks were hypercontractile to U46619 and this was linked to reduced UIC but independent of fT3 and fT4 levels. The RNA-Seq data presented in chapter 4 indicated dilated cardiomyopathy to be the most significantly altered canonical pathway and that expression of genes coding for contractile proteins were significantly increased in SHRSP rats fed LID. Furthermore, cell culture studies described in chapter 5 showed that iodide reduces vascular contractile signalling in mesenteric artery VSMC isolated from male SHRSP but not WKY rats.

Interestingly, the findings in Chapter 3 revealed that homeostatic mechanisms that respond to LID differ between WKY and SHRSP rats. We demonstrated clear evidence for an increase in expression of SLC5a5 in the thyroid gland of WKY but not in SHRSP rats fed LID, and that this increase occurred without significant increase in TSH at that time point. Furthermore, the significant increase in TSH in SHRSP but not WKY male and female rats clearly demonstrated the difference in the ability of the two rat strains to respond to LID. These data suggest that, unlike WKY, SHRSP rats are more likely to reach a subclinical hypothyroid state earlier than WKY which might further escalate to CVD if combined with thyroid dysfunction. It would be of interest in the future to maintain WKY rats longer (16 wks) on LID to establish how long they are able to maintain normal thyroid function. Additionally, it would be interesting to determine thyroid function in SHR and compare it to both SHRSP and WKY rat strains. This would give an

insight on the influence of LID on thyroid function in normotensive, hypertensive, and stroke prone hypertensive rat models. Moreover, we demonstrated the presence of SLC5a5 protein in VSMC from WKY and SHRSP rats, yet iodide had no significant effect on SLC5a5 protein levels. This study is the first to show that SLC5a5 protein is present in VSMC from WKY and SHRSP male rats and it may be involved in active iodide uptake which could provide antioxidant properties in those tissues. Our study therefore adds further evidence to the few previous studies that have suggested the presence of SLC5a5 in extrathyroidal tissues. The presence of SLC5a5 has already been reported in other organs including salivary and mammary glands, which are able to take up iodide, potentially rendering them sensitive to iodine deficiency (Vanderstraeten et al., 2016).

An important discovery in our *ex vivo* studies was that despite the lack of significant difference in BP between the NID and LID-fed rats, LID significantly increased vascular contractility but did not affect endothelial-dependent or -independent relaxation in mesenteric arteries isolated from WKY and SHRSP male rats. Moreover, LID showed a trend towards increased vascular reactivity in female SHRSP rats fed LID when compared to female WKY rats. This implies that feeding LID increases vascular sensitivity to agonist stimulation in mesenteric arteries isolated from WKY and SHRSP rats. These data suggest that iodine deficiency in the longer term may have the potential to raise BP in WKY due to overall increase in peripheral vascular resistance and worsen hypertension in SHRSP rats independent of TH profiles. Previous studies in humans have suggested that circulating iodine levels had a significant negative correlation with age and systolic BP and had no correlation with thyroid volume or biochemical parameters (Menon et al., 2011).

The studies in Chapter 3 led to the proposal that the mechanism behind hypercontractility would be at a molecular level, and therefore in Chapter 4 bulk RNA-Seq was undertaken to identify DEGs influenced by LID. Furthermore, ingenuity pathway analysis (IPA) software was utilised to understand the biology linking to the DEGs in the resultant data set. This study was the first to utilise RNA-Seq to investigate the link between short term low dietary iodine intake and CVD independent of thyroid dysfunction using WKY and SHRSP male rats.

There were no DEGs between NID and LID fed WKY male rats, however 438 DEGs were associated with LID fed SHRSP males. This would suggest that increased vascular contractility observed in WKY fed LID was not through the same mechanism as in SHRSP rats. Despite the lack of significant differences in vascular contractility in female rats, we did observe a trend towards increased vascular contractility in female SHRSP rats fed LID. It would be meaningful in the future to perform RNA-Seq analysis using vascular tissues from female WKY and SHRSP rats to understand how iodine deficiency influences vascular contractility at the molecular level in female rats and how this compares to male rats. The RNA-Seq data suggests that vascular hypercontractility in iodine deficient SHRSP males might have been due to increased expression of genes that code for vascular contractile proteins. Analysis of the DEGs by IPA identified dilated cardiomyopathy as the most significant canonical pathway, and within this pathway expression of contractile genes such as Mhy7, Myh6, Actc1, Tnnc1, Tnni3, Tnnt2 and Ttn was significantly increased in SHRSP fed LID. Generally, these genes are known to be expressed in cardiac muscle cells but not VSMC, however LID might have switched on expression of these genes in VSMC from iodine deficient SHRSP male rats. Evidence for the expression of these genes under LID conditions became apparent during RT-qPCR validation of DEGs where large fold changes in Myh6 and Actc1 normalised to GAPDH were observed. More of the genes in the pathway identified by IPA need to be validated in the future to provide conclusive evidence to support this suggested gene expression induction resulting from LID. Furthermore, future studies are required to understand the mechanisms underlying hypercontractility in iodine deficient WKY male rats since there were no DEGs in this comparison group, even at the least stringent filter of (padj) < 0.05. This indicates that hypercontractility of mesenteric arteries from WKY males observed in Chapter 4 was not a result of increased expression of genes coding for contractile proteins, however it might have been due to impaired Ca^{2+} channels such as the L-type Ca^{2+} voltage gated channels (LTCCs).

Another strength of RNA-Seq is that in addition to protein coding genes, it allows the informative assessment on non-coding RNAs. Many studies have reported that non-coding RNAs play important roles in vascular biology, including vascular development and CVDs (Jin et al., 2018; Liu & Olson, 2010; Uchida & Dimmeler,

2015). Interestingly miRNAs miR -124-3p, miR -155, and MIR 17 HG were implicated in our data set demonstrating increased expression in thoracic aorta from LID-fed SHRSP males. Evidence supporting a pathophysiological role for miRNAs in SMC differentiation and proliferation derives from *in vivo* studies in conditional knockout mice, where smooth muscle cell-specific knockout of the endonuclease Dicer (which cleaves double-stranded RNA to produce miRNA) was associated with dilated, thin-walled arteries, reduced VSMC proliferation, decreased expression of contractile genes, and decreased BP (Albinsson et al., 2010). The transcription of miRNAs is under the control of signalling pathways such as SRF/MYCOD and Jag-1/Notch signalling (Boucher et al., 2011; Cordes et al., 2009; Xin et al., 2009). Interestingly our data showed increased expression of MYCOD and SRF which further demonstrates the negative impact of iodine deficiency in the phenotype modulation of VSMC from a hypertensive rat model. We did not have time to investigate the roles of the identified miRNAs in our data set therefore more comprehensive screening techniques will be essential to delineate the biological effects of these miRNAs. Nevertheless, we identified novel miRNAs involved in vascular contractility and associated with increased expression of genes that code for contractile proteins in VSMC from LID fed SHRSP rats.

To elucidate further the molecular mechanisms underlying hypercontractility of mesenteric arteries of SHRSP and WKY male rats, mesenteric artery VSMCs were isolated and cultured from these rats and incubated in the presence or absence of NaI before incubation with U46619. The results revealed that iodide significantly decreased the levels of phospho-MLC in VSMCs from SHRSP but not WKY. This observation was intriguing as it provided further evidence that the hypercontractility of mesenteric arteries from iodine deficient SHRSP male rats might be due an increased expression of genes and proteins linked with vascular contractility, but due to a different mechanism in WKY rats. The lack of significant increase in phospho-MLC in WKY VSMCs might be attributed to their reduced sensitivity to agonist treatment or reduced sensitivity to iodide. This result supports the findings in Chapter 4, where no DEGs were observed when comparing thoracic aorta from NID and LID fed WKY males. These in vitro studies clearly demonstrated that iodide significantly affected VSMCs from SHRSP but not WKY rats. In future studies it might be beneficial to increase the

concentration of U46619 to stimulate a contractile response in WKY VSMC since a submaximal concentration was used.

To further understand how iodide plays an inhibitory role to contractile signalling in VSMCs from SHRSP male rats, the levels of the pro-contractile protein MLC were determined in SHRSP VSMCs cultured in the presence or absence of NaI. Contrary to the decrease in phospho-MLC levels, VSMC MLC levels were significantly increased when cultured in the presence of NaI. We cannot yet interpret the mechanisms underlying this observation and this requires further investigation. For example, iodide may act by inhibiting the influx of Ca^{2+} into the VSMC cells leading to reduced phosphorylation of MLC (Figure 6-1). It is known that changes in Ca^{2+} influx, and membrane potential lead to Ca^{2+}-calmodulin-mediated phosphorylation of MLC and actin-myosin cross bridge cycling with consequent rapid vasocontraction (Kim et al., 2008). Increased Ca^{2+} influx augments sarcoplasmic reticular Ca^{2+} release and decreases sarcoplasmic reticular Ca^{2+} reuptake, causes activation of the PLC-DAG-IP3 pathway, leading to increased Ca^{2+} signalling, vascular hyperreactivity, and exaggeration of contractile responses to vascular agonists, all of which have been demonstrated in SHR and SHRSP rat models and in human hypertension (Bazan et al., 1992; Goulopoulou & Webb, 2014; Matsuda et al., 1997; Misárková et al., 2016; Touyz et al., 1995). This suggests that LID has the potential to worsen hypertension in hypertensive rat models and may have similar action in humans. Moreover, when diets have sufficient levels of iodide it could potentially act as an antioxidant thereby decreasing the bioavailability of ROS which are also implicated in increased vascular contraction. One study proposed that iodide exerts antioxidative effects, which explained the early release of ROS and NO in response to iodine deficiency in the thyroid gland (Vanderstraeten et al., 2016). Ca^{2+}-independent mechanisms associated with altered Ca^{2+} sensitization and actin filament remodelling and increased bioavailability of ROS also modulate vascular contraction (Matchkov et al., 2012). It is known that redox-regulated Ca^{2+}-sensitive transcription factors, including SRF, nuclear factor of activated T-cells (NFAT), and cyclic adenosine monophosphate (cAMP) response element-binding protein, promote expression of genes encoding contractile proteins, further influencing vascular contractility in hypertension (Goulopoulou & Webb, 2014). It is important to note that the RNA-Seq data

demonstrated increased expression of SRF which occurred upstream of the genes coding for contractile proteins identified in this study. This provides further evidence that enhanced vascular contractility in LID fed SHRSP male rats may be a consequence of significant increases in expression of genes that code for contractile proteins. It would be very useful in the future to determine the levels of Ca^{2+} and ROS in cells following iodide treatment in order to elucidate how iodide prevents phosphorylation of MLC.

Another important discovery in Chapter 4 came from IPA which identified diseases and functions associated with the data set. Growth failure or short stature is one of the diseases/functions associated with LID. Even though we did not observe significant differences in growth rates between the NID and LID fed rats, the RNA-Seq data suggested that SHRSP males fed LID are likely to experience a reduced growth rate which is a known trait associated with severe iodine deficiency more especially in young born from iodine deficient parents. It has been suggested that iodine status may influence growth through its effects on the thyroid axis and it has been demonstrated that administration of T4 to hypothyroid children increases their growth (Hernández-Cassis et al., 1995; Zimmermann et al., 2007). However, we did not see a significant difference in TH levels between the NID and LID fed male SHRSP rats, and this might suggest that reduced growth rate could occur due to LID but independent of TH dysfunction. Taken together these results confirm typical adverse effects of reduced dietary iodine.

To conclude, in this thesis, several novel findings have been presented demonstrating the effect of iodine on the CVS independent of TH, using *in vivo*, *ex vivo*, and *in vitro* models. Furthermore, with the aid of bioinformatic prediction and *in vitro* validation, I have shown that expression of genes coding for contractile proteins were significantly increased in LID fed hypertensive but not normotensive male rats leading to hypercontractility of mesenteric arteries. So, while these findings add to small but growing evidence that dietary iodine directly affects CVD through its antioxidant and anti-inflammatory properties, the current study has demonstrated a direct anticontractile effect of iodide through inhibition of MLC phosphorylation in mesenteric artery VSMC from SHRSP males. Overall, the studies described in this thesis demonstrated that short term

LID has detrimental effects in a hypertensive rat model when compared to the normotensive rat model, suggesting that LID is more likely to affect individuals with hypertension. Thus, if LID precedes CVD, then this potential and modifiable new CVD risk factor might have therapeutic implications and highlight the need for recommending alternatives sources of iodine for people on iodized-salt restriction.

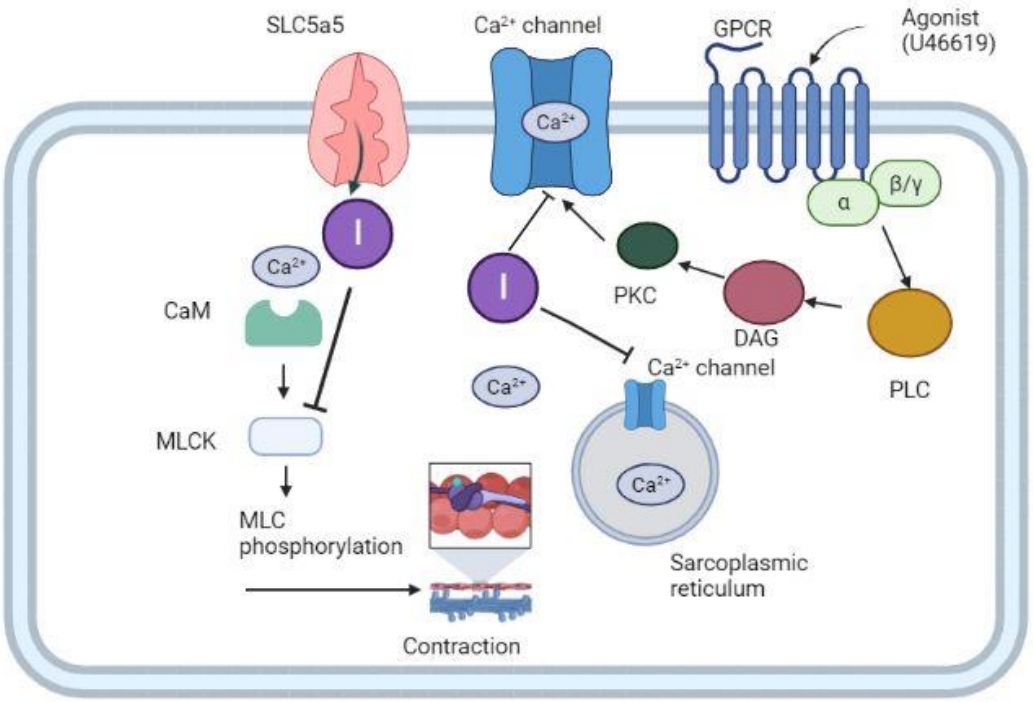

Figure 6-1: Proposed mechanism of iodide action on vascular smooth muscle cell (VSMC) contraction.

Vasoconstrictors induce VSMC contraction by increasing intracellular levels of Ca^{2+}. Vasoactive agonists such as U46619 bind to G protein coupled receptors (GPCRs) activating PLC leading to the formation of DAG which activates PKC. PKC then stimulates Ca^{2+} channel opening. Increased intracellular Ca^{2+} binds to calmodulin and activates MLCK leading to MLC phosphorylation to initiate contraction. Iodide (I^-) transported by the sodium iodide symporter (SLC5a5) inhibits Ca^{2+}entry from extracellular and sarcoplasmic reticulum compartments therefore reducing contractile responses to agonists.

6.1 Limitations and future studies

The major limitation of this PhD work was time. Initially I had planned to determine the effect of dietary iodine on CVD in short- and long-term studies, however, the covid 19 pandemic started a month after the first batch of experimental rats were started and we had to terminate the study. We were on lockdown for more than 7 months and were allowed back into the animal unit in September 2020, and this resulted in us focusing on short term (4 week) dietary effects. Extending our research to a longer-term iodine study would lead to a better understanding of how iodine influences CVD independent of TH. Moreover, I had planned a clinical study, to establish a relationship between UIC and hypertension. In this study I originally intended to use readily available 24 hr urine samples from study participants with and without hypertension (previously collected by Prof Emilie Combet Aspray) and determine their UIC, however this was not possible in the reduced timeframe of my project. In future it will be beneficial to establish the direct effect of iodine and CVD in humans.

SLC5a5 and SLC26a4 gene expression and protein determination should have been extended to other organs such as the kidney since it's the major organ responsible for iodide clearance. Additionally, it would be beneficial to study how iodide deficiency influences mesenteric artery blood flow by determining the expression of SLC5a5 and vascular endothelial growth factor (VEGF) using RT-PCR and immunohistochemistry. It has already been reported that tissues like thyrocytes constantly react to fluctuations in iodide availability by regulating their surrounding microvasculature (Gérard et al., 2008). This would help us understand the homeostatic mechanisms affected by iodide deficiency in blood vessels of normotensive and hypertensive rats and might help explain the differences in vascular function observed in mesenteric arteries from WKY and SHRSP males fed NID compared to those fed LID. TSH-dependent and independent increase in blood flow is mediated, at least in part, by ROS dependent stabilization of the α subunit of hypoxia inducible factor (HIF). HIF-1 transcription factor subunit α is known to bind to HIF-1ß to form active HIF-1 and to stimulate the expression of target genes including VEGF. Furthermore, a previous study reported that salivary glands and stomach respond to iodine deficiency by inducing a microvascular response through the VEGF pathway (Vanderstraeten et al., 2016).

We demonstrated that mesenteric arteries isolated from WKY and SHRSP males fed LID were hypercontractile to U46619 when compared to sex and strain matched rats fed NID. In future it would be interesting to perform wire myography in mesenteric arteries from NID fed male and female WKY and SHRSP rats incubated in PSS containing iodide in a concentration and time course dependent manner. This study would establish ex-vivo, the acute effect of iodide in intact mesenteric arteries from normotensive and hypertensive rat models, which would supplement our vascular function data in chapter 3. Moreover, this would provide further information on the direct effect of iodide on contraction as evidenced in VSMC isolated from mesenteric arteries from WKY and SHRSP male rats covered in chapter 5.

It would have been ideal to perform RNA-Seq on the same tissue as our vascular function studies, however we utilised thoracic aorta mainly because necessary time was taken to dissect mesenteric arteries for wire myography which could have compromised RNA quality. In future it would be beneficial to use mesenteric arteries for our RNA-Seq analysis so we could have meaningful translatable results by using tissue from the same vascular bed. Moreover, our RNA-Seq study demonstrated the significant increase in expression of genes known to control contractile machinery in cardiac muscles. It will therefore be ideal to perform RNA-Seq in cardiac tissue from these animals to establish how LID affects these genes in the heart. Moreover, since the SHRSP stroke as their endpoint of CVD, it would have been meaningful to perform RNA-Seq in brain tissue to determine how LID affects in gene expression in this tissue.

Despite the limitations, this study provides substantial evidence that short-term LID directly impacts CVD independent of TH in a hypertensive rat model and that LID has potential to affect the CVS in normotensive male and female rats.

List of References

Abrams, G. M., & Larsen, P. R. (1973). Triiodothyronine and thyroxine in the serum and thyroid glands of iodine-deficient rats. *J Clin Invest*, *52*(10), 2522-2531. https://doi.org/10.1172/JCI107443

Agarwal, A., Williams, G. H., & Fisher, N. D. (2005). Genetics of human hypertension. *Trends Endocrinol Metab*, *16*(3), 127-133. https://doi.org/10.1016/j.tem.2005.02.009

Ahad, F., & Ganie, S. A. (2010). Iodine, Iodine metabolism and Iodine deficiency disorders revisited. *Indian J Endocrinol Metab*, *14*(1), 13-17. https://www.ncbi.nlm.nih.gov/pubmed/21448409

Al-Attas, O. S., Al-Daghri, N. M., Alkharfy, K. M., Alokail, M. S., Al-Johani, N. J., Abd-Alrahman, S. H., Yakout, S. M., Draz, H. M., & Sabico, S. (2012). Urinary iodine is associated with insulin resistance in subjects with diabetes mellitus type 2. *Exp Clin Endocrinol Diabetes*, *120*(10), 618-622. https://doi.org/10.1055/s-0032-1323816

Al-Dakheel, M. H., Haridi, H. K., Al-Bashir, B. M., Al-Shangiti, A. M., Al-Shehri, S. N., & Hussein, I. (2018). Assessment of household use of iodized salt and adequacy of salt iodization: a cross-sectional National Study in Saudi Arabia. *Nutr J*, *17*(1), 35. https://doi.org/10.1186/s12937-018-0343-0

Albinsson, S., Suarez, Y., Skoura, A., Offermanns, S., Miano, J. M., & Sessa, W. C. (2010). MicroRNAs are necessary for vascular smooth muscle growth, differentiation, and function. *Arterioscler Thromb Vasc Biol*, *30*(6), 1118-1126. https://doi.org/10.1161/ATVBAHA.109.200873

Ambros, V. (2004). The functions of animal microRNAs. *Nature*, *431*(7006), 350-355. https://doi.org/10.1038/nature02871

Andersson, M., de Benoist, B., Delange, F., Zupan, J., & Secretariat, W. (2007). Prevention and control of iodine deficiency in pregnant and lactating women and in children less than 2-years-old: conclusions and recommendations of the Technical Consultation. *Public*

Health Nutr, *10*(12A), 1606-1611. https://doi.org/10.1017/S1368980007361004

Andersson, M., Karumbunathan, V., & Zimmermann, M. B. (2012). Global iodine status in 2011 and trends over the past decade. *J Nutr*, *142*(4), 744-750. https://doi.org/10.3945/jn.111.149393

Arber, S., Barbayannis, F. A., Hanser, H., Schneider, C., Stanyon, C. A., Bernard, O., & Caroni, P. (1998). Regulation of actin dynamics through phosphorylation of cofilin by LIM-kinase. *Nature*, *393*(6687), 805-809. https://doi.org/10.1038/31729

Ardalan, M. R., & Rafieian-Kopaei, M. (2014). Antioxidant supplementation in hypertension. *J Renal Inj Prev*, *3*(2), 39-40. https://doi.org/10.12861/jrip.2014.13

Babuin, L., & Jaffe, A. S. (2005). Troponin: the biomarker of choice for the detection of cardiac injury. *CMAJ*, *173*(10), 1191-1202. https://doi.org/10.1503/cmaj/051291

Bagga, S., & Pasquinelli, A. E. (2006). Identification and analysis of microRNAs. *Genet Eng (N Y)*, *27*, 1-20. https://doi.org/10.1007/0-387-25856-6_1

Bailey, E. L., McBride, M. W., McClure, J. D., Beattie, W., Graham, D., Dominiczak, A. F., Smith, C., & Wardlaw, J. M. (2018). Effects of dietary salt on gene and protein expression in brain tissue of a model of sporadic small vessel disease. *Clin Sci (Lond)*, *132*(12), 1315-1328. https://doi.org/10.1042/CS20171572

Ballantyne, M. D., Pinel, K., Dakin, R., Vesey, A. T., Diver, L., Mackenzie, R., Garcia, R., Welsh, P., Sattar, N., Hamilton, G., Joshi, N., Dweck, M. R., Miano, J. M., McBride, M. W., Newby, D. E., McDonald, R. A., & Baker, A. H. (2016). Smooth Muscle Enriched Long Noncoding RNA (SMILR) Regulates Cell Proliferation. *Circulation*, *133*(21), 2050-2065. https://doi.org/10.1161/CIRCULATIONAHA.115.021019

Baradaran, A., Nasri, H., & Rafieian-Kopaei, M. (2014). Oxidative stress and hypertension: Possibility of hypertension therapy with antioxidants. *J Res Med Sci*, *19*(4), 358-367. https://www.ncbi.nlm.nih.gov/pubmed/25097610

Bartel, D. P. (2004). MicroRNAs: genomics, biogenesis, mechanism, and function. *Cell*, *116*(2), 281-297. https://doi.org/10.1016/s0092-8674(04)00045-5

Bastola, P., Neums, L., Schoenen, F. J., & Chien, J. (2016). VCP inhibitors induce endoplasmic reticulum stress, cause cell cycle arrest, trigger caspase-mediated cell death and synergistically kill ovarian cancer cells in combination with Salubrinal. *Mol Oncol*, *10*(10), 1559-1574. https://doi.org/10.1016/j.molonc.2016.09.005

Bath, S. C., Button, S., & Rayman, M. P. (2012). Iodine concentration of organic and conventional milk: implications for iodine intake. *Br J Nutr*, *107*(7), 935-940. https://doi.org/10.1017/S0007114511003059

Bath, S. C., Combet, E., Scully, P., Zimmermann, M. B., Hampshire-Jones, K. H., & Rayman, M. P. (2016). A multi-centre pilot study of iodine status in UK schoolchildren, aged 8-10 years. *Eur J Nutr*, *55*(6), 2001-2009. https://doi.org/10.1007/s00394-015-1014-y

Bath, S. C., Hill, S., Infante, H. G., Elghul, S., Nezianya, C. J., & Rayman, M. P. (2017). Iodine concentration of milk-alternative drinks available in the UK in comparison with cows' milk. *Br J Nutr*, *118*(7), 525-532. https://doi.org/10.1017/S0007114517002136

Bazan, E., Campbell, A. K., & Rapoport, R. M. (1992). Protein kinase C activity in blood vessels from normotensive and spontaneously hypertensive rats. *Eur J Pharmacol*, *227*(3), 343-348. https://doi.org/10.1016/0922-4106(92)90014-m

Beardsley, A., Fang, K., Mertz, H., Castranova, V., Friend, S., & Liu, J. (2005). Loss of caveolin-1 polarity impedes endothelial cell polarization and directional movement. *J Biol Chem*, *280*(5), 3541-3547. https://doi.org/10.1074/jbc.M409040200

Bell, R. D., Long, X., Lin, M., Bergmann, J. H., Nanda, V., Cowan, S. L., Zhou, Q., Han, Y., Spector, D. L., Zheng, D., & Miano, J. M. (2014). Identification and initial functional characterization of a human vascular cell-enriched long noncoding RNA. *Arterioscler Thromb Vasc Biol*, *34*(6), 1249-1259. https://doi.org/10.1161/ATVBAHA.114.303240

Ben-Ari, Y., Brody, Y., Kinor, N., Mor, A., Tsukamoto, T., Spector, D. L., Singer, R. H., & Shav-Tal, Y. (2010). The life of an mRNA in space and time. *J Cell Sci*, *123*(Pt 10), 1761-1774. https://doi.org/10.1242/jcs.062638

Benotti, J., Benotti, N., Pino, S., & Gardyna, H. (1965). Determination of total iodine in urine, stool, diets, and tissue. *Clin Chem*, *11*(10), 932-936. https://www.ncbi.nlm.nih.gov/pubmed/5837839

Berta, E., Lengyel, I., Halmi, S., Zrínyi, M., Erdei, A., Harangi, M., Páll, D., Nagy, E. V., & Bodor, M. (2019). Hypertension in Thyroid Disorders. *Front Endocrinol (Lausanne)*, *10*, 482. https://doi.org/10.3389/fendo.2019.00482

Bianco, A. C., Anderson, G., Forrest, D., Galton, V. A., Gereben, B., Kim, B. W., Kopp, P. A., Liao, X. H., Obregon, M. J., Peeters, R. P., Refetoff, S., Sharlin, D. S., Simonides, W. S., Weiss, R. E., Williams, G. R., & Action, A. T. A. T. F. o. A. a. S. t. I. T. H. E. a. (2014). American Thyroid Association Guide to investigating thyroid hormone economy and action in rodent and cell models. *Thyroid*, *24*(1), 88-168. https://doi.org/10.1089/thy.2013.0109

Bianco, A. C., & Kim, B. W. (2006). Deiodinases: implications of the local control of thyroid hormone action. *J Clin Invest*, *116*(10), 2571-2579. https://doi.org/10.1172/JCI29812

Biban, B. G., & Lichiardopol, C. (2017). Iodine Deficiency, Still a Global Problem? *Curr Health Sci J*, *43*(2), 103-111. https://doi.org/10.12865/CHSJ.43.02.01

Birben, E., Sahiner, U. M., Sackesen, C., Erzurum, S., & Kalayci, O. (2012). Oxidative stress and antioxidant defense. *World Allergy Organ J*, *5*(1), 9-19. https://doi.org/10.1097/WOX.0b013e3182439613

Bizhanova, A., & Kopp, P. (2009). Minireview: The sodium-iodide symporter NIS and pendrin in iodide homeostasis of the thyroid. *Endocrinology*, *150*(3), 1084-1090. https://doi.org/10.1210/en.2008-1437

Bjoro, T., Holmen, J., Krüger, O., Midthjell, K., Hunstad, K., Schreiner, T., Sandnes, L., & Brochmann, H. (2000). Prevalence of thyroid disease, thyroid dysfunction and

thyroid peroxidase antibodies in a large, unselected population. The Health Study of Nord-Trondelag (HUNT). *Eur J Endocrinol*, *143*(5), 639-647. https://doi.org/10.1530/eje.0.1430639

Blackstone, E., Morrison, M., & Roth, M. B. (2005). H2S induces a suspended animation-like state in mice. *Science*, *308*(5721), 518. https://doi.org/10.1126/science.1108581

Blackstone, E., & Roth, M. B. (2007). Suspended animation-like state protects mice from lethal hypoxia. *Shock*, *27*(4), 370-372. https://doi.org/10.1097/SHK.0b013e31802e27a0

Blaustein, M. P., Leenen, F. H., Chen, L., Golovina, V. A., Hamlyn, J. M., Pallone, T. L., Van Huysse, J. W., Zhang, J., & Wier, W. G. (2012). How NaCl raises blood pressure: a new paradigm for the pathogenesis of salt-dependent hypertension. *Am J Physiol Heart Circ Physiol*, *302*(5), H1031-1049. https://doi.org/10.1152/ajpheart.00899.2011

Blenkiron, C., & Miska, E. A. (2007). miRNAs in cancer: approaches, aetiology, diagnostics and therapy. *Hum Mol Genet*, *16 Spec No 1*, R106-113. https://doi.org/10.1093/hmg/ddm056

Bohlen, H. G. (1986). Localization of vascular resistance changes during hypertension. *Hypertension*, *8*(3), 181-183. https://doi.org/10.1161/01.hyp.8.3.181

Boucher, J. M., Peterson, S. M., Urs, S., Zhang, C., & Liaw, L. (2011). The miR-143/145 cluster is a novel transcriptional target of Jagged-1/Notch signaling in vascular smooth muscle cells. *J Biol Chem*, *286*(32), 28312-28321. https://doi.org/10.1074/jbc.M111.221945

Bouga, M., & Combet, E. (2015). Emergence of Seaweed and Seaweed-Containing Foods in the UK: Focus on Labeling, Iodine Content, Toxicity and Nutrition. *Foods*, *4*(2), 240-253. https://doi.org/10.3390/foods4020240

Braschi, A., Gill, L., & Naismith, D. J. (2009). Partial substitution of sodium with potassium in white bread: feasibility and bioavailability. *Int J Food Sci Nutr*, *60*(6), 507-521. https://doi.org/10.1080/09637480701782118

Braverman, L. E., & Ingbar, S. H. (1963). CHANGES IN THYROIDAL FUNCTION DURING ADAPTATION TO LARGE DOSES OF IODIDE. *J Clin Invest*, *42*(8), 1216-1231. https://doi.org/10.1172/JCI104807

Breschi, A., Gingeras, T. R., & Guigó, R. (2017). Comparative transcriptomics in human and mouse. *Nat Rev Genet*, *18*(7), 425-440. https://doi.org/10.1038/nrg.2017.19

British, heart, & foundation. (2021). *Cardiovascular disease*. Retrieved 05 April from https://www.bhf.org.uk/informationsupport/conditions/cardiovascular-heart-disease

Brozovich, F. V., Nicholson, C. J., Degen, C. V., Gao, Y. Z., Aggarwal, M., & Morgan, K. G. (2016). Mechanisms of Vascular Smooth Muscle Contraction and the Basis for Pharmacologic Treatment of Smooth Muscle Disorders. *Pharmacol Rev*, *68*(2), 476-532. https://doi.org/10.1124/pr.115.010652

Bruhn, T. O., & Jackson, I. M. (1992). Abnormalities of the thyroid hormone negative feedback regulation of TSH secretion in spontaneously hypertensive rats. *Regul Pept*, *38*(3), 221-230. https://doi.org/10.1016/0167-0115(92)90104-3

Buchner, D. A., & Nadeau, J. H. (2015). Contrasting genetic architectures in different mouse reference populations used for studying complex traits. *Genome Res*, *25*(6), 775-791. https://doi.org/10.1101/gr.187450.114

Buelt, A., Richards, A., & Jones, A. L. (2021). Hypertension: New Guidelines from the International Society of Hypertension. *Am Fam Physician*, *103*(12), 763-765. https://www.ncbi.nlm.nih.gov/pubmed/34128614

Buijsse, B., Jacobs, D. R., Steffen, L. M., Kromhout, D., & Gross, M. D. (2015). Plasma Ascorbic Acid, A Priori Diet Quality Score, and Incident Hypertension: A Prospective Cohort Study. *PLoS One*, *10*(12), e0144920. https://doi.org/10.1371/journal.pone.0144920

Burns, R., O'Herlihy, C., & Smyth, P. P. (2013). Regulation of iodide uptake in placental primary cultures. *Eur Thyroid J*, *2*(4), 243-251. https://doi.org/10.1159/000356847

Buttar, H. S., Li, T., & Ravi, N. (2005). Prevention of cardiovascular diseases: Role of exercise, dietary

interventions, obesity and smoking cessation. *Exp Clin Cardiol*, *10*(4), 229-249. https://www.ncbi.nlm.nih.gov/pubmed/19641674

Cai, Y., Manio, M. M., Leung, G. P., Xu, A., Tang, E. H., & Vanhoutte, P. M. (2015). Thyroid hormone affects both endothelial and vascular smooth muscle cells in rat arteries. *Eur J Pharmacol*, *747*, 18-28. https://doi.org/10.1016/j.ejphar.2014.11.036

Cappola, A. R., Desai, A. S., Medici, M., Cooper, L. S., Egan, D., Sopko, G., Fishman, G. I., Goldman, S., Cooper, D. S., Mora, S., Kudenchuk, P. J., Hollenberg, A. N., McDonald, C. L., & Ladenson, P. W. (2019). Thyroid and Cardiovascular Disease: Research Agenda for Enhancing Knowledge, Prevention, and Treatment. *Thyroid*, *29*(6), 760-777. https://doi.org/10.1089/thy.2018.0416

Cappola, A. R., & Ladenson, P. W. (2003). Hypothyroidism and atherosclerosis. *J Clin Endocrinol Metab*, *88*(6), 2438-2444. https://doi.org/10.1210/jc.2003-030398

Cardoso, S. M., Pereira, O. R., Seca, A. M., Pinto, D. C., & Silva, A. M. (2015). Seaweeds as Preventive Agents for Cardiovascular Diseases: From Nutrients to Functional Foods. *Mar Drugs*, *13*(11), 6838-6865. https://doi.org/10.3390/md13116838

Carretero, O. A., & Oparil, S. (2000). Essential hypertension. Part I: definition and etiology. *Circulation*, *101*(3), 329-335. https://doi.org/10.1161/01.cir.101.3.329

Carrillo-Sepúlveda, M. A., & Barreto-Chaves, M. L. (2010). Phenotypic modulation of cultured vascular smooth muscle cells: a functional analysis focusing on MLC and ERK1/2 phosphorylation. *Mol Cell Biochem*, *341*(1-2), 279-289. https://doi.org/10.1007/s11010-010-0459-9

Carvalho, D. P., & Dupuy, C. (2017). Thyroid hormone biosynthesis and release. *Mol Cell Endocrinol*, *458*, 6-15. https://doi.org/10.1016/j.mce.2017.01.038

Casneuf, T., Van de Peer, Y., & Huber, W. (2007). In situ analysis of cross-hybridisation on microarrays and the inference of expression correlation. *BMC Bioinformatics*, *8*, 461. https://doi.org/10.1186/1471-2105-8-461

Castro, S. I., Berthiaume, R., Robichaud, A., & Lacasse, P. (2012). Effects of iodine intake and teat-dipping practices on milk iodine concentrations in dairy cows. *J Dairy Sci*, *95*(1), 213-220. https://doi.org/10.3168/jds.2011-4679

Chamarthi, B., Williams, J. S., & Williams, G. H. (2010). A mechanism for salt-sensitive hypertension: abnormal dietary sodium-mediated vascular response to angiotensin-II. *J Hypertens*, *28*(5), 1020-1026. https://doi.org/10.1097/HJH.0b013e3283375974

Chen, H., Azuma, M., Maeda, K., Kajimoto, N., & Higashino, H. (2000). Impaired heart function and noradrenaline release after ischaemia in stroke-prone spontaneously hypertensive rats. *Clin Exp Pharmacol Physiol*, *27*(9), 664-670. https://doi.org/10.1046/j.1440-1681.2000.03325.x

Chen, J., Kitchen, C. M., Streb, J. W., & Miano, J. M. (2002). Myocardin: a component of a molecular switch for smooth muscle differentiation. *J Mol Cell Cardiol*, *34*(10), 1345-1356. https://doi.org/10.1006/jmcc.2002.2086

Chen, Q., Gruber, H., Swist, E., Pakenham, C., Ratnayake, W. M., & Scoggan, K. A. (2009). Influence of dietary phytosterols and phytostanols on diastolic blood pressure and the expression of blood pressure regulatory genes in SHRSP and WKY inbred rats. *Br J Nutr*, *102*(1), 93-101. https://doi.org/10.1017/S0007114508137904

Chiamolera, M. I., & Wondisford, F. E. (2009). Minireview: Thyrotropin-releasing hormone and the thyroid hormone feedback mechanism. *Endocrinology*, *150*(3), 1091-1096. https://doi.org/10.1210/en.2008-1795

Cho, J. Y., Léveillé, R., Kao, R., Rousset, B., Parlow, A. F., Burak, W. E., Mazzaferri, E. L., & Jhiang, S. M. (2000). Hormonal regulation of radioiodide uptake activity and Na+/I- symporter expression in mammary glands. *J Clin Endocrinol Metab*, *85*(8), 2936-2943. https://doi.org/10.1210/jcem.85.8.6727

Christensen, K. L., & Mulvany, M. J. (2001). Location of resistance arteries. *J Vasc Res*, *38*(1), 1-12. https://doi.org/10.1159/000051024

Christianson, D., Roti, E., Vagenakis, A. G., & Braverman, L. E. (1981). The sex-related difference in serum thyrotropin concentration is androgen mediated. *Endocrinology*, *108*(2), 529-535. https://doi.org/10.1210/endo-108-2-529

Chung, H. R. (2014). Iodine and thyroid function. *Ann Pediatr Endocrinol Metab*, *19*(1), 8-12. https://doi.org/10.6065/apem.2014.19.1.8

Coll-Bonfill, N., de la Cruz-Thea, B., Pisano, M. V., & Musri, M. M. (2016). Noncoding RNAs in smooth muscle cell homeostasis: implications in phenotypic switch and vascular disorders. *Pflugers Arch*, *468*(6), 1071-1087. https://doi.org/10.1007/s00424-016-1821-x

Combet, E. (2017). Iodine Status, Thyroid Function, and Vegetarianism,. In François Mariotti (Ed.), *Vegetarian and Plant-Based Diets in Health and Disease Prevention,* (pp. 769-790). Academic Press,. https://doi.org/https://doi.org/10.1016/B978-0-12-803968-7.00042-3.

Contreras, G. A., Yang, Y., Flood, E. D., Garver, H., Bhattacharya, S., Fink, G. D., & Watts, S. W. (2020). Blood pressure changes PVAT function and transcriptome: use of the mid-thoracic aorta coarcted rat. *Am J Physiol Heart Circ Physiol*, *319*(6), H1313-H1324. https://doi.org/10.1152/ajpheart.00332.2020

Cordes, K. R., Sheehy, N. T., White, M. P., Berry, E. C., Morton, S. U., Muth, A. N., Lee, T. H., Miano, J. M., Ivey, K. N., & Srivastava, D. (2009). miR-145 and miR-143 regulate smooth muscle cell fate and plasticity. *Nature*, *460*(7256), 705-710. https://doi.org/10.1038/nature08195

Coyle, P., & Jokelainen, P. T. (1983). Differential outcome to middle cerebral artery occlusion in spontaneously hypertensive stroke-prone rats (SHRSP) and Wistar Kyoto (WKY) rats. *Stroke*, *14*(4), 605-611. https://doi.org/10.1161/01.str.14.4.605

Cuellar-Rufino, S., Navarro-Meza, M., García-Solís, P., Xochihua-Rosas, I., & Arroyo-Helguera, O. (2017). Iodine levels are associated with oxidative stress and antioxidant status in pregnant women with hypertensive

disease. *Nutr Hosp*, *34*(3), 661-666. https://doi.org/10.20960/nh.460

Dai, G., Levy, O., & Carrasco, N. (1996). Cloning and characterization of the thyroid iodide transporter. *Nature*, *379*(6564), 458-460. https://doi.org/10.1038/379458a0

Dai, Y. S., Cserjesi, P., Markham, B. E., & Molkentin, J. D. (2002). The transcription factors GATA4 and dHAND physically interact to synergistically activate cardiac gene expression through a p300-dependent mechanism. *J Biol Chem*, *277*(27), 24390-24398. https://doi.org/10.1074/jbc.M202490200

Dalen, J. E., Alpert, J. S., Goldberg, R. J., & Weinstein, R. S. (2014). The epidemic of the 20(th) century: coronary heart disease. *Am J Med*, *127*(9), 807-812. https://doi.org/10.1016/j.amjmed.2014.04.015

Daniel, J. M., Bielenberg, W., Stieger, P., Weinert, S., Tillmanns, H., & Sedding, D. G. (2010). Time-course analysis on the differentiation of bone marrow-derived progenitor cells into smooth muscle cells during neointima formation. *Arterioscler Thromb Vasc Biol*, *30*(10), 1890-1896. https://doi.org/10.1161/ATVBAHA.110.209692

Danzi, S., & Klein, I. (2004). Thyroid hormone and the cardiovascular system. *Minerva Endocrinol*, *29*(3), 139-150. https://www.ncbi.nlm.nih.gov/pubmed/15282446

Darras, V. M., & Van Herck, S. L. (2012). Iodothyronine deiodinase structure and function: from ascidians to humans. *J Endocrinol*, *215*(2), 189-206. https://doi.org/10.1530/JOE-12-0204

de Jong, T. V., Chen, H., Brashear, W. A., Kochan, K. J., Hillhouse, A. E., Zhu, Y., Dhande, I. S., Hudson, E. A., Sumlut, M. H., Smith, M. L., Kalbfleisch, T. S., & Doris, P. A. (2022). mRatBN7.2: familiar and unfamiliar features of a new rat genome reference assembly. *Physiol Genomics*, *54*(7), 251-260. https://doi.org/10.1152/physiolgenomics.00017.2022

De Vriese, A. S., Verbeuren, T. J., Van de Voorde, J., Lameire, N. H., & Vanhoutte, P. M. (2000). Endothelial dysfunction in diabetes. *Br J Pharmacol*, *130*(5), 963-974. https://doi.org/10.1038/sj.bjp.0703393

Delbosc, S., Haloui, M., Louedec, L., Dupuis, M., Cubizolles, M., Podust, V. N., Fung, E. T., Michel, J. B., & Meilhac, O. (2008). Proteomic analysis permits the identification of new biomarkers of arterial wall remodeling in hypertension. *Mol Med*, *14*(7-8), 383-394. https://doi.org/10.2119/2008-00030.Delbosc

Della Rocca, G., Costa, M. G., Coccia, C., Pompei, L., Salandin, V., Pierangelo, D. M., & Pietropaoli, P. (2009). Continuous right ventricular end-diastolic volume in comparison with left ventricular end-diastolic area. *Eur J Anaesthesiol*, *26*(4), 272-278. https://doi.org/10.1097/EJA.0b013e328319be8e

Deng, A. Y. (2007). Genetic basis of polygenic hypertension. *Hum Mol Genet*, *16 Spec No. 2*, R195-202. https://doi.org/10.1093/hmg/ddm126

Dhalla, N. S., Temsah, R. M., & Netticadan, T. (2000). Role of oxidative stress in cardiovascular diseases. *J Hypertens*, *18*(6), 655-673. https://doi.org/10.1097/00004872-200018060-00002

Di Castro, S., Scarpino, S., Marchitti, S., Bianchi, F., Stanzione, R., Cotugno, M., Sironi, L., Gelosa, P., Duranti, E., Ruco, L., Volpe, M., & Rubattu, S. (2013). Differential modulation of uncoupling protein 2 in kidneys of stroke-prone spontaneously hypertensive rats under high-salt/low-potassium diet. *Hypertension*, *61*(2), 534-541. https://doi.org/10.1161/HYPERTENSIONAHA.111.00101

Dickhout, J. G., & Lee, R. M. (1998). Blood pressure and heart rate development in young spontaneously hypertensive rats. *Am J Physiol*, *274*(3), H794-800. https://doi.org/10.1152/ajpheart.1998.274.3.H794

Dobrian, A. D., Schriver, S. D., Khraibi, A. A., & Prewitt, R. L. (2004). Pioglitazone prevents hypertension and reduces oxidative stress in diet-induced obesity. *Hypertension*, *43*(1), 48-56. https://doi.org/10.1161/01.HYP.0000103629.01745.59

Dohán, O., De la Vieja, A., Paroder, V., Riedel, C., Artani, M., Reed, M., Ginter, C. S., & Carrasco, N. (2003). The sodium/iodide Symporter (NIS): characterization,

regulation, and medical significance. *Endocr Rev*, *24*(1), 48-77. https://doi.org/10.1210/er.2001-0029

Dugrillon, A. (1996). Iodolactones and iodoaldehydes--mediators of iodine in thyroid autoregulation. *Exp Clin Endocrinol Diabetes*, *104 Suppl 4*, 41-45. https://doi.org/10.1055/s-0029-1211700

Dunn, J. T. (2002). Guarding our nation's thyroid health. *J Clin Endocrinol Metab*, *87*(2), 486-488. https://doi.org/10.1210/jcem.87.2.8346

Dunn, J. T., & Dunn, A. D. (1999). The importance of thyroglobulin structure for thyroid hormone biosynthesis. *Biochimie*, *81*(5), 505-509. https://doi.org/10.1016/s0300-9084(99)80102-3

Dunn, J. T., Semigran, M. J., & Delange, F. (1998). The prevention and management of iodine-induced hyperthyroidism and its cardiac features. *Thyroid*, *8*(1), 101-106. https://doi.org/10.1089/thy.1998.8.101

Dwinell, M. R., Worthey, E. A., Shimoyama, M., Bakir-Gungor, B., DePons, J., Laulederkind, S., Lowry, T., Nigram, R., Petri, V., Smith, J., Stoddard, A., Twigger, S. N., Jacob, H. J., & Team, R. (2009). The Rat Genome Database 2009: variation, ontologies and pathways. *Nucleic Acids Res*, *37*(Database issue), D744-749. https://doi.org/10.1093/nar/gkn842

Eghtedari, B., & Correa, R. (2020). Levothyroxine. In *StatPearls*. StatPearls Publishing

Ehret, G. B., & Caulfield, M. J. (2013). Genes for blood pressure: an opportunity to understand hypertension. *Eur Heart J*, *34*(13), 951-961. https://doi.org/10.1093/eurheartj/ehs455

Ehret, G. B., Munroe, P. B., Rice, K. M., Bochud, M., Johnson, A. D., Chasman, D. I., Smith, A. V., Tobin, M. D., Verwoert, G. C., Hwang, S. J., Pihur, V., Vollenweider, P., O'Reilly, P. F., Amin, N., Bragg-Gresham, J. L., Teumer, A., Glazer, N. L., Launer, L., Zhao, J. H., . . . consortium, C.-H. (2011). Genetic variants in novel pathways influence blood pressure and cardiovascular disease risk. *Nature*, *478*(7367), 103-109. https://doi.org/10.1038/nature10405

Elstner, E. F., Adamczyk, R., Kröner, R., & Furch, A. (1985). [The uptake of potassium iodide and its effect as an antioxidant in isolated rabbit eyes]. *Ophthalmologica*, *191*(2), 122-126. https://doi.org/10.1159/000309572

Emrich, S. J., Barbazuk, W. B., Li, L., & Schnable, P. S. (2007). Gene discovery and annotation using LCM-454 transcriptome sequencing. *Genome Res*, *17*(1), 69-73. https://doi.org/10.1101/gr.5145806

Endo, A., Surks, H. K., Mochizuki, S., Mochizuki, N., & Mendelsohn, M. E. (2004). Identification and characterization of zipper-interacting protein kinase as the unique vascular smooth muscle myosin phosphatase-associated kinase. *J Biol Chem*, *279*(40), 42055-42061. https://doi.org/10.1074/jbc.M403676200

England, J., & Loughna, S. (2013). Heavy and light roles: myosin in the morphogenesis of the heart. *Cell Mol Life Sci*, *70*(7), 1221-1239. https://doi.org/10.1007/s00018-012-1131-1

Farebrother, J., Zimmermann, M. B., & Andersson, M. (2019). Excess iodine intake: sources, assessment, and effects on thyroid function. *Ann N Y Acad Sci*, *1446*(1), 44-65. https://doi.org/10.1111/nyas.14041

Fazio, S., Palmieri, E. A., Lombardi, G., & Biondi, B. (2004). Effects of thyroid hormone on the cardiovascular system. *Recent Prog Horm Res*, *59*, 31-50. https://doi.org/10.1210/rp.59.1.31

Fekete, C., & Lechan, R. M. (2007). Negative feedback regulation of hypophysiotropic thyrotropin-releasing hormone (TRH) synthesizing neurons: role of neuronal afferents and type 2 deiodinase. *Front Neuroendocrinol*, *28*(2-3), 97-114. https://doi.org/10.1016/j.yfrne.2007.04.002

Fernández-Alfonso, M. S. (2004). Regulation of vascular tone: the fat connection. *Hypertension*, *44*(3), 255-256. https://doi.org/10.1161/01.HYP.0000140056.64321.f9

Fisher, N. D., Hurwitz, S., Ferri, C., Jeunemaitre, X., Hollenberg, N. K., & Williams, G. H. (1999). Altered adrenal sensitivity to angiotensin II in low-renin essential hypertension. *Hypertension*, *34*(3), 388-394. https://doi.org/10.1161/01.hyp.34.3.388

Fletcher, A., Read, M. L., Thornton, C. E. M., Larner, D. P., Poole, V. L., Brookes, K., Nieto, H. R., Alshahrani, M., Thompson, R. J., Lavery, G. G., Landa, I., Fagin, J. A., Campbell, M. J., Boelaert, K., Turnell, A. S., Smith, V. E., & McCabe, C. J. (2020). Targeting Novel Sodium Iodide Symporter Interactors ADP-Ribosylation Factor 4 and Valosin-Containing Protein Enhances Radioiodine Uptake. *Cancer Res*, *80*(1), 102-115. https://doi.org/10.1158/0008-5472.CAN-19-1957

Franco, D., Lamers, W. H., & Moorman, A. F. (1998). Patterns of expression in the developing myocardium: towards a morphologically integrated transcriptional model. *Cardiovasc Res*, *38*(1), 25-53. https://doi.org/10.1016/s0008-6363(97)00321-0

Franklyn, J. A., & Boelaert, K. (2012). Thyrotoxicosis. *Lancet*, *379*(9821), 1155-1166. https://doi.org/10.1016/S0140-6736(11)60782-4

Friedman, R. C., Farh, K. K., Burge, C. B., & Bartel, D. P. (2009). Most mammalian mRNAs are conserved targets of microRNAs. *Genome Res*, *19*(1), 92-105. https://doi.org/10.1101/gr.082701.108

Fu, M., Gao, Y., Guo, W., Meng, Q., Jin, Q., Yang, R., Yang, Y., Zhang, Y., & Zhang, W. (2022). Mechanisms of Sodium/Iodide Symporter-Mediated Mammary Gland Iodine Compensation during Lactation. *Nutrients*, *14*(17). https://doi.org/10.3390/nu14173592

Fukui, T., Ishizaka, N., Rajagopalan, S., Laursen, J. B., Capers, Q., Taylor, W. R., Harrison, D. G., de Leon, H., Wilcox, J. N., & Griendling, K. K. (1997). p22phox mRNA expression and NADPH oxidase activity are increased in aortas from hypertensive rats. *Circ Res*, *80*(1), 45-51. https://doi.org/10.1161/01.res.80.1.45

Fürst, D. O., Osborn, M., Nave, R., & Weber, K. (1988). The organization of titin filaments in the half-sarcomere revealed by monoclonal antibodies in immunoelectron microscopy: a map of ten nonrepetitive epitopes starting at the Z line extends close to the M line. *J Cell Biol*, *106*(5), 1563-1572. https://doi.org/10.1083/jcb.106.5.1563

Gelman, S. (2008). Venous function and central venous pressure: a physiologic story. *Anesthesiology*, *108*(4), 735-748. https://doi.org/10.1097/ALN.0b013e3181672607

Gérard, A. C., Poncin, S., Audinot, J. N., Denef, J. F., & Colin, I. M. (2009). Iodide deficiency-induced angiogenic stimulus in the thyroid occurs via HIF- and ROS-dependent VEGF-A secretion from thyrocytes. *Am J Physiol Endocrinol Metab*, *296*(6), E1414-1422. https://doi.org/10.1152/ajpendo.90876.2008

Gérard, A. C., Poncin, S., Caetano, B., Sonveaux, P., Audinot, J. N., Feron, O., Colin, I. M., & Soncin, F. (2008). Iodine deficiency induces a thyroid stimulating hormone-independent early phase of microvascular reshaping in the thyroid. *Am J Pathol*, *172*(3), 748-760. https://doi.org/10.2353/ajpath.2008.070841

Gersh, B. J., Sliwa, K., Mayosi, B. M., & Yusuf, S. (2010). Novel therapeutic concepts: the epidemic of cardiovascular disease in the developing world: global implications. *Eur Heart J*, *31*(6), 642-648. https://doi.org/10.1093/eurheartj/ehq030

Gonzaga-Jauregui, C., Lupski, J. R., & Gibbs, R. A. (2012). Human genome sequencing in health and disease. *Annu Rev Med*, *63*, 35-61. https://doi.org/10.1146/annurev-med-051010-162644

Gonzalez, J. M., & Suki, W. N. (1995). Cell calcium and arterial blood pressure. *Semin Nephrol*, *15*(6), 564-568. https://www.ncbi.nlm.nih.gov/pubmed/8588116

Gopolan, C., & Kirk, E. (2022). Blood pressure, hypertension and excercise. In *Biology of Cardiovascular and Metabolic Diseases*. Academic Press. https://doi.org/https://doi.org/10.1016/C2019-0-04900-X

Gordan, R., Gwathmey, J. K., & Xie, L. H. (2015). Autonomic and endocrine control of cardiovascular function. *World J Cardiol*, *7*(4), 204-214. https://doi.org/10.4330/wjc.v7.i4.204

Goulopoulou, S., & Webb, R. C. (2014). Symphony of vascular contraction: how smooth muscle cells lose harmony to signal increased vascular resistance in

hypertension. *Hypertension*, *63*(3), e33-39. https://doi.org/10.1161/HYPERTENSIONAHA.113.02444

Graham, D. (2019). Vascular Physiology. In R. Touyz & C. Delles (Eds.), *Textbook of Vascular Medicine.* Springer, Cham. https://doi.org/https://doi.org/10.1007/978-3-030-16481-2_2

Graham, D., Hamilton, C., Beattie, E., Spiers, A., & Dominiczak, A. F. (2004). Comparison of the effects of omapatrilat and irbesartan/hydrochlorothiazide on endothelial function and cardiac hypertrophy in the stroke-prone spontaneously hypertensive rat: sex differences. *J Hypertens*, *22*(2), 329-337. https://doi.org/10.1097/00004872-200402000-00017

Grann, M., Comerma-Steffensen, S., Arcanjo, D. D., & Simonsen, U. (2016). Mechanisms Involved in Thromboxane A. *Basic Clin Pharmacol Toxicol*, *119 Suppl 3*, 86-95. https://doi.org/10.1111/bcpt.12544

Greaser, M. L., & Gergely, J. (1973). Purification and properties of the components from troponin. *J Biol Chem*, *248*(6), 2125-2133. https://www.ncbi.nlm.nih.gov/pubmed/4266138

Guyton, A. C. (1991). Blood pressure control--special role of the kidneys and body fluids. *Science*, *252*(5014), 1813-1816. https://doi.org/10.1126/science.2063193

Guzik, T. J., Skiba, D. S., Touyz, R. M., & Harrison, D. G. (2017). The role of infiltrating immune cells in dysfunctional adipose tissue. *Cardiovasc Res*, *113*(9), 1009-1023. https://doi.org/10.1093/cvr/cvx108

Ha, S. K. (2014). Dietary salt intake and hypertension. *Electrolyte Blood Press*, *12*(1), 7-18. https://doi.org/10.5049/EBP.2014.12.1.7

Haeberle, J. R., Hathaway, D. R., & DePaoli-Roach, A. A. (1985). Dephosphorylation of myosin by the catalytic subunit of a type-2 phosphatase produces relaxation of chemically skinned uterine smooth muscle. *J Biol Chem*, *260*(18), 9965-9968. https://www.ncbi.nlm.nih.gov/pubmed/2991287

Hai, C. M., & Murphy, R. A. (1989). Ca2+, crossbridge phosphorylation, and contraction. *Annu Rev Physiol*, *51*,

285-298. https://doi.org/10.1146/annurev.ph.51.030189.001441

Han, H., Xin, P., Zhao, L., Xu, J., Xia, Y., Yang, X., Sun, X., & Hao, L. (2012). Excess iodine and high-fat diet combination modulates lipid profile, thyroid hormone, and hepatic LDLr expression values in mice. *Biol Trace Elem Res*, *147*(1-3), 233-239. https://doi.org/10.1007/s12011-011-9300-x

Han, L., Vickers, K. C., Samuels, D. C., & Guo, Y. (2015). Alternative applications for distinct RNA sequencing strategies. *Brief Bioinform*, *16*(4), 629-639. https://doi.org/10.1093/bib/bbu032

Harvey, A. P., Montezano, A. C., Hood, K. Y., Lopes, R. A., Rios, F., Ceravolo, G., Graham, D., & Touyz, R. M. (2017). Vascular dysfunction and fibrosis in stroke-prone spontaneously hypertensive rats: The aldosterone-mineralocorticoid receptor-Nox1 axis. *Life Sci*, *179*, 110-119. https://doi.org/10.1016/j.lfs.2017.05.002

Hellsten, Y., Nyberg, M., Jensen, L. G., & Mortensen, S. P. (2012). Vasodilator interactions in skeletal muscle blood flow regulation. *J Physiol*, *590*(24), 6297-6305. https://doi.org/10.1113/jphysiol.2012.240762

Hernández-Cassis, C., Cure-Cure, C., & López-Jaramillo, P. (1995). Effect of thyroid replacement therapy on the stature of Colombian children with minimal thyroid dysfunction. *Eur J Clin Invest*, *25*(6), 454-456. https://doi.org/10.1111/j.1365-2362.1995.tb01729.x

Hetzel, B. S. (2002). Eliminating iodine deficiency disorders--the role of the International Council in the global partnership. *Bull World Health Organ*, *80*(5), 410-413; discussion 413-417. https://www.ncbi.nlm.nih.gov/pubmed/12077619

Hetzel, B. S. (2005). Towards the global elimination of brain damage due to iodine deficiency--the role of the International Council for Control of Iodine Deficiency Disorders. *Int J Epidemiol*, *34*(4), 762-764. https://doi.org/10.1093/ije/dyi073

Hiroi, Y., Kim, H. H., Ying, H., Furuya, F., Huang, Z., Simoncini, T., Noma, K., Ueki, K., Nguyen, N. H., Scanlan, T. S., Moskowitz, M. A., Cheng, S. Y., & Liao,

J. K. (2006). Rapid nongenomic actions of thyroid hormone. *Proc Natl Acad Sci U S A*, *103*(38), 14104-14109. https://doi.org/10.1073/pnas.0601600103

Hitzenberger, G. (1961). [Comparative studies on the effects of the Bad Hall iodine cure in hypertensives]. *Arch Phys Ther (Leipz)*, *13*, 91-94. https://www.ncbi.nlm.nih.gov/pubmed/13714683

Hoffmann, T. J., Ehret, G. B., Nandakumar, P., Ranatunga, D., Schaefer, C., Kwok, P. Y., Iribarren, C., Chakravarti, A., & Risch, N. (2017). Genome-wide association analyses using electronic health records identify new loci influencing blood pressure variation. *Nat Genet*, *49*(1), 54-64. https://doi.org/10.1038/ng.3715

Hoption Cann, S. A. (2006). Hypothesis: dietary iodine intake in the etiology of cardiovascular disease. *J Am Coll Nutr*, *25*(1), 1-11. https://doi.org/10.1080/07315724.2006.10719508

Hurst, C., Soto, M., Vina, E. R., & Rodgers, K. E. (2023). Renin-Angiotensin System-Modifying Antihypertensive Drugs Can Reduce the Risk of Cardiovascular Complications in Lupus: A Retrospective Cohort Study. *Am J Med*, *136*(3), 284-293.e284. https://doi.org/10.1016/j.amjmed.2022.11.016

Iannaccone, M., Elgendy, R., Ianni, A., Martino, C., Palazzo, F., Giantin, M., Grotta, L., Dacasto, M., & Martino, G. (2020). Whole-transcriptome profiling of sheep fed with a high iodine-supplemented diet. *Animal*, *14*(4), 745-752. https://doi.org/10.1017/S1751731119002477

Iannaccone, M., Ianni, A., Elgendy, R., Martino, C., Giantin, M., Cerretani, L., Dacasto, M., & Martino, G. (2019). Iodine Supplemented Diet Positively Affect Immune Response and Dairy Product Quality in Fresian Cow. *Animals (Basel)*, *9*(11). https://doi.org/10.3390/ani9110866

Ikawa, T., Watanabe, Y., Okuzaki, D., Goto, N., Okamura, N., Yamanishi, K., Higashino, T., Yamanishi, H., Okamura, H., & Higashino, H. (2019). A new approach to identifying hypertension-associated genes in the mesenteric artery of spontaneously hypertensive rats and stroke-prone spontaneously hypertensive rats. *J*

Hypertens, *37*(8), 1644-1656. https://doi.org/10.1097/HJH.0000000000002083

Intengan, H. D., & Schiffrin, E. L. (2000). Structure and mechanical properties of resistance arteries in hypertension: role of adhesion molecules and extracellular matrix determinants. *Hypertension*, *36*(3), 312-318. https://doi.org/10.1161/01.hyp.36.3.312

Ishikawa, N., Harada, Y., Maruyama, R., Masuda, J., & Nabika, T. (2008). Genetic effects of blood pressure quantitative trait loci on hypertension-related organ damage: evaluation using multiple congenic strains. *Hypertens Res*, *31*(9), 1773-1779. https://doi.org/10.1291/hypres.31.1773

Iwata, A., Morrison, M. L., & Roth, M. B. (2014). Iodide protects heart tissue from reperfusion injury. *PLoS One*, *9*(11), e112458. https://doi.org/10.1371/journal.pone.0112458

Jabbar, A., Pingitore, A., Pearce, S. H., Zaman, A., Iervasi, G., & Razvi, S. (2017). Thyroid hormones and cardiovascular disease. *Nat Rev Cardiol*, *14*(1), 39-55. https://doi.org/10.1038/nrcardio.2016.174

Jayedi, A., Rashidy-Pour, A., Parohan, M., Zargar, M. S., & Shab-Bidar, S. (2019). Dietary and circulating vitamin C, vitamin E, β-carotene and risk of total cardiovascular mortality: a systematic review and dose-response meta-analysis of prospective observational studies. *Public Health Nutr*, *22*(10), 1872-1887. https://doi.org/10.1017/S1368980018003725

Jeffs, B., Clark, J. S., Anderson, N. H., Gratton, J., Brosnan, M. J., Gauguier, D., Reid, J. L., Macrae, I. M., & Dominiczak, A. F. (1997). Sensitivity to cerebral ischaemic insult in a rat model of stroke is determined by a single genetic locus. *Nat Genet*, *16*(4), 364-367. https://doi.org/10.1038/ng0897-364

Jeffs, B., Negrin, C. D., Graham, D., Clark, J. S., Anderson, N. H., Gauguier, D., & Dominiczak, A. F. (2000). Applicability of a "speed" congenic strategy to dissect blood pressure quantitative trait loci on rat chromosome 2. *Hypertension*, *35*(1 Pt 2), 179-187. https://doi.org/10.1161/01.hyp.35.1.179

Jin, L., Lin, X., Yang, L., Fan, X., Wang, W., Li, S., Li, J., Liu, X., Bao, M., Cui, X., Yang, J., Cui, Q., Geng, B., & Cai, J. (2018). AK098656, a Novel Vascular Smooth Muscle Cell-Dominant Long Noncoding RNA, Promotes Hypertension. *Hypertension*, *71*(2), 262-272. https://doi.org/10.1161/HYPERTENSIONAHA.117.09651

Jin, M., Zhang, Z., Li, Y., Teng, D., Shi, X., Ba, J., Chen, B., Du, J., He, L., Lai, X., Teng, X., Chi, H., Liao, E., Liu, C., Liu, L., Qin, G., Qin, Y., Quan, H., Shi, B., . . . Shan, Z. (2020). U-Shaped Associations Between Urinary Iodine Concentration and the Prevalence of Metabolic Disorders: A Cross-Sectional Study. *Thyroid*, *30*(7), 1053-1065. https://doi.org/10.1089/thy.2019.0516

Joanta, A. E., Filip, A., Clichici, S., Andrei, S., & Daicoviciu, D. (2006). Iodide excess exerts oxidative stress in some target tissues of the thyroid hormones. *Acta Physiol Hung*, *93*(4), 347-359. https://doi.org/10.1556/APhysiol.93.2006.4.11

Johnson, A., & Ahrens, T. (2015). Stroke volume optimization: the new hemodynamic algorithm. *Crit Care Nurse*, *35*(1), 11-27. https://doi.org/10.4037/ccn2015427

Kahaly, G. J. (2000). Cardiovascular and atherogenic aspects of subclinical hypothyroidism. *Thyroid*, *10*(8), 665-679. https://doi.org/10.1089/105072500050137743

Kang, K. T. (2014). Endothelium-derived Relaxing Factors of Small Resistance Arteries in Hypertension. *Toxicol Res*, *30*(3), 141-148. https://doi.org/10.5487/TR.2014.30.3.141

Kapil, U. (2007). Health consequences of iodine deficiency. *Sultan Qaboos Univ Med J*, *7*(3), 267-272. https://www.ncbi.nlm.nih.gov/pubmed/21748117

Karki, R., Kim, S. B., & Kim, D. W. (2013). Magnolol inhibits migration of vascular smooth muscle cells via cytoskeletal remodeling pathway to attenuate neointima formation. *Exp Cell Res*, *319*(20), 3238-3250. https://doi.org/10.1016/j.yexcr.2013.07.016

Kearney, P. M., Whelton, M., Reynolds, K., Muntner, P., Whelton, P. K., & He, J. (2005). Global burden of hypertension: analysis of worldwide data. *Lancet*,

365(9455), 217-223. https://doi.org/10.1016/S0140-6736(05)17741-1

Khodadadian, A., Darzi, S., Haghi-Daredeh, S., Sadat Eshaghi, F., Babakhanzadeh, E., Mirabutalebi, S. H., & Nazari, M. (2020). Genomics and Transcriptomics: The Powerful Technologies in Precision Medicine. *Int J Gen Med*, *13*, 627-640. https://doi.org/10.2147/IJGM.S249970

Kim, H. R., Appel, S., Vetterkind, S., Gangopadhyay, S. S., & Morgan, K. G. (2008). Smooth muscle signalling pathways in health and disease. *J Cell Mol Med*, *12*(6A), 2165-2180. https://doi.org/10.1111/j.1582-4934.2008.00552.x

KIRK, E., CHIEFFI, M., & KOUNTZ, W. B. (1949). The correlation between thyroid function and the incidence of arteriosclerosis. *J Gerontol*, *4*(3), 212-217. https://doi.org/10.1093/geronj/4.3.212

Klein, I. (1988). Thyroxine-induced cardiac hypertrophy: time course of development and inhibition by propranolol. *Endocrinology*, *123*(1), 203-210. https://doi.org/10.1210/endo-123-1-203

Klein, I. (1990). Thyroid hormone and the cardiovascular system. *Am J Med*, *88*(6), 631-637. https://doi.org/10.1016/0002-9343(90)90531-h

Klein, I., & Ojamaa, K. (2001a). Thyroid hormone-targeting the heart. *Endocrinology*, *142*(1), 11-12. https://doi.org/10.1210/endo.142.1.7986

Klein, I., & Ojamaa, K. (2001b). Thyroid hormone and the cardiovascular system. *N Engl J Med*, *344*(7), 501-509. https://doi.org/10.1056/NEJM200102153440707

Klieber, M., Czerwenka-Howorka, K., Homan, R., & Pirker, R. (1982). [Ergospirometric studies of circulation in healthy humans. Effect of iodine brine baths on work-induced changes in blood pressure, respiratory gas exchange and metabolic parameters]. *Med Welt*, *33*(33), 1123-1126. https://www.ncbi.nlm.nih.gov/pubmed/7132660

Kogai, T., & Brent, G. A. (2012). The sodium iodide symporter (NIS): regulation and approaches to targeting for cancer therapeutics. *Pharmacol Ther*, *135*(3), 355-370. https://doi.org/10.1016/j.pharmthera.2012.06.007

Kogai, T., Endo, T., Saito, T., Miyazaki, A., Kawaguchi, A., & Onaya, T. (1997). Regulation by thyroid-stimulating hormone of sodium/iodide symporter gene expression and protein levels in FRTL-5 cells. *Endocrinology*, *138*(6), 2227-2232. https://doi.org/10.1210/endo.138.6.5189

Kogai, T., Taki, K., & Brent, G. A. (2006). Enhancement of sodium/iodide symporter expression in thyroid and breast cancer. *Endocr Relat Cancer*, *13*(3), 797-826. https://doi.org/10.1677/erc.1.01143

Kolodney, M. S., Thimgan, M. S., Honda, H. M., Tsai, G., & Yee, H. F. (1999). Ca2+-independent myosin II phosphorylation and contraction in chicken embryo fibroblasts. *J Physiol*, *515 (Pt 1)*(Pt 1), 87-92. https://doi.org/10.1111/j.1469-7793.1999.087ad.x

Komers, R., Oyama, T. T., Beard, D. R., & Anderson, S. (2011). Effects of systemic inhibition of Rho kinase on blood pressure and renal haemodynamics in diabetic rats. *Br J Pharmacol*, *162*(1), 163-174. https://doi.org/10.1111/j.1476-5381.2010.01031.x

König, F., Andersson, M., Hotz, K., Aeberli, I., & Zimmermann, M. B. (2011). Ten repeat collections for urinary iodine from spot samples or 24-hour samples are needed to reliably estimate individual iodine status in women. *J Nutr*, *141*(11), 2049-2054. https://doi.org/10.3945/jn.111.144071

Krajcovicová-Kudlácková, M., Bucková, K., Klimes, I., & Seboková, E. (2003). Iodine deficiency in vegetarians and vegans. *Ann Nutr Metab*, *47*(5), 183-185. https://doi.org/10.1159/000070483

Krämer, A., Green, J., Pollard, J., & Tugendreich, S. (2014). Causal analysis approaches in Ingenuity Pathway Analysis. *Bioinformatics*, *30*(4), 523-530. https://doi.org/10.1093/bioinformatics/btt703

Krupp, P. P., Thomas, L. L., Alpert, N. R., & Frink, R. (1977). The thyroid in the spontaneously hypertensive rat: a light and electron microscopic study. *Am J Anat*, *148*(4), 513-525. https://doi.org/10.1002/aja.1001480407

Kukurba, K. R., & Montgomery, S. B. (2015). RNA Sequencing and Analysis. *Cold Spring Harb Protoc*,

2015(11), 951-969. https://doi.org/10.1101/pdb.top084970

Kuo, I. Y., & Ehrlich, B. E. (2015). Signaling in muscle contraction. *Cold Spring Harb Perspect Biol*, *7*(2), a006023. https://doi.org/10.1101/cshperspect.a006023

Küpper, F. C., Carpenter, L. J., McFiggans, G. B., Palmer, C. J., Waite, T. J., Boneberg, E. M., Woitsch, S., Weiller, M., Abela, R., Grolimund, D., Potin, P., Butler, A., Luther, G. W., Kroneck, P. M., Meyer-Klaucke, W., & Feiters, M. C. (2008). Iodide accumulation provides kelp with an inorganic antioxidant impacting atmospheric chemistry. *Proc Natl Acad Sci U S A*, *105*(19), 6954-6958. https://doi.org/10.1073/pnas.0709959105

Kutikhin, A. G., Sinitsky, M. Y., Yuzhalin, A. E., & Velikanova, E. A. (2018). Whole-Transcriptome Sequencing: a Powerful Tool for Vascular Tissue Engineering and Endothelial Mechanobiology. *High Throughput*, *7*(1). https://doi.org/10.3390/ht7010005

Lakatta, E. G., & Levy, D. (2003). Arterial and cardiac aging: major shareholders in cardiovascular disease enterprises: Part I: aging arteries: a "set up" for vascular disease. *Circulation*, *107*(1), 139-146. https://doi.org/10.1161/01.cir.0000048892.83521.58

Larsen, W. J. (1993). *Human Embryology* (E. Bowman-Schulman, Ed.). Churchill Livingstone Inc.

Lazarus, J. H. (2015). The importance of iodine in public health. *Environ Geochem Health*, *37*(4), 605-618. https://doi.org/10.1007/s10653-015-9681-4

Lazarus, J. H., & Smyth, P. P. (2008). Iodine deficiency in the UK and Ireland. *Lancet*, *372*(9642), 888. https://doi.org/10.1016/S0140-6736(08)61390-2

Leduc, C., Sobilo, L., Toumi, H., Mondon, P., Lespessailles, E., Ossant, F., Kurfurst, R., & Pichon, C. (2016). TGF-beta-induced early gene-1 overexpression promotes oxidative stress protection and actin cytoskeleton rearrangement in human skin fibroblasts. *Biochim Biophys Acta*, *1860*(6), 1071-1078. https://doi.org/10.1016/j.bbagen.2016.02.009

Lee, K. W., Shin, D., & Song, W. O. (2016). Low Urinary Iodine Concentrations Associated with Dyslipidemia in

US Adults. *Nutrients*, *8*(3), 171. https://doi.org/10.3390/nu8030171

Leoni, S. G., Galante, P. A., Ricarte-Filho, J. C., & Kimura, E. T. (2008). Differential gene expression analysis of iodide-treated rat thyroid follicular cell line PCCl3. *Genomics*, *91*(4), 356-366. https://doi.org/10.1016/j.ygeno.2007.12.009

Lervasi, G., & Fommei, E. (2009). Hypertension and hypothyroidism: A thyroid dysfunction frequently associated with abnormal dietary intake. In *Comprehensive handbook of iodine* (pp. 1057-1071).

Levick, J. (2009). Overview of the cardiovascular system. In *An Introduction to Cardiovascular Physiology* (pp. 1-12). Hodder Arnold.

Levy, O., Dai, G., Riedel, C., Ginter, C. S., Paul, E. M., Lebowitz, A. N., & Carrasco, N. (1997). Characterization of the thyroid Na+/I- symporter with an anti-COOH terminus antibody. *Proc Natl Acad Sci U S A*, *94*(11), 5568-5573. https://doi.org/10.1073/pnas.94.11.5568

Li, H. S., & Carayanniotis, G. (2007). Induction of goitrous hypothyroidism by dietary iodide in SJL mice. *Endocrinology*, *148*(6), 2747-2752. https://doi.org/10.1210/en.2007-0082

Li, M. X., & Hwang, P. M. (2015). Structure and function of cardiac troponin C (TNNC1): Implications for heart failure, cardiomyopathies, and troponin modulating drugs. *Gene*, *571*(2), 153-166. https://doi.org/10.1016/j.gene.2015.07.074

Lim, S. S., Vos, T., Flaxman, A. D., Danaei, G., Shibuya, K., Adair-Rohani, H., Amann, M., Anderson, H. R., Andrews, K. G., Aryee, M., Atkinson, C., Bacchus, L. J., Bahalim, A. N., Balakrishnan, K., Balmes, J., Barker-Collo, S., Baxter, A., Bell, M. L., Blore, J. D., . . . Memish, Z. A. (2012). A comparative risk assessment of burden of disease and injury attributable to 67 risk factors and risk factor clusters in 21 regions, 1990-2010: a systematic analysis for the Global Burden of Disease Study 2010. *Lancet*, *380*(9859), 2224-2260. https://doi.org/10.1016/S0140-6736(12)61766-8

Limbruno, U., & De Caterina, R. (2003). Vasomotor effects of iodinated contrast media: just side effects? *Curr Vasc Pharmacol*, *1*(3), 321-328. https://doi.org/10.2174/1570161033476664

Lin, H. Y., Lee, Y. T., Chan, Y. W., & Tse, G. (2016). Animal models for the study of primary and secondary hypertension in humans. *Biomed Rep*, *5*(6), 653-659. https://doi.org/10.3892/br.2016.784

Lister, R., O'Malley, R. C., Tonti-Filippini, J., Gregory, B. D., Berry, C. C., Millar, A. H., & Ecker, J. R. (2008). Highly integrated single-base resolution maps of the epigenome in Arabidopsis. *Cell*, *133*(3), 523-536. https://doi.org/10.1016/j.cell.2008.03.029

Liu, J., Liu, L., Jia, Q., Zhang, X., Jin, X., & Shen, H. (2019). Effects of Excessive Iodine Intake on Blood Glucose, Blood Pressure, and Blood Lipids in Adults. *Biol Trace Elem Res*, *192*(2), 136-144. https://doi.org/10.1007/s12011-019-01668-9

Liu, N., & Olson, E. N. (2010). MicroRNA regulatory networks in cardiovascular development. *Dev Cell*, *18*(4), 510-525. https://doi.org/10.1016/j.devcel.2010.03.010

Llévenes, P., Balfagón, G., & Blanco-Rivero, J. (2018). Thyroid hormones affect nitrergic innervation function in rat mesenteric artery: Role of the PI3K/AKT pathway. *Vascul Pharmacol*, *108*, 36-45. https://doi.org/10.1016/j.vph.2018.05.001

Lockhart, D. J., Dong, H., Byrne, M. C., Follettie, M. T., Gallo, M. V., Chee, M. S., Mittmann, M., Wang, C., Kobayashi, M., Horton, H., & Brown, E. L. (1996). Expression monitoring by hybridization to high-density oligonucleotide arrays. *Nat Biotechnol*, *14*(13), 1675-1680. https://doi.org/10.1038/nbt1296-1675

Loirand, G., & Pacaud, P. (2010). The role of Rho protein signaling in hypertension. *Nat Rev Cardiol*, *7*(11), 637-647. https://doi.org/10.1038/nrcardio.2010.136

Love, M. I., Huber, W., & Anders, S. (2014). Moderated estimation of fold change and dispersion for RNA-seq data with DESeq2. *Genome Biol*, *15*(12), 550. https://doi.org/10.1186/s13059-014-0550-8

Lowe, R., Shirley, N., Bleackley, M., Dolan, S., & Shafee, T. (2017). Transcriptomics technologies. *PLoS Comput Biol*, *13*(5), e1005457. https://doi.org/10.1371/journal.pcbi.1005457

Lowenthal, D. T., Saris, S. D., Haratz, A., Packer, J., Porter, R. S., & Conry, K. (1984). The clinical pharmacology of antihypertensive drugs. *J Hypertens Suppl*, *2*(2), S13-24. https://www.ncbi.nlm.nih.gov/pubmed/6152830

Lozano, R., Naghavi, M., Foreman, K., Lim, S., Shibuya, K., Aboyans, V., Abraham, J., Adair, T., Aggarwal, R., Ahn, S. Y., Alvarado, M., Anderson, H. R., Anderson, L. M., Andrews, K. G., Atkinson, C., Baddour, L. M., Barker-Collo, S., Bartels, D. H., Bell, M. L., . . . Memish, Z. A. (2012). Global and regional mortality from 235 causes of death for 20 age groups in 1990 and 2010: a systematic analysis for the Global Burden of Disease Study 2010. *Lancet*, *380*(9859), 2095-2128. https://doi.org/10.1016/S0140-6736(12)61728-0

Lüscher, T. F., & Vanhoutte, P. M. (1986). Endothelium-dependent contractions to acetylcholine in the aorta of the spontaneously hypertensive rat. *Hypertension*, *8*(4), 344-348. https://doi.org/10.1161/01.hyp.8.4.344

Lyons, G. E., Schiaffino, S., Sassoon, D., Barton, P., & Buckingham, M. (1990). Developmental regulation of myosin gene expression in mouse cardiac muscle. *J Cell Biol*, *111*(6 Pt 1), 2427-2436. https://doi.org/10.1083/jcb.111.6.2427

Ma, J., Li, Y., Yang, X., Liu, K., Zhang, X., Zuo, X., Ye, R., Wang, Z., Shi, R., Meng, Q., & Chen, X. (2023). Signaling pathways in vascular function and hypertension: molecular mechanisms and therapeutic interventions. *Signal Transduct Target Ther*, *8*(1), 168. https://doi.org/10.1038/s41392-023-01430-7

Ma, Z. F., & Skeaff, S. A. (2014). Thyroglobulin as a biomarker of iodine deficiency: a review. *Thyroid*, *24*(8), 1195-1209. https://doi.org/10.1089/thy.2014.0052

Maehre, H. K., Malde, M. K., Eilertsen, K. E., & Elvevoll, E. O. (2014). Characterization of protein, lipid and mineral contents in common Norwegian seaweeds and evaluation of their potential as food and feed. *J Sci Food*

Agric, *94*(15), 3281-3290. https://doi.org/10.1002/jsfa.6681

Maldonado-Araque, C., Valdés, S., Badía-Guillén, R., Lago-Sampedro, A., Colomo, N., Garcia-Fuentes, E., Gutierrez-Repiso, C., Goday, A., Calle-Pascual, A., Castaño, L., Castell, C., Delgado, E., Menendez, E., Franch-Nadal, J., Gaztambide, S., Girbés, J., Chaves, F. J., Soriguer, F., & Rojo-Martínez, G. (2021). Iodine Deficiency and Mortality in Spanish Adults: Di@bet.es Study. *Thyroid*, *31*(1), 106-114. https://doi.org/10.1089/thy.2020.0131

Manolio, T. A., Collins, F. S., Cox, N. J., Goldstein, D. B., Hindorff, L. A., Hunter, D. J., McCarthy, M. I., Ramos, E. M., Cardon, L. R., Chakravarti, A., Cho, J. H., Guttmacher, A. E., Kong, A., Kruglyak, L., Mardis, E., Rotimi, C. N., Slatkin, M., Valle, D., Whittemore, A. S., . . . Visscher, P. M. (2009). Finding the missing heritability of complex diseases. *Nature*, *461*(7265), 747-753. https://doi.org/10.1038/nature08494

Manosroi, W., & Williams, G. H. (2019). Genetics of Human Primary Hypertension: Focus on Hormonal Mechanisms. *Endocr Rev*, *40*(3), 825-856. https://doi.org/10.1210/er.2018-00071

Marković, L., Mihailović-Vucinić, V., & Aritonović, J. (2010). Hormones of thyroid gland in sera of rats treated with different dose of concentrated potassium iodine solutions. *Srp Arh Celok Lek*, *138*(5-6), 323-327. https://doi.org/10.2298/sarh1006323m

Martín-Calvo, N., & Martínez-González, M. (2017). Vitamin C Intake is Inversely Associated with Cardiovascular Mortality in a Cohort of Spanish Graduates: the SUN Project. *Nutrients*, *9*(9). https://doi.org/10.3390/nu9090954

Martinez-Lemus, L. A., Hill, M. A., & Meininger, G. A. (2009). The plastic nature of the vascular wall: a continuum of remodeling events contributing to control of arteriolar diameter and structure. *Physiology (Bethesda)*, *24*, 45-57. https://doi.org/10.1152/physiol.00029.2008

Matsuda, A., & Kosugi, S. (1997). A homozygous missense mutation of the sodium/iodide symporter gene causing

iodide transport defect. *J Clin Endocrinol Metab*, *82*(12), 3966-3971. https://doi.org/10.1210/jcem.82.12.4425

Matsuda, K., Lozinskaya, I., & Cox, R. H. (1997). Augmented contributions of voltage-gated Ca2+ channels to contractile responses in spontaneously hypertensive rat mesenteric arteries. *Am J Hypertens*, *10*(11), 1231-1239. https://doi.org/10.1016/s0895-7061(97)00225-2

McAllister, R. M., Grossenburg, V. D., Delp, M. D., & Laughlin, M. H. (1998). Effects of hyperthyroidism on vascular contractile and relaxation responses. *Am J Physiol*, *274*(5), E946-953. https://doi.org/10.1152/ajpendo.1998.274.5.E946

McAllister, R. M., Luther, K. L., & Pfeifer, P. C. (2000). Thyroid status and response to endothelin-1 in rat arterial vessels. *Am J Physiol Endocrinol Metab*, *279*(2), E252-258. https://doi.org/10.1152/ajpendo.2000.279.2.E252

McBride, M. W., Brosnan, M. J., Mathers, J., McLellan, L. I., Miller, W. H., Graham, D., Hanlon, N., Hamilton, C. A., Polke, J. M., Lee, W. K., & Dominiczak, A. F. (2005). Reduction of Gstm1 expression in the stroke-prone spontaneously hypertension rat contributes to increased oxidative stress. *Hypertension*, *45*(4), 786-792. https://doi.org/10.1161/01.HYP.0000154879.49245.39

McIntyre, M., Bohr, D. F., & Dominiczak, A. F. (1999). Endothelial function in hypertension: the role of superoxide anion. *Hypertension*, *34*(4 Pt 1), 539-545. https://doi.org/10.1161/01.hyp.34.4.539

McKenzie, C., MacDonald, A., & Shaw, A. M. (2009). Mechanisms of U46619-induced contraction of rat pulmonary arteries in the presence and absence of the endothelium. *Br J Pharmacol*, *157*(4), 581-596. https://doi.org/10.1111/j.1476-5381.2008.00084.x

Menon, V. U., Chellan, G., Sundaram, K. R., Murthy, S., Kumar, H., Unnikrishnan, A. G., & Jayakumar, R. V. (2011). Iodine status and its correlations with age, blood pressure, and thyroid volume in South Indian women above 35 years of age (Amrita Thyroid Survey). *Indian J Endocrinol Metab*, *15*(4), 309-315. https://doi.org/10.4103/2230-8210.85584

Milanesi., A., & Brent., G. A. (2016). Iodine and thyroid hormone synthesis, metabolism and action. In J. F. Collins (Ed.), *Molecular, Genetic, and Nutritional Aspects of Major and Trace Minerals* (pp. 143-150). Academic press. https://doi.org/https://doi.org/10.1016/C2014-0-02224-1

Min, H., Dong, J., Wang, Y., Yu, Y., Shan, Z., Xi, Q., Teng, W., & Chen, J. (2017). Marginal Iodine Deficiency Affects Dendritic Spine Development by Disturbing the Function of Rac1 Signaling Pathway on Cytoskeleton. *Mol Neurobiol*, *54*(1), 437-449. https://doi.org/10.1007/s12035-015-9657-5

Mirmiran, P., Hosseini-Esfahani, F., Esfandiar, Z., Hosseinpour-Niazi, S., & Azizi, F. (2022). Associations between dietary antioxidant intakes and cardiovascular disease. *Sci Rep*, *12*(1), 1504. https://doi.org/10.1038/s41598-022-05632-x

Misárková, E., Behuliak, M., Bencze, M., & Zicha, J. (2016). Excitation-contraction coupling and excitation-transcription coupling in blood vessels: their possible interactions in hypertensive vascular remodeling. *Physiol Res*, *65*(2), 173-191. https://doi.org/10.33549/physiolres.933317

Mitchell, J. E., Hellkamp, A. S., Mark, D. B., Anderson, J., Johnson, G. W., Poole, J. E., Lee, K. L., & Bardy, G. H. (2013). Thyroid function in heart failure and impact on mortality. *JACC Heart Fail*, *1*(1), 48-55. https://doi.org/10.1016/j.jchf.2012.10.004

Molnár, I., Magyari, M., & Stief, L. (1998). [Iodine deficiency in cardiovascular diseases]. *Orv Hetil*, *139*(35), 2071-2073. https://www.ncbi.nlm.nih.gov/pubmed/9755626

Moran, C. M., Garriock, R. J., Miller, M. K., Heimark, R. L., Gregorio, C. C., & Krieg, P. A. (2008). Expression of the fast twitch troponin complex, fTnT, fTnI and fTnC, in vascular smooth muscle. *Cell Motil Cytoskeleton*, *65*(8), 652-661. https://doi.org/10.1002/cm.20291

Morcos, S. K., Dawson, P., Pearson, J. D., Jeremy, J. Y., Davenport, A. P., Yates, M. S., Tirone, P., Cipolla, P., de Haën, C., Muschick, P., Krause, W., Refsum, H., Emery, C. J., Liss, P., Nygren, A., Haylor, J., Pugh, N. D., &

Karlsson, J. O. (1998). The haemodynamic effects of iodinated water soluble radiographic contrast media: a review. *Eur J Radiol*, *29*(1), 31-46. https://doi.org/10.1016/s0720-048x(98)00018-7

Morita, T., & Hayashi, K. (2023). Actin-related protein 5 suppresses the cooperative activation of cardiac gene transcription by myocardin and MEF2. *FEBS Open Bio*, *13*(2), 363-379. https://doi.org/10.1002/2211-5463.13549

Morrison, M. L., Iwata, A., Keyes, C. C., Langston, W., Insko, M. A., Langdale, L. A., & Roth, M. B. (2018). Iodide Improves Outcome After Acute Myocardial Infarction in Rats and Pigs. *Crit Care Med*, *46*(11), e1063-e1069. https://doi.org/10.1097/CCM.0000000000003353

Mulvany, M. J., & Halpern, W. (1977). Contractile properties of small arterial resistance vessels in spontaneously hypertensive and normotensive rats. *Circ Res*, *41*(1), 19-26. https://doi.org/10.1161/01.res.41.1.19

Mulvany, M. J., Hansen, O. K., & Aalkjaer, C. (1978). Direct evidence that the greater contractility of resistance vessels in spontaneously hypertensive rats is associated with a narrowed lumen, a thickened media, and an increased number of smooth muscle cell layers. *Circ Res*, *43*(6), 854-864. https://doi.org/10.1161/01.res.43.6.854

Munroe, P. B., Barnes, M. R., & Caulfield, M. J. (2013). Advances in blood pressure genomics. *Circ Res*, *112*(10), 1365-1379. https://doi.org/10.1161/CIRCRESAHA.112.300387

Myung, S. K., Ju, W., Cho, B., Oh, S. W., Park, S. M., Koo, B. K., Park, B. J., & Group, K. M.-A. S. (2013). Efficacy of vitamin and antioxidant supplements in prevention of cardiovascular disease: systematic review and meta-analysis of randomised controlled trials. *BMJ*, *346*, f10. https://doi.org/10.1136/bmj.f10

Nabika, T., Ohara, H., Kato, N., & Isomura, M. (2012). The stroke-prone spontaneously hypertensive rat: still a useful model for post-GWAS genetic studies? *Hypertens Res*, *35*(5), 477-484. https://doi.org/10.1038/hr.2012.30

Nara, Y., Yamori, Y., & Lovenberg, W. (1978). Effect of dietary taurine on blood pressure in spontaneously

hypertensive rats. *Biochem Pharmacol*, *27*(23), 2689-2692. https://doi.org/10.1016/0006-2952(78)90043-6

Natekar, A., Olds, R. L., Lau, M. W., Min, K., Imoto, K., & Slavin, T. P. (2014). Elevated blood pressure: Our family's fault? The genetics of essential hypertension. *World J Cardiol*, *6*(5), 327-337. https://doi.org/10.4330/wjc.v6.i5.327

Network, T. I. G. (2020). Global scorecard of iodine nutrition in 2020 in the general population based on school-age children (SAC).

Network, W. a. I. C. f. t. C. o. I. D. D. G. (2013). *S alt reduction and iodine fortification strategies in public health; Report of a joint technical meeting convened by World Health Organization (WHO) and The George Institute for Global Health in collaboration with the International Council for the Control of Iodine deficiency Disorders Global Network* World Health Organization, Sydney, Australia. http://www.who.int/nutrition/events/2013_technicalconsultation_salt_iodine_strategies_25to27Mar2013/en/

Newby, L. K., Jesse, R. L., Babb, J. D., Christenson, R. H., De Fer, T. M., Diamond, G. A., Fesmire, F. M., Geraci, S. A., Gersh, B. J., Larsen, G. C., Kaul, S., McKay, C. R., Philippides, G. J., & Weintraub, W. S. (2012). ACCF 2012 expert consensus document on practical clinical considerations in the interpretation of troponin elevations: a report of the American College of Cardiology Foundation task force on Clinical Expert Consensus Documents. *J Am Coll Cardiol*, *60*(23), 2427-2463. https://doi.org/10.1016/j.jacc.2012.08.969

NHS. (2023). *Thyroid function tests*. Retrieved 17/07/2023 from https://www.nbt.nhs.uk/severn-pathology/requesting/test-information/thyroid-function-tests

Nicoloff, J. T., Low, J. C., Dussault, J. H., & Fisher, D. A. (1972). Simultaneous measurement of thyroxine and triiodothyronine peripheral turnover kinetics in man. *J Clin Invest*, *51*(3), 473-483. https://doi.org/10.1172/JCI106835

Ohno, M., Zannini, M., Levy, O., Carrasco, N., & di Lauro, R. (1999). The paired-domain transcription factor Pax8 binds to the upstream enhancer of the rat sodium/iodide symporter gene and participates in both thyroid-specific and cyclic-AMP-dependent transcription. *Mol Cell Biol*, *19*(3), 2051-2060. https://doi.org/10.1128/MCB.19.3.2051

Ohta, Y., Tsuchihashi, T., Kiyohara, K., & Oniki, H. (2013). High salt intake promotes a decline in renal function in hypertensive patients: a 10-year observational study. *Hypertens Res*, *36*(2), 172-176. https://doi.org/10.1038/hr.2012.155

Okamoto, K. (1972). *Spontaneous hypertension; its pathogenesis and complications*. Igaku Shoin;
Springer-Verlag.

Okamoto, K., & Aoki, K. (1963). Development of a strain of spontaneously hypertensive rats. *Jpn Circ J*, *27*, 282-293. https://doi.org/10.1253/jcj.27.282

Olson, E., Pravenec, M., Landa, V., Koh-Tan, H. H. C., Dominiczak, A. F., McBride, M. W., & Graham, D. (2019). Transgenic overexpression of glutathione S-transferase μ-type 1 reduces hypertension and oxidative stress in the stroke-prone spontaneously hypertensive rat. *J Hypertens*, *37*(5), 985-996. https://doi.org/10.1097/HJH.0000000000001960

Organisation, W. H. (2007). Assessment of the iodine deficiency disorders and monitoring their elimination. World Health Organization; International Council for the Control
of the Iodine Deficiency Disorders; United Nations Childrens Fund, Geneva.

Organization, W. H. (2007). *Assessment of iodine deficiency disorders and monitoring their elimination : a guide for programme managers*. World Health Organization. https://apps.who.int/iris/handle/10665/43781

Ozemek, C., Laddu, D. R., Arena, R., & Lavie, C. J. (2018). The role of diet for prevention and management of hypertension. *Curr Opin Cardiol*, *33*(4), 388-393. https://doi.org/10.1097/HCO.0000000000000532

Pacific islanders pay heavy price for abandoning traditional diet. (2010). *Bull World Health Organ*, *88*(7), 484-485. https://doi.org/10.2471/BLT.10.010710

Pappachan, J. M., & Buch, H. N. (2017). Endocrine Hypertension: A Practical Approach. *Adv Exp Med Biol*, *956*, 215-237. https://doi.org/10.1007/5584_2016_26

Park, K. W., Dai, H. B., Ojamaa, K., Lowenstein, E., Klein, I., & Sellke, F. W. (1997). The direct vasomotor effect of thyroid hormones on rat skeletal muscle resistance arteries. *Anesth Analg*, *85*(4), 734-738. https://doi.org/10.1097/00000539-199710000-00005

Patel, R. S., Masi, S., & Taddei, S. (2017). Understanding the role of genetics in hypertension. *Eur Heart J*, *38*(29), 2309-2312. https://doi.org/10.1093/eurheartj/ehx273

Pearce, E. N. (2007). National trends in iodine nutrition: is everyone getting enough? *Thyroid*, *17*(9), 823-827. https://doi.org/10.1089/thy.2007.0102

Pearce, E. N., Pino, S., He, X., Bazrafshan, H. R., Lee, S. L., & Braverman, L. E. (2004). Sources of dietary iodine: bread, cows' milk, and infant formula in the Boston area. *J Clin Endocrinol Metab*, *89*(7), 3421-3424. https://doi.org/10.1210/jc.2003-032002

Pedraza, P. E., Obregon, M. J., Escobar-Morreale, H. F., del Rey, F. E., & de Escobar, G. M. (2006). Mechanisms of adaptation to iodine deficiency in rats: thyroid status is tissue specific. Its relevance for man. *Endocrinology*, *147*(5), 2098-2108. https://doi.org/10.1210/en.2005-1325

Pehrsson, P. R., Patterson, K. Y., Spungen, J. H., Wirtz, M. S., Andrews, K. W., Dwyer, J. T., & Swanson, C. A. (2016). Iodine in food- and dietary supplement-composition databases. *Am J Clin Nutr*, *104 Suppl 3*, 868S-876S. https://doi.org/10.3945/ajcn.115.110064

Pfister, R., Sharp, S. J., Luben, R., Wareham, N. J., & Khaw, K. T. (2011). Plasma vitamin C predicts incident heart failure in men and women in European Prospective Investigation into Cancer and Nutrition-Norfolk prospective study. *Am Heart J*, *162*(2), 246-253. https://doi.org/10.1016/j.ahj.2011.05.007

Pickering, D., & Stevens, S. (2013). How to measure and record blood pressure. *Community Eye Health*, *26*(84), 76. https://www.ncbi.nlm.nih.gov/pubmed/24782587

Pino, S., Fang, S. L., & Braverman, L. E. (1996). Ammonium persulfate: a safe alternative oxidizing reagent for measuring urinary iodine. *Clin Chem*, *42*(2), 239-243. https://www.ncbi.nlm.nih.gov/pubmed/8595717

Pinto, Y. M., Paul, M., & Ganten, D. (1998). Lessons from rat models of hypertension: from Goldblatt to genetic engineering. *Cardiovasc Res*, *39*(1), 77-88. https://doi.org/10.1016/s0008-6363(98)00077-7

Poy, M. N., Eliasson, L., Krutzfeldt, J., Kuwajima, S., Ma, X., Macdonald, P. E., Pfeffer, S., Tuschl, T., Rajewsky, N., Rorsman, P., & Stoffel, M. (2004). A pancreatic islet-specific microRNA regulates insulin secretion. *Nature*, *432*(7014), 226-230. https://doi.org/10.1038/nature03076

Poy, M. N., Spranger, M., & Stoffel, M. (2007). microRNAs and the regulation of glucose and lipid metabolism. *Diabetes Obes Metab*, *9 Suppl 2*, 67-73. https://doi.org/10.1111/j.1463-1326.2007.00775.x

Prabhakar, N. R., Peng, Y. J., Kumar, G. K., & Nanduri, J. (2015). Peripheral chemoreception and arterial pressure responses to intermittent hypoxia. *Compr Physiol*, *5*(2), 561-577. https://doi.org/10.1002/cphy.c140039

Pugh, N. D., Griffith, T. M., & Karlsson, J. O. (1995). Effects of iodinated contrast media on peripheral blood flow. *Acta Radiol Suppl*, *399*, 155-163. https://doi.org/10.1177/0284185195036s39918

Rafieian-Kopaei, M., Baradaran, A., & Rafieian, M. (2013). Plants antioxidants: From laboratory to clinic. *J Nephropathol*, *2*(2), 152-153. https://doi.org/10.12860/JNP.2013.26

Rajani, R. M., Quick, S., Ruigrok, S. R., Graham, D., Harris, S. E., Verhaaren, B. F. J., Fornage, M., Seshadri, S., Atanur, S. S., Dominiczak, A. F., Smith, C., Wardlaw, J. M., & Williams, A. (2018). Reversal of endothelial dysfunction reduces white matter vulnerability in cerebral small vessel disease in rats. *Sci Transl Med*, *10*(448). https://doi.org/10.1126/scitranslmed.aam9507

Rakoczy, R., Kopeć, A., Piątkowska, E., Smoleń, S., Skoczylas, Ł., Leszczyńska, T., & Sady, W. (2016). The Iodine Content in Urine, Faeces and Selected Organs of Rats Fed Lettuce Biofortified with Iodine Through Foliar Application. *Biol Trace Elem Res*, *174*(2), 347-355. https://doi.org/10.1007/s12011-016-0717-0

Razvi, S., Bhana, S., & Mrabeti, S. (2019). Challenges in Interpreting Thyroid Stimulating Hormone Results in the Diagnosis of Thyroid Dysfunction. *J Thyroid Res*, *2019*, 4106816. https://doi.org/10.1155/2019/4106816

Razvi, S., Jabbar, A., Pingitore, A., Danzi, S., Biondi, B., Klein, I., Peeters, R., Zaman, A., & Iervasi, G. (2018). Thyroid Hormones and Cardiovascular Function and Diseases. *J Am Coll Cardiol*, *71*(16), 1781-1796. https://doi.org/10.1016/j.jacc.2018.02.045

Réhault-Godbert, S., Guyot, N., & Nys, Y. (2019). The Golden Egg: Nutritional Value, Bioactivities, and Emerging Benefits for Human Health. *Nutrients*, *11*(3). https://doi.org/10.3390/nu11030684

Rhee, C. M., Alexander, E. K., Bhan, I., & Brunelli, S. M. (2013). Hypothyroidism and mortality among dialysis patients. *Clin J Am Soc Nephrol*, *8*(4), 593-601. https://doi.org/10.2215/CJN.06920712

Riesco-Eizaguirre, G., Santisteban, P., & De la Vieja, A. (2021). The complex regulation of NIS expression and activity in thyroid and extrathyroidal tissues. *Endocr Relat Cancer*, *28*(10), T141-T165. https://doi.org/10.1530/ERC-21-0217

Rietzschel, E. R., Langlois, M., De Buyzere, M. L., Segers, P., De Bacquer, D., Bekaert, S., Cooman, L., Van Oostveldt, P., Verdonck, P., De Backer, G. G., Gillebert, T. C., & Investigators, A. (2008). Oxidized low-density lipoprotein cholesterol is associated with decreases in cardiac function independent of vascular alterations. *Hypertension*, *52*(3), 535-541. https://doi.org/10.1161/HYPERTENSIONAHA.108.114439

Rimoldi, S. F., Scherrer, U., & Messerli, F. H. (2014). Secondary arterial hypertension: when, who, and how to

screen? *Eur Heart J*, *35*(19), 1245-1254. https://doi.org/10.1093/eurheartj/eht534

Rivas, A. M., Pena, C., Kopel, J., Dennis, J. A., & Nugent, K. (2021). Hypertension and Hyperthyroidism: Association and Pathogenesis. *Am J Med Sci*, *361*(1), 3-7. https://doi.org/10.1016/j.amjms.2020.08.012

Roberts, C. G., & Ladenson, P. W. (2004). Hypothyroidism. *Lancet*, *363*(9411), 793-803. https://doi.org/10.1016/S0140-6736(04)15696-1

Rohner, F., Zimmermann, M., Jooste, P., Pandav, C., Caldwell, K., Raghavan, R., & Raiten, D. J. (2014). Biomarkers of nutrition for development--iodine review. *J Nutr*, *144*(8), 1322S-1342S. https://doi.org/10.3945/jn.113.181974

Rong, J. X., Shapiro, M., Trogan, E., & Fisher, E. A. (2003). Transdifferentiation of mouse aortic smooth muscle cells to a macrophage-like state after cholesterol loading. *Proc Natl Acad Sci U S A*, *100*(23), 13531-13536. https://doi.org/10.1073/pnas.1735526100

Rottger, A. S., Halle, I., Wagner, H., Breves, G., Danicke, S., & Flachowsky, G. (2012). The effects of iodine level and source on iodine carry-over in eggs and body tissues of laying hens. *Arch Anim Nutr*, *66*(5), 385-401. https://doi.org/10.1080/1745039X.2012.719795

Rouse, I. L., Beilin, L. J., Armstrong, B. K., & Vandongen, R. (1983). Blood-pressure-lowering effect of a vegetarian diet: controlled trial in normotensive subjects. *Lancet*, *1*(8314-5), 5-10. https://doi.org/10.1016/s0140-6736(83)91557-x

Royaux, I. E., Suzuki, K., Mori, A., Katoh, R., Everett, L. A., Kohn, L. D., & Green, E. D. (2000). Pendrin, the protein encoded by the Pendred syndrome gene (PDS), is an apical porter of iodide in the thyroid and is regulated by thyroglobulin in FRTL-5 cells. *Endocrinology*, *141*(2), 839-845. https://doi.org/10.1210/endo.141.2.7303

Rust, P., & Ekmekcioglu, C. (2017). Impact of Salt Intake on the Pathogenesis and Treatment of Hypertension. *Adv Exp Med Biol*, *956*, 61-84. https://doi.org/10.1007/5584_2016_147

Rutter, L., Moran Lauter, A. N., Graham, M. A., & Cook, D. (2019). Visualization methods for differential expression analysis. *BMC Bioinformatics*, *20*(1), 458. https://doi.org/10.1186/s12859-019-2968-1

Ryödi, E., Salmi, J., Jaatinen, P., Huhtala, H., Saaristo, R., Välimäki, M., Auvinen, A., & Metso, S. (2014). Cardiovascular morbidity and mortality in surgically treated hyperthyroidism - a nation-wide cohort study with a long-term follow-up. *Clin Endocrinol (Oxf)*, *80*(5), 743-750. https://doi.org/10.1111/cen.12359

Sacks, F. M., Rosner, B., & Kass, E. H. (1974). Blood pressure in vegetarians. *Am J Epidemiol*, *100*(5), 390-398. https://doi.org/10.1093/oxfordjournals.aje.a112050

Saito, I., Ito, K., & Saruta, T. (1983). Hypothyroidism as a cause of hypertension. *Hypertension*, *5*(1), 112-115. https://doi.org/10.1161/01.hyp.5.1.112

Samuel, S., Zhang, K., Tang, Y. D., Gerdes, A. M., & Carrillo-Sepulveda, M. A. (2017). Triiodothyronine Potentiates Vasorelaxation via PKG/VASP Signaling in Vascular Smooth Muscle Cells. *Cell Physiol Biochem*, *41*(5), 1894-1904. https://doi.org/10.1159/000471938

Santos, J. A. R., Christoforou, A., Trieu, K., McKenzie, B. L., Downs, S., Billot, L., Webster, J., & Li, M. (2019). Iodine fortification of foods and condiments, other than salt, for preventing iodine deficiency disorders. *Cochrane Database Syst Rev*, *2*, CD010734. https://doi.org/10.1002/14651858.CD010734.pub2

Savoia, C., Burger, D., Nishigaki, N., Montezano, A., & Touyz, R. M. (2011). Angiotensin II and the vascular phenotype in hypertension. *Expert Rev Mol Med*, *13*, e11. https://doi.org/10.1017/S1462399411001815

Schaub, M. C., & Perry, S. V. (1969). The relaxing protein system of striated muscle. Resolution of the troponin complex into inhibitory and calcium ion-sensitizing factors and their relationship to tropomyosin. *Biochem J*, *115*(5), 993-1004. https://doi.org/10.1042/bj1150993

Schiffrin, E. L. (1992). Reactivity of small blood vessels in hypertension: relation with structural changes. State of the art lecture. *Hypertension*, *19*(2 Suppl), II1-9. https://doi.org/10.1161/01.hyp.19.2_suppl.ii1-a

Schiffrin, E. L. (1997). Resistance arteries as endpoints in hypertension. *Blood Press Suppl*, *2*, 24-30. https://www.ncbi.nlm.nih.gov/pubmed/9495622

Schneider, C. A., Rasband, W. S., & Eliceiri, K. W. (2012). NIH Image to ImageJ: 25 years of image analysis. *Nat Methods*, *9*(7), 671-675. https://doi.org/10.1038/nmeth.2089

Schughart, K., Libert, C., Kas, M. J., & consortium, S. (2013). Controlling complexity: the clinical relevance of mouse complex genetics. *Eur J Hum Genet*, *21*(11), 1191-1196. https://doi.org/10.1038/ejhg.2013.79

Schumacker, P. T. (2003). Current paradigms in cellular oxygen sensing. *Adv Exp Med Biol*, *543*, 57-71. https://doi.org/10.1007/978-1-4419-8997-0_5

Scientific Opinion on Dietary Reference Values for iodine. (2014). EFSA Panel on Dietetic Products, Nutrition and Allergies (NDA). *EFSA Journal 2014;12(5):3660*, *12 (5)*, 3660. https://doi.org/10.2903/j.efsa.2014.3660

Serrano-Nascimento, C., Calil-Silveira, J., & Nunes, M. T. (2010). Posttranscriptional regulation of sodium-iodide symporter mRNA expression in the rat thyroid gland by acute iodide administration. *Am J Physiol Cell Physiol*, *298*(4), C893-899. https://doi.org/10.1152/ajpcell.00224.2009

Shendure, J. (2008). The beginning of the end for microarrays? *Nat Methods*, *5*(7), 585-587. https://doi.org/10.1038/nmeth0708-585

Sheng, Q., Vickers, K., Zhao, S., Wang, J., Samuels, D. C., Koues, O., Shyr, Y., & Guo, Y. (2017). Multi-perspective quality control of Illumina RNA sequencing data analysis. *Brief Funct Genomics*, *16*(4), 194-204. https://doi.org/10.1093/bfgp/elw035

Sievert, R., Goldstein, M. L., & Surks, M. I. (1996). Graves' disease and autoimmune factor VIII deficiency. *Thyroid*, *6*(3), 245-247. https://doi.org/10.1089/thy.1996.6.245

Silva, J. E. (1995). Thyroid hormone control of thermogenesis and energy balance. *Thyroid*, *5*(6), 481-492. https://doi.org/10.1089/thy.1995.5.481

Singh, S., Shankar, R., & Singh, G. P. (2017). Prevalence and Associated Risk Factors of Hypertension: A Cross-

Sectional Study in Urban Varanasi. *Int J Hypertens*, *2017*, 5491838. https://doi.org/10.1155/2017/5491838

Small, H. Y., McNeilly, S., Mary, S., Sheikh, A. M., & Delles, C. (2019). Resistin Mediates Sex-Dependent Effects of Perivascular Adipose Tissue on Vascular Function in the Shrsp. *Sci Rep*, *9*(1), 6897. https://doi.org/10.1038/s41598-019-43326-z

Small, H. Y., Morgan, H., Beattie, E., Griffin, S., Indahl, M., Delles, C., & Graham, D. (2016). Abnormal uterine artery remodelling in the stroke prone spontaneously hypertensive rat. *Placenta*, *37*, 34-44. https://doi.org/10.1016/j.placenta.2015.10.022

Smyth, P. P. (2003). Role of iodine in antioxidant defence in thyroid and breast disease. *Biofactors*, *19*(3-4), 121-130. https://doi.org/10.1002/biof.5520190304

Smyth, P. P. A. (2021). Iodine, Seaweed, and the Thyroid. *Eur Thyroid J*, *10*(2), 101-108. https://doi.org/10.1159/000512971

Song, E., Park, M. J., Kim, J. A., Roh, E., Yu, J. H., Kim, N. H., Yoo, H. J., Seo, J. A., Kim, S. G., Baik, S. H., & Choi, K. M. (2022). Impact of urinary iodine concentration on blood glucose levels and blood pressure: a nationwide population-based study. *Eur J Nutr*, *61*(6), 3227-3234. https://doi.org/10.1007/s00394-022-02888-x

Sorokin, V., Vickneson, K., Kofidis, T., Woo, C. C., Lin, X. Y., Foo, R., & Shanahan, C. M. (2020). Role of Vascular Smooth Muscle Cell Plasticity and Interactions in Vessel Wall Inflammation. *Front Immunol*, *11*, 599415. https://doi.org/10.3389/fimmu.2020.599415

Spiers, A., & Padmanabhan, N. (2005). A guide to wire myography. *Methods Mol Med*, *108*, 91-104. https://doi.org/10.1385/1-59259-850-1:091

Spitzweg, C., Harrington, K. J., Pinke, L. A., Vile, R. G., & Morris, J. C. (2001). Clinical review 132: The sodium iodide symporter and its potential role in cancer therapy. *J Clin Endocrinol Metab*, *86*(7), 3327-3335. https://doi.org/10.1210/jcem.86.7.7641

Sprague, M., Chau, T. C., & Givens, D. I. (2021). Iodine Content of Wild and Farmed Seafood and Its Estimated

Contribution to UK Dietary Iodine Intake. *Nutrients*, *14*(1). https://doi.org/10.3390/nu14010195

Strahorn, P., Graham, D., Charchar, F. J., Sattar, N., McBride, M. W., & Dominiczak, A. F. (2005). Genetic determinants of metabolic syndrome components in the stroke-prone spontaneously hypertensive rat. *J Hypertens*, *23*(12), 2179-2186. https://doi.org/10.1097/01.hjh.0000191904.26853.b8

Streeten, D. H., Anderson, G. H., Howland, T., Chiang, R., & Smulyan, H. (1988). Effects of thyroid function on blood pressure. Recognition of hypothyroid hypertension. *Hypertension*, *11*(1), 78-83. https://doi.org/10.1161/01.hyp.11.1.78

Sudharsanan, N., Theilmann, M., Kirschbaum, T. K., Manne-Goehler, J., Azadnajafabad, S., Bovet, P., Chen, S., Damasceno, A., De Neve, J. W., Dorobantu, M., Ebert, C., Farzadfar, F., Gathecha, G., Gurung, M. S., Jamshidi, K., Jørgensen, J. M. A., Labadarios, D., Lemp, J., Lunet, N., . . . Geldsetzer, P. (2021). Variation in the Proportion of Adults in Need of Blood Pressure-Lowering Medications by Hypertension Care Guideline in Low- and Middle-Income Countries: A Cross-Sectional Study of 1 037 215 Individuals From 50 Nationally Representative Surveys. *Circulation*, *143*(10), 991-1001. https://doi.org/10.1161/CIRCULATIONAHA.120.051620

Sustainable elimination of iodine deficiency. (2008). United Nations Children's Fund, New York.

Suzuki, Y. J., & Ford, G. D. (1992). Superoxide stimulates IP3-induced Ca2+ release from vascular smooth muscle sarcoplasmic reticulum. *Am J Physiol*, *262*(1 Pt 2), H114-116. https://doi.org/10.1152/ajpheart.1992.262.1.H114

Takami, T., Ito, H., Suzuki, T., & Okamoto, K. (1991). Changes in TSH and 11-deoxycorticosterone (DOC) in hypertension. *Clin Exp Hypertens A*, *13*(5), 991-998. https://doi.org/10.3109/10641969109042105

Takeda, Y., Yoneda, T., Demura, M., Furukawa, K., Miyamori, I., & Mabuchi, H. (2001). Effects of high sodium intake on cardiovascular aldosterone synthesis in stroke-prone spontaneously hypertensive rats. *J Hypertens*, *19*(3 Pt

2), 635-639. https://doi.org/10.1097/00004872-200103001-00017

Taki, K., Kogai, T., Kanamoto, Y., Hershman, J. M., & Brent, G. A. (2002). A thyroid-specific far-upstream enhancer in the human sodium/iodide symporter gene requires Pax-8 binding and cyclic adenosine 3',5'-monophosphate response element-like sequence binding proteins for full activity and is differentially regulated in normal and thyroid cancer cells. *Mol Endocrinol*, *16*(10), 2266-2282. https://doi.org/10.1210/me.2002-0109

Tamargo, M., & Tamargo, J. (2017). Future drug discovery in renin-angiotensin-aldosterone system intervention. *Expert Opin Drug Discov*, *12*(8), 827-848. https://doi.org/10.1080/17460441.2017.1335301

Tang, E. H., Leung, F. P., Huang, Y., Feletou, M., So, K. F., Man, R. Y., & Vanhoutte, P. M. (2007). Calcium and reactive oxygen species increase in endothelial cells in response to releasers of endothelium-derived contracting factor. *Br J Pharmacol*, *151*(1), 15-23. https://doi.org/10.1038/sj.bjp.0707190

Tang, F. (1985). Effect of sex and age on serum aldosterone and thyroid hormones in the laboratory rat. *Horm Metab Res*, *17*(10), 507-509. https://doi.org/10.1055/s-2007-1013590

Tardiff, J. C. (2005). Sarcomeric proteins and familial hypertrophic cardiomyopathy: linking mutations in structural proteins to complex cardiovascular phenotypes. *Heart Fail Rev*, *10*(3), 237-248. https://doi.org/10.1007/s10741-005-5253-5

Tatzber, F., Griebenow, S., Wonisch, W., & Winkler, R. (2003). Dual method for the determination of peroxidase activity and total peroxides-iodide leads to a significant increase of peroxidase activity in human sera. *Anal Biochem*, *316*(2), 147-153. https://doi.org/10.1016/s0003-2697(02)00652-8

Tayie, F. A., & Jourdan, K. (2010). Hypertension, dietary salt restriction, and iodine deficiency among adults. *Am J Hypertens*, *23*(10), 1095-1102. https://doi.org/10.1038/ajh.2010.120

Tazebay, U. H., Wapnir, I. L., Levy, O., Dohan, O., Zuckier, L. S., Zhao, Q. H., Deng, H. F., Amenta, P. S., Fineberg, S., Pestell, R. G., & Carrasco, N. (2000). The mammary gland iodide transporter is expressed during lactation and in breast cancer. *Nat Med*, *6*(8), 871-878. https://doi.org/10.1038/78630

Teas, J., Pino, S., Critchley, A., & Braverman, L. E. (2004). Variability of iodine content in common commercially available edible seaweeds. *Thyroid*, *14*(10), 836-841. https://doi.org/10.1089/thy.2004.14.836

Thom, S. (1997). Arterial structural modifications in hypertension. Effects of treatment. *Eur Heart J*, *18 Suppl E*, E2-4. https://doi.org/10.1016/s0195-668x(97)90001-4

Touré, F., Fritz, G., Li, Q., Rai, V., Daffu, G., Zou, Y. S., Rosario, R., Ramasamy, R., Alberts, A. S., Yan, S. F., & Schmidt, A. M. (2012). Formin mDia1 mediates vascular remodeling via integration of oxidative and signal transduction pathways. *Circ Res*, *110*(10), 1279-1293. https://doi.org/10.1161/CIRCRESAHA.111.262519

Touyz, R. M., Alves-Lopes, R., Rios, F. J., Camargo, L. L., Anagnostopoulou, A., Arner, A., & Montezano, A. C. (2018). Vascular smooth muscle contraction in hypertension. *Cardiovasc Res*, *114*(4), 529-539. https://doi.org/10.1093/cvr/cvy023

Touyz, R. M., Deng, L. Y., & Schiffrin, E. L. (1995). Ca2+ and contractile responses of resistance vessels of WKY rats and SHR to endothelin-1. *J Cardiovasc Pharmacol*, *26 Suppl 3*, S193-196. https://www.ncbi.nlm.nih.gov/pubmed/8587360

Tran, H. V., Erskine, N. A., Kiefe, C. I., Barton, B. A., Lapane, K. L., Do, V. T. H., & Goldberg, R. J. (2017). Is low iodine a risk factor for cardiovascular disease in Americans without thyroid dysfunction? Findings from NHANES. *Nutr Metab Cardiovasc Dis*, *27*(7), 651-656. https://doi.org/10.1016/j.numecd.2017.06.001

Trøan, G., Dahl, L., Meltzer, H. M., Abel, M. H., Indahl, U. G., Haug, A., & Prestløkken, E. (2015). A model to secure a stable iodine concentration in milk. *Food Nutr Res*, *59*, 29829. https://doi.org/10.3402/fnr.v59.29829

Turner, K. B. (1933). STUDIES ON THE PREVENTION OF CHOLESTEROL ATHEROSCLEROSIS IN RABBITS : I. THE EFFECTS OF WHOLE THYROID AND OF POTASSIUM IODIDE. *J Exp Med*, *58*(1), 115-125. https://doi.org/10.1084/jem.58.1.115

Uchida, S., & Dimmeler, S. (2015). Long noncoding RNAs in cardiovascular diseases. *Circ Res*, *116*(4), 737-750. https://doi.org/10.1161/CIRCRESAHA.116.302521

Uder, M., Heinrich, M., Jansen, A., Humke, U., Utz, J., Trautwein, W., & Kramann, B. (2002). cAMP and cGMP do not mediate
the vasorelaxation induced by iodinated radiographic contrast media in isolated
swine renal arteries. *43*(1), 104-110.
https://pubmed.ncbi.nlm.nih.gov/11972472/

Uyttersprot, N., Pelgrims, N., Carrasco, N., Gervy, C., Maenhaut, C., Dumont, J. E., & Miot, F. (1997). Moderate doses of iodide in vivo inhibit cell proliferation and the expression of thyroperoxidase and Na+/I-symporter mRNAs in dog thyroid. *Mol Cell Endocrinol*, *131*(2), 195-203. https://doi.org/10.1016/s0303-7207(97)00108-1

Vanderstraeten, J., Baselet, B., Buset, J., Ben Said, N., de Ville de Goyet, C., Many, M. C., Gérard, A. C., & Derradji, H. (2020). Modulation of VEGF Expression and Oxidative Stress Response by Iodine Deficiency in Irradiated Cancerous and Non-Cancerous Breast Cells. *Int J Mol Sci*, *21*(11). https://doi.org/10.3390/ijms21113963

Vanderstraeten, J., Derradji, H., Craps, J., Sonveaux, P., Colin, I. M., Many, M. C., & Gérard, A. C. (2016). Iodine deficiency induces a VEGF-dependent microvascular response in salivary glands and in the stomach. *Histol Histopathol*, *31*(8), 897-909. https://doi.org/10.14670/HH-11-727

Vanhoutte, P. M., Shimokawa, H., Feletou, M., & Tang, E. H. (2017). Endothelial dysfunction and vascular disease - a 30th anniversary update. *Acta Physiol (Oxf)*, *219*(1), 22-96. https://doi.org/10.1111/apha.12646

Vardi, M., Levy, N. S., & Levy, A. P. (2013). Vitamin E in the prevention of cardiovascular disease: the importance of proper patient selection. *J Lipid Res*, *54*(9), 2307-2314. https://doi.org/10.1194/jlr.R026641

Vardouli, L., Moustakas, A., & Stournaras, C. (2005). LIM-kinase 2 and cofilin phosphorylation mediate actin cytoskeleton reorganization induced by transforming growth factor-beta. *J Biol Chem*, *280*(12), 11448-11457. https://doi.org/10.1074/jbc.M402651200

Vejbjerg, P., Knudsen, N., Perrild, H., Laurberg, P., Andersen, S., Rasmussen, L. B., Ovesen, L., & Jørgensen, T. (2009). Estimation of iodine intake from various urinary iodine measurements in population studies. *Thyroid*, *19*(11), 1281-1286. https://doi.org/10.1089/thy.2009.0094

Velculescu, V. E., Zhang, L., Vogelstein, B., & Kinzler, K. W. (1995). Serial analysis of gene expression. *Science*, *270*(5235), 484-487. https://doi.org/10.1126/science.270.5235.484

Venturi, S., & Venturi, M. (1999). Iodide, thyroid and stomach carcinogenesis: evolutionary story of a primitive antioxidant? *Eur J Endocrinol*, *140*(4), 371-372. https://doi.org/10.1530/eje.0.1400371

Vicinanza, R., Coppotelli, G., Malacrino, C., Nardo, T., Buchetti, B., Lenti, L., Celi, F. S., & Scarpa, S. (2013). Oxidized low-density lipoproteins impair endothelial function by inhibiting non-genomic action of thyroid hormone-mediated nitric oxide production in human endothelial cells. *Thyroid*, *23*(2), 231-238. https://doi.org/10.1089/thy.2011.0524

Vinogradova, M. N., Mandrykina, T. A., Lavrov, G. K., & Shchegoleva, E. A. (1990). [The effect of molecular-iodine baths on the central hemodynamics of patients with hypertension and ischemic heart disease]. *Vopr Kurortol Fizioter Lech Fiz Kult*(4), 15-18. https://www.ncbi.nlm.nih.gov/pubmed/2275098

Vitale, M., Di Matola, T., D'Ascoli, F., Salzano, S., Bogazzi, F., Fenzi, G., Martino, E., & Rossi, G. (2000). Iodide excess induces apoptosis in thyroid cells through a p53-independent mechanism involving oxidative stress.

Endocrinology, *141*(2), 598-605. https://doi.org/10.1210/endo.141.2.7291

Wang, D., Chang, P. S., Wang, Z., Sutherland, L., Richardson, J. A., Small, E., Krieg, P. A., & Olson, E. N. (2001). Activation of cardiac gene expression by myocardin, a transcriptional cofactor for serum response factor. *Cell*, *105*(7), 851-862. https://doi.org/10.1016/s0092-8674(01)00404-4

Wang, G., Jacquet, L., Karamariti, E., & Xu, Q. (2015). Origin and differentiation of vascular smooth muscle cells. *J Physiol*, *593*(14), 3013-3030. https://doi.org/10.1113/JP270033

Wang, J., Li, A., Wang, Z., Feng, X., Olson, E. N., & Schwartz, R. J. (2007). Myocardin sumoylation transactivates cardiogenic genes in pluripotent 10T1/2 fibroblasts. *Mol Cell Biol*, *27*(2), 622-632. https://doi.org/10.1128/MCB.01160-06

Wang, K. C., & Chang, H. Y. (2011). Molecular mechanisms of long noncoding RNAs. *Mol Cell*, *43*(6), 904-914. https://doi.org/10.1016/j.molcel.2011.08.018

Wang, Q., Reiter, R. S., Huang, Q. Q., Jin, J. P., & Lin, J. J. (2001). Comparative studies on the expression patterns of three troponin T genes during mouse development. *Anat Rec*, *263*(1), 72-84. https://doi.org/10.1002/ar.1078

Wang, R., Sauvé, R., & de Champlain, J. (1995). Abnormal regulation of cytosolic free calcium in vascular endothelial cells from spontaneously hypertensive rats. *J Hypertens*, *13*(9), 993-1001. https://www.ncbi.nlm.nih.gov/pubmed/8586835

Wang, Z., Gerstein, M., & Snyder, M. (2009). RNA-Seq: a revolutionary tool for transcriptomics. *Nat Rev Genet*, *10*(1), 57-63. https://doi.org/10.1038/nrg2484

Wang, Z., Wang, D. Z., Pipes, G. C., & Olson, E. N. (2003). Myocardin is a master regulator of smooth muscle gene expression. *Proc Natl Acad Sci U S A*, *100*(12), 7129-7134. https://doi.org/10.1073/pnas.1232341100

Warren, H. R., Evangelou, E., Cabrera, C. P., Gao, H., Ren, M., Mifsud, B., Ntalla, I., Surendran, P., Liu, C., Cook, J. P., Kraja, A. T., Drenos, F., Loh, M., Verweij, N., Marten, J., Karaman, I., Lepe, M. P., O'Reilly, P. F., Knight, J., . .

. group, U. B. C. C. B. w. (2017). Genome-wide association analysis identifies novel blood pressure loci and offers biological insights into cardiovascular risk. *Nat Genet*, *49*(3), 403-415. https://doi.org/10.1038/ng.3768

Webb, R. C. (2003). Smooth muscle contraction and relaxation. *Adv Physiol Educ*, *27*(1-4), 201-206. https://doi.org/10.1152/advan.00025.2003

Weiss, S. J., Philp, N. J., & Grollman, E. F. (1984). Iodide transport in a continuous line of cultured cells from rat thyroid. *Endocrinology*, *114*(4), 1090-1098. https://doi.org/10.1210/endo-114-4-1090

WHO. (2014). *Global Status Report on Noncommunicable Disease*.

WHO. (2017, May 17). *Cardiovascular diseases (CVDs)*. https://www.who.int/news-room/fact-sheets/detail/cardiovascular-diseases-(cvds)

Wilson, C., Zhang, X., Buckley, C., Heathcote, H. R., Lee, M. D., & McCarron, J. G. (2019). Increased Vascular Contractility in Hypertension Results From Impaired Endothelial Calcium Signaling. *Hypertension*, *74*(5), 1200-1214. https://doi.org/10.1161/HYPERTENSIONAHA.119.13791

Winkler, R., Griebenow, S., & Wonisch, W. (2000). Effect of iodide on total antioxidant status of human serum. *Cell Biochem Funct*, *18*(2), 143-146. https://doi.org/10.1002/(SICI)1099-0844(200006)18:2<143::AID-CBF857>3.0.CO;2-#

Wolff, J., & Chaikoff, I. L. (1948). Plasma inorganic iodide as a homeostatic regulator of thyroid function. *J Biol Chem*, *174*(2), 555-564. https://www.ncbi.nlm.nih.gov/pubmed/18865621

World health organization. (2013). *Global Health Observatory (GHO), World health statistics 2013*. https://www.who.int/gho/publications/world_health_statistics/2013/en/ <p class="EndNoteBibliography" style="margin-left:36.0pt
text-indent:-36.0pt
line-height:150%">

World Health Organization., & International Atomic Energy Agency. (1989). *Minor and trace elements in breast milk*

: report of a joint WHO/IAEA collaborative study. World Health Organization ; Albany, NY : WHO Publications Center USA distributor.

Wu, R., Millette, E., Wu, L., & de Champlain, J. (2001). Enhanced superoxide anion formation in vascular tissues from spontaneously hypertensive and desoxycorticosterone acetate-salt hypertensive rats. *J Hypertens*, *19*(4), 741-748. https://doi.org/10.1097/00004872-200104000-00011

Xia, X. D., Zhou, Z., Yu, X. H., Zheng, X. L., & Tang, C. K. (2017). Myocardin: A novel player in atherosclerosis. *Atherosclerosis*, *257*, 266-278. https://doi.org/10.1016/j.atherosclerosis.2016.12.002

Xiang, X., Li, S., Zhuang, X., & Shi, L. (2016). Arhgef1 negatively regulates neurite outgrowth through activation of RhoA signaling pathways. *FEBS Lett*, *590*(17), 2940-2955. https://doi.org/10.1002/1873-3468.12339

Xin, M., Small, E. M., Sutherland, L. B., Qi, X., McAnally, J., Plato, C. F., Richardson, J. A., Bassel-Duby, R., & Olson, E. N. (2009). MicroRNAs miR-143 and miR-145 modulate cytoskeletal dynamics and responsiveness of smooth muscle cells to injury. *Genes Dev*, *23*(18), 2166-2178. https://doi.org/10.1101/gad.1842409

Yabu, Y., Miyai, K., Hayashizaki, S., Endo, Y., Hata, N., Iijima, Y., & Fushimi, R. (1986). Measurement of iodide in urine using the iodide-selective ion electrode. *Endocrinol Jpn*, *33*(6), 905-911. https://doi.org/10.1507/endocrj1954.33.905

Yamori, Y. (1984). The stroke-prone spontaneously hypertensive rat: Contribution to risk factor analysis and prevention of hypertensive diseases. In D. J. W (Ed.), *Handbook of Hypertension* (pp. 240–255). Elsevier.

Yamori, Y., Nara, Y., Tsubouchi, T., Sogawa, Y., Ikeda, K., & Horie, R. (1986). Dietary prevention of stroke and its mechanisms in stroke-prone spontaneously hypertensive rats--preventive effect of dietary fibre and palmitoleic acid. *J Hypertens Suppl*, *4*(3), S449-452. https://www.ncbi.nlm.nih.gov/pubmed/3023589

Yamori, Y., & Okamoto, K. (1974). Spontaneous hypertension in the rat. A model for human "essential" hypertension.

Verh Dtsch Ges Inn Med, *80*, 168-170. https://doi.org/10.1007/978-3-642-85449-1_25

Yamori, Y., Sagara, M., Mori, H., Mori, M., & Group, C. S. (2022). Stroke-Prone SHR as Experimental Models for Cardiovascular Disease Risk Reduction in Humans. *Biomedicines*, *10*(11). https://doi.org/10.3390/biomedicines10112974

Yogi, A., Callera, G. E., Aranha, A. B., Antunes, T. T., Graham, D., McBride, M., Dominiczak, A., & Touyz, R. M. (2011). Sphingosine-1-phosphate-induced inflammation involves receptor tyrosine kinase transactivation in vascular cells: upregulation in hypertension. *Hypertension*, *57*(4), 809-818. https://doi.org/10.1161/HYPERTENSIONAHA.110.162719

Yoshida, M., Mukama, A., Hosomi, R., Fukunaga, K., & Nishiyama, T. (2014). Serum and tissue iodine concentrations in rats fed diets supplemented with kombu powder or potassium iodide. *J Nutr Sci Vitaminol (Tokyo)*, *60*(6), 447-449. https://doi.org/10.3177/jnsv.60.447

Young, W. F. (2010). Endocrine hypertension: then and now. *Endocr Pract*, *16*(5), 888-902. https://doi.org/10.4158/EP10205.RA

Yu, T., Jing, M., Gao, Y., Liu, C., Liu, L., Jia, H., Liu, P., & Chang, M. (2020). Study on the relationship between hyperthyroidism and vascular endothelial cell damage. *Sci Rep*, *10*(1), 6992. https://doi.org/10.1038/s41598-020-62796-0

Zabka, T. S., Fielden, M. R., Garrido, R., Tao, J., Fretland, A. J., Fretland, J. L., Albassam, M. A., Singer, T., & Kolaja, K. L. (2011). Characterization of xenobiotic-induced hepatocellular enzyme induction in rats: anticipated thyroid effects and unique pituitary gland findings. *Toxicol Pathol*, *39*(4), 664-677. https://doi.org/10.1177/0192623311406934

Zaragoza, C., Gomez-Guerrero, C., Martin-Ventura, J. L., Blanco-Colio, L., Lavin, B., Mallavia, B., Tarin, C., Mas, S., Ortiz, A., & Egido, J. (2011). Animal models of

cardiovascular diseases. *J Biomed Biotechnol*, *2011*, 497841. https://doi.org/10.1155/2011/497841

Zhang, B., Pu, L., Zhao, T., Wang, L., Shu, C., Xu, S., Sun, J., Zhang, R., & Han, L. (2023). Global Burden of Cardiovascular Disease from 1990 to 2019 Attributable to Dietary Factors. *J Nutr*, *153*(6), 1730-1741. https://doi.org/10.1016/j.tjnut.2023.03.031

Zhang, L., Zhou, W., Velculescu, V. E., Kern, S. E., Hruban, R. H., Hamilton, S. R., Vogelstein, B., & Kinzler, K. W. (1997). Gene expression profiles in normal and cancer cells. *Science*, *276*(5316), 1268-1272. https://doi.org/10.1126/science.276.5316.1268

Zhang, M., Li, C., He, C., Cui, Y., Li, Y., Ma, Y., Cheng, J., Wen, J., Li, P., & Yang, Y. (2022). Thromboxane-induced contractile response of mesenteric arterioles is diminished in the older rats and the older hypertensive rats. *Front Pharmacol*, *13*, 1019511. https://doi.org/10.3389/fphar.2022.1019511

Zhang, M., Zou, X., Lin, X., Bian, J., Meng, H., & Liu, D. (2015). Effect of Excessive Potassium Iodide on Rat Aorta Endothelial Cells. *Biol Trace Elem Res*, *166*(2), 201-209. https://doi.org/10.1007/s12011-015-0264-0

Zhang, X., Jiang, Y., Han, W., Liu, A., Xie, X., Han, C., Fan, C., Wang, H., Zhang, H., Ding, S., Shan, Z., & Teng, W. (2016). Effect of Prolonged Iodine Overdose on Type 2 Iodothyronine Deiodinase Ubiquitination-Related Enzymes in the Rat Pituitary. *Biol Trace Elem Res*, *174*(2), 377-386. https://doi.org/10.1007/s12011-016-0723-2

Zhao, J., Yu, J., Shan, Z., Teng, W., Liu, C., Chong, W., & Mao, J. (2021). MicroRNA expression profiles of the thyroid after goiter formation and involution in rats under different iodine regimens. *Endocrine*, *73*(3), 598-608. https://doi.org/10.1007/s12020-021-02679-0

Zhao, S. J., Ye, Y., Sun, F. J., Tian, E. J., & Chen, Z. P. (2011). The impact of dietary iodine intake on lipid metabolism in mice. *Biol Trace Elem Res*, *142*(3), 581-588. https://doi.org/10.1007/s12011-010-8767-1

Zimmermann, M. B. (2009). Iodine deficiency. *Endocr Rev*, *30*(4), 376-408. https://doi.org/10.1210/er.2009-0011

Zimmermann, M. B. (2012). The effects of iodine deficiency in pregnancy and infancy. *Paediatr Perinat Epidemiol*, *26 Suppl 1*, 108-117. https://doi.org/10.1111/j.1365-3016.2012.01275.x

Zimmermann, M. B., & Andersson, M. (2012). Assessment of iodine nutrition in populations: past, present, and future. *Nutr Rev*, *70*(10), 553-570. https://doi.org/10.1111/j.1753-4887.2012.00528.x

Zimmermann, M. B., & Andersson, M. (2021). GLOBAL ENDOCRINOLOGY: Global perspectives in endocrinology: coverage of iodized salt programs and iodine status in 2020. *Eur J Endocrinol*, *185*(1), R13-R21. https://doi.org/10.1530/EJE-21-0171

Zimmermann, M. B., & Boelaert, K. (2015). Iodine deficiency and thyroid disorders. *Lancet Diabetes Endocrinol*, *3*(4), 286-295. https://doi.org/10.1016/S2213-8587(14)70225-6

Zimmermann, M. B., Jooste, P. L., & Pandav, C. S. (2008). Iodine-deficiency disorders. *Lancet*, *372*(9645), 1251-1262. https://doi.org/10.1016/S0140-6736(08)61005-3

Appendices

Appendix I: Nutritional (mineral) composition of normal iodine diet (ND) and the low iodine diet (LID)

Supplementary Table 1: Amount of macro and micro minerals in normal iodine diet

NUTRIENTS		Total	Supp (9)
Glutamic Acid	%	3.17	
Proline	%	1.20	
Serine	%	0.56	
Hydroxyproline	%		
Hydroxylysine	%		
Alanine	%	0.16	
Macro Minerals			
Calcium	%	0.73	0.63
Total Phosphorus	%	0.52	0.04
Phytate Phosphorus	%	0.24	
Available Phosphorus	%	0.28	0.04
Sodium	%	0.25	0.19
Chloride	%	0.38	0.32
Potassium	%	0.67	
Magnesium	%	0.23	
Micro Minerals			
Iron	mg/kg	159.30	82.50
Copper	mg/kg	11.50	1.94
Manganese	mg/kg	72.44	19.22
Zinc	mg/kg	35.75	
Cobalt	µg/kg	634.10	550.00
Iodine	µg/kg	1202.69	1085.00
Selenium	µg/kg	298.99	100.00
Fluorine	mg/kg	10.49	

The diets were prepared by Special Diets Services (SDS). The compressed normal iodine diet contained 1202.69 µg/kg of iodine from background ingredients with 1085 µg/kg supplementation. The normal iodine diet (NID) contained 1.2 mg/kg iodine.

Supplementary Table 2: Amount of macro and micro minerals in low iodine diet

		VALUE
MACRO & MICRO MINERALS		
Ca	%	0.7
SUPP Ca	%	0.62
P	%	0.5
SUPP P	%	0.04
PHYTATE P	%	0.23
AVAILABLE P	%	0.26
Na	%	0.22
SUPP Na	%	0.19
Cl	%	0.36
SUPP Cl	%	0.31
K	%	0.65
SUPP K	%	0.0
Mg	%	0.2
SUPP Mg	%	0.0
Fe	mg/kg	175
SUPP Fe	mg/kg	89
Cu	mg/kg	12.1
SUPP Cu	mg/kg	1.9
MN	mg/kg	70
SUPP Mn	mg/kg	19
Zn	mg/kg	34.5
SUPP Zn	mg/kg	0.0
Co	µg/kg	694
SUPP Co	µg/kg	632
I*	**µg/kg**	**76**
SUPP I*	**µg/kg**	**0.0**
Se	µg/kg	288
SUPP Se	µg/kg	100

The diets were prepared by Special Diets Services (SDS). The compressed low iodine diet (LID) contained 76 µg/kg (highlighted in bold) of iodine from background ingredients with no supplementation. The low iodine diet (LID) contained 0.211, 0.039 and 0.0907 mg/kg iodine (Figure 7-1, 7-2 and 7-3).

Special Diets Services

Monday, 03 February 2020

SDS - Analysis Report – 827053 - RM1 Iodine Deficient (P) - 41305

Product Code	827053
Product Name	RM1 Iodine Deficient (P)
Product Batch Number	41305
Date of Manufacture Completion	30/12/2019

Please find below the results of the diet samples as referenced above.

Parameter analysed	Units	Result	Notes i.e. Expected Homogeneity / Laboratory Precision
Iodine	Mg/kg	0.211	*

* The results are in line with expected values.

Please come back to me if I can be of any further help.

Yours sincerely,

Rosie

Roseanna Barclay
Assistant Nutritionist

Special Diet Services.
PO Box 705
Witham
Essex/
England
CM8 3AD
Tel: + 44 (0) 1376 536 000
Fax: + 44 (0) 1376 511 247
e-mail:

Supplementary Figure 1: First batch low iodine diet iodine concentration analysis report.

The amount of iodine in low iodine diet was determined my Special diet service and found to be 0.211 mg/kg.

Special Diets Services

Thursday, 08 October 2020

SDS - Analysis Report – 827053 - RM1 Iodine Deficient (P) - 41587

Product Code	827053
Product Name	RM1 Iodine Deficient (P)
Product Batch Number	41587
Date of Manufacture Completion	08/09/2020

Please find below the results of the diet samples as referenced above.

Parameter analysed	Units	Result	Notes i.e. Expected Homogeneity / Laboratory Precision
Iodine	Mg/kg	0.039	*

* The results are in line with expected values.

Please come back to me if I can be of any further help.

Yours sincerely,

Rosie

Roseanna Barclay
Assistant Nutritionist

Special Diet Services.
PO Box 705
Witham
Essex/
England
CM8 3AD
Tel: + 44 (0) 1376 536 000
Fax: + 44 (0) 1376 511 247
e-mail:

Supplementary Figure 2: Second batch low iodine diet iodine concentration analysis report.

The amount of iodine in low iodine diet was determined my Special diet service and found to be 0.039 mg/kg.

Special Diets Services

Tuesday, 29 March 2022

SDS - Analysis Report – 827053 - RM1 Iodine Deficient (P) - 42148

Product Code	827053
Product Name	RM1 Iodine Deficient (P)
Product Batch Number	42148
Date of Manufacture Completion	08/03/2022

Please find below the results of the diet samples as referenced above.

Parameter analysed	Units	Result	Notes i.e. Expected Homogeneity / Laboratory Precision
Iodine	mg/kg	0.0907	*

* The results are in line with expected values.

Please come back to me if I can be of any further help.

Yours sincerely,
Juliette

Juliette Marshall
Senior Nutritionist

Special Diet Services.
PO Box 705
Witham
Essex/
England
CM8 3AD
Tel: + 44 (0) 1376 536 000
Fax: + 44 (0) 1376 511 247
Email:

Supplementary Figure 3: Third batch low iodine diet iodine concentration analysis report.

The amount of iodine in low iodine diet was determined my Special diet service and found to be 0.0907 mg/kg.

Appendix II: WIRE MYOGRAPHY STANDARD OPERATING PROCEDURE

ABBREVIATIONS

I. Physiological Salt Solution: PSS
II. Oxygen: O_2
III. Carbon Dioxide: CO_2
IV. Micrometer: µM

PROCEDURE

- **Set-up**

I. Turn on the myograph, Powerlab and computer.
II. Open the current settings file and save the document with an appropriate name.
III. Turn on the gas supply and ensure each bath is gassed with 95% O_2 / 5 % CO_2. A low constant stream of bubbles is sufficient.
IV. Rinse each bath with deionised water 3 times.
V. Fill each bath with 5 mL of cold PSS and then drain the bath contents. Repeat a further 2 times, leaving the PSS in the bath on the final rinse.

- **Mounting**

I. The mounting of tissue should be completed under a microscope.
II. Following dissection, cut the tissue into approximately 2 mm ring segments.
III. Thread one 40 µM diameter wire (or 25 µM wire) through the lumen of the tissue, taking care not to damage the endothelium for example, by scraping the wire along the wall.
IV. Once threaded, transfer the vessel and wire into a myograph bath.
V. Clamp the wire between the 2 jaws, ensuring the jaws are not pushed together too tightly as this could damage the transducer.
VI. Attach the wire to one of the heads by wrapping it round the screws in a clockwise direction. Ensure the tissue is sitting in the middle of the jaws and the wire is secured tightly with no slack.
VII. Carefully thread a second 40 µM wire through the lumen of the tissue. Again, take care not to damage the endothelium or to cross the wires.

VIII. Secure the second wire between the 2 jaws and attached it to the second head.

IX. Make sure the wires are level at this stage.

X. Carefully open the jaws slightly so that the wires are not touching but there is no stretch on the tissue.

XI. See supplementary figure 4 below for an illustration of the complete myograph set up.

XII. Place the myograph bath onto the base plate and plug in the transducer (if required, make sure the appropriate arrow on the interface is pressed to temporarily block the transducer).

XIII. Place a cap and funnel over the bath. Ensure the bath is gassing.

XIV. Repeat these steps for all baths.

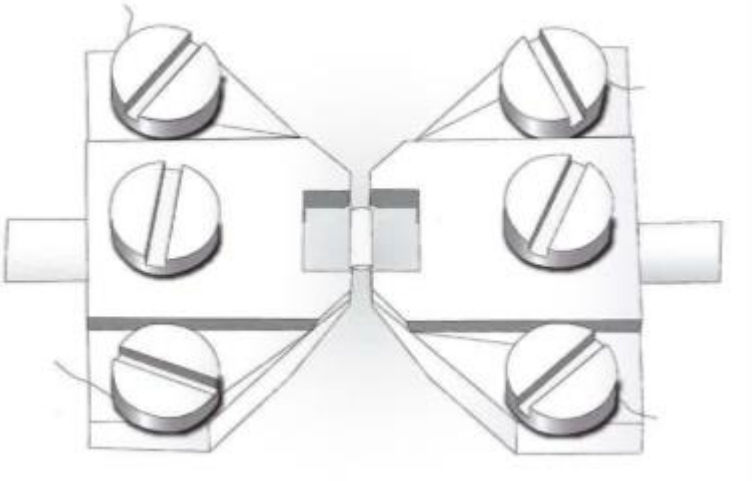

Supplementary Figure 4: Illustration showing a mounted tissue in a wire myograph

- **Equilibration**

I. Following mounting of the tissue, turn on the heat.

II. Allow the baths to slowly reach 37 °C and the tissue to equilibrate for approximately 30 minutes.

- **Normalisation or stretching**

I. Depending on the tissue mounted, the tissue may either be stretched or normalised

II. Tissue such as airways will be stretched:

III. Zero all transducers.

IV. Stretch the tissue to the desired tension (detailed in the protocol) slowly over a number of stretches.

V. Once the desired tension is reached allow the trace to stabilise.

VI. Wash the baths 3 times with warm PSS, leaving the PSS in the bath on the third rinse.

VII. Dependent on the tissue, a second 90 minute period of equilibration may be entered. This will be detailed in the protocol.

Tissue such as resistance arteries will be normalised:

I. The objective of normalisation is to determine the optimal passive tension of each vessel.

II. Before starting a group of experiments with a new tissue it is important to conduct a passive and active length tension curve in order to determine the normalisation factor (the IC_1/IC_{100} ratio (this may be changed to a physiologically relevant ratio. For example, if using pulmonary arteries, which are at a much lower pressure, you may want use a ratio of $IC_1/IC_{10)}$).

III. Stretch the tissue in a small increment and record the force generated. Once the response has plateaued, add 62.5 mM KPSS to the bath. Record this response.

IV. Wash out the bath 3 times with PSS.

V. Repeat these steps until a plateau in KPSS response is reached.

VI. Calculate the pressure at each point using the following formula:

Pressure=2π x force / 2 x length of vessel x (205.6 + (2 x distance stretched))

VII. Plot the points on a graph and draw an isobar line (a horizontal line at 13.3 kPa (this may be at 5 kPa for pulmonary arteries))

VIII. The IC_{100} is the point at which the isobar line crosses the passive length tension curve.

IX. The IC_1 is the maximal response in the active length tension curve. Select the middle point of the plateau to allow the maximal response to be observes for slightly larger or smaller vessels.

X. Calculate the ratio between $IC_1/IC_{100.}$ Once this ratio is calculated, the length tension curves do not have to be repeated. This value is used in the normalisation module in LabChart. See supplementary figure 5 below for an overview of the calculating the normalisation factor

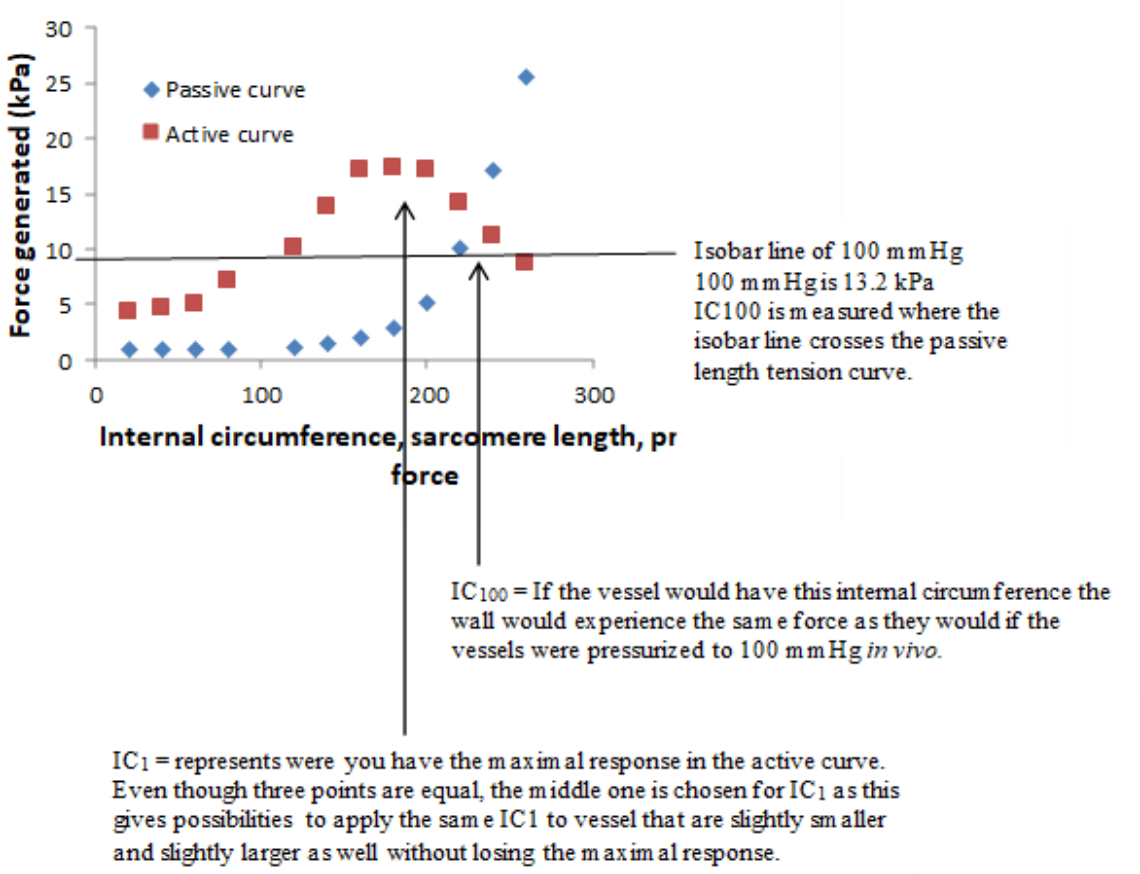

Supplementary Figure 5: Overview of calculating the normalisation factor

XI. To start normalisation, zero all transducers.

XII. Open the DMT normalisation module on chart and enter the eyepiece calibration (if using a ruler to measure the vessel length then enter 1 in this box), target pressure and IC_1/IC_{100}. For each channel enter the tissue length and initial micrometer reading.

XIII. Stretch the vessel in small increments and enter the micrometer reading at each stretch. The programme will calculate the pressure at each stretch.

XIV. Once the vessel has reached the target pressure (13.3 kPa for resistance arteries) LabChart will calculate the optimum stretch for the vessel and will detail the appropriate micrometer reading.

XV. Set your micrometer to the indicated level.

XVI. Wash the baths 3 times with warm PSS.

XVII. Once the response has plateaued, zero the transducers.

XVIII. At this stage, normalisation is complete.

- **Wake Up procedure.**

I. Empty the baths and add 5 mL of 62.5 mM KPSS.

II. Following maximum response wash all baths three times with PSS, leaving PSS in the bath following the third wash and allow steady baseline generation.

III. Repeat steps I and II a further two times, three times in total.

- **Endothelial Check**
    - U46619 pre-constriction.

I. Add 15 µl of $1x10^{-5}$ M = $3x10^{-8}$ M in bath

II. Following plateau of the above response, add ACh to the bath to assess endothelial function. (Add 5 µl of $1x10^{-3}$ M = $1x10^{-6}$ M in bath)

III. Following maximal ACh response, wash baths with PSS three times leaving PSS in the bath after the final wash. Allow steady baseline generation.

NOTE: Functional endothelium = minimum of 50 % relaxation

Denuded vessel = maximum of 20% relaxation.

- **U46619 cumulative concentration-response curves**
    - Conduct a CCRC to U46619 as follows:

Add 5 µl of $1x10^{-7}$ M = $1x10^{-10}$ M in bath

Add 10 µl of $1x10^{-7}$ M = $3x10^{-10}$ M in bath

Add 3.5 µl of $1x10^{-6}$ M = $1x10^{-9}$ M in bath

Add 10 µl of $1x10^{-6}$ M = $3x10^{-9}$ M in bath

Add 3.5 µl of $1x10^{-5}$ M = $1x10^{-8}$ M in bath

Add 10 µl of $1x10^{-5}$ M = $3x10^{-8}$ M in bath

Add 3.5 µl of $1x10^{-4}$ M = $1x10^{-7}$ M in bath

Add 10 µl of $1x10^{-4}$ M = $3x10^{-7}$ M in bath

Add 3.5 µl of $1x10^{-3}$ M = $1x10^{-6}$ M in bath

Add 10 µl of $1x10^{-3}$ M = $3x10^{-6}$ M in bath

Add 3.5 µl of $1x10^{-2}$ M = $1x10^{-5}$ M in bath

I. Additions are made after 5 minutes when no response is observed or following maximal response of the preceding concentration.

II. Following completion of the above CCRC wash baths three times with PSS, leaving the PSS in the bath after the third wash. Allow steady baseline generation.

- **ACh cumulative concentration-response curves**

I. Following a steady baseline, pre-constrict the vessels with U46619:

Add 15 µl of $1x10^{-5}$ M U46619 = $3x10^{-8}$ M in bath

II. Following plateau of the above response, conduct a CCRC to ACh as follows:

Add 5 µl of $1x10^{-7}$ M = $1x10^{-10}$ M in bath
Add 10 µl of $1x10^{-7}$ M = $3x10^{-10}$ M in bath
Add 3.5 µl of $1x10^{-6}$ M = $1x10^{-9}$ M in bath
Add 10 µl of $1x10^{-6}$ M = $3x10^{-9}$ M in bath
Add 3.5 µl of $1x10^{-5}$ M = $1x10^{-8}$ M in bath
Add 10 µl of $1x10^{-5}$ M = $3x10^{-8}$ M in bath
Add 3.5 µl of $1x10^{-4}$ M = $1x10^{-7}$ M in bath
Add 10 µl of $1x10^{-4}$ M = $3x10^{-7}$ M in bath
Add 3.5 µl of $1x10^{-3}$ M = $1x10^{-6}$ M in bath
Add 10 µl of $1x10^{-3}$ M = $3x10^{-6}$ M in bath
Add 3.5 µl of $1x10^{-2}$ M = $1x10^{-5}$ M in bath
Add 10 µl of $1x10^{-2}$ M = $3x10^{-5}$ M in bath

III. Additions are made after 5 minutes when no response is observed or following maximal response of the preceding concentration.

IV. Following completion of the above CCRC, wash baths three times with PSS, leaving the PSS in the bath after the third wash. Allow steady baseline generation.

- **SNP cumulative concentration-response curves**

I. Following a steady baseline, pre-constrict the vessels with U46619:

Add 15 µl of $1x10^{-5}$ M U46619 = $3x10^{-8}$ M in bath

II. Following plateau of the above response, conduct a CCRC to SNP as follows:

Add 5 µl of $1x10^{-7}$ M = $1x10^{-10}$ M in bath
Add 10 µl of $1x10^{-7}$ M = $3x10^{-10}$ M in bath

Add 3.5 µl of $1x10^{-6}$ M = $1x10^{-9}$ M in bath

Add 10 µl of $1x10^{-6}$ M = $3x10^{-9}$ M in bath

Add 3.5 µl of $1x10^{-5}$ M = $1x10^{-8}$ M in bath

Add 10 µl of $1x10^{-5}$ M = $3x10^{-8}$ M in bath

Add 3.5 µl of $1x10^{-4}$ M = $1x10^{-7}$ M in bath

Add 10 µl of $1x10^{-4}$ M = $3x10^{-7}$ M in bath

Add 3.5 µl of $1x10^{-3}$ M = $1x10^{-6}$ M in bath

Add 10 µl of $1x10^{-3}$ M = $3x10^{-6}$ M in bath

Add 3.5 µl of $1x10^{-2}$ M = $1x10^{-5}$ M in bath

Add 10 µl of $1x10^{-2}$ M = $3x10^{-5}$ M in bath

III. Additions are made after 5 minutes when no response is observed or following maximal response of the preceding concentration.

- **End of Experiment**

I. Stop data acquisition and save the file.

II. Unplug baths from the myograph.

III. Drain baths and carefully remove tissue. If required, use a microscope to remove the tissue. Discard tissue in a yellow biohazard waste bag.

IV. Fill baths with 8 % acetic acid and leave in the baths for approximately 5 minutes.

V. Using a cotton bud, clean all surfaces of the myograph (inside and outside of bath).

NOTE: Ensure the gas is still on when cleaning the myographs.

VI. Wash all baths three times with dH_2O.

VII. Wipe down outer surfaces of the myograph using dH_2O and blue roll.

VIII. Finally, dry all surfaces of the myograph, including the under surface of the bath/interface.

IX. Wipe down all benching with disinfectant.

X. Turn off all equipment and the gas supply (both from the tap and cylinder).

Appendix III: Making solutions.

Western blot solutions

Making running SDS gel

Supplementary Table 3: Solutions for preparing 12% running gel for Tris-glycine SDS-Polyacrylamide Gel Electrophoresis.

	Component volumes (mL) per gel mold volume of			
Solution components	5 mL	10 mL	15 mL	20 mL
H_2O	1.6	3.3	4.9	6.6
30% acrylamide mix	2.0	4.0	6.0	8.0
1.5 M tris (pH 8.8)	1.3	2.5	3.8	5.0
10% SDS	0.05	0.1	0.15	0.2
10% ammonium persulfate	0.05	0.1	0.15	0.2
TEMED	0.002	0.004	0.006	0.008

Supplementary Table 4: Solutions for preparing 5% stacking gel for Tris-glycine SDS-Polyacrylamide Gel Electrophoresis

	Component volumes (mL) per gel mold volume of			
Solution components	1 mL	2 mL	3 mL	4 mL
H_2O	0.68	1.4	2.1	2.7
30% acrylamide mix	0.17	0.33	0.5	0.67
1.5 M tris (pH 8.8)	0.13	0.25	0.38	0.5
10% SDS	0.01	0.02	0.03	0.04
10% ammonium persulfate	0.01	0.02	0.03	0.04
TEMED	0.001	0.002	0.003	0.004

SDS-PAGE SDS Running Buffer (10x) Preparation and Recipe

In SDS-PAGE (sodium dodecyl sulfate-polyacrylamide gel electrophoresis), SDS Running Buffer is used as the electrophoresis buffer during stacking and resolution.

Supplementary Table 5: Reagents to prepare 1L 10X SDS-PAGE SDS Running Buffer

Component	Amount	Concentration
Tris base (mw: 121.14 g/mol)	30.3 g	0.2501 M
Glycine (mw: 75.07 g/mol)	144.4 g	1.924 M
SDS (mw: 288.38 g/mol)	10 g	0.03467 M

To prepare 1L 10X SDS-PAGE SDS Running Buffer (10x):

I. Prepare 800 mL of distilled water in a suitable container.

II. Add 30.3 g of Tris base to the solution.

III. Add 144.4 g of Glycine to the solution.

IV. Add 10 g of SDS to the solution.

V. Add distilled water until the volume is 1 L.

To make 1X: do a 1:10 dilution in distilled water (100mL of 10X and 900mL of distilled water)

Transfer buffer

Supplementary Table 6: Reagents to make 1L 10X transfer buffer

Component	Amount	Concentration
Tris base (mw: 121.14 g/mol)	30.3 g	0.2501 M
Glycine (mw: 75.07 g/mol)	144.4 g	1.924 M

To make 1L 10X transfer buffer;

I. Prepare 800 mL of distilled water in a suitable container.

II. Add 30.3 g of Tris base to the solution.

III. Add 144.4 g of Glycine to the solution.

IV. Add distilled water until the volume is 1 L.

To make 1X (1L):

I. 100mL of 10X transfer buffer

II. 200mL ethanol

III. 700mL distilled water

Tris-Buffered Saline (TBS) 10X Stock Solution for Western Blots

Tris-buffered saline (TBS) is an excellent wash buffer for many types of immunoassays. To make 1 L of 10X TBS stock solution, dissolve 24 g Tris and 88 g NaCl in 900 mL of water and then adjust the pH to 7.6 and final volume to 1 L.

Supplementary Table 7: Reagents for making Tris Buffered saline 10X stock solution

Component	Amount
Tris Base (mw: 121.14)	24g
NaCl (mw: 58.44)	88g

To make 1X TBS, 100mL of 10X TBS in 900 ml of distilled water

Tris-buffered saline with 0.1% Tween® 20 detergent (TBST)

Tris-buffered saline with 0.1% Tween® 20 detergent (TBST) is an effective wash buffer for many immunoassays. To make 1 L of TBST wash buffer, add 100 mL of 10X TBS and **1 mL Tween® 20** detergent to 900 mL of water.